frontiers | Research Topics

Pharmacological approaches targeting neutrophilic inflammation: Volume II

Edited by
Galina Sud'ina, Boris Victor Chernyak, Tsong-Long Hwang,
Alexey Victorovich Sokolov and Roman A. Zinovkin

Published in
Frontiers in Pharmacology
Frontiers in Immunology

ISSN 1664-8714
ISBN 978-2-83250-945-6
DOI 10.3389/978-2-83250-945-6

About Frontiers

Frontiers is more than just an open access publisher of scholarly articles: it is a pioneering approach to the world of academia, radically improving the way scholarly research is managed. The grand vision of Frontiers is a world where all people have an equal opportunity to seek, share and generate knowledge. Frontiers provides immediate and permanent online open access to all its publications, but this alone is not enough to realize our grand goals.

Frontiers journal series

The Frontiers journal series is a multi-tier and interdisciplinary set of open-access, online journals, promising a paradigm shift from the current review, selection and dissemination processes in academic publishing. All Frontiers journals are driven by researchers for researchers; therefore, they constitute a service to the scholarly community. At the same time, the *Frontiers journal series* operates on a revolutionary invention, the tiered publishing system, initially addressing specific communities of scholars, and gradually climbing up to broader public understanding, thus serving the interests of the lay society, too.

Dedication to quality

Each Frontiers article is a landmark of the highest quality, thanks to genuinely collaborative interactions between authors and review editors, who include some of the world's best academicians. Research must be certified by peers before entering a stream of knowledge that may eventually reach the public - and shape society; therefore, Frontiers only applies the most rigorous and unbiased reviews. Frontiers revolutionizes research publishing by freely delivering the most outstanding research, evaluated with no bias from both the academic and social point of view. By applying the most advanced information technologies, Frontiers is catapulting scholarly publishing into a new generation.

What are Frontiers Research Topics?

Frontiers Research Topics are very popular trademarks of the *Frontiers journals series*: they are collections of at least ten articles, all centered on a particular subject. With their unique mix of varied contributions from Original Research to Review Articles, Frontiers Research Topics unify the most influential researchers, the latest key findings and historical advances in a hot research area.

Find out more on how to host your own Frontiers Research Topic or contribute to one as an author by contacting the Frontiers editorial office: frontiersin.org/about/contact

Pharmacological approaches targeting neutrophilic inflammation: Volume II

Topic editors

Galina Sud'ina — Lomonosov Moscow State University, Russia
Boris Victor Chernyak — Lomonosov Moscow State University, Russia
Tsong-Long Hwang — Chang Gung University, Taiwan
Alexey Victorovich Sokolov — Institute of Experimental Medicine (RAS), Russia
Roman A. Zinovkin — Lomonosov Moscow State University, Russia

Citation

Sud'ina, G., Chernyak, B. V., Hwang, T.-L., Sokolov, A. V., Zinovkin, R. A., eds. (2022). *Pharmacological approaches targeting neutrophilic inflammation: Volume II*. Lausanne: Frontiers Media SA. doi: 10.3389/978-2-83250-945-6

Table of contents

frontiers | Frontiers in Pharmacology

TYPE Editorial
PUBLISHED 22 November 2022
DOI 10.3389/fphar.2022.1084026

OPEN ACCESS

EDITED AND REVIEWED BY
Paola Patrignani,
University of Studies G.d'Annunzio Chieti and Pescara, Italy

*CORRESPONDENCE
Galina F. Sud'ina,
sudina@genebee.msu.ru

SPECIALTY SECTION
This article was submitted to Inflammation Pharmacology, a section of the journal Frontiers in Pharmacology

RECEIVED 29 October 2022
ACCEPTED 07 November 2022
PUBLISHED 22 November 2022

CITATION
Sokolov AV, Chernyak BV, Zinovkin RA, Hwang T-L and Sud'ina GF (2022), Editorial: Pharmacological approaches targeting neutrophilic inflammation: Volume II.
Front. Pharmacol. 13:1084026.
doi: 10.3389/fphar.2022.1084026

Editorial: Pharmacological approaches targeting neutrophilic inflammation: Volume II

Alexey V. Sokolov[1], Boris V. Chernyak[2], Roman A. Zinovkin[2,3], Tsong-Long Hwang[4,5,6] and Galina F. Sud'ina[2]*

[1]Institute of Experimental Medicine, St. Petersburg, Russia, [2]Belozersky Institute of Physico-Chemical Biology, Lomonosov Moscow State University, Moscow, Russia, [3]The "Russian Clinical Research Center for Gerontology" of the Ministry of Healthcare of the Russian Federation, Pirogov Russian National Research Medical University, Moscow, Russia, [4]Graduate Institute of Natural Products, Chang Gung University, Taoyuan, Taiwan, [5]Graduate Institute of Health Industry Technology, Chang Gung University of Science and Technology, Taoyuan, Taiwan, [6]Department of Anesthesiology, Chang Gung Memorial Hospital, Taoyuan, Taiwan

KEYWORDS

neutrophils, inflammation, acute lung injury, sepsis, neutrophil extracellular traps (NETs), phagocytosis

Editorial on the Research Topic
Pharmacological Approaches targeting neutrophilic inflammation: Volume II

Neutrophils are essential for maintaining homeostasis and the functioning of the innate immune system. Neutrophils are the first immune cells to respond, and they release numerous types of substances that are crucial for eliminating microbes. However, it can also result in collateral tissue damage if neutrophilic activity is overdone. Thus, regulation of neutrophilic activity is of great importance for the treatment of many pathological conditions. The Research Topic aims to highlight the ongoing advancement in the pharmacological approaches targeting neutrophilic inflammation.

Many acute and chronic lung disorders are accompanied by increased neutrophilic infiltration. Acute lung injury (ALI) and acute respiratory distress syndrome (ARDS) are the main causes of acute respiratory failure in seriously ill patients, with critical role of neutrophils in epithelial and endothelial dysfunction. It is not surprising that nearly half of the papers on this Research Topic are devoted to inflammatory diseases of the respiratory tract.

Earlier studies has demonstrated increased levels of the pro-fibrotic, ß-galactoside-binding lectin Galectin-3, which is involved in neutrophils recruitment and stimulation, increased in the lungs during ALI (Humphries et al., 2021). It has been suggested that Galectin-3 inhibition may be a promising therapeutic approach in the treatment of ALI. In this Research Topic, the same research group by Humphries et al. reported that the Galectin-3 inhibitor GB0139 reduced inflammation and decreased neutrophil activation

in an ALI model. GB0139 inhibited neutrophil recruitment in LPS-induced lung inflammation while accelerating neutrophil apoptosis. The study supports the development of Galectin-3 inhibitors as a therapeutic agent for the treatment of ALI.

In asthma, airways neutrophils recruitment and neutrophil extracellular traps (NETs) formation are associated with disease severity (Janssen et al., 2022), and neutrophilic asthma is poorly controlled by conventional therapy. Kim et al. have explored targeting of extracellular traps formed by host DNA of leukocyte origin to inhibit inflammatory asthma. The authors found that microRNA (miR)-155 regulated the release of extracellular traps. The level of miR-155 was increased in asthma and the inhibition of miR-155 mitigated neutrophilic asthma.

The pharmacological approach to ALI treatment by classical Chinese medicine Qing-Jin-Hua-Tang-Decoction (QJHTD) was conducted by Xiao et al. Network pharmacology with experimental validation identified the active components, effective targets and potential mechanisms of action of QJHTD in ALI. Some components prevented thrombosis in ALI. Direct binding to thrombin and inhibition of its activity in micromolar range was evidenced for baicalein, wogonin, and baicalin. Interestingly, QJHTD also inhibited NETs formation. The formation of NETs containing chromatin makes a significant contribution to antimicrobial protection but also to the pathogenesis of various inflammatory diseases. In particular, excessive NETs formation has been shown to play an important role in ALI and coronavirus disease 2019 (COVID-19) (Cesta et al., 2021) (Scozzi et al., 2022).

Hyperinflammation in COVID-19 is characterized by elevated blood levels of neutrophils and neutrophil activation, accompanied by hypercoagulability and blood clotting, which is the main cause of death in this disease. The urgent task is the search for possible approaches to reduce the pro-inflammatory functions of neutrophils while preserving their protective functions. Masso-Silva et al. have found, that intravenous immunoglobulin (IVIG) reduced neutrophil inflammatory pathways in patients with COVID-19. IVIG was shown to dose-dependently inhibit NETs production and oxidative burst but did not affect *ex vivo* neutrophil phagocytosis. Plasma levels of both extracellular DNA and neutrophil elastase in patients with COVID-19 were significantly lower after IVIG treatment. These findings present a new perspective for the application of neutrophil modulators to the therapeutic repertoire of COVID-19.

In severe COVID-19, neutrophils play an important role in the pathogenesis of ARDS, vascular disease, and sepsis (Ventura-Santana et al., 2022). Huang et al. presented an interesting report on the protective effects of D-tagatose in ARDS model induced by oleic acid in rats, as a basis for the development of new therapeutic approaches. D-tagatose improved oxygenation function, reduced respiratory acidosis, improved vascular permeability, and maintained the stability of the alveolar structure.

Chronic viral infections induce sustained inflammatory cytokine signaling and oxidative stress that are associated with atherogenesis. However, the impact of hyperinflammation in COVID-19 on atherogenesis remains unclear. The study by Nie et al. showed that circulating endotoxin levels and intestinal neutrophil elastase activity positively correlated with the progression of atherosclerosis in patients. The selective neutrophil elastase inhibitor sivelestat reduced intestinal permeability and endotoxemia in Apo E−/− atherosclerotic mice. In conclusion, application of sivelestat was proposed as a promising approach to the treatment of atherosclerosis and the protection of intestinal homeostasis, which plays a critical role in pathogenesis of atherosclerosis.

Neonatal neutrophils are less sensitive to many stimuli, making children more susceptible to sepsis than adults (Fleischmann-Struzek et al., 2018). The role of checkpoint inhibitor proteins in the immune response to sepsis in both adults and neonates is reviewed by Hensler et al. The authors point out to significant gaps in the management of neonatal sepsis and suggest that checkpoint inhibitor proteins such as PD-1, PD-L1, VISTA, and HVEM may be useful for the diagnosis and treatment of patients with sepsis.

Neutrophils are involved in defense mechanisms against microbial pathogens *via* phagocytosis and ROS production. At the same time, neutrophils may also be involved in the pathogenesis of some infections by inducing oxidative stress, releasing toxic granules and NETs. The role of neutrophils in malaria infection has been reviewed by Babatunde and Adenuga. The malaria parasite is known to inhibit the antimicrobial functions of neutrophils, making malaria patients more susceptible to secondary opportunistic *Salmonella* infections. Hemolysis of red blood cells in malaria is responsible for the inhibition of phagocytosis, ROS production and neutrophil migration. The authors discussed some conflicting data on the use of murine models to study the role of neutrophils in malaria.

Bacterial infections remain the leading cause of death, and pharmacological approaches to enhance phagocytosis are in high demand. Jacob S. Brenner and colleagues recently published the study identifying the properties of nanoparticle leading to neutrophil tropism in inflamed lungs (Myerson et al., 2022). In continuation to these studies, Rubey et al. developed an approach to enhance bacterial neutrophil phagocytosis. The authors studied a wide class of neutrophil-tropic nanoparticles and demonstrated that they enhance phagocytosis and enter the same sites as bacteria inside neutrophils. It has been suggested that these nanoparticles can serve as useful drug carriers to alleviate bacterial diseases.

The regulatory role of microRNAs (miRNAs) in phagocytosis has been reviewed by Wang et al. The authors noticed that the effects of miRNAs on neutrophils and macrophages are highly environmentally dependent and formulated further steps to determine the therapeutic utility of miRNAs.

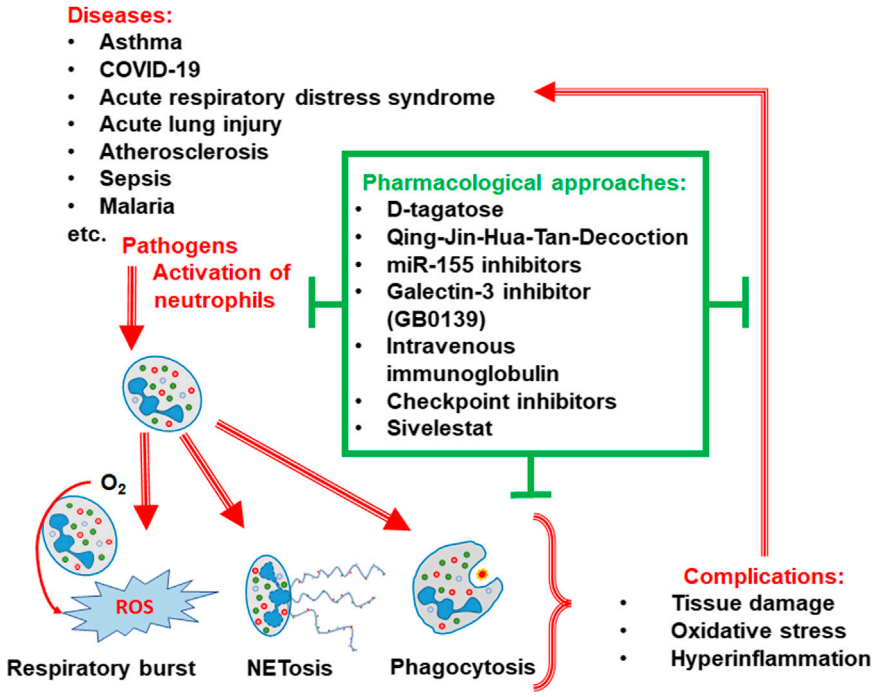

SCHEME 1
Pharmacological approaches targeting neutrophilic inflammation.

In summary, the papers in this topic issue illustrate the involvement of neutrophils in various pathologies and the role of neutrophils in host immunity (Scheme 1).

Author contributions

All authors listed have made a substantial, direct and intellectual contribution to the work, and approved it for publication.

Funding

RZ was supported by the Russian Science Foundation (project 20-14-00268).

Acknowledgements

We thank the contributors of this Research Topic and the referees for their attentive review. This editorial was partly supported by the Interdisciplinary Scientific and Educational School of Moscow University « Molecular Technologies of the Living Systems and Synthetic Biology».

Conflict of interest

The authors declare that the research was conducted in the absence of any commercial or financial relationships that could be construed as a potential conflict of interest.

Publisher's note

All claims expressed in this article are solely those of the authors and do not necessarily represent those of their affiliated organizations, or those of the publisher, the editors and the reviewers. Any product that may be evaluated in this article, or claim that may be made by its manufacturer, is not guaranteed or endorsed by the publisher.

References

Cesta, M. C., Zippoli, M., Marsiglia, C., Gavioli, E. M., Mantelli, F., Allegretti, M., et al. (2021). The role of interleukin-8 in lung inflammation and injury: Implications for the management of COVID-19 and hyperinflammatory acute respiratory distress syndrome. *Front. Pharmacol.* 12, 808797. doi:10.3389/fphar.2021.808797

Fleischmann-Struzek, C., Goldfarb, D. M., Schlattmann, P., Schlapbach, L. J., Reinhart, K., and Kissoon, N. (2018). The global burden of paediatric and neonatal sepsis: A systematic review. *Lancet. Respir. Med.* 6, 223–230. doi:10.1016/S2213-2600(18)30063-8

Humphries, D. C., Mills, R., Dobie, R., Henderson, N. C., Sethi, T., and Mackinnon, A. C. (2021). Selective myeloid depletion of galectin-3 offers protection against acute and chronic lung injury. *Front. Pharmacol.* 12, 715986. doi:10.3389/fphar.2021.715986

Janssen, P., Tosi, I., Hego, A., Marechal, P., Marichal, T., and Radermecker, C. (2022). Neutrophil extracellular traps are found in bronchoalveolar lavage fluids of horses with severe asthma and correlate with asthma severity. *Front. Immunol.* 13, 921077. doi:10.3389/fimmu.2022.921077

Myerson, J. W., Patel, P. N., Rubey, K. M., Zamora, M. E., Zaleski, M. H., Habibi, N.., et al. (2022). Supramolecular arrangement of protein in nanoparticle structures predicts nanoparticle tropism for neutrophils in acute lung inflammation. *Nat. Nanotechnol.* 17, 86–97. doi:10.1038/s41565-021-00997-y

Scozzi, D., Liao, F., Krupnick, A. S., Kreisel, D., and Gelman, A. E. (2022). The role of neutrophil extracellular traps in acute lung injury. *Front. Immunol.* 13, 953195. doi:10.3389/fimmu.2022.953195

Ventura-Santana, E., Ninan, J. R., Snyder, C. M., and Okeke, E. B. (2022). Neutrophil extracellular traps, sepsis and COVID-19 - a tripod stand. *Front. Immunol.* 13, 902206. doi:10.3389/fimmu.2022.902206

frontiers | Frontiers in Pharmacology

ORIGINAL RESEARCH
published: 04 April 2022
doi: 10.3389/fphar.2022.838688

Sivelestat Alleviates Atherosclerosis by Improving Intestinal Barrier Function and Reducing Endotoxemia

Hezhongrong Nie[1]†, Qingquan Xiong[2]†, Guanghui Lan[2], Chunli Song[1], Xiaohong Yu[1], Lei Chen[1], Daming Wang[1], Tingyu Ren[1], Zeyan Chen[1], Xintong Liu[1] and Yiwen Zhou[1]**

[1]Center of Clinical Laboratory, Shenzhen Hospital, Southern Medical University, Shenzhen, China, [2]Department of General Surgery, Shenzhen Hospital, Southern Medical University, Shenzhen, China

Emerging evidence suggests that atherosclerosis, one of the leading phenotypes of cardiovascular diseases, is a chronic inflammatory disease. During the atherosclerotic process, immune cells play critical roles in vascular inflammation and plaque formation. Meanwhile, gastrointestinal disorder is considered a risk factor in mediating the atherosclerotic process. The present study aimed to utilize sivelestat, a selective inhibitor of neutrophil elastase, to investigate its pharmacological benefits on atherosclerosis and disclose the gastrointestinal–vascular interaction. The activation of intestinal neutrophil was increased during atherosclerotic development in Western diet-fed ApoE$^{-/-}$ mice. Administration of sivelestat attenuated atherosclerotic phenotypes, including decreasing toxic lipid accumulation, vascular monocyte infiltration, and inflammatory cytokines. Sivelestat decreased intestinal permeability and endotoxemia in atherosclerotic mice. Mechanistically, sivelestat upregulated the expression of zonula occludens-1 in the atherosclerotic mice and recombinant neutrophil elastase protein-treated intestinal epithelial cells. Meanwhile, treatment of sivelestat suppressed the intestinal expression of inflammatory cytokines and NF-κB activity. In contrast, administration of lipopolysaccharides abolished the anti-atherosclerotic benefits of sivelestat in the Western diet-fed ApoE$^{-/-}$ mice. Further clinical correlation study showed that the circulating endotoxin level and intestinal neutrophil elastase activity were positively correlated with carotid intima-medial thickness in recruited subjects. In conclusion, sivelestat had pharmacological applications in protection against atherosclerosis, and intestinal homeostasis played one of the critical roles in atherosclerotic development.

Keywords: atherosclerosis, sivelestat, intestinal permeability, endotoxemia, inflammation

OPEN ACCESS

Edited by:
Galina Sud'ina, Lomonosov Moscow State University, Russia

Reviewed by:
Mingxue Zhou, Capital Medical University, China
Roman A. Zinovkin, Lomonosov Moscow State University, Russia
Alexey Victorovich Sokolov, Institute of Experimental Medicine (RAS), Russia

***Correspondence:**
Hezhongrong Nie
hezrnie@hotmail.com
Yiwen Zhou
yiwenzhou21@aliyun.com

†*These authors have contributed equally to this work*

Specialty section:
This article was submitted to Inflammation Pharmacology, a section of the journal Frontiers in Pharmacology

Received: *18 December 2021*
Accepted: *08 March 2022*
Published: *04 April 2022*

Citation:
Nie H, Xiong Q, Lan G, Song C, Yu X, Chen L, Wang D, Ren T, Chen Z, Liu X and Zhou Y (2022) Sivelestat Alleviates Atherosclerosis by Improving Intestinal Barrier Function and Reducing Endotoxemia. Front. Pharmacol. 13:838688. doi: 10.3389/fphar.2022.838688

INTRODUCTION

Atherosclerosis, one of the major phenotypes of cardiovascular diseases (CVDs), is the leading cause of cardiovascular morbidity and mortality (Libby et al., 2016). It is associated with increased vascular inflammation and plaque formation. Recently, emerging studies have disclosed the potential crosstalk between the cardiovascular system and gastrointestinal homeostasis (Cani et al., 2007; Pendyala et al., 2012). In patients with atherosclerosis, there was obvious induction of plasma endotoxin activity, which was accompanied by intestinal

injuries (Pendyala et al., 2012). Administration of intestinal toxic lipopolysaccharides (LPS) accelerated vascular inflammation and atherosclerotic plaque formation by eliminating anti-atherosclerotic benefits of healthy intestinal bacteria in apolipoprotein (Apo) E-deficient mice (Jin Li et al., 2016). Trimethylamine N-oxide (TMAO), a product of intestinal microorganisms, could promote the atherosclerosis process and accelerate the pathological process of cerebrovascular diseases (Wang et al., 2015). Apo A-I, synthesized in small intestinal cells, was a potential target for protection against atherosclerosis (Chen et al., 2020). Therefore, targeting intestinal homeostasis has therapeutic benefits in combating atherosclerosis.

Structural disorders of the gastrointestinal system mainly involve disruption of intestinal permeability, leakage of toxic substances into circulation, and a consequent inflammatory response (Andreasen et al., 2008). In patients with cardiovascular diseases, the intestinal barrier was disrupted, whereas circulating toxic factors were remarkably upregulated (Kim et al., 2018; Noval Rivas et al., 2019). Western diet-induced atherosclerotic mice exhibited abnormal intestinal permeability, but improvement of intestinal permeability could alleviate diet-induced intestinal disorders and atherosclerotic plaque formation (Jin Li et al., 2016; Zhu et al., 2018). Mechanistic studies identified intestinal epithelial zonulin proteins, majorly controlled by zonula occludens-1 (ZO-1), and determined the intestinal permeability (Fasano, 2011; Carrera-Bastos et al., 2018). The circulating level of zonulin was closely associated with plasma endotoxin concentrations in patients with myocardial infarction (Carrera-Bastos et al., 2018). Western diet-induced atherosclerotic mice had a lower expression of intestinal ZO-1 but severe endotoxemia (Jin Li et al., 2016). Meanwhile, the biogenesis and activity of intestinal epithelial ZO-1 were dampened by the local intestinal and systemic inflammation. In patients with immune diseases, the tight junction integrity was severely disrupted by the upregulation of the inflammatory response (Fasano, 2011). All these previous findings supported the fact that intestinal tight junction and endotoxin were potential critical mediators during atherosclerosis development.

Sivelestat, with the formula of $C_{20}H_{22}N_2O_7S$, is one of the selective neutrophil elastase inhibitors for alleviating acute respiratory distress syndrome (Kawabata et al., 1991). For COVID-19 treatment, sivelestat also exhibited therapeutic benefits in recovering some patients with severe symptoms (Sahebnasagh et al., 2020). More recently, administration of sivelestat suppressed the endotoxin-induced neutrophil activity *in vitro* (Okeke et al., 2020). Multiple studies have supported excessive intestinal accumulation of neutrophil elastase; one of key neutrophil serine proteinases injured the mucosal structure and debilitated intestinal diseases, such as the thrombotic tendency (Maloy and Powrie, 2011; Li et al., 2020). Besides, neutrophil elastase exacerbated cardiovascular diseases (Warnatsch et al., 2015; Wen et al., 2018). Therefore, targeting neutrophil elastase by sivelestat had potential pharmacological benefits in improving the inflammatory response and related systemic diseases.

The present study aimed to utilize sivelestat to disclose the crosstalk between intestinal neutrophils and atherosclerotic development. Atherosclerotic Apo $E^{-/-}$ mice were administered sivelestat, and we further investigated its pharmacological effects on atherosclerotic development and intestinal homeostasis. Our findings provided evidence that sivelestat was a potential drug to combat atherosclerosis, and the intestine/vascular interaction could explain the pharmacological effects of sivelestat on cardiovascular diseases.

MATERIALS AND METHODS

Reagents

The Oil Red O staining kit (#MAK194), hematoxylin (#MHS32), eosin solution (#HT110116), sivelestat (#S7198), and lipopolysaccharides (#L2630) were purchased from Sigma (Sigma Chemicals, St. Louis). Anti-Ly6G antibody (#561105) was purchased from BD (BD Biosciences). Anti-moma-2 antibody (#ab33451) was purchased from Abcam (Cambridge, United Kingdom). Anti-ZO-1 (#5406), anti-Tubulin (#5568), anti-phosphorylated IκB (#2859), and anti-IκB (#9242) antibodies were purchased from Cell Signaling Technology, Inc. (Danvers, MA). DX-4000-FITC (#46944) was purchased from Sigma (Sigma chemicals, St. Louis), and the endotoxin kit (#88282) was from Pierce (Thermo Fisher, CA). Intestinal protein levels of TNF-α (#BMS607-3), IL-1β (#BMS6002), and MCP-1 (#BMS6005) were measured by using ELISA kits from Invitrogen (Thermo Fisher, CA). The intestinal neutrophil elastase activity was measured with a commercial kit (# ab204730) purchased from Abcam (Cambridge, United Kingdom).

Treatment of Sivelestat *In Vivo*

All mouse experimental procedures were approved by the Animal Research and Teaching Committee at Southern Medical University (Guangzhou, China). The mice were housed in 21 ± 2 °C condition and were given free access to diet and tap water. In detail, male aged 6-week ApoE-deficient mice ($ApoE^{-/-}$) were purchased from the Shanghai Model Organisms Center (Shanghai, China), and every group included six mice. Mice were fed with high-fat high-cholesterol diet (HFHC, 40% fat and 1.25% cholesterol, Cat#D12108C, research diets). After being fed with HFHC for 4-week, the $ApoE^{-/-}$ mice were administered with sivelestat (50 mg/kg per day, intraperitoneal injection) or phosphate-buffered saline (Veh) for another 8 weeks. For lipopolysaccharide stimulation, the $ApoE^{-/-}$ mice were fed with HFHC for 4 weeks and then treated with sivelestat (50 mg/kg per day, intraperitoneal injection) and LPS (25 μg/day, subcutaneous injection) or Veh for 8 weeks. Then, mouse tissues, including the aorta, small intestine, and serum, were collected for further measurement.

Measurement of Intestinal Permeability

For the analysis, 500 mg/kg FITC-labeled dextran was orally gavaged into mice, and the serum samples were collected for further analysis. The serum concentration of DX-4000-FITC was

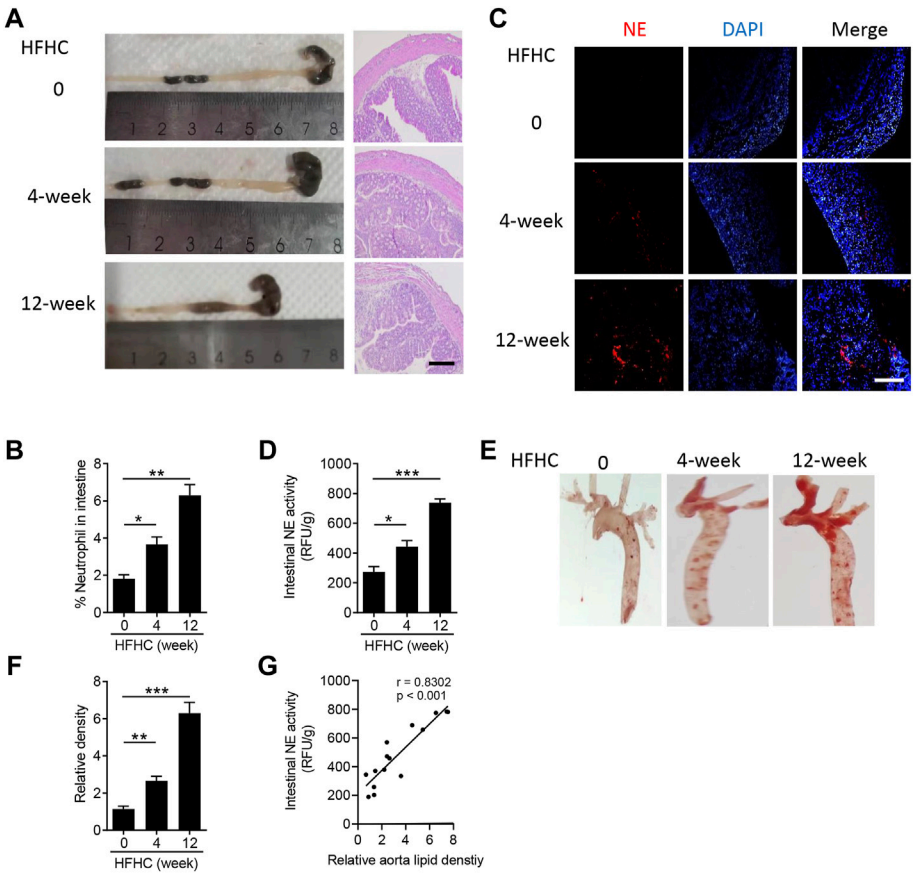

FIGURE 1 | Neutrophils infiltrate into the intestine during the atherosclerotic process. Male Apo $E^{-/-}$ mice were fed with high-fat high-cholesterol diet (HFHC) for 4 and 12 weeks, and $ApoE^{-/-}$ mice were fed with normal diet as the control group. **(A)** Representative images of the mouse colon (left panel) and hematoxylin-eosin staining of the colon structure (right panel). Scale bar = 100 μm. **(B)** Flow cytometry analysis of the percentage of $Cd11b^{+}Ly6G^{+}$ neutrophils in the intestine. **(C)** Immunofluorescence staining of neutrophil elastase (NE, red color, neutrophil marker), and the nuclei were stained with DAPI (blue color). Scale bar = 100 μm. **(D)** Measurement of the neutrophil elastase (NE) activity in intestinal lysates. **(E,F)** Oil Red O staining of the en face aorta **(E)** and the quantitative analysis of the relative lipid density **(F)**. **(G)** Correlation of the intestinal NE activity and aorta lipid density. Data are shown as mean ± SEM. n = 5 mice/group, and $^{*}p < 0.05$, $^{**}p < 0.01$, $^{***}p < 0.001$.

measured by using a fluorescence spectrophotometer (Synergy H1, BioTek, VT) with an excitation wavelength of 485 nm and an emission wavelength of 535 nm.

Histological Staining of the Aorta and Intestine

For lipid staining of the en face aorta and aorta root, whole aorta or 10-μm frozen sections of the aorta root were stained with the Oil Red O staining kit. For hematoxylin and eosin staining, the aorta and colon were fixed in 4% paraformaldehyde and embedded in paraffin. Then, 5-μm paraffin sections were dehydrated and stained with hematoxylin and eosin solution. For immunofluorescence staining, 5-μm aorta sections were hydrated, blocked with 3% BSA solution, and incubated with the anti-moma-2 antibody at 1:100 dilution. After washing in PBS, the sections were stained with the fluorescence-labeled secondary antibody at 1:500 dilution. The nuclei were stained with DAPI. The images were viewed and captured by using a fluorescence microscope (Nikon, Tokyo), and relative lipid contents were measured in 50 images/per mouse by ImageJ software.

Flow Cytometry Analysis of Intestinal Neutrophils

Intestinal resident cells were isolated from 5 to 8 cm of the intestine. Briefly, intestinal segments were excised, cleaned, and cut into small pieces. Samples were then washed with sterile bovine serum-free RPMI 1640 medium three times and digested in 10 ml RPMI containing 1 mg/ml collagenase A (Roche #10103578001) for 30 min at 37°C and 200 rpm in a shaking incubator. Digestion was quenched with FACS buffer and centrifuged for 5 min at 800 g. After washing with PBS t three times, the samples were passed through a 100-μm cell strainer to obtain a single cell suspension. For neutrophil staining, the cells were stained with anti-Cd11b and anti-Ly6G antibodies at 1:100

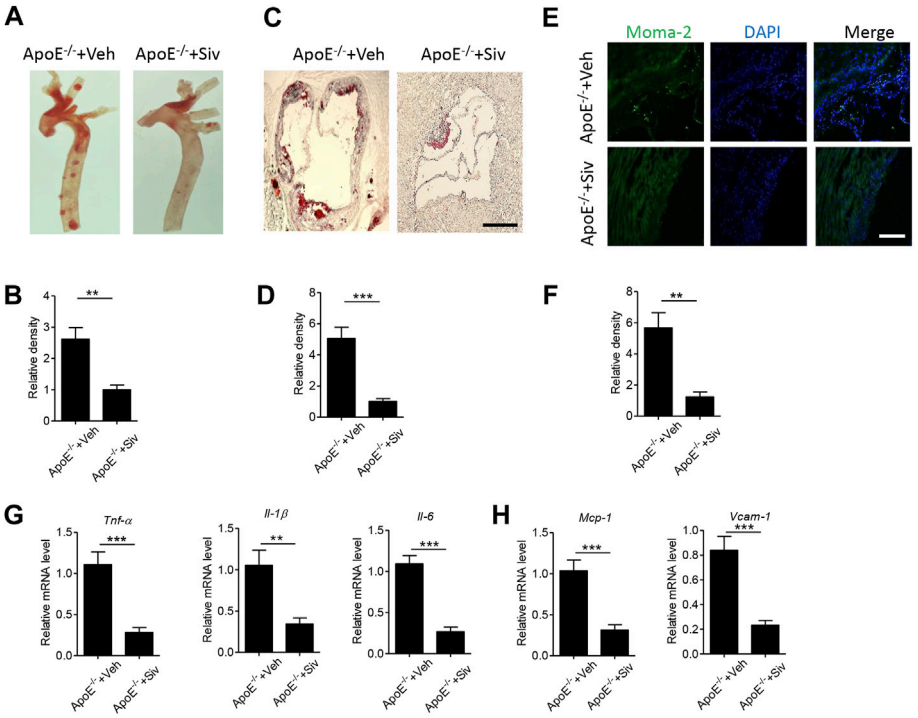

FIGURE 2 | Sivelestat attenuates HFHC-induced atherosclerotic plaque formation and vascular inflammation in Apo $E^{-/-}$ mice. Male Apo $E^{-/-}$ mice were fed with HFHC diet for 4 weeks and then treated with sivelestat (Siv, 50 mg/kg per day, intraperitoneal injection) or phosphate-buffered saline (Veh) for 8 weeks. (A-B) Oil Red O staining of the en face aorta **(A)** and quantitative analysis of the relative lipid density **(B)**. **(C-D)** Oil red O staining of the aorta root **(C)** and quantitative analysis of the relative lipid density **(D)**. Scale bar = 200 μm. **(E-F)** Immunofluorescence staining of aorta root sections with anti-moma-2 antibody **(E)** and quantitative analysis of the relative density **(F)**. Scale bar = 100 μm. **(G-H)** Real-time PCR analysis of gene levels of inflammatory cytokines **(G)**, including *Tnf-α*, *Il-1β*, and *Il-6*, and chemokines **(H)** including *Mcp-1* and *Vcam-1*. Data are shown as mean ± SEM. n = 6 mice/group, and $^{**}p < 0.01$ and $^{***}p < 0.001$.

dilution. The cell percentage was analyzed by using a flow cytometer (BD FACSAria™ III).

Culture of Rat Intestinal Epithelial Cells

The rat intestinal epithelial cell line (#IEC-18, ATCC) was gifted from Dr. Ning Zhu (Zhejiang University). Cells were cultured in DMEM containing 10% FBS and 1% penicillin/streptomycin antibiotics in a humidified chamber (37°C, 21% O_2, and 5% CO_2). For cell experiments, 1×10^6 cells were pretreated with sivelestat (100 μM) or DMSO and stimulated with 0.1 μg/ml human neutrophil elastase recombinant protein for 24 h.

Real-Time PCR Analysis of the Gene Expression

Total RNA from the whole aorta or intestine tissues was extracted by using TRIzol (Invitrogen), according to the manufacturer's instructions. Complementary DNA was reverse-transcribed using the PrimeScript™ RT reagent kit with gDNA Eraser (Takara Biotech, Dalian, China), and qPCR was performed with the SYBR Green quantitative kit (Applied Biosystems, CA). The primer sequences used in this study were listed as follows: mouse *Zo-1*: F-5′-CAACATACAGTGACGCTTCACA-3'; R-5′- CACTATTGACGTTTCCCCACTC-3′, mouse *Tnf-α*: F-5′-ACGGCATGGATCTCAAAGAC-3' R-5′-AGATAGCAAATCGGCTGACG-3′, mouse *Il-1β*: F-5′-CTGGTGTGTGACGTTCCCATTA-3'; R-5′-CCGACAGCACGAGGCTTT-3′, mouse *Il-6*: F-5′-CCACGGCCTTCCCTAC-3'; R-5′- AAGTGCATCATCGTTGT-3′, mouse *Mcp-1*: F-5′-CCACTCACCTGCTGCTACTCA-3'; R-5′-TGGTGATCCTCTTGTAGCTCTCC-3′, mouse *Vcam-1*: F-5′-CCGGCATATACGAGTGTGAA-3'; R-5′-TAGAGTGCAAGGAGTTCGGG-3′, and mouse *Gapdh*: F-5′-AGGAGCGAGACCCCACTAAC-3'; R-5′-GATGACCCTTTTGGCTCCAC-3'. The relative gene expression was calculated by normalizing to the *Gapdh* level.

Immunoblot Analysis

Protein lysates were extracted from the intestinal tissues or epithelial cells, and the protein concentration was measured by using a BCA assay kit (Thermo Fisher, CA). 50 μg protein was subjected to 10% SDS–PAGE electrophoresis and electro-transferred to polyvinylidene difluoride membranes (Amersham Biosciences). Then, the membranes were blocked with 10% non-fat milk and incubated with anti-ZO-1, anti-phos-IκB, IκB, or anti-Tubulin antibody at 1:1,000 dilution and relative secondary antibodies at 1:5,000 dilution. The relative protein expression was visualized by using enhanced chemiluminescence reagents (Bio-Rad, CA) and quantitatively analyzed by ImageJ software.

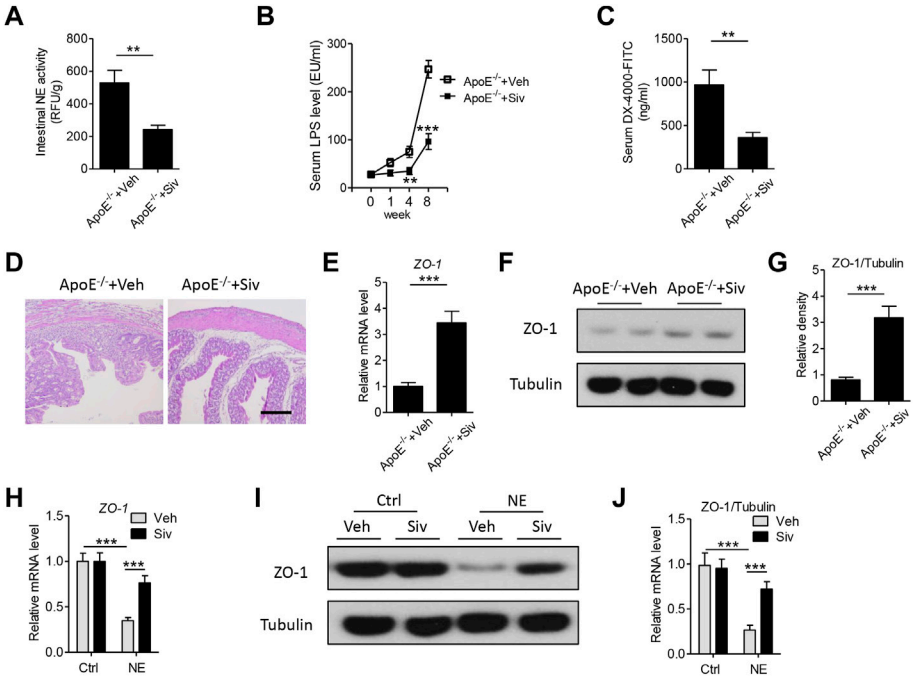

FIGURE 3 | Sivelestat decreases HFHC-induced endotoxemia and intestinal structural disorders by upregulating the intestinal zonula occludens-1 expression in Apo $E^{-/-}$ mice and intestinal epithelial cells. **(A–F)** Male Apo $E^{-/-}$ mice were fed with HFHC diet for 4 weeks and then treated with sivelestat (Siv, 50 mg/kg per day, intraperitoneal injection) or Veh for 8 weeks. **(A)** Mouse intestinal NE activity. **(B)** Measurement of circulating lipopolysaccharide (LPS) levels after sivelestat treatment for 0, 1, 4, and 8 weeks. **(C)** Mice were orally administered with FITC-labeled dextran, and the circulating concentration of DX-4000-FITC was analyzed. **(D)** Hematoxylin and eosin (HE) staining of the colon. Scale bar = 100 μm. **(E)** Gene expression of intestinal zonula occludens (ZO)-*1*. **(F–G)** Immunoblot analysis of intestinal ZO-1 **(F)** and quantitative analysis of the relative density of ZO-1/Tubulin **(G)**. **(H–J)** 1 × 10^6 rat intestinal epithelial cells were pretreated with sivelestat (100 μM) or DMSO and stimulated with 0.1 μg/ml human neutrophil elastase recombinant protein for 24 h. **(H)** Real-time PCR analysis of the ZO-1 gene level. **(I–J)** Immunoblot analysis of ZO-1 protein expression **(I)** and quantitative analysis of the relative density of ZO-1/Tubulin **(J)**. Data are shown as mean ± SEM. n = 6 mice/group or n = 5 independent experiments, and $^{**}p < 0.01$, $^{***}p < 0.001$.

Clinical Study

This study included 26 individuals, including nine atherosclerotic subjects with carotid intima-medial thickness (IMT) ≥ 0.85 mm and 17 healthy subjects with IMT <0.85 mm, who were recruited from July 2019 to May 2020 at the Shenzhen Hospital of Southern Medical University (NYSZYYEC20190005). The basic clinical parameters of these subjects are showed in **Supplementary Table S1**. Furthermore, among these subjects, 12 patients were under intestinal polyp surgery (3 patients with ≥0.85 mm and nine subjects with IMT <0.85 mm). The subjects with IMT <0.85 mm were characterized with no history of angina and other heart diseases, a normal resting ECG, and normal exercise ECG stress testing. In patients under the intestinal polyp surgery, the intestinal activity was measured by using the commercial kit. Before statistical analysis, the Shapiro–Wilk test was conducted to identify the distribution for normality. Then, Pearson analysis was conducted for clinical correlation. All participants have been informed clinical consent, and the related analysis protocol was approved by the Human Ethics Committee of Southern Medical University.

Statistical Analysis

Data were shown as mean ± SEM. The Student's *t*-test was used for comparing two groups, and ANOVA was used for multiple groups (GraphPad, San Diego, CA). Pearson analysis was used for analyzing the statistical correlation. $p < 0.05$ was considered to be significant.

RESULTS

Neutrophils Infiltrate Into the Intestine During the Atherosclerotic Process

Multiple studies have addressed high-fat diet severely injured intestinal homeostasis, such as intestinal shortening, disruption of the intestinal barrier, and inflammatory response (Araújo et al., 2017; Rohr et al., 2020). To identify the pathological changes of the intestine in atherosclerotic mice, at first, we measured the tissue remodeling of colon. As shown in **Figure 1A**, the length of the colon was significantly decreased after the mice were fed with high-fat high-cholesterol (HFHC) diet for 4 and 12 weeks, and HFHC feeding also induced colic structural disorders. For an inflammatory response, flow cytometry analysis indicated $Cd11b^{+}Ly6G^{+}$ neutrophils obviously infiltrated into the intestine (**Figure 1B**), especially in the HFHC-fed mice for 12 weeks ($p < 0.01$). Furthermore, neutrophil elastase (NE), one of the neutrophil serine proteases, was also highly expressed in the intestines of HFHC-fed mice (**Figure 1C**),

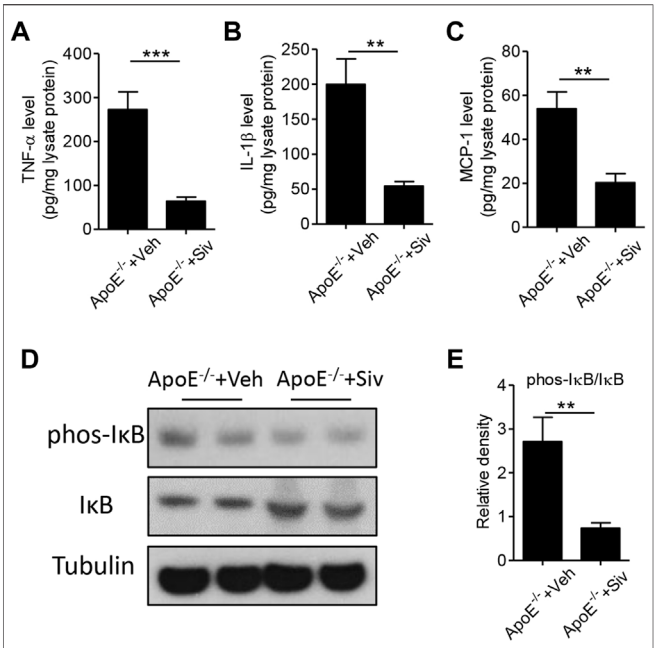

FIGURE 4 | Sivelestat attenuates intestinal inflammation in HFHC-fed Apo $E^{-/-}$ mice and NE-treated intestinal epithelial cells. **(A–E)** Male Apo $E^{-/-}$ mice were fed with HFHC diet for 4 weeks and then treated with sivelestat (Siv, 50 mg/kg per day, intraperitoneal injection) or Veh for 8 weeks. ELISA analysis of intestinal protein levels of TNF-α **(A)**, IL-1β **(B)**, and MCP-1 **(C)**. Immunoblot analysis of protein expressions of phosphorylated (phos-) IκB and IκB **(D)** and quantitative analysis of the relative density of phos-IκB/IκB **(E)**. Data are shown as mean ± SEM. n = 6 mice/group, and $^{**}p < 0.01$ and $^{***}p < 0.001$.

and the intestinal NE activity was increased time-dependently during HFHC feeding (**Figure 1D**). Meanwhile, as shown in **Figures 1E,F**, mice with HFHC feeding had remarkable lipid plaque formation in the aorta. To testify the possible role of intestinal NE in atherosclerotic development, Pearson analysis showed the intestinal NE levels had a positive correlation of the aorta lipid deposit (**Figure 1G**).

Administration of Sivelestat Attenuates HFHC Diet-Induced Atherosclerosis and Vascular Inflammation in ApoE$^{-/-}$ Mice

Neutrophils play critical roles in the inflammatory response (Kolaczkowska and Kubes, 2013) and participated in the progress of cardiovascular diseases (Gaul et al., 2017). Sivelestat, as a selective inhibitor of neutrophil elastase, could suppress inflammation in several inflammatory diseases (Endo et al., 2006; Shimoda et al., 2008). In the present study, we aimed to explore the pharmacological effects of sivelestat on atherosclerosis in mice. Consistent with previous studies (Jin Li et al., 2016; Zhu et al., 2018), high-fat high-cholesterol (HFHC) diet accelerated lipid accumulation in the aorta from Apo $E^{-/-}$ mice (**Figures 2A–D**). But the administration of sivelestat significantly decreased lipid contents in en-face aorta (**Figures 2A,B**, $p < 0.01$) and the sections of the aorta root (**Figures 2C,D**, $p < 0.001$). Infiltration of immune cells, including macrophages and other monocytes, was a key phenotype of atherosclerosis (Hansson, 2005). As shown in **Figures 2E,F**, treatment of sivelestat inhibited the infiltration of monocytes and macrophages ($p < 0.01$). Meanwhile, sivelestat also decreased the gene levels of inflammatory factors, including pro-inflammatory cytokines (**Figure 2G**, $p < 0.01$) and chemokines (**Figure 2H**, $p < 0.001$). However, sivelestat had no significant effects on the other basic parameters of a mouse, including body weight, the fasting blood glucose level, and serum lipid profiles (**Supplementary Table S2**).

Administration of Sivelestat Decreases Endotoxemia by Improving Zonula Occludens-1-Mediated Intestinal Permeability and Intestinal Inflammatory Response *In Vivo* and *In Vitro*

The abnormal induction of intestinal permeability and subsequent endotoxemia could initiate the progress of atherosclerotic plaque formation (Zhu et al., 2018). In the present study, we found the treatment of sivelestat led to a significant reduction in the intestinal NE activity (**Figure 3A**) and the circulating level of endotoxin in the HFHC-fed ApoE$^{-/-}$ mice (**Figure 3B**). Next, we measured intestinal permeability by treating mice with fluorescent-labeled dextran (DX-4000-FITC). As shown in **Figure 3C**, the circulating concentration of DX-4000-FITC was decreased in sivelestat-treated Apo $E^{-/-}$ mice ($p < 0.01$). H&E staining of the colon also showed the HFHC diet loosened the structure of mucosa, which facilitated the leakage of toxic substances into circulation, whereas sivelestat improved the intestinal structure (**Figure 3D**). Intestinal permeability was mainly controlled by zonula occludens (ZO)-1, one of the key epithelial tight junction proteins (Van Itallie et al., 2009). As shown in **Figure 3E**, the intestinal gene level of ZO-1 was upregulated in sivelestat-treated Apo $E^{-/-}$ mice ($p < 0.001$). The protein expression of ZO-1 was also significantly upregulated in sivelestat-treated Apo $E^{-/-}$ mice, as compared with Veh-treated Apo $E^{-/-}$ mice (**Figures 3F,G**). To determine the direct pharmacological effects of sivelestat on the ZO-1 protein expression, intestinal epithelial cells were treated with NE recombinant protein with or without sivelestat. **Figures 3H–J** showed NE recombinant protein decreased the gene and protein expression of ZO-1 ($p < 0.001$), whereas sivelestat attenuated NE-induced ZO-1 reduction in intestinal epithelial cells ($p < 0.05$).

Previous studies have showed there were abnormal immune responses in the gastrointestinal homeostasis of patients with atherosclerosis (Cani et al., 2007; Pendyala et al., 2012). Therefore, we investigated the effects of sivelestat on the intestinal inflammatory response in the HFHC-fed Apo $E^{-/-}$ mice. As shown in **Figures 4A–C**, the protein levels of inflammatory cytokines, including TNF-α (**Figure 4A**, $p < 0.001$), IL-1β (**Figure 4B**, $p < 0.01$), and MCP-1 (**Figure 4C**, $p < 0.01$), were significantly decreased in intestinal lysates from sivelestat-treated ApoE$^{-/-}$ mice. NF-κB signaling is one of the key transcriptional factors in regulating the inflammatory response

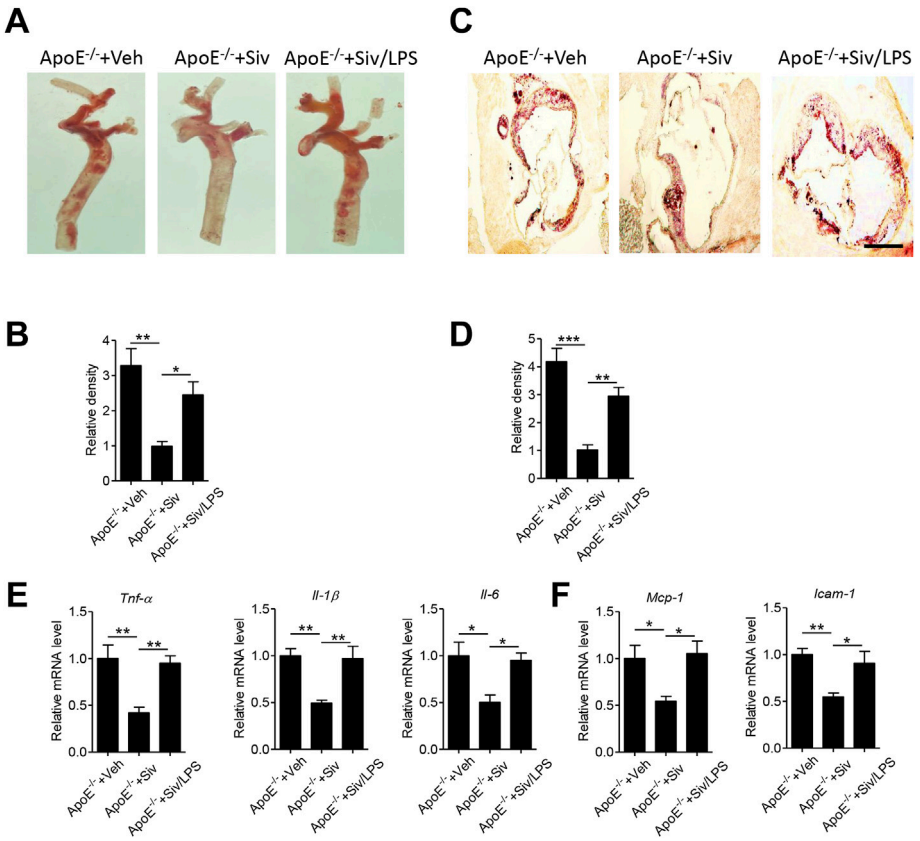

FIGURE 5 | Administration of lipopolysaccharides eliminates anti-atherosclerotic benefits of sivelestat in Apo $E^{-/-}$ mice. Male Apo $E^{-/-}$ mice were fed with HFHC diet for 4 weeks and then treated with sivelestat (Siv, 50 mg/kg per day, intraperitoneal injection) and LPS (25 μg/day, subcutaneous injection) or Veh for 8 weeks. **(A–B)** Oil Red O staining of en face aorta **(A)** and the quantitative analysis of relative lipid density **(B)**. **(C–D)** Oil red O staining of the aorta root **(C)** and the quantitative analysis of the relative lipid density **(D)**. Scale bar = 200 μm. **(E–F)** Real-time PCR analysis of gene levels of inflammatory cytokines **(E)**, including *Tnf-α*, *Il-1β*, and *Il-6*, and chemokines **(F)** including *Mcp-1* and *Vcam-1*. Data are shown as mean ± SEM. n = 6 mice/group and $^{*}p < 0.05$, $^{**}p < 0.01$, $^{***}p < 0.001$.

(Pan et al., 2012; Pan et al., 2014). To this end, we measured the expression of phosphorylated (phos-) IκB and IκB in intestinal tissues. **Figures 4D,E** showed sivelestat inhibited NF-κB activation by decreasing phos-IκB and increasing the IκB level ($p < 0.01$).

Administration of Lipopolysaccharides Eliminates the Anti-Atherosclerotic Benefits of Sivelestat in HFHC-Fed ApoE$^{-/-}$ Mice

To clarify whether the pharmacological benefits of sivelestat is dependent on lowering endotoxemia, we subcutaneously injected lipopolysaccharides (LPS) into sivelestat-treated ApoE$^{-/-}$ mice. Administration of sivelestat decreased lipid accumulation in the aorta of Apo $E^{-/-}$ mice (**Figures 1A–D**), but co-treatment with LPS reversely increased lipid contents in the en-face aorta (**Figures 5A,B**, $p < 0.05$) and the sections of the aorta root (**Figures 5C,D**, $p < 0.01$). Real-time PCR analysis of the mouse aorta further showed LPS eliminated the benefits of sivelestat on suppression of vascular inflammation, characterized by reduction of pro-inflammatory cytokines and chemokines (**Figures 5E,F**, $p < 0.05$).

Circulating Endotoxin Level and Intestinal NE Activity Were Potential Clinical Diagnostic Biomarkers of Atherosclerosis

To address the clinical applications, 26 volunteers were recruited for atherosclerotic analysis, including 12 patients with intestinal polyp surgery. The circulating endotoxin level and carotid intima-medial thickness (IMT) were measured in all subjects (**Supplementary Table S1**). As shown in Pearson analysis, the carotid IMT value was positively associated with the circulating level of endotoxin (**Figure 6A**) and intestinal NE activity (**Figure 6B**). Furthermore, there were structural disorders and higher expression of NE in atherosclerotic patients, as compared with healthy subjects (**Figure 6C**).

DISCUSSION

Emerging studies have demonstrated modulation of intestinal homeostasis as one of the potential approaches for protection against atherosclerosis (Jin Li et al., 2016; Zhu et al., 2018). In patients with atherosclerosis, there was excessive inflammation

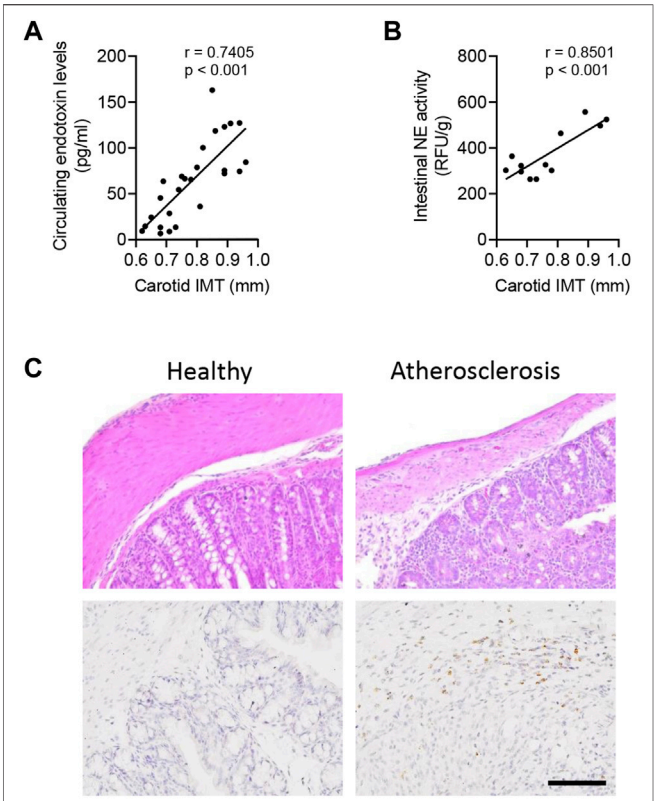

FIGURE 6 | Intestinal NE level is closely associated with the human atherosclerotic status. In total, 26 volunteers were recruited, including 12 patients with intestinal polyp surgery. **(A)** Correlation between circulating levels of endotoxin and carotid intima-medial thickness (IMT). **(B)** Measurement of intestinal NE activity in 12 patients with intestinal polyp surgery and further correlation of the intestinal NE activity and carotid IMT. **(C)** HE staining and immunohistological staining of NE in human intestines.

and disruption of intestinal permeability, characterized by disorders of tight junction (Chuanwei Li et al., 2016). By utilizing sivelestat as a research tool, the present study identified that neutrophil elastase, one of the essential inflammatory mediators, contributed to atherosclerotic plaque formation. Administration of sivelestat attenuated diet-induced aorta plaque formation and vascular inflammation, accompanied by lowering endotoxemia. Mechanistically, sivelestat improved diet- or recombinant neutrophil elastase protein-induced intestinal permeability by upregulation of zonula occludens-1 and inhibited the intestinal inflammatory response. However, replenishment of lipopolysaccharides eliminated the anti-atherosclerotic benefits of sivelestat in mice. Pearson analysis of clinical parameters further supported circulating endotoxin and intestinal NE, which were potential diagnostic biomarkers of atherosclerotic patients.

The crosstalk between gastrointestinal homeostasis and cardiovascular disease is an attractive topic in recent years. Intestinal metabolites, such as TMAO, promoted atherosclerotic plaque formation in humans and mice (Koeth et al., 2013). Moreover, TMAO activated the cardiac autonomic nervous system and deteriorated ischemia-induced ventricular arrhythmia (Meng et al., 2019). Intestinally derived lysophosphatidic acid accelerated the atherosclerotic process dependent on hyperlipidemia and excessive inflammatory response (Navab et al., 2015). In addition, the incidence of cardiovascular diseases was closely associated with the component of intestinal microbiota. Administration of beneficial microbial species, such as *Akkermansia muciniphila*, improved Western diet-induced atherosclerosis in atherosclerotic Apo $E^{-/-}$ mice (Jin Li et al., 2016). In contrast, one microbial component named *Citrobacter*, a species of toxic bacteria, was positively correlated with carotid intima-media thickness in a Bangladesh population (Wu et al., 2019).

Furthermore, intestinal homeostasis also depends on the structural maintenance of the intestinal epithelium. A higher level of circulating endotoxin, as a consequence of abnormal intestinal leakage, contributed to the development of multiple diseases. Abnormal intestinal permeability and the consequence of endotoxemia were some key characteristics in patients with fatty liver diseases (Parlesak et al., 2000). In atherosclerotic mice, it was observed that severe abruption of intestinal permeability and endotoxemia but improvement of intestinal homeostasis could attenuate atherosclerotic plaque formation and vascular inflammation (Jin Li et al., 2016; Zhu et al., 2018). Mechanistically, tight junction proteins, such as zonula occludens-1 (ZO-1) and occludin, determined the intestinal structure and permeability (Van Itallie et al., 2009; Hamada et al., 2010). The expression profile of ZO-1 was a key biomarker of atherosclerotic development, whereas upregulation of ZO-1 could improve intestinal permeability and vascular plaque formation (Zhang et al., 2020). Moreover, a variety of studies have demonstrated that the transcriptional biogenesis and activity of ZO-1 were closely associated with the intestinal inflammatory response. Chronic, excessive inflammation injured the tight junction barrier in multiple diseases (Fasano, 2011). Suppression of intestinal inflammation, such as inhibition of nuclear factor (NF)-κB signaling, was one of the therapeutic approaches to improve intestinal homeostasis and consequent disorders (Arakawa et al., 2019; Nunes et al., 2019). Consistently, the present study also found the intestinal ZO-1 expression was decreased in atherosclerotic mice but induction of ZO-1 concurred in sivelestat-treated Apo $E^{-/-}$ mice. Meanwhile, administration of sivelestat decreased the diet-induced excessive expression of intestinal inflammatory cytokines and NF-κB activity.

Neutrophils, as one of the early pro-inflammatory cells, have been shown to affect plaque formation and plaque rupture (Zernecke et al., 2008; Ionita et al., 2010). Due to their relatively short lifespan, neutrophils are rarely detected in atherosclerotic lesions (Nathan, 2006; Galli et al., 2011). Emerging studies have demonstrated that neutrophils may exacerbate cardiovascular diseases through the release of neutrophil serine proteinases, thus inducing atherosclerotic plaque formation (Warnatsch et al., 2015; Wen et al., 2018). More recently, Wen et al. (2018), reported pharmacologic inhibitors of neutrophil elastase could improve the

atherosclerotic process in Apo $E^{-/-}$ mice. Okeke et al. (2020), interestingly, found suppression of neutrophil elastase rescued mice from endotoxic shock, which indicated the close links between the neutrophil elastase activity and endotoxemia. However, there was no direct evidence providing the roles of neutrophil elastase in mediating intestine/vascular crosstalk.

Sivelestat, with the formula C20H22N2O7S, is a selective neutrophil elastase inhibitor for alleviating acute respiratory distress syndrome (Kawabata et al., 1991). In a lipopolysaccharide-induced septic mouse model, sivelestat attenuated alveolar collapse and stromal tissue thickening (Inoue et al., 2005). More recently, administration of sivelestat suppressed NET formation *in vitro* but rescued mice from lipopolysaccharide-induced endotoxic shock (Okeke et al., 2020). However, there was no report to disclose the pharmacological effects of sivelestat in atherosclerotic formation and vascular inflammation. Our present findings, for the first time, uncovered the anti-atherosclerotic effects of sivelestat in genetic Apo $E^{-/-}$ mice; then, we determined the intestine/vascular axis was a potential explanation for the therapeutic benefits of sivelestat *in vivo* and *in vitro*.

In conclusion, the present findings supported intestinal NE-regulated intestinal permeability and inflammatory response in the development of atherosclerosis, and administration of sivelestat had benefits in protection against atherosclerosis.

DATA AVAILABILITY STATEMENT

The raw data supporting the conclusion of this article will be made available by the authors, without undue reservation.

ETHICS STATEMENT

The studies involving human participants were reviewed and approved by the Human Ethics committee of Southern Medical University. The patients/participants provided their written informed consent to participate in this study. The animal study was reviewed and approved by the Animal Welfare Committee of Southern Medical University.

AUTHOR CONTRIBUTIONS

QX, CS, TR, DW, and XL performed the experiments and analyzed data. GL, LC, and XY discussed data. HN and YZ guided the experiments and discussed data. HN wrote the manuscript.

FUNDING

This work was financially supported by the National Natural Science Foundation of China (81902113 and 81702088), the Natural Science Foundation of Guangdong Province (2018A030310466 and 2018A030313740), the Seeding Program of Shenzhen Hospital of Southern Medical University (2018MM02), the Research Fund of Innovation and Technology Bureau of Baoan District (2019JD443 and 2021JD293), and the Research Foundation of Shenzhen Hospital of Southern Medical University (PY2020ZY09).

SUPPLEMENTARY MATERIAL

The Supplementary Material for this article can be found online at: https://www.frontiersin.org/articles/10.3389/fphar.2022.838688/full#supplementary-material

REFERENCES

Andreasen, A. S., Krabbe, K. S., Krogh-Madsen, R., Taudorf, S., Pedersen, B. K., and Møller, K. (2008). Human Endotoxemia as a Model of Systemic Inflammation. *Curr. Med. Chem.* 15, 1697–1705. doi:10.2174/092986708784872393

Arakawa, K., Ishigami, T., Nakai-Sugiyama, M., Chen, L., Doi, H., Kino, T., et al. (2019). Lubiprostone as a Potential Therapeutic Agent to Improve Intestinal Permeability and Prevent the Development of Atherosclerosis in Apolipoprotein E-Deficient Mice. *PloS one* 14, e0218096. doi:10.1371/journal.pone.0218096

Araújo, J. R., Tomas, J., Brenner, C., and Sansonetti, P. J. (2017). Impact of High-Fat Diet on the Intestinal Microbiota and Small Intestinal Physiology before and after the Onset of Obesity. *Biochimie* 141, 97–106. doi:10.1016/j.biochi.2017.05.019

Cani, P. D., Amar, J., Iglesias, M. A., Poggi, M., Knauf, C., Bastelica, D., et al. (2007). Metabolic Endotoxemia Initiates Obesity and Insulin Resistance. *Diabetes* 56, 1761–1772. doi:10.2337/db06-1491

Carrera-Bastos, P., Picazo, Ó., Fontes-Villalba, M., Pareja-Galeano, H., Lindeberg, S., Martínez-Selles, M., et al. (2018). Serum Zonulin and Endotoxin Levels in Exceptional Longevity versus Precocious Myocardial Infarction. *Aging Dis.* 9, 317–321. doi:10.14336/AD.2017.0630

Chen, W., Wu, Y., Lu, Q., Wang, S., and Xing, D. (2020). Endogenous ApoA-I Expression in Macrophages: A Potential Target for protection against Atherosclerosis. *Clin. Chim. Acta* 505, 55–59. doi:10.1016/j.cca.2020.02.025

Chuanwei Li, C., Gao, M., Zhang, W., Chen, C., Zhou, F., Hu, Z., et al. (2016). Zonulin Regulates Intestinal Permeability and Facilitates Enteric Bacteria Permeation in Coronary Artery Disease. *Sci. Rep.* 6, 29142. doi:10.1038/srep29142

Endo, S., Sato, N., Yaegashi, Y., Suzuki, Y., Kojika, M., Yamada, Y., et al. (2006). Sivelestat Sodium Hydrate Improves Septic Acute Lung Injury by Reducing Alveolar Dysfunction. *Res. Commun. Mol. Pathol. Pharmacol.* 119, 53–65. doi:10.1097/01.shk.0000144423.40270.96

Fasano, A. (2011). Zonulin and its Regulation of Intestinal Barrier Function: the Biological Door to Inflammation, Autoimmunity, and Cancer. *Physiol. Rev.* 91, 151–175. doi:10.1152/physrev.00003.2008

Galli, S. J., Borregaard, N., and Wynn, T. A. (2011). Phenotypic and Functional Plasticity of Cells of Innate Immunity: Macrophages, Mast Cells and Neutrophils. *Nat. Immunol.* 12, 1035–1044. doi:10.1038/ni.2109

Gaul, D. S., Stein, S., and Matter, C. M. (2017). Neutrophils in Cardiovascular Disease. *Eur. Heart J.* 38, 1702–1704. doi:10.1093/eurheartj/ehx244

Hamada, K., Shitara, Y., Sekine, S., and Horie, T. (2010). Zonula Occludens-1 Alterations and Enhanced Intestinal Permeability in Methotrexate-Treated Rats. *Cancer Chemother. Pharmacol.* 66, 1031–1038. doi:10.1007/s00280-010-1253-9

Hansson, G. K. (2005). Inflammation, Atherosclerosis, and Coronary Artery Disease. *N. Engl. J. Med.* 352, 1685–1695. doi:10.1056/NEJMra043430

Inoue, Y., Seiyama, A., Tanaka, H., Ukai, I., Akimau, P., Nishino, M., et al. (2005). Protective Effects of a Selective Neutrophil Elastase Inhibitor (Sivelestat) on Lipopolysaccharide-Induced Acute Dysfunction of the Pulmonary

Microcirculation. *Crit. Care Med.* 33, 1814–1822. doi:10.1097/01.ccm.0000172547.54086.ad

Ionita, M. G., van den Borne, P., Catanzariti, L. M., Moll, F. L., de Vries, J. P., Pasterkamp, G., et al. (2010). High Neutrophil Numbers in Human Carotid Atherosclerotic Plaques Are Associated with Characteristics of Rupture-Prone Lesions. *Arterioscler Thromb. Vasc. Biol.* 30, 1842–1848. doi:10.1161/ATVBAHA.110.209296

Jin Li, J., Lin, S., Vanhoutte, P. M., Woo, C. W., and Xu, A. (2016). Akkermansia Muciniphila Protects against Atherosclerosis by Preventing Metabolic Endotoxemia-Induced Inflammation in Apoe-/- Mice. *Circulation* 133, 2434–2446. doi:10.1161/CIRCULATIONAHA.115.019645

Kawabata, K., Suzuki, M., Sugitani, M., Imaki, K., Toda, M., and Miyamoto, T. (1991). ONO-5046, a Novel Inhibitor of Human Neutrophil Elastase. *Biochem. Biophys. Res. Commun.* 177, 814–820. doi:10.1016/0006-291x(91)91862-7

Kim, S., Goel, R., Kumar, A., Qi, Y., Lobaton, G., Hosaka, K., et al. (2018). Imbalance of Gut Microbiome and Intestinal Epithelial Barrier Dysfunction in Patients with High Blood Pressure. *Clin. Sci. (Lond)* 132, 701–718. doi:10.1042/CS20180087

Koeth, R. A., Wang, Z., Levison, B. S., Buffa, J. A., Org, E., Sheehy, B. T., et al. (2013). Intestinal Microbiota Metabolism of L-Carnitine, a Nutrient in Red Meat, Promotes Atherosclerosis. *Nat. Med.* 19, 576–585. doi:10.1038/nm.3145

Kolaczkowska, E., and Kubes, P. (2013). Neutrophil Recruitment and Function in Health and Inflammation. *Nat. Rev. Immunol.* 13, 159–175. doi:10.1038/nri3399

Li, T., Wang, C., Liu, Y., Li, B., Zhang, W., Wang, L., et al. (2020). Neutrophil Extracellular Traps Induce Intestinal Damage and Thrombotic Tendency in Inflammatory Bowel Disease. *J. Crohns Colitis* 14, 240–253. doi:10.1093/ecco-jcc/jjz132

Libby, P., Bornfeldt, K. E., and Tall, A. R. (2016). Atherosclerosis: Successes, Surprises, and Future Challenges. *Circ. Res.* 118, 531–534. doi:10.1161/CIRCRESAHA.116.308334

Maloy, K. J., and Powrie, F. (2011). Intestinal Homeostasis and its Breakdown in Inflammatory Bowel Disease. *Nature* 474, 298–306. doi:10.1038/nature10208

Meng, G., Zhou, X., Wang, M., Zhou, L., Wang, Z., Wang, M., et al. (2019). Gut Microbe-Derived Metabolite Trimethylamine N-Oxide Activates the Cardiac Autonomic Nervous System and Facilitates Ischemia-Induced Ventricular Arrhythmia via Two Different Pathways. *EBioMedicine* 44, 656–664. doi:10.1016/j.ebiom.2019.03.066

Nathan, C. (2006). Neutrophils and Immunity: Challenges and Opportunities. *Nat. Rev. Immunol.* 6, 173–182. doi:10.1038/nri1785

Navab, M., Chattopadhyay, A., Hough, G., Meriwether, D., Fogelman, S. I., Wagner, A. C., et al. (2015). Source and Role of Intestinally Derived Lysophosphatidic Acid in Dyslipidemia and Atherosclerosis. *J. Lipid Res.* 56, 871–887. doi:10.1194/jlr.M056614

Noval Rivas, M., Wakita, D., Franklin, M. K., Carvalho, T. T., Abolhesn, A., Gomez, A. C., et al. (2019). Intestinal Permeability and IgA Provoke Immune Vasculitis Linked to Cardiovascular Inflammation. *Immunity* 51, 508–e6. doi:10.1016/j.immuni.2019.05.021

Nunes, C., Freitas, V., Almeida, L., and Laranjinha, J. (2019). Red Wine Extract Preserves Tight Junctions in Intestinal Epithelial Cells under Inflammatory Conditions: Implications for Intestinal Inflammation. *Food Funct.* 10, 1364–1374. doi:10.1039/c8fo02469c

Okeke, E. B., Louttit, C., Fry, C., Najafabadi, A. H., Han, K., Nemzek, J., et al. (2020). Inhibition of Neutrophil Elastase Prevents Neutrophil Extracellular Trap Formation and Rescues Mice from Endotoxic Shock. *Biomaterials* 238, 119836. doi:10.1016/j.biomaterials.2020.119836

Pan, Y., Wang, Y., Cai, L., Cai, Y., Hu, J., Yu, C., et al. (2012). Inhibition of High Glucose-Induced Inflammatory Response and Macrophage Infiltration by a Novel Curcumin Derivative Prevents Renal Injury in Diabetic Rats. *Br. J. Pharmacol.* 166, 1169–1182. doi:10.1111/j.1476-5381.2012.01854.x

Pan, Y., Wang, Y., Zhao, Y., Peng, K., Li, W., Wang, Y., et al. (2014). Inhibition of JNK Phosphorylation by a Novel Curcumin Analog Prevents High Glucose-Induced Inflammation and Apoptosis in Cardiomyocytes and the Development of Diabetic Cardiomyopathy. *Diabetes* 63, 3497–3511. doi:10.2337/db13-1577

Parlesak, A., Schäfer, C., Schütz, T., Bode, J. C., and Bode, C. (2000). Increased Intestinal Permeability to Macromolecules and Endotoxemia in Patients with Chronic Alcohol Abuse in Different Stages of Alcohol-Induced Liver Disease. *J. Hepatol.* 32, 742–747. doi:10.1016/s0168-8278(00)80242-1

Pendyala, S., Walker, J. M., and Holt, P. R. (2012). A High-Fat Diet Is Associated with Endotoxemia that Originates from the Gut. *Gastroenterology* 142, 1100–e2. doi:10.1053/j.gastro.2012.01.034

Rohr, M. W., Narasimhulu, C. A., Rudeski-Rohr, T. A., and Parthasarathy, S. (2020). Negative Effects of a High-Fat Diet on Intestinal Permeability: A Review. *Adv. Nutr.* 11, 77–91. doi:10.1093/advances/nmz061

Sahebnasagh, A., Saghafi, F., Safdari, M., Khataminia, M., Sadremomtaz, A., Talaei, Z., et al. (2020). Neutrophil Elastase Inhibitor (Sivelestat) May Be a Promising Therapeutic Option for Management of Acute Lung Injury/acute Respiratory Distress Syndrome or Disseminated Intravascular Coagulation in COVID-19. *J. Clin. Pharm. Ther.* 45, 1515–1519. doi:10.1111/jcpt.13251

Shimoda, M., Iwasaki, Y., Okada, T., Sawada, T., and Kubota, K. (2008). Protective Effect of Sivelestat in a Porcine Hepatectomy Model Prepared Using an Intermittent Pringle Method. *Eur. J. Pharmacol.* 587, 248–252. doi:10.1016/j.ejphar.2008.02.064

Van Itallie, C. M., Fanning, A. S., Bridges, A., and Anderson, J. M. (2009). ZO-1 Stabilizes the Tight junction Solute Barrier through Coupling to the Perijunctional Cytoskeleton. *Mol. Biol. Cel* 20, 3930–3940. doi:10.1091/mbc.e09-04-0320

Wang, Z., Roberts, A. B., Buffa, J. A., Levison, B. S., Zhu, W., Org, E., et al. (2015). Non-lethal Inhibition of Gut Microbial Trimethylamine Production for the Treatment of Atherosclerosis. *Cell* 163, 1585–1595. doi:10.1016/j.cell.2015.11.055

Warnatsch, A., Ioannou, M., Wang, Q., and Papayannopoulos, V. (2015). Inflammation. Neutrophil Extracellular Traps License Macrophages for Cytokine Production in Atherosclerosis. *Science* 349, 316–320. doi:10.1126/science.aaa8064

Wen, G., An, W., Chen, J., Maguire, E. M., Chen, Q., Yang, F., et al. (2018). Genetic and Pharmacologic Inhibition of the Neutrophil Elastase Inhibits Experimental Atherosclerosis. *J. Am. Heart Assoc.* 7, e008187. doi:10.1161/JAHA.117.008187

Wu, F., Yang, L., Islam, M. T., Jasmine, F., Kibriya, M. G., Nahar, J., et al. (2019). The Role of Gut Microbiome and its Interaction with Arsenic Exposure in Carotid Intima-media Thickness in a Bangladesh Population. *Environ. Int.* 123, 104–113. doi:10.1016/j.envint.2018.11.049

Zernecke, A., Bot, I., Djalali-Talab, Y., Shagdarsuren, E., Bidzhekov, K., Meiler, S., et al. (2008). Protective Role of CXC Receptor 4/CXC Ligand 12 Unveils the Importance of Neutrophils in Atherosclerosis. *Circ. Res.* 102, 209–217. doi:10.1161/CIRCRESAHA.107.160697

Zhang, L., Wang, F., Wang, J., Wang, Y., and Fang, Y. (2020). Intestinal Fatty Acid-Binding Protein Mediates Atherosclerotic Progress through Increasing Intestinal Inflammation and Permeability. *J. Cel Mol Med* 24, 5205–5212. doi:10.1111/jcmm.15173

Zhu, L., Zhang, D., Zhu, H., Zhu, J., Weng, S., Dong, L., et al. (2018). Berberine Treatment Increases Akkermansia in the Gut and Improves High-Fat Diet-Induced Atherosclerosis in Apoe-/- Mice. *Atherosclerosis* 268, 117–126. doi:10.1016/j.atherosclerosis.2017.11.023

Conflict of Interest: The authors declare that the research was conducted in the absence of any commercial or financial relationships that could be construed as a potential conflict of interest.

Publisher's Note: All claims expressed in this article are solely those of the authors and do not necessarily represent those of their affiliated organizations, or those of the publisher, the editors, and the reviewers. Any product that may be evaluated in this article, or claim that may be made by its manufacturer, is not guaranteed or endorsed by the publisher.

frontiers | Frontiers in Immunology

REVIEW
published: 11 May 2022
doi: 10.3389/fimmu.2022.901166

The Regulatory Role of MicroRNAs on Phagocytes: A Potential Therapeutic Target for Chronic Diseases

Yongbo Wang[1,2], Xingyu Liu[1,2], Panpan Xia[1], Zhangwang Li[2], Xinxi FuChen[1], Yunfeng Shen[1], Peng Yu[1] and Jing Zhang[3]**

[1] Department of Metabolism and Endocrinology, The Second Affiliated Hospital of Nanchang University, Jiangxi, China, [2] The Second Clinical Medical College of Nanchang University, The Second Affiliated Hospital of Nanchang University, Jiangxi, China, [3] Department of Anesthesiology, The Second Affiliated Hospital of Nanchang University, Jiangxi, China

An effective acute inflammatory response results in the elimination of infectious microorganisms, followed by a smooth transition to resolution and repair. During the inflammatory response, neutrophils play a crucial role in antimicrobial defense as the first cells to reach the site of infection damage. However, if the neutrophils that have performed the bactericidal effect are not removed in time, the inflammatory response will not be able to subside. Anti-inflammatory macrophages are the main scavengers of neutrophils and can promote inflammation towards resolution. MicroRNAs (miRNAs) have great potential as clinical targeted therapy and have attracted much attention in recent years. This paper summarizes the involvement of miRNAs in the process of chronic diseases such as atherosclerosis, rheumatoid arthritis and systemic lupus erythematosus by regulating lipid metabolism, cytokine secretion, inflammatory factor synthesis and tissue repair in two types of cells. This will provide a certain reference for miRNA-targeted treatment of chronic diseases.

Keywords: chronic disease, miRNA, immunity, neutrophils, macrophages

OPEN ACCESS

Edited by:
Galina Sud'ina,
Lomonosov Moscow State University, Russia

Reviewed by:
Jun Yin,
Shanghai Jiao Tong University, China
Sujata Mohanty,
All India Institute of Medical Sciences, India

***Correspondence:**
Peng Yu
yu8220182@163.com
Jing Zhang
zhangjing666doc@163.com

Specialty section:
This article was submitted to Inflammation, a section of the journal Frontiers in Immunology

Received: *21 March 2022*
Accepted: *19 April 2022*
Published: *11 May 2022*

Citation:
Wang Y, Liu X, Xia P, Li Z, FuChen X, Shen Y, Yu P and Zhang J (2022) The Regulatory Role of MicroRNAs on Phagocytes: A Potential Therapeutic Target for Chronic Diseases. Front. Immunol. 13:901166. doi: 10.3389/fimmu.2022.901166

1 INTRODUCTION

Inflammation is a cascade reaction of human tissues and organs response to harmful stimuli such as pathogens (1). On the cellular level, inflammation that is manifested as mutual damage between damage factors and histiocytes, as well as the regeneration of parenchymal cells and interstitial cells are often followed by tissue dysfunction due to changes in protein activity, changes in cellular metabolites, and connective tissue reorganization (2). The solution of inflammation mainly includes two aspects: one is anti-inflammatory, that is to prevent the re-recruitment of inflammatory cells; the other is decomposition, that is to remove apoptotic inflammatory cells (mainly neutrophils) (3). However, unresolved inflammatory cascades that bring new features to tissues and cells may promote he establishment of chronic inflammation leading to tissue and organ dysfunction (4). Thus, chronic inflammation can contribute to many potential chronic diseases, including diabetes (5), cardiovascular disease (CVD) (6), rheumatoid arthritis (RA) (7), inflammatory bowel disease (IBD) (8), neurodegenerative diseases (9) and systemic lupus erythematosus (SLE) (10).

Both neutrophils and macrophages belong to phagocytic cells, but they play different important roles in inflammatory response. Neutrophils are "whistlers" of the inflammatory response, which means they are the first immune cells to be recruited to the site of infection or injury. The phagocytosis of neutrophils can destroy pathogens and some damage factors. However, if it is not cleared in time, the derived death induction pathways such as oxidation and hydrolysis can form an inflammation amplification loop, causing serious tissue damage and developing the inflammatory response into a chronic disease (11). Inflammatory cells such as neutrophils are often eliminated by macrophages. Macrophages can not only phagocytose pathogens and damage factors, but also phagocytose apoptotic cells and participate in lipid metabolism. For example, the efferocytosis of macrophages enables the apoptotic cells to be eliminated before necrosis, releasing anti-inflammatory cytokines and specialized proresolving mediators (SPMs) at the same time, and establishing immune tolerance (12). Therefore, macrophages are the "finalizers" of the inflammatory response and play a key role in the resolution and regression of inflammation. Macrophages play distinct roles in the different stages of inflammatory response. The dysfunction of macrophages in the late stage of the inflammatory response is likely to prevent the inflammation from resolving.

Studies on the relationship between non-coding RNAs (ncRNA) and the control of chronic inflammatory diseases in some species have shown that ncRNA has become a key regulatory factor for the development and function of the immune system (13–15). miRNAs belong to a major subfamily of ncRNA and are endogenous non-coding ribonucleic acid with a length of about 20 nucleotides (16). miRNAs mediate specific gene silencing through complementarity to mRNA sequences (17, 18). A miRNA can be targeted to multiple mRNAs, while an mRNA can also be targeted by many different or related miRNAs. miRNAs often control multiple targets within a signal axis to amplify and regulate the utility. In addition to directly targeting mRNAs, miRNAs can further coordinate inflammation by targeting enzymes or transcription factors exerting indirect effects (16, 18–21). These basic properties of miRNA make it very suitable for regulating chronic inflammatory (2). miRNAs regulate inflammatory cascades by regulating target gene levels, which determine whether phagocytosis occurs, how strong the response is, and the threshold at which inflammation subside (16). For example, under the stimulation of inflammatory mediators and mildly oxidized low-density lipoprotein, the expression of miR-155 is up-regulated. MiR-155 directly targets B-cell lymphoma 6 protein (Bcl6), enhances the expression of inflammatory mediators (such as CCL2) in macrophages, and damages the efferent cytosis of macrophages, leading to the accumulation of inflammatory cells at the infected site of injury and secondary necrosis of apoptotic cells, which eventually develops into atherosclerosis (22).

The existing literature on miRNA is extensive and focuses particularly on the regulation of various signaling pathways by miRNA. In recent years, there has been growing recognition of the vital links between miRNAs and immune cells. miRNAs are active in inflammatory responses. For example, miRNAs regulate the levels and types of chemokines by targeting chemokine (C-X-C motif) ligand (CXCL) (23), cholesterol metabolism by targeting ATP binding cassette transporter A1 (ABCA1) and ATP binding cassette transporter G1 (ABCG1) (24), the release of inflammatory factors by targeting the nuclear factor kappa-B (NF-κB) signaling pathway (25), and tissue repair by targeting suppressor of cytokine signaling-1 (SOCS1) (26).

Although there are many reports in the literature on regulation of specific miRNA on phagocytes (neutrophils and macrophages), most are restricted to functional elucidations without reference to specific chronic diseases. There has been very little systematic summery of the regulations of miRNA on phagocytes in specific diseases. We fills a gap in the research on this aspect. The primary aim of this paper is to review recent research into the regulation mechanism of miRNA on phagocytes in different chronic diseases, explore the relationship between miRNAs and phagocytes in different chronic diseases, and provide empirical evidence for the claim that miRNA can become a potential therapeutic target for chronic diseases eventually.

2 MECHANISM OF INFLAMMATORY RESPONSE AND CHRONIC INFLAMMATION

2.1 Function and Mechanism of Inflammatory Response

Under normal conditions, the homeostatic control mechanism maintains the acceptable range of the environmental parameters near the predetermined equilibrium point (27). Abnormal conditions may cause certain parameters to deviate from their normal homeostasis range, resulting in stress response (28). Acute and chronic inflammation are two distinct adaptive stresses triggered by inadequate or ineffective other homeostatic mechanisms. When body tissue is damaged, the inflammatory process is a protective cascade of local blood vessels characterized by redness, swelling, pain, heat and dysfunction, which can aid in the removal of foreign bodies and tissue repair (29, 30). The inflammatory cascade is preprogrammed and pervasive, and can be triggered by almost every tissue, playing an important physiological role in tissue homeostasis (31).

When the body faces threats such as infection and injury, it induces its own acute inflammatory response, which usually lasts for minutes to days (32). The inflammatory response is controlled by a complex regulatory networds consisting of inducers, sensors, mediators, and effectors, and the inflammatory response can be determined according to the components of the regulatory networks (33). The recognition of pattern recognition receptors (PRR) initiates an immune response that identifies structural components of pathogens as pathogen-associated molecular patterns (PAMPs) and chemicals produced by injured cells as damage-associated molecular patterns (DAMPs) (34–36). Different receptors in immune cells recognize these patterns, and upon triggering these receptors, inflammatory cytokines

such as TNF-α and IL-6 are released, causing changes in endothelial cells and allowing immune cells to flow through endothelial cells to tissues (29, 37). DAMPs are a class of substances released by cells into the surrounding interstitial fluid when cells are stimulated by injury, hypoxia and stress, including degraded matrix molecules, leukocyte degranulation molecules, and heat shock proteins (HSP). They are considered harmful signals that trigger inflammatory responses through pattern recognition receptors such as Toll-like receptors or NOD (nucleotide binding oligomer domain protein)-like receptors (34–36, 38). For example, TLR4 can identify endogenous substrates such as free fatty acids (FFA) (38). PAMPs are ligand receptors that are recognized and bound by PRRs, including some highly conserved molecular structures shared on the surface of pathogenic microorganisms, such as the lipopolysaccharide of PAMPs are ligand receptors that are recognized and bound by PRRs, including some highly conserved molecular structures shared on the surface of pathogenic microorganisms, such as the lipopolysaccharide of G^- (gram-negative) bacterium. They also include some common molecular structures on the surface of host apoptotic cells, such as phosphatidyl serine (33). NADPH oxidase utilizes the respiratory burst in hexose phosphate to convert oxygen molecules into superoxide anions. Superoxide anion generates hydrogen peroxide under the action of superoxide dismutase (SOD), which can be bactericidal, and can further generate oxides with strong bactericidal power under the action of myeloperoxide (MPO), such as OCl^-. However, reactive oxygen species (ROS) generated during oxidative sterilization of neutrophils may leak into surrounding tissues. Strong bactericidal oxidants may also cause damage to neutral proteases that inhibit lysosome release, thereby harming surrounding tissues (39).

Infection and tissue damage are well-known inflammatory triggers that attract leukocytes and plasma proteins to tissue damage (4). Furthermore, tissue stress or dysfunction induces an adaptive response called para-inflammation, which occurs between essential homeostasis and canonical inflammatory responses and is mediated primarily by tissue-resident macrophages (4, 40). Regardless of the cause of the inflammatory response, the ultimate goal is to eliminate or isolate the source of the interference, allowing the host to adapt to the abnormal condition and restore tissue function and homeostasis. However, part of the inflammation can develop into chronic disease due to persistent tissue dysfunction due to environmental variables, genetic mutations and even modern unhealthy human diseases (31, 41).

2.2 The Role of Neutrophils and Macrophages in the Inflammatory Response

At the most basic level, acute inflammatory responses induced by infection or tissue damage result in the coordinated distribution of blood components (plasma and leukocytes) to the site of disease or injury. This process can be roughly divided into: First, blood vessel flow and tiny blood vessels become larger, and newly formed capillaries and larger arterioles help increase blood flow to areas of inflammation (4). Then, vasodilation and vascular permeability increase, leading to leakage of microcirculatory plasma and phagocytosis of leukocytes. Endothelial cell selectins on the surface of vascular endothelial cells can inducibly connect with leukocyte integrins and chemokine receptors. This connection allows endothelial cell modification, increased microvascular permeability, and preferential access of plasma proteins and white blood cells (mainly neutrophils) to infected or injured tissues through the posterior capillary vein (32). Neutrophils are activated by direct stimulation of cytokines released by pathogens or tissue resident cells, and activated neutrophils capture bacteria *via* phagosomes and then begin almost simultaneously degranulation-dependent non-oxygen bactericidal action and triphosphopyridine nucleotide (NADPH) oxidation enzyme (NOX2)-dependent aerobic bactericidal action (42). Under the degranulation-dependent non-oxygen sterilization, various bactericides and hydrolytic enzymes in the granules are released, including lysozyme, bactericidal/permeability increasing protein polypeptide (BPI) protein, defensin, elastase, cathepsin G, protease 3, azurocidin (CAP37) and acid β-glycerophosphatase (43). However, if these bactericides and hydrolases in granules are exocytosed into tissues outside neutrophils, they will damage normal tissues and further aggravate inflammation (44). In oxygen-dependent sterilization, activated neutrophils are highly phosphorylated by the serine residues in $p47^{phox}$, which bind to the $p67^{phox}$ $p40^{phox}$ complex, and then migrate to the plasma membrane to bind to cytochrome b_{558}. At this point, an NADPH oxidase is assembled (45).

After neutrophils play a bactericidal role at the site of inflammation, they often produce pus. The main forms include necrosis, pyroptosis, and neutrophils external traps (NET) (**Figure 1**) (46). Necrosis is often triggered by intracellular parasites, manifested by the activation of intracellular TLRs, interferon (IFN)-α and granulocyte-macrophage colony-stimulating factor receptors (47). Pyroptosis is activated by the cleavage of Gasdermin D (GSDMD) by the intracellular pathogen inflammasome. Under the action of necrosis and pyroptosis, neutrophils release inflammatory factors, such as interleukin-1β (IL-1β), and the area of tissue damage increases and the degree of damage is more serious (48). The neutrophil extracellular trap is a suicide system that captures and kills microorganisms. The neutrophil extracellular trap is an externalized form of the nucleus and mitochondria, consisting of DNA, histones, and granule proteins. ROS surge activates the proteins arginine deiminase 4 (PAD_4), neutrophil elastase (NE) and Gasdermin D under the action of the respiratory burst of neutrophils (49). These proteases catalyze the processes of chromatin decondensation, nuclear membrane disassembly, assembly of antimicrobial proteins on chromatin, and cell rupture. Likewise, the cellular contents released by NET will further exacerbate the damage to surrounding tissue. Unlike the first two, NET can also cause autoimmune diseases by exposing cellular endogenous components to immune cells (50).

Conversely, in response to inflammation, neutrophils also die by a non-inflammatory pathway, that is macrophage-mediated

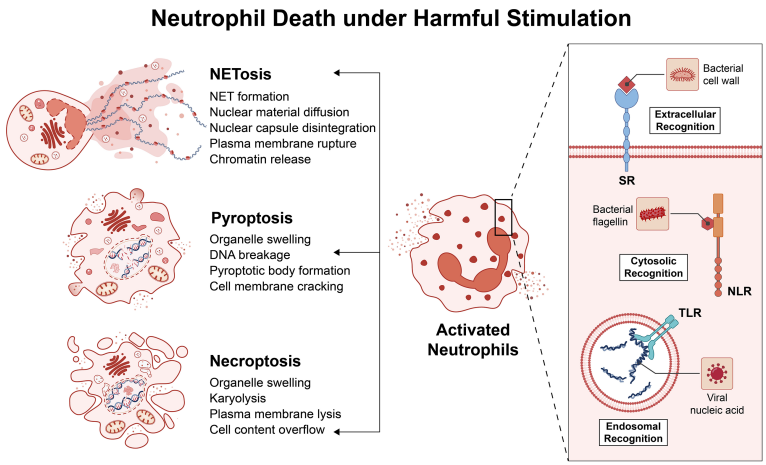

FIGURE 1 | Neutrophil Death under Harmful Stimulation. Neutrophils recognize pathogens through pattern recognition receptors (PRRs). The main PRRs are Toll-like receptors (TLR) or NOD-like receptors (NLR), and there are some other PRRs, such as scavenger receptors (SR). These PRRs can recognize pathogens in the extracellular cytoplasm and endosomes. Neutrophils are activated after recognizing the pathogen and begin to kill the pathogen. The final outcome of an inflammatory environment is often: necrosis, pyroptosis, and neutrophils external traps. These death pathways have different characteristics, but all exacerbate the inflammatory response.

efferocytosis. Macrophage uptake of dying neutrophils can rapidly clear cells to prevent secondary necrosis, and can also trigger anti-inflammatory signaling pathways that play an important role in inflammation resolution. If efferent pleocytosis malfunctions, amplifying loops that promote secondary necrosis and exacerbate inflammation (51). It is not difficult to see that macrophages play an important role in the resolution of inflammation. Anti-inflammatory macrophages can secrete various anti-inflammatory mediators (such as IL-10) and express programmed cell death ligand (PD-L), thereby suppressing inflammation (52). However, if pro-inflammatory macrophages cannot complete the transformation to anti-inflammatory macrophages during the initial period of inflammation, a large number of pro-inflammatory macrophages will accumulate, the inflammatory response will continue, and tissue repair will be delayed (53).

3 THE CONNECTION BETWEEN CHRONIC INFLAMMATION AND CHRONIC DISEASE

Chronic inflammation is associated with persistent production of pro-inflammatory mediators and persistent activation of pro-inflammatory signaling pathways, and phagocytic-associated inflammasomes, cell differentiation, lipid metabolism, tissue repair, and microbiota contribute to aging-related phenotypes and chronic disease (54).

3.1 Inflammation Resolution and Chronic Diseases

Acute inflammation is characterized by a complex but well-coordinated inflammatory response with a resolution period of acute inflammation. Numerous pro-inflammatory cytokines rapidly released by neutrophils characterize the inflammatory environment (TNF and IL-1), and omega-6 pro-inflammatory arachidonic acid (AA)-derived eicosenoic acid (prostaglandins and leukotrienes) (55). These potent pro-inflammatory factors are difficult to identify microbes and their host cells, and thus are prone to irreversible damage to surrounding tissues (4, 56). In an effective acute inflammatory response, damaging factors are rapidly eliminated, while endothelial and immune cells undergo a "lipid mediator switch" that converts pro-inflammatory SPMs into anti-inflammatory prostaglandins, which trigger inflammation subsided, effectively preventing persistent inflammation and tissue necrosis (57). Regression is the process by which inflammation ceases and has historically been seen as a passive process (58). Numerous studies published over the past few years have shown that regression is an active process, manifested by a complex set of mediators that regulate cellular events necessary for inflammatory cell clearance from the site of infection or injury and restoration of tissue function (3, 40). Inflammation can be resolved by removal of inflammatory stimuli, inhibition of proinflammatory signaling, catabolism of proinflammatory mediators, and cellular burial (3). Inflammation may resolve if granulocytes are eliminated during the inflammatory response and the monocyte population (macrophages and lymphocytes) within the tissue returns to pre-inflammatory numbers and phenotypes (59). However, if the inflammatory response persists, a normally healthy immune response can degrade into a dangerous chronic inflammatory disease that can be fatal.

While immune responses are required for successful pathogen clearance, symbiotic contact with commensal microorganisms, wound repair, and overall tissue homeostasis, they can become dysfunctional and initiate persistent responses

without resolution phases (4). Persistent stimulation, pro-inflammatory signaling, or damage to pro-catabolic/anti-inflammatory pathways can lead to irreversible inflammatory responses, in which inflammatory cells such as neutrophils and monocytes/macrophages infiltrate the tissue, leaving the tissue chronically inflammatory (31). When these events occur, a normal healthy immune response can deteriorate into a chronic inflammatory state, a hallmark of chronic disease (41). Chronic inflammation has a post-resolution phase involving Ly6Chi inflammatory monocytes (iMOs) and dendritic cells that enhance the adaptive branch of the response, while macrophages in tissues preferentially deplete apoptotic Polymorphonuclear neutrophils (PMNs), thereby connecting innate and adaptive immune system (60–62). The organism tries to establish 'adaptive homeostasis' in this new phase, but this may be beneficial in shaping the developmental environment of chronic disease (3). Indeed, adaptive changes are often induced at the expense of many other physiological activities, leading to the formation of non-adaptive traits. In evolution, a balance is established between the beneficial effects of adaptive traits and the undesired effects of non-adaptive traits (4). However, long-term changes in environmental conditions can upset this balance, increase the burden on the body, and lead to the development of chronic diseases. For example, prolonged secondary infection induces autoimmune activation at a lower cost than endogenous antigens, such as those released by apoptotic cells (63). We can conclude that many chronic inflammatory diseases are characterized by persistent acute inflammation combined with failed attempts at adaptive immunity, resulting in immune maladaptation.

3.2 Possible Factors Leading to Chronic Diseases

Even though the etiology of some chronic inflammatory diseases is unknown, early detection and treatment are essential to stop their progression. According to Karen T. Feehan et al, the factors that lead to chronic diseases can be roughly divided into (3):

a. Aging: Over the years, extensive research has demonstrated an age-related increase in cellular inflammation. Senescent cells secrete large amounts of soluble factors, collectively referred to as the senescence-associated secretory phenotype (SASP), which include large amounts of pro-inflammatory cytokines and chemokines, growth factors, and extracellular matrix (ECM) remodeling enzymes, all of which contribute to A phenomenon known as "aging inflammation" (64). Multiple molecular pathways contribute to the acquisition of cellular senescence-associated secretory phenotypes, including persistent DNA damage response (DDR) (65), unfolded protein response (UPR) (66) and missense nucleic acids (67, 68). By activating NF-κB, these specific intracellular receptors can be detected (69). Sustained activation of NF-κB leads to transcription of numerous genes involved in the control of inflammatory responses, including adhesion molecules such as vascular cell adhesion molecule-1 (VCAM-1) and cytokines such as interleukin (IL-6) and tumor necrosis factor (TNF) (70). Notably, SASP can metastasize senescence by detonating in neighboring cells, a so-called bystander effect, thus creating a pro-inflammatory environment during systemic horizontal spread (71, 72). In addition to the aging-associated secretory phenotype that contributes to senescent inflammation, the thymus produces fewer T cells as we age, reducing our ability to respond to neoantigens and memory for new infections or immunities (73). Increased autoantibodies against self-tissue, memory phenotype T cells release greater amounts of pro-inflammatory cytokines in response to persistent/chronic viral infection (74).
b. Self-antigens lead to autoimmune diseases: Chronic inflammation may be induced to a large extent by immune responses to self-tissues. Immune complexes are produced *in situ* or in various organs, including nuclear residues derived from apoptotic cells. The formation of autoantibodies (AAbs) against double-stranded DNA (dsDNA) and other nuclear autoantigens is an important feature of systemic lupus erythematosus, which is easily associated with NETs mentioned above. Strikingly, nearly 100 SLE-associated autoantibodies, including nuclear DNA and nuclear proteins, were detected in NETs (75). Nucleic acid-carrying ICs (immune complexes) may also be phagocytosed by macrophages, releasing pro-inflammatory cytokines. NET components, such as elastase, cathepsin G, and citrullinated histone H3, were also detected in the serum and synovial fluid of RA patients, and these components all have certain damage to the cartilage matrix (76).
c. Damage-Associated Molecular Patterns: DAMPs trigger chronic immune responses that alter tissue function, produced and detected by TLRs or NLRs on innate immune cells (77). Obesity is mainly caused by fat cell hypertrophy and excessive calorie intake, and the accumulation of lipids in the bloodstream is the root cause of cardiovascular disease (78). In the pathogenesis of atherosclerosis, early-stage macrophages take up oxidized low-density lipoprotein and other lipids through their TLR ligands, activate NF-κB signaling and trigger the release of inflammatory factors (79). However, the continuous influx of lipoproteins overwhelms the lipid-handling capacity of macrophages and renders macrophage-based lipid clearance systems ineffective (51). Due to the accumulation of lipids in the endoplasmic reticulum membrane, the macrophages are persistently in an inflammatory state, the macrophages are dysfunctional in the efferocytosis of neutrophils, the inflammatory response never enters a regressive state, and chronic inflammation form.
d. Microbiota and its secretions: The microbiota in the gut has a significant impact on human health. Chronic inflammation can also be caused by the microbiota due to their ability to affect the gut and surrounding tissues (80). Studies have shown that the diversity of gut microbiota in health and disease and its impact on the environment can vary from protective to pro-inflammatory in animal models of

inflammatory bowel disease. Although gut bacteria are known to activate the immune system, persistent inflammation can alter gut microbiota and lead to ecological imbalances (8). During intestinal inflammation, monocyte recruitment was increased, but IL-10 levels were consistently low. In this case, monocytes are insensitive to inflammatory stimuli and acquire the M1 phenotype, secreting a large amount of inflammatory substances such as IL-1β, TNF-α, ROS (59). Furthermore, in IBD, defects in neutrophil migration at sites of inflammation, neutrophil-related oxidative stress, inflammatory factors, disruption of tissue integrity, increased epithelial and vascular permeability, enhanced immune cell recruitment and Inflammation polarizes and hinders wound healing (81). However, due to the complex assemblage of different species, the study of disease phenotypes by specific microbial members is still ongoing.

4 mIRNAS REGULATE PHAGOCYTES IN THE PATHOGENESIS OF CHRONIC DISEASES

Chronic inflammation is involved in the production of chronic relapsing diseases characterized by excessive activation of the immune response and high levels of autoantibodies, which are autoimmune diseases. Interaction of gene expression and environment plays an important role in the pathogenesis of chronic relapsing disease (82–84). miRNAs are rheostats of gene transcription and are widely involved in innate immune regulation such as phagocytosis, exocytosis, induction of endotoxin tolerance, and cytokine responses (85). Exosomes are extracellular vesicles (MVs) that transport miRNAs between immune cells *via* membrane budding and endocytosis. Notably, some miRNAs are activated during inflammatory responses and can limit excessive immune responses. The imbalance of these miRNAs can lead to uncontrolled production of inflammatory cytokines, which can lead to the occurrence of various diseases. It is not difficult to see that miRNAs are key regulators of innate immune cell development and function and maintenance of immune homeostasis (86). Phagocytes, including neutrophils and macrophages, are the whistleblowers and finishers of the inflammatory response, respectively, and are important in the resolution of inflammation and the development of chronic diseases. In the following sections, we will use these two types of cells as examples to illustrate the regulatory role of miRNAs on them and how they affect chronic diseases.

4.1 Neutrophils

Neutrophils are the most abundant innate immune cells in the blood, and during the development of an immune response, neutrophils first reach the site of inflammation/functional damage (87). Myeloblasts in the bone marrow develop into granulosa cells through several morphologically distinct stages, including promyelocytes, myeloid cells, mesenchymal cells, and ribbon cells (88). Granulocyte generation is characterized by differential expression of transcription factors and cyclins, a process controlled by granulocyte-colony stimulating factor (G-CSF) (89). During inflammation, the number of neutrophils at the site of infection damage increases. Normally, neutrophils should be cleared by efferocytosis of macrophages after their mission is complete. This process leads to the down-regulation of the synthesis of inflammatory factors such as IL-23 in cells, thereby reducing the release of G-CSF, and the inflammatory response tends to subside (90, 91).

4.1.1 miRNA and the Function of Neutrophils

Typically, neutrophils are seen as short-lived cells that perform very repetitive roles, such as releasing antimicrobial chemicals, until more specialized cells reach the site of inflammation, enabling a more effective attack. As a result of the activation of multiple cytokines, growth factors, and bacterial products, neutrophils are more complex than initially thought, exhibiting phenotypic and functional diversity and participating in the pathogenesis of health and disease (43, 92). Evidence suggests that neutrophils help activate other immune cells, regulate inflammation and wound healing, which are critical for tissue integrity and the control and resolution of inflammatory processes (92, 93). When exposed to specific stimuli (serum amyloid A17), specific mature neutrophils (which eventually grow into fully formed granules and segmental nuclei) may proliferate outside the bone marrow, prolonging their time in the tissue. Although longer lifespans may allow neutrophils to perform more complex activities in tissues, such as helping resolve inflammation or building adaptive immune responses, their persistence in tissues can damage other cells (94).

Neutrophils are a specialized form of phagocytic cells. When bacteria come into contact with these cells, they eat and destroy the bacteria. Neutrophils engulfing bacteria produce reactive oxygen species (ROS) through an electron transfer system called NADPH, such as O^{2-}, HO^{-} and H_2O_2 being converted to hypochlorous acid (HOCl) by myeloperoxidase (MPO), which in turn kills bacteria (43, 95). In addition, the bactericidal effect of neutrophils is also reflected in the transport of a variety of different cellular particles with different components and functions (96). Neutrophil granules contain MPO, neutrophil proteases (elastase, cathepsin G, protease 3, azurin) and membrane permeability factors (lysozyme, defensins, bacterial permeability increasing proteins) and are the major germicidal granules (97, 98). This means that neutrophil activation and migration need to be tightly controlled to prevent tissue damage and uncontrolled inflammation.

When discussing inflammatory processes, neutrophils are often viewed as passive components that die and are eliminated over days or weeks, rather than as active participants. They are now known to produce pro-resolution lipid mediators, suggesting that they are actively involved in the resolution-inducing process. GPCRs (G-protein-coupled receptors) and their analogous G-protein-coupled compounds (GPCRs) play important roles in the transport and activation of neutrophils in the *in vivo* environment (99). LXA4 is a

lipopolysaccharide (also known as FPR2) that inhibits neutrophil recruitment by binding to its G protein-coupled receptor LXA4R at the end of an acute inflammatory response. By blocking and removing chemokines and cytokines, neutrophils also contribute to the resolution of inflammation (100). Lipolytic mediators such as LXA4, resolvin E1, and protectin D1 promote C-C chemokine receptor type 5 (CCR5) production through apoptotic neutrophils, which then act as functional decoys and scavengers of chemokine (C-C motif) ligand 3 (CCL3) and CCR5 (101).

As a rule, neutrophils are regarded as short-lived cells that perform a very recurring role, such as releasing antibacterial chemicals, until more specialized cells arrive at the inflammatory site, allowing for more effective attacks. Half-lives in mice and humans are 1.5 and 8 hours, respectively (102, 103).To ensure that neutrophils are present at the site of inflammation, they are activated, and their life span is enhanced severalfold during the inflammatory process (104). Neutrophils are more complex than first thought. They exhibit phenotypic and functional diversity and are involved in the pathogenesis of both health and disease (43, 92), as a result of activation by a variety of cytokines, growth factors, and bacterial products (105). There is evidence that neutrophils contribute to the activation of other immune cells, regulation of inflammation, and wound healing, which is crucial for tissue integrity and ordinance and resolution of the inflammation process (92, 93). Upon exposure to specific stimuli, such as serum amyloid A17, particular mature neutrophils (which eventually grow into fully-formed granules and segmented nuclei) may multiply outside the bone marrow, lengthening their time in the tissue. Even though a more extended lifespan may allow neutrophils to perform more complex activities in the tissue, such as helping to resolve inflammation or establishing an adaptive immune response, their continuing presence in the tissue may harm other cells (94).

Finally, the treatment of apoptotic neutrophils is a critical step in addressing inflammation, which is carefully regulated by the expression of an "eat me" signal that initiates an anti-inflammatory program in phagocytes (106, 107). Indeed, the recognition and uptake of apoptotic neutrophils can influence the phenotype of macrophages (106), and macrophages themselves also polarize towards an anti-inflammatory type when they perform efferocytosis on apoptotic neutrophils, release anti-inflammatory factors and promote tissue repair (108, 109). Thus, neutrophils are part of the cellular cascade that coordinates the resolution of inflammation. They are important for shutting down the inflammatory response early and preventing the development of chronic inflammation.

One of the most effective ways neutrophils fight infection and tissue damage is through their immune system. Neutrophils are a specialist form of phagocyte. These cells can eat and destroy bacteria when they come into touch with them. An electron transfer system known as NADPH is a multi-protein electron transfer system that can be assembled and activated to generate reactive oxygen species (ROS) such as O^{2-}, HO^{-}, and H_2O_2 (43, 95). Myeloperoxidase(MPO) converts H_2O_2 to hypochlorous acid (HOCl). Neutrophils transport a variety of different cell particles with distinct components and functions (96). The neutrophil granules contain MPO, neutral protease (elastase, cathepsin G, protease 3, and azurin), and membrane permeability factors (lysozyme, defensin, and bacterial permeability-increasing protein), which are the main bactericidal granules (97, 98). This means that neutrophil activation and migration need to be strictly controlled in order to prevent tissue damage and inflammation from becoming out of control. GPCRs (G protein-coupled receptors) and their analogous G protein-coupled compounds (GPCCs) play an essential role in the trafficking and activation of neutrophils *in vivo* environments (99).

miRNAs play key roles in cellular processes such as granulocyte proliferation, activation, and apoptosis. Mef2c is an important regulator of granulocyte development. Johnnidis et al. found that miR-223-deficient mice had neutrophil hyperactivity and hyperinflammatory function caused by direct targeting of transcription factor MEF2C, suggesting that miR-223 is a negative regulator of granulocyte production and inflammatory response (110). These findings suggest that miR-223 acts as a regulator of granulocyte activation, effectively suppressing pathogenic immune responses (111). The overexpression of miR-21 is closely related to the activation of granulocytes (112). Elevation of miR-199 reduces neutrophil chemotaxis and migration by inhibiting the cyclin-dependent kinase 2 (Cdk2) pathway, ultimately reducing the inflammatory response (113). MiR-9 is a component of the feedback loop of granulocyte-induced inflammation, and miR-9 inhibits the synthesis of NF-κB by regulating the TLR4 pathway, thereby activating neutrophils (114). The role of miR-155 in granulocytes has been revealed *in vitro* and *in vivo*. MiR-155 is essential for granulocyte proliferation by regulating SH2-containing inositol 5'-phosphatase 1 (SHP1). An animal model study showed that elevated miR-155 produces myeloproliferative disorders, suggesting that miR-155 is critical for maintaining the balance of innate immune cells (96, 115).

4.1.2 miRNA and NETs

Under inflammatory conditions, neutrophils release a network of complexes consisting of chromatin DNA, histones, and granule proteins into the extracellular environment, leading to extracellular death, a structure known as a neutrophil extracellular trap (116). Granular proteins that have been identified in NET include antimicrobial proteins (such as lactoferrin, cathepsin G, defensins, LL37, and bacterial permeability-increasing proteins), proteases (such as neutrophil elastase, protease 3 (PR3), and gelatin enzymes) or enzymes responsible for the production of reactive oxygen species such as myeloperoxidase (MPO) (116). Recent evidence suggests that NETs and their components may be detrimental to host tissues and have contributed to the development of many non-infectious diseases (117), such as atherosclerosis (118), systemic lupus erythematosus (119), vasculitis (120), and thrombosis (121, 122). Antineutrophil cytoplasmic antibody (ANCA)-associated vasculitis (AAV) is a systemic necrotizing vasculitis of small vessels characterized by the production of antineutrophil

cytoplasmic antibodies against neutrophil cytoplasmic proteins (ANCA) (123, 124), targeting some NET components such as MPO, PR3 and neutrophil elastase (125). Methods such as DNase and NET-DNA targeting using NET-associated proteins have demonstrated that inhibiting the production of NETs can prevent tissue damage (126).

Recent studies have shown that NET and miRNA are very closely related. Linhares-Laseda et al. are the first to demonstrate the presence of NET-associated miRNA vectors and miRNAs in NET-enriched supernatants (NET-miRs). This provides a new class of molecules and a new protein platform that can be created and delivered in NETs. Their research revealed a novel role for NET in cellular communication, facilitating the transport of miRNAs from neutrophils to neighboring cells. NET, as a negative feedback loop, reduces hyperreactivity and maintains normal regulation of inflammatory responses (**Figure 2**). In monocytes/macrophages, the protein kinase C (PKC) pathway is involved in adhesion/migration, M1/M2 polarization, TLR activation and inflammatory cytokine production (127). It has been shown that the role of miRNA-142-3p may also affect these activities, suggesting that NET may allow extensive control of surrounding cellular functions through the release of miRNAs. Specifically, miRNA-142-3p carried by NET downregulates protein kinase Cα (PKCα) and regulates TNF-α production in macrophages when NET interacts with macrophages (128–130). Not only that, miRNAs released by surrounding cells *via* exosomes can also affect neutrophil NETosis formation. In Yong-Zhanggan et al.' s study, exosomal miR-146a produced by oxLDL-treated macrophages stimulated ROS and NET production and worsened atherosclerosis by targeting SOD2 (131). The study by Reyes-García AML et al. showed that NET represents an important relationship between inflammation and thrombosis, and that both NET components DNA and H4 lead to increased HNF4A mRNA expression, which may suggest that it is partly involved in the Coagulation factor regulation. They determined that H4 induced decreased expression of specific miRNAs in the miR-17/92 cluster, which partially explains why H4 induced increased TF expression (132).

4.1.3 miRNAs Regulate Neutrophil-Involved Chronic Diseases

Although it has been traditionally believed that the primary role of neutrophils is to effectively eliminate extracellular pathogenic factors, it is not surprising that neutrophils play an important role in the pathogenesis of many diseases based on the recent discovery of a wide range of neutrophil functions. Some results indicate that neutrophils have become an important determinant of chronic inflammation (133). In the following section we would discuss about the role of miRNAs in regulating neutrophils in chronic diseases such as sepsis, asthma, systemic lupus erythematosus and so on (**Table 1**).

4.1.3.1 Sepsis

When ill individuals encounter an inappropriate immune response, it can lead to exacerbations of sepsis, and the cardiovascular system is a susceptible system to sepsis (150). On the anti-inflammatory side, miR-21 drives an overwhelming inflammatory response by indirectly inhibiting the expression of the anti-infective mediator prostaglandin E2(PGE 2)/IL-10 (134). MiR-let-7b directly targets toll-like receptor 4 (TLR4) and nuclear factor κB (NF-κB), reducing interleukin-6 (IL-6), IL-8, tumor necrosis factor alpha (TNF-α) and other pro-inflammatory factors, up-regulate the anti-inflammatory factor IL-11 (140). In terms of pro-inflammatory, up-regulation of miR-146a, miR-887-3p, miR-155, and down-regulation of miR-223-3p play important roles. miR-146a modulates inflammatory responses by inhibiting

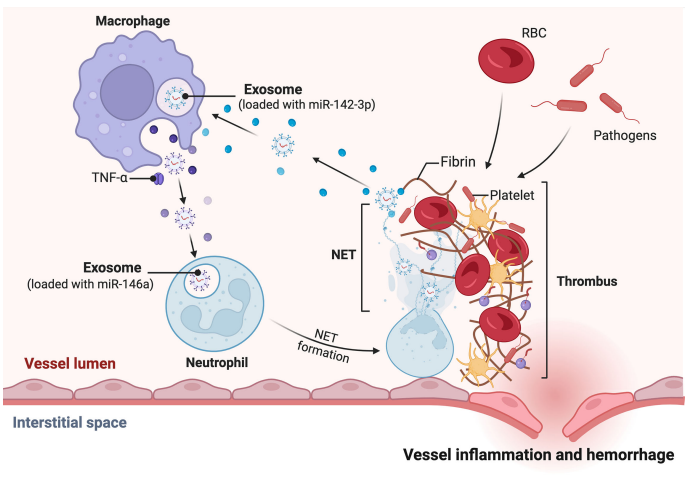

FIGURE 2 | miRNA-mediated regulation of inflammatory factors by NET released in neutrophils. Under the influence of the vascular inflammatory environment, neutrophils, for example, mature macrophages release exosome-loaded miR-146, which stimulates neutrophil development and maturation to form NETs. The NETs supernatant contains miRNA, such as miR-142-3p. miR-142-3p targets macrophages to release more pro-inflammatory factors, which in turn accelerate the formation of a pro-inflammatory environment.

TABLE 1 | miRNAs regulate neutrophil-involved chronic diseases.

miRNA	Expression level	Target	Function	Chronic diseases	Ref.
miR-21	↑	PGE 2/IL-10	pro-inflammation	sepsis	(134)
miR-223-3p	↓	MKNK1	pro-inflammation	sepsis	(135)
miR-146a	↑	NF-κB SOD2	pro-inflammation promote NETosis	sepsis	(136, 137)
miR-887-3p	↑	IL-1β VCAM-1	pro-inflammation	sepsis	(138)
miR-155	↑	NF-κB	pro-inflammation	sepsis	(139)
miR-let-7b	↑	TLR4 NF-κB	anti-inflammation	sepsis	(140)
miR-223	↑	NLRP3/IL-1β	anti-inflammation	asthma	(141)
hsa-miR-223-3p	↑	TLR/Th17	endoplasmic reticulum stress	asthma	(142)
miR-199a-5p	↑	WNT2 WNT4	inhibit lung regeneration	asthma	(143)
miR-629-3p	↑	IL-8	pro-inflammation	asthma	(144)
miR-4512	↓	TLR4 CXCL2	promote NETosis	SLE	(23)
miR-let-7b	↑	TLR-7	pro-inflammation	SLE	(145)
miR-125a	↓	IL-16	pro-inflammation	SLE	(146)
miR-223-3p	↑	GM-CSF TRAF4	anti-inflammation	COPD	(147)
miR-1285	↑	SP11	pro-inflammation inhibit tissue repair	IBD	(144)
miR-23a	↑	Lamin B1	inhibit tissue repair	IBD	(148)
miR-155		RAD51	pro-inflammation		
miR-223	↑	IL-18	anti-inflammation	AOSD	(149)

PGE 2, prostaglandin E2; IL-10, interleukin-10; MKNK1, mitogen-activated protein kinase interacting serine/threonine kinase 1; NF-κB, nuclear factor kappa light-chain enhancer of activated B cells; SOD2, manganese superoxide dismutase, superoxide dismutase 2; VCAM-1, vascular cell adhesion molecule-1; TLR4, toll-like receptor 4; NLRP3, Nucleotide-binding oligomerization domain, leucine-rich repeat and pyrin domain-containing 3; Th17, helper T cell 17; WNT, Wingless-Type MMTV Integration Site Family; CXCL2, Chemokine(C-X-Cmotif) ligand10; GM-CSF, granulocyte monocyte-colony stimulation factor; TRAF4, (TNF) tumor necrosis factor-receptor-associated factor 4; SP11, S-locusprotein 11; RAD51, a homologous recombination regulator homologous recombination; SLE, Systemic lupus erythematosus; COPD, chronic obstructive pulmonary disease; IBD, inflammatory bowel disease; AOSD, Adult-onset Still's disease.

↑ Represents expression level rises.

↓ Represents expression level decreases.

the Toll-like receptor/NF-κB axis and sod2 and modulates NET formation by altering its senescence phenotype (136, 137). MiR-887-3p released by neutrophils increases endothelial release of chemokines and promotes transendothelial leukocyte migration (138). Furthermore, neutrophils promote vascular inflammation and atherosclerosis by delivering miR-155-carrying microvesicles to disease-prone areas (139). Downregulation of miR-223-3p promotes the expression of mitogen-activated protein kinase (MAPK)-interacting serum/threonine kinase 1 (MKNK 1), which regulates the abundance of neutrophil-expressed inflammatory factors involved in sepsis (135).

4.1.3.2 Asthma

Asthma is a chronic respiratory disease. Airway obstruction in asthma includes bronchial smooth muscle spasms and different degrees of airway inflammation, which are characterized by edema, mucus secretion, and inflow of various inflammatory cells (151). Expression of miR-223 in neutrophils inhibits the NLRP3/IL-1β axis, reduces airway inflammation, and reduces NLRP3 (Nucleotide-binding oligomerization domain, leucine-rich repeat and pyrin domain-containing 3) levels and IL-1β release (141). Has-miR-223-3P, a neurotropic miRNA, regulates TLR/Th17 signaling and endoplasmic reticulum stress by inhibiting the TLR/Th17 pathway (142). The up-regulation of miR-199a-5p in neutrophils is negatively correlated with lung function (143). MiR-629-3p damages the bronchial epithelium by inducing IL-8 mRNA expression and promoting inflammatory response (144). In addition, miR-26a, miR-146a, and miR-31 are also related to the levels of interleukin-5 (IL-5), IL-8, IL-12, and tumor necrosis factor-α (TNF-α) (152).

4.1.3.3 Systemic Lupus Erythematosus

Systemic lupus erythematosus is a chronic autoimmune disease characterized by the loss of self-tolerance and the formation of nuclear autoantigens and immune complexes. The disease has a wide range of manifestations, which can involve multiple organ system inflammations. The course of the disease is chronic or relapsed and alleviated, leading to significant morbidity and even mortality (153). In SLE, the down-regulation of miR-4512 in neutrophils promotes the expression of TLR4 and CXCL2, which has the function of promoting the formation of NETs (23). As a TLR-7 agonist, miR-let-7b appears in pro-inflammatory neutrophils (low-density granulocytes (LDGs)) NET of SLE and plays a role in inducing vascular cell pro-inflammatory response (145). In addition, the down-regulation of miR-125a weakened the original inhibitory effect on IL-16 gene, and the up-regulation of IL-16 expression directly acts on lung epithelial

cells, thereby significantly enhancing the expression of neutrophil chemokines, leading to lung injury (146).

4.1.3.4 Other Chronic Diseases

In inflammatory bowel disease (IBD), miR-23a and miR-155 enhance the deleterious effects of neutrophils by targeting lamin B1 and RAD51 (a homologous recombination regulator), inhibiting tissue healing responses (148). Neutrophil-derived traces (NDTR) are membrane-derived vesicles produced by neutrophil migration toward inflammatory foci and contain pro-inflammatory miRNAs, such as miR-1285. MiR-1285 promotes intestinal inflammation and inhibits tissue repair by targeting the S-locusprotein 11 (SP11) gene. Other miRNAs in NDTR, including miR-1260, miR-4454, and miR-7975, have similar utility (144). In atherosclerosis, miR-146a (a brake of inflammatory response) is downregulated, thereby increasing NETosis and increasing thrombotic risk (137). In rheumatoid arthritis, citrullinated protein antigen and TNF-α decreased the expression of many miRNAs and their biogenesis-related genes, such as miRNA-223, miRNA-126 and miRNA-148a, thereby increasing their potential mRNA target. These miRNAs are mainly associated with migration and inflammation in synovial fluid neutrophils (154).In chronic pulmonary disease (COPD), miR-223-3P suppressed Granulocyte monocyte-colony stimulation factor (GM-CSF) secret and gene expression of the pro-Inflammatory transcription factor traf4, which is related to neutrophilic inflammation (147). In Adult-onset Still's disease (AOSD), the expression of miR-223 in neutrophils is suppressed (149). In IBD, miR-23a and miR-155 can enhance the harmful effects of polymorphonuclears (PMNs) and inhibit the tissue healing response (148).

4.2 Macrophages

Macrophages are ubiquitous in our body, and most tissue-resident macrophages are seeded in the yolk sac in embryonic form for long-term self-renewal (155). Tissue macrophages are specialized according to the microenvironment of the tissue in which they live and have specific functions. Therefore, they are not only immune cells, but also participate in the formation of living tissues through specialized auxiliary functions, such as osteoclasts in bone (156), macrophages in intestinal muscularis (157), and small keratinocytes in brain tissue (158). The remaining macrophages were derived from monocyte-macrophages. Monocytes are present in the blood circulation and have a high degree of functional plasticity, providing the necessary support for their involvement in the initiation and subsequent resolution of inflammatory responses (4, 159). In an inflammatory response, damaged infected areas can chemotactically recruit mature monocytes, expose them to several cytokines and bacterial products, and differentiate into macrophages. They participate in inflammatory processes together with tissue-resident macrophages to maintain the macrophage pool in the tissue (160, 161).

Dynamic regulation of complex gene networks and signaling cascades that control macrophage polarization, priming, and plasticity through multiple layers of regulation of gene expression (162). Transcription and translation are complex processes that are tightly regulated and strongly influence cellular function. Specific miRNA subsets induced by different microenvironmental signals have been shown to modulate transcriptional output to obtain distinct macrophage activation patterns and polarization states, ranging from M1 phenotype to M2 phenotype (163), affecting multiple macrophages biology, such as monocyte differentiation and development, macrophage polarization, infection, inflammatory activation, cholesterol homeostasis, cell survival, and phagocytosis (164).

4.2.1 miRNA and the Plasticity of Macrophages

Macrophages are an important plastic cell. The local microenvironment can make macrophages directional polarization, from one phenotype to another phenotype (165). Macrophages are heterogeneous, and their phenotype and function are regulated by the surrounding microenvironment. Macrophages are generally divided into two distinct subpopulations: a) M1 macrophages (typically activated macrophages), induced to differentiate by lipopolysaccharide (LPS) alone or in combination with Th1 cytokines such as IFN-γ and TNF-α, secrete high levels of pro-inflammatory cells Factors, such as interleukin-1β (IL-1β), IL-6, IL-12, and cyclo-oxygen-ase-2 (COX-2), have pro-inflammatory effects. M1 macrophages have potent antibacterial and antitumor activities and are able to mediate ROS-induced tissue damage while impairing tissue regeneration and wound healing (166–169). b) M2 macrophages (alternately activated macrophages), which have anti-inflammatory and immunomodulatory effects, are polarized by Th2 cytokines (such as IL-4, IL-13) and produce anti-inflammatory cytokines (such as IL- 10, TGF-β). Exposure of M2 macrophages to the M1 signaling environment results in "repolarization" or "reprogramming" of differentiated M2 macrophages and vice versa (165, 168, 170, 171). M1 macrophages and M2 macrophages have distinct functional and transcriptional profiles, and the balance of polarization between them determines the fate of inflamed or injured organs. When in an infection or inflammatory response, macrophages first exhibit the M1 phenotype to resist the stimulation to release anti-inflammatory factors such as TNF-α and IL-1β. At this time, M2 macrophages secrete a large amount of IL-10 and TGF-β to inhibit inflammation, promote tissue repair, angiogenesis, and maintain environmental stability (51).

MiRNA-125, miR-127, miRNA-146, miRNA-155 and miRNA-let-7a/f were involved in the polarization of M1 macrophages, while miRNA-9, miRNA-21, miRNA-146, miRNA-147 and miR-223 regulates the polarization of M2 macrophages. Compared with miR-155 and miR-142-3p, miRNA-let-7a reduced macrophage proliferation. Macrophage apoptosis is negatively regulated by miR-21 and miRNA-let-7e (172–174). GATA binding protein 3(GATA3) is targeted by miR-720, whereas BCL6 is targeted by miR-127 and miR-155, all of which induce M1 polarization. The polarization of M2 macrophages is dependent on these two miRNAs (175, 176). On the other hand, overexpression of miR-720 reduces M2 polarization (175). There is evidence that miR-127 and miR-155 increase pro-inflammatory cytokines, and that M2

macrophages can be transformed into M1 macrophages by overexpression of miR-155 (22, 176–178). MiR-146a increases the expression of M2 marker genes (such as CD206) in peritoneal macrophages and decreases the expression of M1 phenotypic markers, resulting in M2 polarization of macrophages (such as IL-12) (179).

The role of miRNAs in regulating macrophage polarization allows it to influence the duration and intensity of the innate immune response, which helps prevent excessive macrophage inflammation. miRNAs may transform macrophages from pro-inflammatory to anti-inflammatory by affecting the expression of immune proteins (180, 181). MiR-146a and miR-155 are the earliest expressed miRNAs in LPS-induced macrophages and are controlled by NF-κB (182, 183). Numerous studies have confirmed that there is a negative feedback loop in the production of miRNAs in the NF-κB pathway (**Figure 3**). The NF-κB pathway is inhibited by miR-146a, which increases transcription of two distinct miR-146a targets: the adaptor proteins TNF receptor associated factor 6 (TRAF6) and interleukin-1 receptor associated kinase 1 (IRAK1) (182). MiR-155, a pro-inflammatory miRNA, is also involved in this negative feedback regulation, rapidly increasing NF-κB expression in macrophages using TLR ligands and type 1 interferons (184). Notably, miR-155 is a key component of various feed forward networks that regulate the length and intensity of inflammatory responses (185, 186).

Members of the same miRNA family may have completely opposite regulatory effects. LPS-activated macrophages express distinct miR-125a and miR-125b, which play an antagonistic role in cellular inflammatory responses. In contrast to miR-125a, the level of miR-125b was decreased at an early stage in LPS-induced macrophages. Enhanced expression of miR-125b induces stronger IFN-γ responses and maintains activation of pro-inflammatory cells by targeting innovation and research focus (IRF4), thereby promoting M2 macrophage polarization (187, 188). Similarly, miR-146a and miR-146b may act as a relay system to buffer TLR4 trigger-induced expression of proinflammatory genes (189).

4.2.2 miRNAs Regulate Macrophage-Involved Chronic Diseases

Macrophages play a central role in the innate immune response and are the link between the innate and adaptive immune responses. Macrophages directly neutralize pathogens by phagocytosis and secrete chemokines and cytokines to coordinate the response of other immune cells (such as neutrophils and lymphocytes) and the stroma (159). Macrophages have a variety of functions, including: a) phagocytosis and killing, b) antigen presentation, c) mediating inflammatory responses, which include interleukin-1 (IL-1), IL-6, and TNF-α with different types of cytokines to achieve (190, 191), d) Tissue repair, regeneration and fibrosis (53), e) lipid metabolism (192).

As stated in "The Doctor's Dilemma" (Act 1): "There is really only one truly scientific cure for all diseases, and that is to stimulate phagocytes." Macrophages are key in chronic inflammation and related pathological processes cell (193). While macrophages are critical for effective control and clearance of infections, clearance of pathogens and dead cells, and promotion of tissue repair and wound healing, they may also cause tissue damage and pathological changes during infections and inflammatory diseases (194). What is more needed now is to calm them down so that the inflammatory response can be addressed. M2 macrophages play a key role in the resolution of inflammatory responses. Phagocytic debris, damaged or dead cells, and apoptotic neutrophils are essential functions of M2 macrophages in this process. During tissue breakdown,

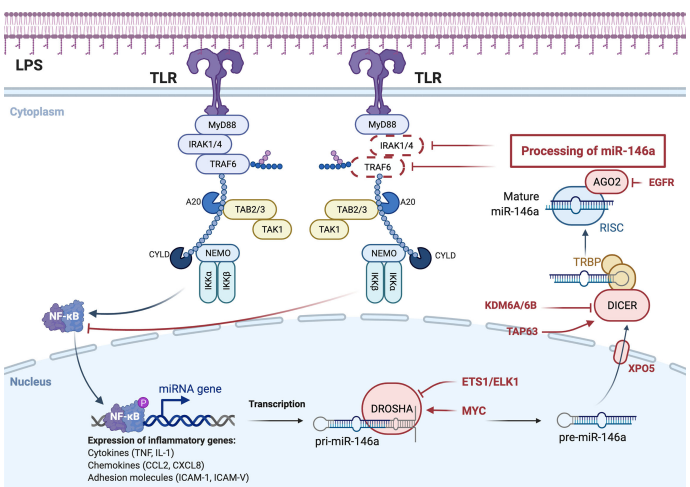

FIGURE 3 | miRNA-mediated negative feedback loop of macrophage polarization to M1 type. TLR on the macrophage cell membrane, stimulated by bacterial LPS, activates NF-κB pathway, which in turn promotes the formation of miR-146a, and the formation of miR-146a inhibits NF-κB pathway by inhibiting IRAK1 and TRAF6. Expression and function are two distinct concepts for the same miRNA family members.

macrophages are the main source of lipid mediators and produce anti-inflammatory cytokines, and IL-10 and TGF-β are involved in tissue breakdown (195, 196). After being stimulated by the extracellular environment, macrophages can adjust their own miRNA secretion levels to adapt to the environment. In addition, miRNAs secreted by macrophages can also be transported to other cells through extracellular vesicles, thereby regulating the functions of these cells. The following summarizes the role of miRNAs in regulating macrophages in some chronic diseases (**Table 2**).

4.2.2.1 Atherosclerosis

Vascular wounds heal slowly when stimulated by hyperglycemia, hypertension or nicotine. In the early stage of atherosclerosis, the vascular injury area becomes an inflammatory microenvironment, and inflammatory cells (such as neutrophils and macrophages) gather, making the vascular endothelium vulnerable to injury. In the mid-stage, lipids rich in blood impair the regenerative capacity of endothelial cells and cause the accumulation of moxLDL in macrophages, transforming into foam cells. In the advanced stage, it is difficult for the vascular wound to heal. The constant influx of lipoproteins causes the lipid clearance system of macrophages to fail. Cholesterol accumulation in the endoplasmic reticulum of macrophages leads to the same effects as activation of toll-like receptors 2 (TLR2) and 4 (TLR4) and inflammatory activation of macrophages (12). It can be seen that in the process of AS, macrophages are gradually damaged, resulting in secondary necrosis of apoptotic cells and aggravation of inflammation.

The regulation of macrophages by miRNAs exists in various stages of atherosclerosis. In the early stage of trauma, monocytes-macrophages are rapidly recruited by inflammatory factors and differentiate into large numbers of macrophages. Under the influence of a diminished generation of nitrotyrosine, miR-342–5p is up-regulated in macrophages and induces macrophages to produce pro-inflammatory factors (such as Nos2, IL-1β, and IL-6) by an Akt (protein kinase B) 1- and miRNA-155-dependent pathway. Up-regulation of miR-342-5p also results in decreased expression of Bmpr2 (bone morphogenetic protein receptor, type II). Bmpr2 mRNA may regulate the synthesis of inflammatory mediators in macrophages by binding to miR-342-5p, which competes with Akt1 (197). MiR-92a directly targets Krüppel-like factor 2 (KLF2) to increase the expression of KLF

2, endothelial nitric oxide synthase, and thrombomodulin (198). The expression of miR-155 in macrophages is increased. miR-155 can inhibit the proliferation of macrophages and reduce the content of diseased macrophages by targeting colony-stimulating factor-1 (178). The down-regulation of miR-383 in macrophages also has a similar effect. The down-regulation of miR-383 reduces energy consumption and increases the cell survival rate of bone marrow-derived macrophages by reducing the inhibition of the poly (ADP-ribose)-glycopyrrolate gene (PARG) (199). In addition, miR-10a is upregulated in macrophages and mediates Dicer lipolytic and anti-inflammatory effects by inhibiting ligand-dependent nuclear receptors and promoting fatty acid oxidation (200). In the late stage, under the induction of Free Cholesterol-Induced Macrophase Apoptotic Cells (FC-AM), miR-10b in resident peritoneal macrophages (RPM) was up-regulated to reduce the expression of ABCA1 in RPM, thereby reducing the size of late plaques and enhancing the stability of plaques (201). Stimulated by a variety of inflammatory mediators, including mildly oxidized low-density lipoprotein (moxLDL), miR-155 reduces the anti-infectious signaling proteins (Bcl-6) and phosphorylated-stat-3, thereby enhancing the expression of inflammatory mediators in macrophages (such as CCL2) and impairing efferocytosis. In the hypercholesterolemia environment, miR-302a is up-regulated to inhibit the expression of ATP-binding cassette transporter A1 (ABCA1), to stimulate the lipid-cleaning function of macrophages with cholesterol accumulation in plaques (202).

In addition, miR-17-5p, miR-140a, and miR-146a played a pro-inflammatory role in AS. SNHG16 is up-regulated and inhibits the expression of miR-17-5p, the proliferation, infectious factors, and NF-κB signaling factors are increased in macrophages, thus promoting the inflammatory response in AS patients and the proliferation of THP-1 macrophages (25). Monocyte-derived miR-140a inhibits IL-10 expression, enhances the pro-inflammatory capacity of ox-LDL-stimulated differentiated macrophages, and reduces IL-10-mediated anti-inflammatory response (205). MiR-146a, on the other hand, promoted the release of ROS and NETs by inhibiting SOD2 (131). In terms of anti-inflammatory, miR-155 from THP-1 macrophages inhibits foam cell formation and enhances cholesterol efflux (203). miR-34a regulates macrophage cholesterol efflux and reverses cholesterol transport by inhibiting ATP-binding cassette subfamily G member 1 (ABCG1) and liver x receptor α (204). In the aspect of tissue repair, exosomes derived from nicotine-treated macrophages inhibit phosphatase and tension homologue deleted from chromosome 10 (PTEN) by releasing miR-21-3p to promote the migration and proliferation of vascular smooth muscle cells (VSMCs) (206).

4.2.2.2 Obesity and Type 2 Diabetes Mellitus

Type 2 diabetes mellitus (T2DM) is a chronic low-grade inflammatory disease characterized by insulin resistance (IR) and pancreatic β -cell dysfunction. MiRNA-34a, miR-210, miR-690, and miR-467a-5p are related to insulin metabolism. Under the infiltration of adipose tissues, miR-34a in macrophages is up-regulated and inhibits Krüppel-like factor 4 (Klf4), which is able to inhibit the anti-inflammatory polarization of macrophages. miRNA is positively correlated with insulin resistance and metabolic inflammatory parameters (207). The macrophages in adipose tissues directly target the NADH dehydrogenase ubiquinone 1 α subcomplex 4 (NDUFA 4) gene by releasing miR-210 and promoting the onset of obesity-related diabetes by regulating glucose uptake and mitochondrial CIV activity (208). Anti-inflammatory M2-type macrophages are important to maintain normal metabolic homeostasis. M2-polarized bone marrow-derived macrophages (BMDM) secrete exosomes (Exos) containing miRNA, and miR-690 in the exosomes acts as an insulin sensitizer by inhibiting NAD kinase (NADK), thereby improving glucose tolerance (209). MiR-467a-5p, by targeting

TABLE 2 | miRNAs regulate macrophage-involved chronic diseases.

miRNA	Expression level	Target	Function	Chronic diseases	Ref.
miR-342-5p	↑	Akt1	pro-inflammation	in early AS	(197)
miR-155	↑	CSF-1	inhibit macrophage lesion	in early AS	(178)
miR-92a	↑	KLF2	pro-inflammation	in early AS	(198)
miR-383	↓	Parg	promote macrophage survival	in early AS	(199)
miR-10a	↑	LCoR	promote lipid metabolism	in early AS	(200)
miR-10b	↑	ABCA1	reduclate plaque	in advanced AS	(201)
miR-155	↑	Bcl6	pro-inflammation weaken efferocytosis	in advanced AS	(22)
miR- 302a	↑	ABCA1	promote lipid metabolism	in advanced AS	(202)
miR-155	↑	CEH	inhibit foam cell	AS	(203)
miR-17-5p	↓	NF-κB	promote lipid metabolism	AS	(25)
miR-34a	↑	ABCG1 liver X receptor α	pro-inflammation	AS	(204)
miR-146a	↑	SOD2	pro-inflammation	AS	(131)
miR-140a	↑	IL-10	pro-inflammation	AS	(205)
miR-21-3p	↑	PTEN	promote tissue repair	AS	(206)
miR-34a	↑	KLF4	pro-inflammation promote insulin resistance	Obesity T2DM	(207)
miR-210	↑	NDUFA4	promote insulin resistance	Obesity T2DM	(208)
miR-690	↑	Nadk	insulin sensitizer	Obesity T2DM	(209)
miR-467a-5p	↑	THBS1	prevent insulin resistance	Obesity T2DM	(210)
miR-505-3p	↓	RUNX1	pro-inflammation	Obesity T2DM	(211)
miR-29	↑	TRAF3	pro-inflammation	Obesity T2DM	(212)
miR-712	↓	LRRK2	anti-inflammation	Obesity T2DM	(213)
miR-128-2	↑	ABCA1 ABCG1 RXRa	promote lipid metabolism	Obesity T2DM	(214)
miR-33a	↑	ABCA1 ABCG1	inhibit lipid metabolism	Obesity T2DM	(24)
miR-221-3p	↓	JAK3	pro-inflammation	RA	(215)
miR-29b	↑	HBP1	pro-inflammation	RA	(216)
miR-132	↑	COX2	promote osteoclastogenesis	RA	(217)
miR-574-5p	↑	TLR 7/8	promote osteoclastogenesis	RA	(218)
miR-20a	↑	RANKL	inhibit osteoclastogenesis	RA	(219)
miR-6089	↑	TLR4	inhibit osteoclastogenesis	RA	(220)
miR-148a	↓	GP130 IKKα IKKβ IL1R1 TNFR2	pro-inflammation	IBD	(221)
miR-590-3p	↑	LATS1	anti-inflammation promote tissue repair	IBD	(222)
miR-378a-5p	↑	NLRP3	anti-inflammation promote tissue repair	IBD	(223)
miR-142-5p	↑	SOCS1	promote fibrosis	liver cirrhosis	(26)
miR-130a-3p	↓	PPARγ	promote fibrosis	liver cirrhosis	(26)
miR-4512	↓	TLR4 CXCL2	pro-inflammation	SLE	(23)
miR-20a	↑	IL-18	anti-inflammation	AOSD	(149)
miR-181b	↑	PKCδ	regulate macrophage polarization	Myocardial infarction	(224)

Akt1, serine/threonine protein kinase 1; CSF-1,colony-stimulating factor-1; KLF2,Krüppel-like factor 2; Parg, poly(ADP-ribose)-glycohydrolase; LCoR, ligand-dependent nuclear receptor corepressor; Bcl6, B-cell lymphoma 6 protein; RXRα, Retinoid X receptors α; ABCA1, ATP-binding cassette transporter A1; ABCG1, ATP-binding cassette subfamily G member 1; JAK3, Janus kinase 3 tyrosine-protein kinase; COX, Cyclooxygenase; IKK, inhibitor of nuclear factor kappa-B kinase; PTEN, phosphatase and tension homologue deleted from chromosome 10; KLF4, Krüppel-like factor 4; NDUFA4, NADH dehydrogenas, ubiquinone 1 alpha subcomplex 4; THBS1, thrombospondin 1; IL1R1, interleukin 1 receptor type 1; TNFR2, TNF receptor superfamily member 1b; TRAF3,TNF-receptor-associated factor 3; NF-κB, nuclear factor kappa light-chain enhancer of activated B cells; HBP1, the high-mobility group box-containing protein 1; TLR,Toll-like receptor; RANKL, receptor activation of nuclear factor-κB ligand; NLRP3, NOD-like receptor family, pyrin domain-containing 3; SOCS1,suppressor of cytokine signaling 1; PPARγ, peroxisome proliferator-activated receptor γ; PKCδ,protein kinase C δ; AS, atherosclerosis; T2DM, diabetes mellitus type 2; AR, rheumatoid arthritis; IBD, inflammatory bowel disease; SLE, Systemic lupus erythematosus; AOSD, Adult-onset Still's disease.

thrombospondin 1 (THBS1), increases the infiltration of macrophages in adipose tissues, increases the level of IL-6 in adipose tissues, and can prevent insulin resistance (210). Both miR-505-3p and miR-29 have pro-inflammatory effects. miR-505-3p is down-regulated and promotes the expression of the transcription factor (RUNX1). CCR3, CCR4, CXCR, and RUNX1 are increased in MΦ (macrophage), and this increase promotes pro-inflammatory macrophages (211). The miR-29 exosome promotes inflammation by promoting the recruitment and activation of circulating monocytes and macrophages in a TNF-receptor-associated factor 3 (TRAF3) dependent manner (212). Furthermore, our results show that pancreatic β cells regulate systemic inflammatory tone and glucose homeostasis through miR-29 in response to nutrient overload (212). Persistence of pro-inflammatory M1 macrophages in diabetic wounds contributes to the persistence of chronic inflammation in diabetic wounds. The persistence of M1 macrophage phenotype and its failure to remodel into M2-type macrophages play a key role in diabetic wound injury. The level of miR-21 has staged characteristics in diabetic wound healing. In the early and late stages of diabetic wound repair, miR-21 level is high, while in the middle stage of trauma, miR-21 level is significantly low. In macrophages, M1-polarized bacteriophage showed up-regulation of miR-21 and the pro-inflammatory factors IL-1β, TNF-α, and IL-6. In addition, hyperglycemia induces NOX2 expression and ROS production through the HG/miR-21/PI3K/NOX2/ROS signaling cascade. Dysregulation of miR-21 may lead to abnormal inflammation and persistent M1 macrophage polarization in diabetic wounds (225). The down-regulation of miR-712 reduces and inhibits the phosphorylation of p38 and ERK1/2 kinases and inhibits the pro-inflammatory transformation of macrophages by promoting the expression of apotant infectious gene LRRk2 (213). MiR-128-2 and miR-467a-5p participate in the regulation of macrophage cholesterol transport by inhibiting ATP-binding cassette transporter A1 (ABCA1), ATP-binding cassette subfamily G member 1 (ABCG1) and Retinoid X receptors α (RXRα) (24, 214).

4.2.2.3 Rheumatoid Arthritis

Rheumatoid arthritis is chronic inflammatory arthritis that can lead to irreversible cartilage and bone damage, characterized by persistent synovitis, systemic inflammation, and autoantibodies (226). The down-regulation of miR-221-3p promotes the expression of Janus kinase 3 tyrosine-protein kinase (JAK3) and drives M2 macrophages to show M1 cytokine characteristics, resulting in weakened anti-inflammatory response and enhanced pro-inflammatory response (215). The upregulation of miR-29b targets the high-mobility group box-containing protein 1 (HBP1) and promotes the persistent existence of CD14-positive peripheral blood mononuclear cells (PBMs) at inflammatory sites (216). Up-regulation of miR-20a inhibits receptor activation of NF-κB ligand (RANKL), thereby inhibiting the proliferation and differentiation potential of osteoclasts (219). MiR-132 and miR-574-5p target COX2 and TLR 7/8 signaling, respectively, to promote osteoclastogenesis and intensify rheumatoid arthritis (217, 218). MiR-6089 inhibits lipopolysaccharide (LPS)-induced cell proliferation and activation of macrophase-like THP-1 cells by inhibiting the level of TLR4 (220).

4.2.2.4 Infectious Bowel Disease

Infectious bowel disease (IBD) is a chronic and recurrent inflammatory bowel disease that is an abnormal immune response to intestinal microflora triggered by environmental factors in susceptible hosts. MiR-590-3p can activate the transcription regulated by YAP/β-catenin in macrophages, reduce inflammatory signals and promote epithelial regeneration by directly targeting large tumor suppressor, homolog 1 (LATS1) (222). The down-regulation of miR-148a increases the levels of GP130, inhibitor of nuclear factor kappa-B kinase α (IKKα), IKKβ, interleukin 1 receptor type 1 (IL1R1), and TNF receptor superfamily member 1b (TNFR2), resulting in the decreased activation of NF-κB and signal transducer and activator of transcription 3 (STAT3) in macrophages and colon tissues, and promotion of colitis (221). MiR-378a-5p, on the other hand, plays a vital role in the repair of colitis by targeting to nod-like receptor family, pyrin domain-containing 3 (NLRP3) (223).

4.2.2.5 Other Chronic Diseases

In liver cirrhosis and idiopathic pulmonary fibrosis, miR-142-5p prolongs STAT6 phosphorylation by inhibiting suppressor of cytokine signaling 1 (SOCS1) protein, leading to increased IgE, eosinophil infiltration, fibroblast proliferation and collagen synthesis, and aggravates tissue fibrosis (26). MiR-130a-3p attenuates its repression of peroxisome proliferator-activated receptor γ (PPARγ), which coordinates STAT6 signaling, and also promotes tissue fibrosis (26). In systemic lupus erythematosus (SLE), downregulation of miR-4512 leads to high expression of TLR4 and CXCL2 in macrophages, which release more pro-inflammatory factors (23). In adult-onset still's disease (AOSD), miR-20a is upregulated in macrophages and suppresses the expression of the proinflammatory factor IL-18 (149). PKCδ (protein kinase C δ) is an important mediator of inducing Mϕ polarization. In myocardial infarction, miR-181b regulates macrophage polarization by targeting PKCδ. We summarize the above content in **Table 2**.

5 CONCLUSION AND FUTURE PERSPECTIVES

In this paper, the latest progress of miRNA in regulating neutrophils and macrophages is reviewed. miRNAs can determine the resolution of inflammatory responses by regulating the functions of neutrophils and macrophages, and thus serve as potential therapeutic targets for chronic diseases. miRNA can regulate the level of inflammatory factors in injured or infected sites by influencing the differentiation and function of neutrophils and the formation of NET, play a role in polycytosis of self-apoptosis, and participate in the development of chronic diseases through oxidation and hydrolysis derived from phagocytosis and killing. For macrophages, miRNA mainly participates in chronic diseases by regulating the polarization,

phagocytosis, efferent cytopenia, and lipid metabolism of macrophages, and repairing, regenerating, and fibrosis of tissues.

However, it is not difficult to find from the foregoing that most of the current effects of miRNAs are concentrated in a certain part of a specific disease. For example, miR-223-3p is anti-inflammatory in the context of sepsis (135) while pro-inflammatory in the context of COPD (147). We can conclude from this that the effects of miRNAs are environment-specific, that is, the functions of miRNAs on neutrophils and macrophages are highly dependent on surrounding environmental factors, which makes miRNAs have inevitable side effects. Therefore, extensive experiments are needed to evaluate the global regulatory network of miRNAs to determine the therapeutic utility of miRNAs before they can be put into the clinic.

AUTHOR CONTRIBUTIONS

PY and JZ: Conceptualization, Methodology, Funding acquisition. YW: Writing-Original draft preparation and Reviewing. XL: Visualization and Investigation. PX: Software and Supervision. ZL: Validation and Editing. XF and YS: Reviewing and Supervision. All authors contributed to the article and approved the submitted version.

FUNDING

This research was supported by grants from the Key Science and Technology Research Project of Education Department of Jiangxi Province (GJJ180004).

REFERENCES

1. Schmid-Schönbein GW. Analysis of Inflammation. *Annu Rev BioMed Eng* (2006) 8:93–151. doi: 10.1146/annurev.bioeng.8.061505.095708
2. Alexander M, O'Connell RM. Noncoding RNAs and Chronic Inflammation Micro-Man. *BioEssays* (2015) 37:1005–15. doi: 10.1002/bies.201500054
3. Feehan KT, Gilroy DW. Is Resolution the End of Inflammation? *Trends Mol Med* (2019) 25:198–214. doi: 10.1016/j.molmed.2019.01.006
4. Medzhitov R. Origin and Physiological Roles of Inflammation. *Nature* (2008) 454:428–35. doi: 10.1038/nature07201
5. Poznyak A, Grechko AV, Poggio P, Myasoedova VA, Alfieri V, Orekhov AN. The Diabetes Mellitus–Atherosclerosis Connection: The Role of Lipid and Glucose Metabolism and Chronic Inflammation. *Int J Mol Sci* (2020) 21:1835. doi: 10.3390/ijms21051835
6. Ferrucci L, Fabbri E. Inflammageing: Chronic Inflammation in Ageing, Cardiovascular Disease, and Frailty. *Nat Rev Cardiol* (2018) 15:505–22. doi: 10.1038/s41569-018-0064-2
7. Firestein GS, McInnes IB. Immunopathogenesis of Rheumatoid Arthritis. *Immunity* (2017) 46:183–96. doi: 10.1016/j.immuni.2017.02.006
8. Ni J, Wu GD, Albenberg L, Tomov VT. Gut Microbiota and IBD: Causation or Correlation? *Nat Rev Gastroenterol Hepatol* (2017) 14:573–84. doi: 10.1038/nrgastro.2017.88
9. Mayne K, White JA, McMurran CE, Rivera FJ, de la Fuente AG. Aging and Neurodegenerative Disease: Is the Adaptive Immune System a Friend or Foe? *Front Aging Neurosci* (2020) 12:572090. doi: 10.3389/fnagi.2020.572090
10. Weindel CG, Richey LJ, Bolland S, Mehta AJ, Kearney JF, Huber BT. B Cell Autophagy Mediates TLR7-Dependent Autoimmunity and Inflammation. *Autophagy* (2015) 11:1010–24. doi: 10.1080/15548627.2015.1052206
11. Jones HR, Robb CT, Perretti M, Rossi AG. The Role of Neutrophils in Inflammation Resolution. *Semin Immunol* (2016) 28:137–45. doi: 10.1016/j.smim.2016.03.007
12. Tajbakhsh A, Bianconi V, Pirro M, Gheibi Hayat SM, Johnston TP, Sahebkar A. Efferocytosis and Atherosclerosis: Regulation of Phagocyte Function by MicroRNAs. *Trends Endocrinol Metab* (2019) 30:672–83. doi: 10.1016/j.tem.2019.07.006
13. Heward JA, Lindsay MA. Long non-Coding RNAs in the Regulation of the Immune Response. *Trends Immunol* (2014) 35:408–19. doi: 10.1016/j.it.2014.07.005
14. Xiao C, Rajewsky K. MicroRNA Control in the Immune System: Basic Principles. *Cell* (2009) 136:26–36. doi: 10.1016/j.cell.2008.12.027
15. O'Connell RM, Rao DS, Chaudhuri AA, Baltimore D. Physiological and Pathological Roles for microRNAs in the Immune System. *Nat Rev Immunol* (2010) 10:111–22. doi: 10.1038/nri2708
16. Ebert MS, Sharp PA. Roles for MicroRNAs in Conferring Robustness to Biological Processes. *Cell* (2012) 149:515–24. doi: 10.1016/j.cell.2012.04.005
17. Zeng Y, Wagner EJ, Cullen BR. Both Natural and Designed Micro RNAs Can Inhibit the Expression of Cognate mRNAs When Expressed in Human Cells. *Mol Cell* (2002) 9:1327–33. doi: 10.1016/S1097-2765(02)00541-5
18. Zeng Y, Yi R, Cullen BR. MicroRNAs and Small Interfering RNAs can Inhibit mRNA Expression by Similar Mechanisms. *Proc Natl Acad Sci* (2003) 100:9779–84. doi: 10.1073/pnas.1630797100
19. Baek D, Villén J, Shin C, Camargo FD, Gygi SP, Bartel DP. The Impact of microRNAs on Protein Output. *Nature* (2008) 455:64–71. doi: 10.1038/nature07242
20. Ivanovska I, Cleary MA. Combinatorial microRNAs: Working Together to Make a Difference. *Cell Cycle* (2008) 7:3137–42. doi: 10.4161/cc.7.20.6923
21. Bracken CP, Khew-Goodall Y, Goodall GJ. Network-Based Approaches to Understand the Roles of miR-200 and Other microRNAs in Cancer. *Cancer Res* (2015) 75:2594–9. doi: 10.1158/0008-5472.CAN-15-0287
22. Nazari-Jahantigh M, Wei Y, Noels H, Akhtar S, Zhou Z, Koenen RR, et al. MicroRNA-155 Promotes Atherosclerosis by Repressing Bcl6 in Macrophages. *J Clin Invest* (2012) 122:4190–202. doi: 10.1172/JCI61716
23. Yang B, Huang X, Xu S, Li L, Wu W, Dai Y, et al. Decreased miR-4512 Levels in Monocytes and Macrophages of Individuals With Systemic Lupus Erythematosus Contribute to Innate Immune Activation and Neutrsophil NETosis by Targeting TLR4 and CXCL2. *Front Immunol* (2021) 12:756825. doi: 10.3389/fimmu.2021.756825
24. Marquart TJ, Allen RM, Ory DS, Baldan A. miR-33 Links SREBP-2 Induction to Repression of Sterol Transporters. *Proc Natl Acad Sci* (2010) 107:12228–32. doi: 10.1073/pnas.1005191107
25. An J-H, Chen Z-Y, Ma Q-L, Wang H-J, Zhang J-Q, Shi F-W. LncRNA SNHG16 Promoted Proliferation and Inflammatory Response of Macrophages Through miR-17-5p/NF-κb Signaling Pathway in Patients With Atherosclerosis. *Eur Rev Med Pharmacol Sci* (2019) 23:8665–77. doi: 10.26355/eurrev_201910_19184
26. Su S, Zhao Q, He C, Huang D, Liu J, Chen F, et al. miR-142-5p and miR-130a-3p are Regulated by IL-4 and IL-13 and Control Profibrogenic Macrophage Program. *Nat Commun* (2015) 6:8523. doi: 10.1038/ncomms9523
27. Peake JM, Suzuki K, Coombes JS. The Influence of Antioxidant Supplementation on Markers of Inflammation and the Relationship to Oxidative Stress After Exercise. *J Nutr Biochem* (2007) 18:357–71. doi: 10.1016/j.jnutbio.2006.10.005
28. Fullerton JN, Gilroy DW. Resolution of Inflammation: A New Therapeutic Frontier. *Nat Rev Drug Discovery* (2016) 15:551–67. doi: 10.1038/nrd.2016.39
29. Medzhitov R. Inflammation 2010: New Adventures of an Old Flame. *Cell* (2010) 140:771–6. doi: 10.1016/j.cell.2010.03.006
30. Stewart A, Beart P. Inflammation: Maladies, Models, Mechanisms and Molecules: Inflammation: Maladies, Models, Mechanisms and Molecules. *Br J Pharmacol* (2016) 173:631–4. doi: 10.1111/bph.13389
31. Suzuki K. Chronic Inflammation as an Immunological Abnormality and Effectiveness of Exercise. *Biomolecules* (2019) 9:223. doi: 10.3390/biom9060223
32. Markiewski MM, Lambris JD. The Role of Complement in Inflammatory Diseases From Behind the Scenes Into the Spotlight. *Am J Pathol* (2007) 171:715–27. doi: 10.2353/ajpath.2007.070166

33. Varela ML, Mogildea M, Moreno I, Lopes A. Acute Inflammation and Metabolism. *Inflammation* (2018) 41:1115–27. doi: 10.1007/s10753-018-0739-1
34. Kotas ME, Medzhitov R. Homeostasis, Inflammation, and Disease Susceptibility. *Cell* (2015) 160:816–27. doi: 10.1016/j.cell.2015.02.010
35. Takeuchi O, Akira S. Pattern Recognition Receptors and Inflammation. *Cell* (2010) 140:805–20. doi: 10.1016/j.cell.2010.01.022
36. Lee J-W, Nam H, Kim LE, Jeon Y, Min H, Ha S, et al. TLR4 (Toll-Like Receptor 4) Activation Suppresses Autophagy Through Inhibition of FOXO3 and Impairs Phagocytic Capacity of Microglia. *Autophagy* (2019) 15:753–70. doi: 10.1080/15548627.2018.1556946
37. Mills KHG. TLR-Dependent T Cell Activation in Autoimmunity. *Nat Rev Immunol* (2011) 11:807–22. doi: 10.1038/nri3095
38. Lee JY, Sohn KH, Rhee SH, Hwang D. Saturated Fatty Acids, But Not Unsaturated Fatty Acids, Induce the Expression of Cyclooxygenase-2 Mediated Through Toll-Like Receptor 4. *J Biol Chem* (2001) 276:16683–9. doi: 10.1074/jbc.M011695200
39. Soehnlein O, Steffens S, Hidalgo A, Weber C. Neutrophils as Protagonists and Targets in Chronic Inflammation. *Nat Rev Immunol* (2017) 17:248–61. doi: 10.1038/nri.2017.10
40. Buckley CD, Gilroy DW, Serhan CN, Stockinger B, Tak PP. The Resolution of Inflammation. *Nat Rev Immunol* (2013) 13:59–66. doi: 10.1038/nri3362
41. Leuti A, Fazio D, Fava M, Piccoli A, Oddi S, Maccarrone M. Bioactive Lipids, Inflammation and Chronic Diseases. *Adv Drug Delivery Rev* (2020) 159:133–69. doi: 10.1016/j.addr.2020.06.028
42. Kobayashi H, Higashiura Y, Shigetomi H, Kajihara H. Pathogenesis of Endometriosis: The Role of Initial Infection and Subsequent Sterile Inflammation (Review). *Mol Med Rep* (2014) 9:9–15. doi: 10.3892/mmr.2013.1755
43. Liew PX, Kubes P. The Neutrophil's Role During Health and Disease. *Physiol Rev* (2019) 99:1223–48. doi: 10.1152/physrev.00012.2018
44. Silvestre-Roig C, Braster Q, Ortega-Gomez A, Soehnlein O. Neutrophils as Regulators of Cardiovascular Inflammation. *Nat Rev Cardiol* (2020) 17:327–40. doi: 10.1038/s41569-019-0326-7
45. Ley K, Hoffman HM, Kubes P, Cassatella MA, Zychlinsky A, Hedrick CC, et al. Neutrophils: New Insights and Open Questions. *Sci Immunol* (2018) 3: eaat4579. doi: 10.1126/sciimmunol.aat4579
46. Lawrence SM, Corriden R, Nizet V. How Neutrophils Meet Their End. *Trends Immunol* (2020) 41:531–44. doi: 10.1016/j.it.2020.03.008
47. Greenlee-Wacker MC, Rigby KM, Kobayashi SD, Porter AR, DeLeo FR, Nauseef WM. Phagocytosis of Staphylococcus Aureus by Human Neutrophils Prevents Macrophage Efferocytosis and Induces Programmed Necrosis. *J Immunol* (2014) 192:4709–17. doi: 10.4049/jimmunol.1302692
48. Kambara H, Liu F, Zhang X, Liu P, Bajrami B, Teng Y, et al. Gasdermin D Exerts Anti-Inflammatory Effects by Promoting Neutrophil Death. *Cell Rep* (2018) 22:2924–36. doi: 10.1016/j.celrep.2018.02.067
49. Lee KH, Kronbichler A, Park DD-Y, Park Y, Moon H, Kim H, et al. Neutrophil Extracellular Traps (NETs) in Autoimmune Diseases: A Comprehensive Review. *Autoimmun Rev* (2017) 16:1160–73. doi: 10.1016/j.autrev.2017.09.012
50. Castanheira FVS, Kubes P. Neutrophils and NETs in Modulating Acute and Chronic Inflammation. *Blood* (2019) 133:2178–85. doi: 10.1182/blood-2018-11-844530
51. Shapouri-Moghaddam A, Mohammadian S, Vazini H, Taghadosi M, Esmaeili S, Mardani F, et al. Macrophage Plasticity, Polarization, and Function in Health and Disease. *J Cell Physiol* (2018) 233:6425–40. doi: 10.1002/jcp.26429
52. Tabas I, Bornfeldt KE. Intracellular and Intercellular Aspects of Macrophage Immunometabolism in Atherosclerosis. *Circ Res* (2020) 126:1209–27. doi: 10.1161/CIRCRESAHA.119.315939
53. Wynn TA, Vannella KM. Macrophages in Tissue Repair, Regeneration, and Fibrosis. *Immunity* (2016) 44:450–62. doi: 10.1016/j.immuni.2016.02.015
54. Liu CH, Abrams ND, Carrick DM, Chander P, Dwyer J, Hamlet MRJ, et al. Biomarkers of Chronic Inflammation in Disease Development and Prevention: Challenges and Opportunities. *Nat Immunol* (2017) 18:1175–80. doi: 10.1038/ni.3828
55. Dennis EA, Norris PC. Eicosanoid Storm in Infection and Inflammation. *Nat Rev Immunol* (2015) 15:511–23. doi: 10.1038/nri3859
56. Nathan C. Points of Control in Inflammation. *Nature* (2002) 420:846–52. doi: 10.1038/nature01320
57. Serhan CN, Savill J. Resolution of Inflammation: The Beginning Programs the End. *Nat Immunol* (2005) 6:1191–7. doi: 10.1038/ni1276
58. Buckley CD, Gilroy DW, Serhan CN. Proresolving Lipid Mediators and Mechanisms in the Resolution of Acute Inflammation. *Immunity* (2014) 40:315–27. doi: 10.1016/j.immuni.2014.02.009
59. Onali S, Favale A, Fantini MC. The Resolution of Intestinal Inflammation: The Peace-Keeper's Perspective. *Cells* (2019) 8:344. doi: 10.3390/cells8040344
60. Uderhardt S, Herrmann M, Oskolkova OV, Aschermann S, Bicker W, Ipseiz N, et al. 12/15-Lipoxygenase Orchestrates the Clearance of Apoptotic Cells and Maintains Immunologic Tolerance. *Immunity* (2012) 36:834–46. doi: 10.1016/j.immuni.2012.03.010
61. Wakim LM, Bevan MJ. Cross-Dressed Dendritic Cells Drive Memory CD8+ T-Cell Activation After Viral Infection. *Nature* (2011) 471:629–32. doi: 10.1038/nature09863
62. Nakano H, Lin KL, Yanagita M, Charbonneau C, Cook DN, Kakiuchi T, et al. Blood-Derived Inflammatory Dendritic Cells in Lymph Nodes Stimulate Acute T Helper Type 1 Immune Responses. *Nat Immunol* (2009) 10:394–402. doi: 10.1038/ni.1707
63. Newson J, Motwani MP, Kendall AC, Nicolaou A, Muccioli GG, Alhouayek M, et al. Inflammatory Resolution Triggers a Prolonged Phase of Immune Suppression Through COX-1/mPGES-1-Derived Prostaglandin E 2. *Cell Rep* (2017) 20:3162–75. doi: 10.1016/j.celrep.2017.08.098
64. Chung HY, Kim DH, Lee EK, Chung KW, Chung S, Lee B, et al. Redefining Chronic Inflammation in Aging and Age-Related Diseases: Proposal of the Senoinflammation Concept. *Aging Dis* (2019) 10:367. doi: 10.14336/AD.2018.0324
65. Hook M, Roy S, Williams EG, Bou Sleiman M, Mozhui K, Nelson JF, et al. Genetic Cartography of Longevity in Humans and Mice: Current Landscape and Horizons. *Biochim Biophys Acta BBA - Mol Basis Dis* (2018) 1864:2718–32. doi: 10.1016/j.bbadis.2018.01.026
66. González-Quiroz M, Blondel A, Sagredo A, Hetz C, Chevet E, Pedeux R. When Endoplasmic Reticulum Proteostasis Meets the DNA Damage Response. *Trends Cell Biol* (2020) 30:881–91. doi: 10.1016/j.tcb.2020.09.002
67. Dufey E, Bravo-San Pedro JM, Eggers C, González-Quiroz M, Urra H, Sagredo AI, et al. Genotoxic Stress Triggers the Activation of IRE1α-Dependent RNA Decay to Modulate the DNA Damage Response. *Nat Commun* (2020) 11:2401. doi: 10.1038/s41467-020-15694-y
68. Abdullah A, Ravanan P. The Unknown Face of IRE1α – Beyond ER Stress. *Eur J Cell Biol* (2018) 97:359–68. doi: 10.1016/j.ejcb.2018.05.002
69. Prattichizzo F, Bonafè M, Giuliani A, Costantini A, Storci G, Sabbatinelli J, et al. Response to: Letter to the Editor on "Bonafè M, Prattichizzo F, Giuliani A, Storci G, Sabbatinelli J, Olivieri F. Inflamm-Aging: Why Older Men are the Most Susceptible to SARS-CoV-2 Complicated Outcomes. Cytokine Growth Factor Rev" by Eugenia Quiros-Roldan, Giorgio Biasiotto and Isabella Zanella. *Cytokine Growth Factor Rev* (2021) 58:141–3. doi: 10.1016/j.cytogfr.2020.07.013
70. Acosta JC, Banito A, Wuestefeld T, Georgilis A, Janich P, Morton JP, et al. A Complex Secretory Program Orchestrated by the Inflammasome Controls Paracrine Senescence. *Nat Cell Biol* (2013) 15:978–90. doi: 10.1038/ncb2784
71. Kadota T, Fujita Y, Yoshioka Y, Araya J, Kuwano K, Ochiya T. Emerging Role of Extracellular Vesicles as a Senescence-Associated Secretory Phenotype: Insights Into the Pathophysiology of Lung Diseases. *Mol Aspects Med* (2018) 60:92–103. doi: 10.1016/j.mam.2017.11.005
72. Fafián-Labora JA, O'Loghlen A. Classical and Nonclassical Intercellular Communication in Senescence and Ageing. *Trends Cell Biol* (2020) 30:628–39. doi: 10.1016/j.tcb.2020.05.003
73. Dooley J, Liston A. Molecular Control Over Thymic Involution: From Cytokines and Micro RNA to Aging and Adipose Tissue: HIGHLIGHTS. *Eur J Immunol* (2012) 42:1073–9. doi: 10.1002/eji.201142305
74. Haynes L, Swain SL. Why Aging T Cells Fail: Implications for Vaccination. *Immunity* (2006) 24:663–6. doi: 10.1016/j.immuni.2006.06.003
75. Sherer Y, Gorstein A, Fritzler MJ, Shoenfeld Y. Autoantibody Explosion in Systemic Lupus Erythematosus: More Than 100 Different Antibodies Found in SLE Patients. *Semin Arthritis Rheum* (2004) 34:501–37. doi: 10.1016/j.semarthrit.2004.07.002
76. Spengler J, Lugonja B, Jimmy Ytterberg A, Zubarev RA, Creese AJ, Pearson MJ, et al. Release of Active Peptidyl Arginine Deiminases by Neutrophils Can

Explain Production of Extracellular Citrullinated Autoantigens in Rheumatoid Arthritis Synovial Fluid: ENZYMATICALLY ACTIVE PADs AND AUTOANTIGEN PRODUCTION IN RA Sf. *Arthritis Rheumatol* (2015) 67:3135–45. doi: 10.1002/art.39313

77. Allen IC, TeKippe EM, Woodford R-MT, Uronis JM, Holl EK, Rogers AB, et al. The NLRP3 Inflammasome Functions as a Negative Regulator of Tumorigenesis During Colitis-Associated Cancer. *J Exp Med* (2010) 207:1045–56. doi: 10.1084/jem.20100050
78. Madsen CM, Varbo A, Nordestgaard BG. Extreme High High-Density Lipoprotein Cholesterol is Paradoxically Associated With High Mortality in Men and Women: Two Prospective Cohort Studies. *Eur Heart J* (2017) 38:2478–86. doi: 10.1093/eurheartj/ehx163
79. Chistiakov DA, Bobryshev YV, Nikiforov NG, Elizova NV, Sobenin IA, Orekhov AN. Retraction Notice to Macrophage Phenotypic Plasticity in Atherosclerosis: The Associated Features and the Peculiarities of the Expression of Inflammatory Genes, International Journal of Cardiology, Volume 184, 1 April 2015, Pages 436–445. *Int J Cardiol* (2021) 325:186. doi: 10.1016/j.ijcard.2020.12.067
80. Nicholson JK, Holmes E, Kinross J, Burcelin R, Gibson G, Jia W, et al. Host-Gut Microbiota Metabolic Interactions. *Science* (2012) 336:1262–7. doi: 10.1126/science.1223813
81. Zigmond E, Jung S. Intestinal Macrophages: Well Educated Exceptions From the Rule. *Trends Immunol* (2013) 34:162–8. doi: 10.1016/j.it.2013.02.001
82. Kreiner E, Waage J, Standl M, Brix S, Pers TH, Couto Alves A, et al. Shared Genetic Variants Suggest Common Pathways in Allergy and Autoimmune Diseases. *J Allergy Clin Immunol* (2017) 140:771–81. doi: 10.1016/j.jaci.2016.10.055
83. Li B, Selmi C, Tang R, Gershwin ME, Ma X. The Microbiome and Autoimmunity: A Paradigm From the Gut–Liver Axis. *Cell Mol Immunol* (2018) 15:595–609. doi: 10.1038/cmi.2018.7
84. Grolleau-Julius A, Ray D, Yung RL. The Role of Epigenetics in Aging and Autoimmunity. *Clin Rev Allergy Immunol* (2010) 39:42–50. doi: 10.1007/s12016-009-8169-3
85. Van Roosbroeck K, Calin GA. Cancer Hallmarks and MicroRNAs: The Therapeutic Connection. *Adv Cancer Res* (2017) 135:119–49. doi: 10.1016/bs.acr.2017.06.002
86. Kumar Kingsley SM, Vishnu Bhat B. Role of MicroRNAs in the Development and Function of Innate Immune Cells. *Int Rev Immunol* (2017) 36:154–75. doi: 10.1080/08830185.2017.1284212
87. Hidalgo A, Chilvers ER, Summers C, Koenderman L. The Neutrophil Life Cycle. *Trends Immunol* (2019) 40:584–97. doi: 10.1016/j.it.2019.04.013
88. Bjerregaard MD, Jurlander J, Klausen P, Borregaard N, Cowland JB. The *In Vivo* Profile of Transcription Factors During Neutrophil Differentiation in Human Bone Marrow. *Blood* (2003) 101:4322–32. doi: 10.1182/blood-2002-03-0835
89. Klausen P, Bjerregaard MD, Borregaard N, Cowland JB. End-Stage Differentiation of Neutrophil Granulocytes *In Vivo* is Accompanied by Up-Regulation of P27kip1 and Down-Regulation of CDK2, CDK4, and CDK6. *J Leukoc Biol* (2004) 75:569–78. doi: 10.1189/jlb.1003474
90. Smith E, Stark MA, Zarbock A, Burcin TL, Bruce AC, Vaswani D, et al. IL-17a Inhibits the Expansion of IL-17a-Producing T Cells in Mice Through "Short-Loop" Inhibition *via* IL-17 Receptor. *J Immunol* (2008) 181:1357–64. doi: 10.4049/jimmunol.181.2.1357
91. Stark MA, Huo Y, Burcin TL, Morris MA, Olson TS, Ley K. Phagocytosis of Apoptotic Neutrophils Regulates Granulopoiesis *via* IL-23 and IL-17. *Immunity* (2005) 22:285–94. doi: 10.1016/j.immuni.2005.01.011
92. Silvestre-Roig C, Hidalgo A, Soehnlein O. Neutrophil Heterogeneity: Implications for Homeostasis and Pathogenesis. *Blood* (2016) 127:2173–81. doi: 10.1182/blood-2016-01-688887
93. Headland SE, Norling LV. The Resolution of Inflammation: Principles and Challenges. *Semin Immunol* (2015) 27:149–60. doi: 10.1016/j.smim.2015.03.014
94. Kolaczkowska E, Kubes P. Neutrophil Recruitment and Function in Health and Inflammation. *Nat Rev Immunol* (2013) 13:159–75. doi: 10.1038/nri3399
95. Nguyen GT, Green ER, Mecsas J. Neutrophils to the ROScue: Mechanisms of NADPH Oxidase Activation and Bacterial Resistance. *Front Cell Infect Microbiol* (2017) 7:373. doi: 10.3389/fcimb.2017.00373
96. Yin C, Heit B. Armed for Destruction: Formation, Function and Trafficking of Neutrophil Granules. *Cell Tissue Res* (2018) 371:455–71. doi: 10.1007/s00441-017-2731-8
97. Falloon J, Gallin J. Neutrophil Granules in Health and Disease. *J Allergy Clin Immunol* (1986) 77:653–62. doi: 10.1016/0091-6749(86)90404-5
98. Borregaard N. Neutrophils, From Marrow to Microbes. *Immunity* (2010) 33:657–70. doi: 10.1016/j.immuni.2010.11.011
99. Metzemaekers M, Gouwy M, Proost P. Neutrophil Chemoattractant Receptors in Health and Disease: Double-Edged Swords. *Cell Mol Immunol* (2020) 17:433–50. doi: 10.1038/s41423-020-0412-0
100. Serhan CN, Chiang N, Van Dyke TE. 70Resolving Inflammation: Dual Anti-Inflammatory and Pro-Resolution Lipid Mediators. *Nat Rev Immunol* (2008) 8:349–61. doi: 10.1038/nri2294
101. Ariel A, Fredman G, Sun Y-P, Kantarci A, Van Dyke TE, Luster AD, et al. 75Apoptotic Neutrophils and T Cells Sequester Chemokines During Immune Response Resolution Through Modulation of CCR5 Expression. *Nat Immunol* (2006) 7:1209–16. doi: 10.1038/ni1392
102. Tofts PS, Chevassut T, Cutajar M, Dowell NG, Peters AM. Doubts Concerning the Recently Reported Human Neutrophil Lifespan of 54 Days. *Blood* (2011) 117:6050–2. doi: 10.1182/blood-2010-10-310532
103. Pillay J, den Braber I, Vrisekoop N, Kwast LM, de Boer RJ, Borghans JAM, et al. *In Vivo* Labeling With 2H2O Reveals a Human Neutrophil Lifespan of 5.4 Days. *Blood* (2010) 116:625–7. doi: 10.1182/blood-2010-01-259028
104. Summers C, Rankin SM, Condliffe AM, Singh N, Peters AM, Chilvers ER. Neutrophil Kinetics in Health and Disease. *Trends Immunol* (2010) 31:318–24. doi: 10.1016/j.it.2010.05.006
105. Kim M-H, Granick JL, Kwok C, Walker NJ, Borjesson DL, Curry F-RE, et al. Neutrophil Survival and C-Kit+-Progenitor Proliferation in Staphylococcus Aureus–Infected Skin Wounds Promote Resolution. *Blood* (2011) 117:3343–52. doi: 10.1182/blood-2010-07-296970
106. Fox S, Leitch AE, Duffin R, Haslett C, Rossi AG. Neutrophil Apoptosis: Relevance to the Innate Immune Response and Inflammatory Disease. *J Innate Immun* (2010) 2:216–27. doi: 10.1159/000284367
107. Jeannin P, Jaillon S, Delneste Y. Pattern Recognition Receptors in the Immune Response Against Dying Cells. *Curr Opin Immunol* (2008) 20:530–7. doi: 10.1016/j.coi.2008.04.013
108. Biswas SK, Mantovani A. Macrophage Plasticity and Interaction With Lymphocyte Subsets: Cancer as a Paradigm. *Nat Immunol* (2010) 11:889–96. doi: 10.1038/ni.1937
109. Bystrom J, Evans I, Newson J, Stables M, Toor I, van Rooijen N, et al. Resolution-Phase Macrophages Possess a Unique Inflammatory Phenotype That is Controlled by cAMP. *Blood* (2008) 112:4117–27. doi: 10.1182/blood-2007-12-129767
110. Johnnidis JB, Harris MH, Wheeler RT, Stehling-Sun S, Lam MH, Kirak O, et al. Regulation of Progenitor Cell Proliferation and Granulocyte Function by microRNA-223. *Nature* (2008) 451:1125–9. doi: 10.1038/nature06607
111. Zhang L, Wu H, Zhao M, Chang C, Lu Q. Clinical Significance of miRNAs in Autoimmunity. *J Autoimmun* (2020) 109:102438. doi: 10.1016/j.jaut.2020.102438
112. Kim C, Hu B, Jadhav RR, Jin J, Zhang H, Cavanagh MM, et al. Activation of miR-21-Regulated Pathways in Immune Aging Selects Against Signatures Characteristic of Memory T Cells. *Cell Rep* (2018) 25:2148–2162.e5. doi: 10.1016/j.celrep.2018.10.074
113. Hsu AY, Wang D, Liu S, Lu J, Syahirah R, Bennin DA, et al. Phenotypical microRNA Screen Reveals a Noncanonical Role of CDK2 in Regulating Neutrophil Migration. *Proc Natl Acad Sci* (2019) 116:18561–70. doi: 10.1073/pnas.1905221116
114. Mussbacher M, Salzmann M, Brostjan C, Hoesel B, Schoergenhofer C, Datler H, et al. Cell Type-Specific Roles of NF-κb Linking Inflammation and Thrombosis. *Front Immunol* (2019) 10:85. doi: 10.3389/fimmu.2019.00085
115. O'Connell RM, Chaudhuri AA, Rao DS, Baltimore D. Inositol Phosphatase SHIP1 is a Primary Target of miR-155. *Proc Natl Acad Sci* (2009) 106:7113–8. doi: 10.1073/pnas.0902636106
116. Brinkmann V, Reichard U, Goosmann C, Fauler B, Uhlemann Y, Weiss DS, et al. Neutrophil Extracellular Traps Kill Bacteria. *Science* (2004) 303:1532–5. doi: 10.1126/science.1092385

117. Clark SR, Ma AC, Tavener SA, McDonald B, Goodarzi Z, Kelly MM, et al. Platelet TLR4 Activates Neutrophil Extracellular Traps to Ensnare Bacteria in Septic Blood. *Nat Med* (2007) 13:463–9. doi: 10.1038/nm1565
118. Megens RTA, Vijayan S, Lievens D, Döring Y, van Zandvoort MAMJ, Grommes J, et al. Presence of Luminal Neutrophil Extracellular Traps in Atherosclerosis. *Thromb Haemost* (2012) 107:597–8. doi: 10.1160/TH11-09-0650
119. Knight JS, Kaplan MJ. Lupus Neutrophils: 'Net' Gain in Understanding Lupus Pathogenesis. *Curr Opin Rheumatol* (2012) 24:441–50. doi: 10.1097/BOR.0b013e3283546703
120. Ray K. Disordered NETs Implicated in Pathogenesis of MPO-ANCA-Associated Vasculitis. *Nat Rev Rheumatol* (2012) 8:501–1. doi: 10.1038/nrrheum.2012.123
121. Jorch SK, Kubes P. An Emerging Role for Neutrophil Extracellular Traps in Noninfectious Disease. *Nat Med* (2017) 23:279–87. doi: 10.1038/nm.4294
122. von Brühl M-L, Stark K, Steinhart A, Chandraratne S, Konrad I, Lorenz M, et al. Monocytes, Neutrophils, and Platelets Cooperate to Initiate and Propagate Venous Thrombosis in Mice In Vivo. *J Exp Med* (2012) 209:819–35. doi: 10.1084/jem.20112322
123. Kitching AR, Anders H-J, Basu N, Brouwer E, Gordon J, Jayne DR, et al. ANCA-Associated Vasculitis. *Nat Rev Dis Primer* (2020) 6:71. doi: 10.1038/s41572-020-0204-y
124. Hilhorst M, van Paassen P, Tervaert JWC. Proteinase 3-ANCA Vasculitis Versus Myeloperoxidase-ANCA Vasculitis. *J Am Soc Nephrol* (2015) 26:2314–27. doi: 10.1681/ASN.2014090903
125. Kessenbrock K, Krumbholz M, Schönermarck U, Back W, Gross WL, Werb Z, et al. Netting Neutrophils in Autoimmune Small-Vessel Vasculitis. *Nat Med* (2009) 15:623–5. doi: 10.1038/nm.1959
126. Kolaczkowska E, Jenne CN, Surewaard BGJ, Thanabalasuriar A, Lee W-Y, Sanz M-J, et al. Molecular Mechanisms of NET Formation and Degradation Revealed by Intravital Imaging in the Liver Vasculature. *Nat Commun* (2015) 6:6673. doi: 10.1038/ncomms7673
127. Linhares-Lacerda L, Temerozo JR, Ribeiro-Alves M, Azevedo EP, Mojoli A, Nascimento MTC, et al. Neutrophil Extracellular Trap-Enriched Supernatants Carry microRNAs Able to Modulate TNF-α Production by Macrophages. *Sci Rep* (2020) 10:2715. doi: 10.1038/s41598-020-59486-2
128. Castrillo A, Pennington DJ, Otto F, Parker PJ, Owen MJ, Boscá L. Protein Kinase Cε Is Required for Macrophage Activation and Defense Against Bacterial Infection. *J Exp Med* (2001) 194:1231–42. doi: 10.1084/jem.194.9.1231
129. Wu Z, Zhao G, Peng L, Du J, Wang S, Huang Y, et al. Protein Kinase C Beta Mediates CD40 Ligand-Induced Adhesion of Monocytes to Endothelial Cells. *PloS One* (2013) 8:e72593. doi: 10.1371/journal.pone.0072593
130. Parihar SP, Ozturk M, Marakalala MJ, Loots DT, Hurdayal R, Maasdorp DB, et al. Protein Kinase C-Delta (Pkcδ), a Marker of Inflammation and Tuberculosis Disease Progression in Humans, is Important for Optimal Macrophage Killing Effector Functions and Survival in Mice. *Mucosal Immunol* (2018) 11:496–511. doi: 10.1038/mi.2017.68
131. Zhang Y-G, Song Y, Guo X-L, Miao R-Y, Fu Y-Q, Miao C-F, et al. Exosomes Derived From oxLDL-Stimulated Macrophages Induce Neutrophil Extracellular Traps to Drive Atherosclerosis. *Cell Cycle* (2019) 18:2672–82. doi: 10.1080/15384101.2019.1654797
132. de Los Reyes–García AM, Aroca A, Arroyo A, García–Barbera N, Vicente V, González–Conejero R, et al. Neutrophil Extracellular Trap Components Increase the Expression of Coagulation Factors. *BioMed Rep* (2019) 10 (3):195–201. doi: 10.3892/br.2019.1187
133. Mantovani A, Cassatella MA, Costantini C, Jaillon S. Neutrophils in the Activation and Regulation of Innate and Adaptive Immunity. *Nat Rev Immunol* (2011) 11:519–31. doi: 10.1038/nri3024
134. De Melo P, Pineros Alvarez AR, Ye X, Blackman A, Alves-Filho JC, Medeiros AI, et al. Macrophage-Derived MicroRNA-21 Drives Overwhelming Glycolytic and Inflammatory Response During Sepsis *via* Repression of the PGE 2/IL-10 Axis. *J Immunol* (2021) 207:902–12. doi: 10.4049/jimmunol.2001251
135. Fu M, Zhang K. MAPK Interacting Serine/Threonine Kinase 1 (MKNK1), One Target Gene of miR-223-3p, Correlates With Neutrophils in Sepsis Based on Bioinformatic Analysis. *Bioengineered* (2021) 12:2550–62. doi: 10.1080/21655979.2021.1935405
136. Arroyo AB, Águila S, Fernández-Pérez MP, de los Reyes-García AM, Reguilón-Gallego L, Zapata-Martínez L, et al. miR-146a in Cardiovascular Diseases and Sepsis: An Additional Burden in the Inflammatory Balance? *Thromb Haemost* (2021) 121:1138–50. doi: 10.1055/a-1342-3648
137. Arroyo AB, Fernández-Pérez MP, del Monte A, Águila S, Méndez Rl, Hernández-Antolín R, et al. miR-146a is a Pivotal Regulator of Neutrophil Extracellular Trap Formation Promoting Thrombosis. *Haematologica* (2020) 106:1636–46. doi: 10.3324/haematol.2019.240226
138. Goodwin AJ, Li P, Halushka PV, Cook JA, Sumal AS, Fan H. Circulating miRNA 887 is Differentially Expressed in ARDS and Modulates Endothelial Function. *Am J Physiol-Lung Cell Mol Physiol* (2020) 318:L1261–9. doi: 10.1152/ajplung.00494.2019
139. Gomez I, Ward B, Souilhol C, Recarti C, Ariaans M, Johnston J, et al. Neutrophil Microvesicles Drive Atherosclerosis by Delivering miR-155 to Atheroprone Endothelium. *Nat Commun* (2020) 11:214. doi: 10.1038/s41467-019-14043-y
140. Chen B, Han J, Chen S, Xie R, Yang J, Zhou T, et al. MicroLet-7b Regulates Neutrophil Function and Dampens Neutrophilic Inflammation by Suppressing the Canonical TLR4/NF-κb Pathway. *Front Immunol* (2021) 12:653344. doi: 10.3389/fimmu.2021.653344
141. Xu W, Wang Y, Ma Y, Yang J. MiR-223 Plays a Protecting Role in Neutrophilic Asthmatic Mice Through the Inhibition of NLRP3 Inflammasome. *Respir Res* (2020) 21:116. doi: 10.1186/s12931-020-01374-4
142. Gomez JL, Chen A, Diaz MP, Zirn N, Gupta A, Britto C, et al. A Network of Sputum MicroRNAs Is Associated With Neutrophilic Airway Inflammation in Asthma. *Am J Respir Crit Care Med* (2020) 202:51–64. doi: 10.1164/rccm.201912-2360OC
143. Huang Y, Zhang S, Fang X, Qin L, Fan Y, Ding D, et al. Plasma miR-199a-5p is Increased in Neutrophilic Phenotype Asthma Patients and Negatively Correlated With Pulmonary Function. *PloS One* (2018) 13:e0193502. doi: 10.1371/journal.pone.0193502
144. Maes T, Cobos FA, Schleich F, Sorbello V, Henket M, De Preter K, et al. Asthma Inflammatory Phenotypes Show Differential microRNA Expression in Sputum. *J Allergy Clin Immunol* (2016) 137:1433–46. doi: 10.1016/j.jaci.2016.02.018
145. Blanco LP, Wang X, Carlucci PM, Torres-Ruiz JJ, Romo-Tena J, Sun H, et al. RNA Externalized by Neutrophil Extracellular Traps Promotes Inflammatory Pathways in Endothelial Cells. *Arthritis Rheumatol* (2021) 73:2282–92. doi: 10.1002/art.41796
146. Smith S, Wu PW, Seo JJ, Fernando T, Jin M, Contreras J, et al. IL-16/miR-125a Axis Controls Neutrophil Recruitment in Pristane-Induced Lung Inflammation. *JCI Insight* (2018) 3:e120798. doi: 10.1172/jci.insight.120798
147. Roffel MP, Maes T, Brandsma C-A, van den Berge M, Vanaudenaerde BM, Joos GF, et al. MiR-223 is Increased in Lungs of Patients With COPD and Modulates Cigarette Smoke-Induced Pulmonary Inflammation. *Am J Physiol-Lung Cell Mol Physiol* (2021) 321:L1091–104. doi: 10.1152/ajplung.00252.2021
148. Butin-Israeli V, Bui TM, Wiesolek HL, Mascarenhas L, Lee JJ, Mehl LC, et al. Neutrophil-Induced Genomic Instability Impedes Resolution of Inflammation and Wound Healing. *J Clin Invest* (2019) 129:712–26. doi: 10.1172/JCI122085
149. Liao T-L, Chen Y-M, Tang K-T, Chen P-K, Liu H-J, Chen D-Y. MicroRNA-223 Inhibits Neutrophil Extracellular Traps Formation Through Regulating Calcium Influx and Small Extracellular Vesicles Transmission. *Sci Rep* (2021) 11:15676. doi: 10.1038/s41598-021-95028-0
150. Merx MW, Weber C. Sepsis and the Heart. *Circulation* (2007) 116:793–802. doi: 10.1161/CIRCULATIONAHA.106.678359
151. Sockrider M, Fussner L. What Is Asthma? *Am J Respir Crit Care Med* (2020) 202:P25–6. doi: 10.1164/rccm.2029P25
152. Shi Z-G, Sun Y, Wang K-S, Jia J-D, Yang J, Li Y-N. Effects of miR-26a/miR-146a/miR-31 on Airway Inflammation of Asthma Mice and Asthma Children. *Eur Rev Med Pharmacol Sci* (2019) 23:5432–40. doi: 10.26355/eurrev_201906_18212
153. Durcan L, O'Dwyer T, Petri M. Management Strategies and Future Directions for Systemic Lupus Erythematosus in Adults. *Lancet* (2019) 393:2332–43. doi: 10.1016/S0140-6736(19)30237-5
154. De la Rosa IA, Perez-Sanchez C, Ruiz-Limon P, Patiño-Trives A, Torres-Granados C, Jimenez-Gomez Y, et al. Impaired microRNA Processing in

Neutrophils From Rheumatoid Arthritis Patients Confers Their Pathogenic Profile. Modulation by Biological Therapies. *Haematologica* (2020) 105:2250–61. doi: 10.3324/haematol.2018.205047
155. Epelman S, Lavine KJ, Randolph GJ. Origin and Functions of Tissue Macrophages. *Immunity* (2014) 41:21–35. doi: 10.1016/j.immuni.2014.06.013
156. Boyle WJ, Simonet WS, Lacey DL. Osteoclast Differentiation and Activation. *Nature* (2003) 423:337–42. doi: 10.1038/nature01658
157. Muller PA, Koscsó B, Rajani GM, Stevanovic K, Berres M-L, Hashimoto D, et al. Crosstalk Between Muscularis Macrophages and Enteric Neurons Regulates Gastrointestinal Motility. *Cell* (2014) 158:300–13. doi: 10.1016/j.cell.2014.04.050
158. Parkhurst CN, Yang G, Ninan I, Savas JN, Yates JR, Lafaille JJ, et al. Microglia Promote Learning-Dependent Synapse Formation Through Brain-Derived Neurotrophic Factor. *Cell* (2013) 155:1596–609. doi: 10.1016/j.cell.2013.11.030
159. Varol C, Mildner A, Jung S. Macrophages: Development and Tissue Specialization. *Annu Rev Immunol* (2015) 33:643–75. doi: 10.1146/annurev-immunol-032414-112220
160. Gordon S, Plüddemann A. Tissue Macrophages: Heterogeneity and Functions. *BMC Biol* (2017) 15:53. doi: 10.1186/s12915-017-0392-4
161. Kuznetsova T, Prange KHM, Glass CK, de Winther MPJ. Transcriptional and Epigenetic Regulation of Macrophages in Atherosclerosis. *Nat Rev Cardiol* (2020) 17:216–28. doi: 10.1038/s41569-019-0265-3
162. Zhang Q, Wang J, Zhang J, Wen J, Zhao G, Li Q. Differential mRNA and miRNA Profiles Reveal the Potential Roles of Genes and miRNAs Involved in LPS Infection in Chicken Macrophages. *Genes* (2021) 12:760. doi: 10.3390/genes12050760
163. Natoli G, Ghisletti S, Barozzi I. The Genomic Landscapes of Inflammation. *Genes Dev* (2011) 25:101–6. doi: 10.1101/gad.2018811
164. Wei Y, Schober A. MicroRNA Regulation of Macrophages in Human Pathologies. *Cell Mol Life Sci* (2016) 73:3473–95. doi: 10.1007/s00018-016-2254-6
165. Sica A, Mantovani A. Macrophage Plasticity and Polarization: *In Vivo* Veritas. *J Clin Invest* (2012) 122:787–95. doi: 10.1172/JCI59643
166. Funes SC, Rios M, Escobar-Vera J, Kalergis AM. Implications of Macrophage Polarization in Autoimmunity. *Immunology* (2018) 154:186–95. doi: 10.1111/imm.12910
167. Murray PJ, Allen JE, Biswas SK, Fisher EA, Gilroy DW, Goerdt S, et al. Macrophage Activation and Polarization: Nomenclature and Experimental Guidelines. *Immunity* (2014) 41:14–20. doi: 10.1016/j.immuni.2014.06.008
168. Sica A, Invernizzi P, Mantovani A. Macrophage Plasticity and Polarization in Liver Homeostasis and Pathology: Sica Et al. *Hepatology* (2014) 59:2034–42. doi: 10.1002/hep.26754
169. Muñoz J, Akhavan NS, Mullins AP, Arjmandi BH. Macrophage Polarization and Osteoporosis: A Review. *Nutrients* (2020) 12:2999. doi: 10.3390/nu12102999
170. Jetten N, Verbruggen S, Gijbels MJ, Post MJ, De Winther MPJ, Donners MMPC. Anti-Inflammatory M2, But Not Pro-Inflammatory M1 Macrophages Promote Angiogenesis In Vivo. *Angiogenesis* (2014) 17:109–18. doi: 10.1007/s10456-013-9381-6
171. Braga TT, Agudelo JSH, Camara NOS. Macrophages During the Fibrotic Process: M2 as Friend and Foe. *Front Immunol* (2015) 6:602. doi: 10.3389/fimmu.2015.00602
172. Takeuch O, Akira S. Epigenetic Control of Macrophage Polarization. *Eur J Immunol* (2011) 41:2490–3. doi: 10.1002/eji.201141792
173. Ivashkiv LB. Epigenetic Regulation of Macrophage Polarization and Function. *Trends Immunol* (2013) 34:216–23. doi: 10.1016/j.it.2012.11.001
174. Van den Bossche J, Neele AE, Hoeksema MA, de Winther MPJ. Macrophage Polarization: The Epigenetic Point of View. *Curr Opin Lipidol* (2014) 25:367–73. doi: 10.1097/MOL.0000000000000109
175. Zhong Y, Yi C. MicroRNA-720 Suppresses M2 Macrophage Polarization by Targeting GATA3. *Biosci Rep* (2016) 36:e00363. doi: 10.1042/BSR20160105
176. Ying H, Kang Y, Zhang H, Zhao D, Xia J, Lu Z, et al. MiR-127 Modulates Macrophage Polarization and Promotes Lung Inflammation and Injury by Activating the JNK Pathway. *J Immunol* (2015) 194:1239–51. doi: 10.4049/jimmunol.1402088
177. Pasca S, Jurj A, Petrushev B, Tomuleasa C, Matei D. MicroRNA-155 Implication in M1 Polarization and the Impact in Inflammatory Diseases. *Front Immunol* (2020) 11:625. doi: 10.3389/fimmu.2020.00625
178. Wei Y, Zhu M, Corbalán-Campos J, Heyll K, Weber C, Schober A. Regulation of Csf1r and Bcl6 in Macrophages Mediates the Stage-Specific Effects of MicroRNA-155 on Atherosclerosis. *Arterioscler Thromb Vasc Biol* (2015) 35:796–803. doi: 10.1161/ATVBAHA.114.304723
179. Vergadi E, Vaporidi K, Theodorakis EE, Doxaki C, Lagoudaki E, Ieronymaki E, et al. Akt2 Deficiency Protects From Acute Lung Injury *via* Alternative Macrophage Activation and miR-146a Induction in Mice. *J Immunol* (2014) 192:394–406. doi: 10.4049/jimmunol.1300959
180. Wang Z, Brandt S, Medeiros A, Wang S, Wu H, Dent A, et al. MicroRNA 21 Is a Homeostatic Regulator of Macrophage Polarization and Prevents Prostaglandin E2-Mediated M2 Generation. *PloS One* (2015) 10:e0115855. doi: 10.1371/journal.pone.0115855
181. Curtale G, Mirolo M, Renzi TA, Rossato M, Bazzoni F, Locati M. Negative Regulation of Toll-Like Receptor 4 Signaling by IL-10-Dependent microRNA-146b. *Proc Natl Acad Sci* (2013) 110:11499–504. doi: 10.1073/pnas.1219852110
182. Taganov KD, Boldin MP, Chang K-J, Baltimore D. NF- B-Dependent Induction of microRNA miR-146, an Inhibitor Targeted to Signaling Proteins of Innate Immune Responses. *Proc Natl Acad Sci* (2006) 103:12481–6. doi: 10.1073/pnas.0605298103
183. O'Connell RM, Taganov KD, Boldin MP, Cheng G, Baltimore D. MicroRNA-155 is Induced During the Macrophage Inflammatory Response. *Proc Natl Acad Sci* (2007) 104:1604–9. doi: 10.1073/pnas.0610731104
184. Wang P, Hou J, Lin L, Wang C, Liu X, Li D, et al. Inducible microRNA-155 Feedback Promotes Type I IFN Signaling in Antiviral Innate Immunity by Targeting Suppressor of Cytokine Signaling 1. *J Immunol* (2010) 185:6226–33. doi: 10.4049/jimmunol.1000491
185. Pashangzadeh S, Motallebnezhad M, Vafashoar F, Khalvandi A, Mojtabavi N. Implications the Role of miR-155 in the Pathogenesis of Autoimmune Diseases. *Front Immunol* (2021) 12:669382. doi: 10.3389/fimmu.2021.669382
186. Bala S, Csak T, Saha B, Zatsiorsky J, Kodys K, Catalano D, et al. The Pro-Inflammatory Effects of miR-155 Promote Liver Fibrosis and Alcohol-Induced Steatohepatitis. *J Hepatol* (2016) 64:1378–87. doi: 10.1016/j.jhep.2016.01.035
187. Wang JK, Wang Z, Li G. MicroRNA-125 in Immunity and Cancer. *Cancer Lett* (2019) 454:134–45. doi: 10.1016/j.canlet.2019.04.015
188. Tiedt S, Prestel M, Malik R, Schieferdecker N, Duering M, Kautzky V, et al. RNA-Seq Identifies Circulating miR-125a-5p, miR-125b-5p, and miR-143-3p as Potential Biomarkers for Acute Ischemic Stroke. *Circ Res* (2017) 121:970–80. doi: 10.1161/CIRCRESAHA.117.311572
189. Ding J, Zhang Y, Cai X, Zhang Y, Yan S, Wang J, et al. Extracellular Vesicles Derived From M1 Macrophages Deliver miR-146a-5p and miR-146b-5p to Suppress Trophoblast Migration and Invasion by Targeting TRAF6 in Recurrent Spontaneous Abortion. *Theranostics* (2021) 11:5813–30. doi: 10.7150/thno.58731
190. Mantovani A, Sica A, Sozzani S, Allavena P, Vecchi A, Locati M. The Chemokine System in Diverse Forms of Macrophage Activation and Polarization. *Trends Immunol* (2004) 25:677–86. doi: 10.1016/j.it.2004.09.015
191. Moreira Lopes TC, Mosser DM, Gonçalves R. Macrophage Polarization in Intestinal Inflammation and Gut Homeostasis. *Inflammation Res* (2020) 69:1163–72. doi: 10.1007/s00011-020-01398-y
192. Remmerie A, Scott CL. Macrophages and Lipid Metabolism. *Cell Immunol* (2018) 330:27–42. doi: 10.1016/j.cellimm.2018.01.020
193. Netea MG, Balkwill F, Chonchol M, Cominelli F, Donath MY, Giamarellos-Bourboulis EJ, et al. Author Correction: A Guiding Map for Inflammation. *Nat Immunol* (2021) 22:254–4. doi: 10.1038/s41590-020-00846-5
194. Bashir S, Sharma Y, Elahi A, Khan F. Macrophage Polarization: The Link Between Inflammation and Related Diseases. *Inflammation Res* (2016) 65:1–11. doi: 10.1007/s00011-015-0874-1
195. Locati M, Curtale G, Mantovani A. Diversity, Mechanisms, and Significance of Macrophage Plasticity. *Annu Rev Pathol Mech Dis* (2020) 15:123–47. doi: 10.1146/annurev-pathmechdis-012418-012718

196. Das A, Sinha M, Datta S, Abas M, Chaffee S, Sen CK, et al. Monocyte and Macrophage Plasticity in Tissue Repair and Regeneration. *Am J Pathol* (2015) 185:2596–606. doi: 10.1016/j.ajpath.2015.06.001
197. Wei Y, Nazari-Jahantigh M, Chan L, Zhu M, Heyll K, Corbalán-Campos J, et al. The microRNA-342-5p Fosters Inflammatory Macrophage Activation Through an Akt1- and microRNA-155 –Dependent Pathway During Atherosclerosis. *Circulation* (2013) 127:1609–19. doi: 10.1161/CIRCULATIONAHA.112.000736
198. Lin C-M, Wang B-W, Pan C-M, Fang W-J, Chua S-K, Cheng W-P, et al. Chrysin Boosts KLF2 Expression Through Suppression of Endothelial Cell-Derived Exosomal microRNA-92a in the Model of Atheroprotection. *Eur J Nutr* (2021) 60:4345–55. doi: 10.1007/s00394-021-02593-1
199. Karshovska E, Wei Y, Subramanian P, Mohibullah R, Geißler C, Baatsch I, et al. HIF-1α (Hypoxia-Inducible Factor-1α) Promotes Macrophage Necroptosis by Regulating miR-210 and miR-383. *Arterioscler Thromb Vasc Biol* (2020) 40:583–96. doi: 10.1161/ATVBAHA.119.313290
200. Wei Y, Corbalán-Campos J, Gurung R, Natarelli L, Zhu M, Exner N, et al. Dicer in Macrophages Prevents Atherosclerosis by Promoting Mitochondrial Oxidative Metabolism. *Circulation* (2018) 138:2007–20. doi: 10.1161/CIRCULATIONAHA.117.031589
201. Wang D, Wang W, Lin W, Yang W, Zhang P, Chen M, et al. Apoptotic Cell Induction of miR-10b in Macrophages Contributes to Advanced Atherosclerosis Progression in ApoE−/− Mice. *Cardiovasc Res* (2018) 114:1794–805. doi: 10.1093/cvr/cvy132
202. Meiler S, Baumer Y, Toulmin E, Seng K, Boisvert WA. MicroRNA 302a Is a Novel Modulator of Cholesterol Homeostasis and Atherosclerosis. *Arterioscler Thromb Vasc Biol* (2015) 35:323–31. doi: 10.1161/ATVBAHA.114.304878
203. Zhang F, Zhao J, Sun D, Wei N. MiR-155 Inhibits Transformation of Macrophages Into Foam Cells *via* Regulating CEH Expression. *BioMed Pharmacother* (2018) 104:645–51. doi: 10.1016/j.biopha.2018.05.068
204. Xu Y, Xu Y, Zhu Y, Sun H, Juguilon C, Li F, et al. Macrophage miR-34a Is a Key Regulator of Cholesterol Efflux and Atherosclerosis. *Mol Ther* (2020) 28:202–16. doi: 10.1016/j.ymthe.2019.09.008
205. Yang H-X, Jiang H-B, Luo L. MiR-140a Contributes to the Pro-Atherosclerotic Phenotype of Macrophages by Downregulating Interleukin-10. *Eur Rev Med Pharmacol Sci* (2020) 24:9139–46. doi: 10.26355/eurrev_202009_22861
206. Zhu J, Liu B, Wang Z, Wang D, Ni H, Zhang L, et al. Exosomes From Nicotine-Stimulated Macrophages Accelerate Atherosclerosis Through miR-21-3p/PTEN-Mediated VSMC Migration and Proliferation. *Theranostics* (2019) 9:6901–19. doi: 10.7150/thno.37357
207. Pan Y, Hui X, Hoo RLC, Ye D, Chan CYC, Feng T, et al. Adipocyte-Secreted Exosomal microRNA-34a Inhibits M2 Macrophage Polarization to Promote Obesity-Induced Adipose Inflammation. *J Clin Invest* (2019) 129:834–49. doi: 10.1172/JCI123069
208. Tian F, Tang P, Sun Z, Zhang R, Zhu D, He J, et al. miR-210 in Exosomes Derived From Macrophages Under High Glucose Promotes Mouse Diabetic Obesity Pathogenesis by Suppressing NDUFA4 Expression. *J Diabetes Res* (2020) 2020:1–12. doi: 10.1155/2020/6894684
209. Ying W, Gao H, Dos Reis FCG, Bandyopadhyay G, Ofrecio JM, Luo Z, et al. MiR-690, an Exosomal-Derived miRNA From M2-Polarized Macrophages, Improves Insulin Sensitivity in Obese Mice. *Cell Metab* (2021) 33:781–90.e5. doi: 10.1016/j.cmet.2020.12.019
210. Gajeton J, Krukovets I, Yendamuri R, Verbovetskiy D, Vasanji A, Sul L, et al. miR-467 Regulates Inflammation and Blood Insulin and Glucose. *J Cell Mol Med* (2021) 25:2549–62. doi: 10.1111/jcmm.16224
211. Escate R, Mata P, Cepeda JM, Padró T, Badimon L. miR-505-3p Controls Chemokine Receptor Up-Regulation in Macrophages: Role in Familial Hypercholesterolemia. *FASEB J* (2018) 32:601–12. doi: 10.1096/fj.201700476RR
212. Sun Y, Zhou Y, Shi Y, Zhang Y, Liu K, Liang R, et al. Expression of miRNA-29 in Pancreatic β Cells Promotes Inflammation and Diabetes *via* TRAF3. *Cell Rep* (2021) 34:108576. doi: 10.1016/j.celrep.2020.108576
213. Talari M, Nayak TKS, Kain V, Babu PP, Misra P, Parsa KVL. MicroRNA-712 Restrains Macrophage Pro-Inflammatory Responses by Targeting LRRK2 Leading to Restoration of Insulin Stimulated Glucose Uptake by Myoblasts. *Mol Immunol* (2017) 82:1–9. doi: 10.1016/j.molimm.2016.12.014
214. Adlakha YK, Khanna S, Singh R, Singh VP, Agrawal A, Saini N. Pro-Apoptotic miRNA-128-2 Modulates ABCA1, ABCG1 and Rxrα Expression and Cholesterol Homeostasis. *Cell Death Dis* (2013) 4:e780–0. doi: 10.1038/cddis.2013.301
215. Quero L, Tiaden AN, Hanser E, Roux J, Laski A, Hall J, et al. miR-221-3p Drives the Shift of M2-Macrophages to a Pro-Inflammatory Function by Suppressing JAK3/STAT3 Activation. *Front Immunol* (2020) 10:3087. doi: 10.3389/fimmu.2019.03087
216. Ren B, Liu J, Wu K, Zhang J, Lv Y, Wang S, et al. TNF-α-Elicited miR-29b Potentiates Resistance to Apoptosis in Peripheral Blood Monocytes From Patients With Rheumatoid Arthritis. *Apoptosis* (2019) 24:892–904. doi: 10.1007/s10495-019-01567-3
217. Donate PB, Alves de Lima K, Peres RS, Almeida F, Fukada SY, Silva TA, et al. Cigarette Smoke Induces miR-132 in Th17 Cells That Enhance Osteoclastogenesis in Inflammatory Arthritis. *Proc Natl Acad Sci* (2021) 118:e2017120118. doi: 10.1073/pnas.2017120118
218. Hegewald AB, Breitwieser K, Ottinger SM, Mobarrez F, Korotkova M, Rethi B, et al. Extracellular miR-574-5p Induces Osteoclast Differentiation *via* TLR 7/8 in Rheumatoid Arthritis. *Front Immunol* (2020) 11:585282. doi: 10.3389/fimmu.2020.585282
219. Kong XH. MicroRNA-20a Suppresses RANKL-Modulates Osteoclastogenesis and Prevents Bone Erosion in Mice With Rheumatoid Arthritis Through the TLR4/p38 Pathway. *J Biol Regul Homeost Agents* (2021) 35(3):921–31. doi: 10.23812/20-604-A
220. Xu D, Song M, Chai C, Wang J, Jin C, Wang X, et al. Exosome-Encapsulated miR-6089 Regulates Inflammatory Response *via* Targeting TLR4. *J Cell Physiol* (2019) 234:1502–11. doi: 10.1002/jcp.27014
221. Zhu Y, Gu L, Li Y, Lin X, Shen H, Cui K, et al. miR-148a Inhibits Colitis and Colitis-Associated Tumorigenesis in Mice. *Cell Death Differ* (2017) 24:2199–209. doi: 10.1038/cdd.2017.151
222. Deng F, Yan J, Lu J, Luo M, Xia P, Liu S, et al. M2 Macrophage-Derived Exosomal miR-590-3p Attenuates DSS-Induced Mucosal Damage and Promotes Epithelial Repair *via* the LATS1/YAP/ β-Catenin Signalling Axis. *J Crohns Colitis* (2021) 15:665–77. doi: 10.1093/ecco-jcc/jjaa214
223. Cai X, Zhang Z, Yuan J, Ocansey DKW, Tu Q, Zhang X, et al. hucMSC-Derived Exosomes Attenuate Colitis by Regulating Macrophage Pyroptosis *via* the miR-378a-5p/NLRP3 Axis. *Stem Cell Res Ther* (2021) 12:416. doi: 10.1186/s13287-021-02492-6
224. Guo F, Tang C, Li Y, Liu Y, Lv P, Wang W, et al. The Interplay of Lnc RNA ANRIL and miR-181b on the Inflammation-Relevant Coronary Artery Disease Through Mediating NF -κb Signalling Pathway. *J Cell Mol Med* (2018) 22:5062–75. doi: 10.1111/jcmm.13790
225. Liechty C, Hu J, Zhang L, Liechty KW, Xu J. Role of microRNA-21 and Its Underlying Mechanisms in Inflammatory Responses in Diabetic Wounds. *Int J Mol Sci* (2020) 21:3328. doi: 10.3390/ijms21093328
226. Smolen JS, Aletaha D, McInnes IB. Rheumatoid Arthritis. *Lancet* (2016) 388:2023–38. doi: 10.1016/S0140-6736(16)30173-8

Conflict of Interest: The authors declare that the research was conducted in the absence of any commercial or financial relationships that could be construed as a potential conflict of interest.

frontiers | Frontiers in Immunology

REVIEW
published: 04 July 2022
doi: 10.3389/fimmu.2022.940930

The Neonatal Innate Immune Response to Sepsis: Checkpoint Proteins as Novel Mediators of This Response and as Possible Therapeutic/Diagnostic Levers

Emily Hensler[1,2], *Habesha Petros*[2], *Chyna C. Gray*[1,2], *Chun-Shiang Chung*[1,2], *Alfred Ayala*[1,2*†] *and Eleanor A. Fallon*[1,2†]

[1] Division of Surgical Research, Department of Surgery, Rhode Island Hospital, Providence, RI, United States, [2] Graduate Program in Biotechnology, Brown University, Providence, RI, United States

Sepsis, a dysfunctional immune response to infection leading to life-threatening organ injury, represents a significant global health issue. Neonatal sepsis is disproportionately prevalent and has a cost burden of 2-3 times that of adult patients. Despite this, no widely accepted definition for neonatal sepsis or recommendations for management exist and those created for pediatric patients are significantly limited in their applicability to this unique population. This is in part due to neonates' reliance on an innate immune response (which is developmentally more prominent in the neonate than the immature adaptive immune response) carried out by dysfunctional immune cells, including neutrophils, antigen-presenting cells such as macrophages/monocytes, dendritic cells, etc., natural killer cells, and innate lymphoid regulatory cell sub-sets like iNKT cells, γδ T-cells, etc.

Immune checkpoint inhibitors are a family of proteins with primarily suppressive/inhibitory effects on immune and tumor cells and allow for the maintenance of self-tolerance. During sepsis, these proteins are often upregulated and are thought to contribute to the long-term immunosuppression seen in adult patients. Several drugs targeting checkpoint inhibitors, including PD-1 and PD-L1, have been developed and approved for the treatment of various cancers, but no such therapeutics have been approved for the management of sepsis. In this review, we will comparatively discuss the role of several checkpoint inhibitor proteins, including PD-1, PD-L1, VISTA, and HVEM, in the immune response to sepsis in both adults and neonates, as well as posit how they may uniquely propagate their actions through the neonatal innate immune response. We will also consider the possibility of leveraging these proteins in the clinical setting as potential therapeutics/diagnostics that might aid in mitigating neonatal septic morbidity/mortality.

Keywords: sepsis, neonate, checkpoint inhibitor, PD-1, PD-L1, VISTA, HVEM

OPEN ACCESS

Edited by:
Galina Sud'ina, Lomonosov Moscow State University, Russia

Reviewed by:
Lan Wu, Vanderbilt University Medical Center, United States
Juan Carlos Andreu-Ballester, Fundacion para el Fomento de la Investigacion Sanitaria y Biomedica de la Comunitat Valenciana (FISABIO), Spain
Edward Sherwood, Vanderbilt University Medical Center, United States

***Correspondence:**
Alfred Ayala
aayala@lifespan.org

†These authors have contributed equally to this work and share senior authorship

This article was submitted to Inflammation, a section of the journal Frontiers in Immunology

Specialty section:
Received: *10 May 2022*
Accepted: *07 June 2022*
Published: *04 July 2022*

Citation:
Hensler E, Petros H, Gray CC, Chung CS, Ayala A and Fallon EA (2022) The Neonatal Innate Immune Response to Sepsis: Checkpoint Proteins as Novel Mediators of This Response and as Possible Therapeutic/Diagnostic Levers. Front. Immunol. 13:940930. doi: 10.3389/fimmu.2022.940930

PREVALENCE AND BURDEN OF NEONATAL SEPSIS

Neonates accounted for 47% of all mortalities in children under five years worldwide in 2020 (1). Sepsis, defined as a dysfunctional immune response to infection resulting in life-threatening organ injury (2), is the third leading cause of death in this group after prematurity or complications occurring during birth (3). Neonatal sepsis accounts for 13% of neonatal deaths and 42% of mortality in the first week of life (4). Globally, there are an estimated 2200 cases of neonatal sepsis per 100,000 live births with mortality ranging from 11 to 19% (5). Preterm infants are particularly susceptible, with premature neonates being 1000 times as likely as term counterparts to experience sepsis, as well as suffering from higher mortality and long-term morbidity (6).

In the United States, there is an overall mortality rate of 10% for septic infants, with a sharp increase up to 30% for those with any comorbidity (7). 36% of premature neonates born before 28 weeks gestation had at least one episode of bacteremia during their initial hospitalization with a mortality rate of up to 50% (6). Neonates in the US also have the highest rate of ICU admissions for sepsis of any age group and disproportionately high health care costs of 2-3 times those of adult septic patients, accounting for $1.1 billion in annual health care costs (7). Despite the high prevalence and significant health care burden of neonatal sepsis, reductions in mortality have lagged behind those seen in the overall pediatric population (4). In addition, the percentage of deaths in children under five years of age attributed to neonates has risen (1) showing that there is still significant room for improvement in the care of this vulnerable population.

NEONATAL VS PEDIATRIC SEPSIS

The rising incidence of sepsis, as well as its significant rates of mortality and long-term morbidity, led to the development of consensus definitions and recommendations for adult patients in 1991 (8) which have had multiple revisions based on updated evidence (2). Initial guidelines for pediatric patients were published in 2020 (9) and included 77 recommendations on the management of sepsis in children, 49 of which were classified as weak recommendations based on limited and low-quality evidence. While neonates born at 37 weeks gestation or later are intended to be covered by these guidelines, premature infants (a significant proportion of the neonatal population) and studies addressing concerns specific to neonates, such as those related to perinatal infections, were excluded. This somewhat limits the application of these guidelines to neonatal sepsis.

Several distinct differences between neonates and older children need to be considered in the diagnosis and management of sepsis. Neonates likely have exposure to different pathogens than older infants or other children due to intrauterine infections or vertical transmission during birth (10). Neonates are also affected differently by exposure to certain organisms, with those often dismissed as contaminants in older children or adults causing significant morbidity and mortality in the neonatal population. The long-term impact of neonatal sepsis must also be considered given the rapid development of the brain during this period. Studies have shown that patients who experience sepsis as neonates go on to have neurodevelopmental changes that persist even decades later (11–13).

Even amongst neonates there is considerable heterogeneity. These differences are due to varied gestational age of the population, timing of sepsis (early vs late), and source of the infection (10). Rapid changes in renal function (14) and the ability to metabolize medications (15) also occur in the first few weeks of life, causing variability in how individual patients may respond to a given treatment. Changes in the normal values for vital signs (16) and common laboratory tests (17) also occur in the first weeks to months of life and most clinical signs of sepsis in children and adults lack specificity in neonates (10). Even blood cultures are unreliable, with as few as 1% of cases having positive cultures due to the need for small samples and antenatal maternal antibiotic administration. All of these issues present significant challenges in forming widely-applicable definitions and recommendations for the diagnosis and management of neonatal sepsis.

ANIMAL MODELS OF NEONATAL SEPSIS

While well-established models of sepsis in adult animals have vastly increased our understanding of the immune response to sepsis, the unique challenges posed by neonatal septic patients

Abbreviations: (-/-), Knockout; Akt, Protein kinase B; ALT, Alanine transaminase; AP-1, Activator protein 1; APC, Antigen presenting cell; AST, Aspartate aminotransferase; Bcl-xL, B-cell lymphoma- extra large; BTLA, B and T lymphocyte attenuator; CD, Cluster of differentiation; CLP, Cecal ligation and puncture; CS, Cecal slurry; CTLA, Cytotoxic T-lymphocyte associated protein; Dies1, Differentiation of embryonic stem cells 1; EAE, Experimental autoimmune encephalomyelitis; FOXP3, Forkhead box P3; GI – Gastrointestinal; HSV, Herpes simplex virus; HVEM, Herpesvirus entry mediator; ICU, Intensive care unit; IFN-γ, Interferon gamma; IgC, Immunoglobulin constant; IgV, Immunoglobulin variable; IL, Interleukin; iNKT, Invariant natural killer T-cell; IP, Intraperitoneal; ITIM, Immunoreceptor tyrosine-based inhibitory motif; ITSM, Immunoreceptor tyrosine-based switch motif; IV, Intravenous; LIGHT, Homologous to lymphotoxin, exhibits inducible expression and competes with HSV glycoprotein D for binding to HVEM, a receptor expressed on T-lymphocytes; LTα, Lymphotoxin alpha; LTβR, Lymphotoxin beta receptor; MAPK, Mitogen-activated protein kinase; MCP, Monocyte chemoattractant protein; MHC, Major histocompatibility complex; NEC, Necrotizing enterocolitis; NET, Neutrophil extracellular trap; NFκB, Nuclear factor kappa light chain enhancer of activated B-cells; NK, Natural killer; PAMPs, Pathogen-associated molecular patterns; PD-1, Programmed cell death protein 1; PD-1H, Programmed death 1 homolog; PD-L1, Programmed death ligand 1; PD-L2, Programmed death ligand 2; PI3K, Phosphatidylinositol 3-kinase; PKCθ, Protein kinase C theta; PRRs, Pathogen recognition receptors; PSGL-1, P-selectin glycoprotein ligand 1; SHP, Src homology 2 domain-containing protein tyrosine phosphatase; SISP1, Stress induced secreted protein 1; STAT, Signal transducer and activator of transcription; TCR, T-cell receptor; TLR, Toll-like receptor; TNF-α, Tumor necrosis factor alpha; TRAF, Tumor necrosis factor receptor-associated factors; T-reg, Regulatory T-cell; VISTA, V-domain Ig suppressor of T-cell activation; VSIG3, V-set and immunoglobulin domain containing 3; VSIR, V-set immunoregulatory receptor; WT, Wildtype; ZAP70, Zeta-chain-associated protein kinase 70.

necessitate ongoing research using neonatal animals. Several models for neonatal sepsis have been developed to meet this need. Cecal ligation and puncture (CLP) is a commonly used model of intraabdominal polymicrobial sepsis in adult mice (18). This model has limitations in neonates, largely due to their small size and increased risk of cannibalization of the surgically manipulated neonates by the mothers (19). The cecal slurry (CS) model was developed to combat these issues. In this model, the cecal contents of adult mice are mixed with crystalloid fluid to create the slurry, which is then administered *via* IP injection to the study animals. The cecal slurry model induces bacteremia with mortality typically occurring between 12- and 72-hours following injection (20). This timeline is similar to that seen in septic human neonates (21). In addition to induction of sepsis *via* IP injection, pure bacteremia models utilizing IV injection of pathogens (22) as well as pneumonia models using intranasal administration (23) have been developed in rodents.

Models have also been developed to closely mimic necrotizing enterocolitis (NEC), a disease process most commonly seen in premature infants. These models typically involve gavage feeding of formula and either a single pathogen (24) or polymicrobial slurry (25, 26), often followed by induction of hypoxia to mimic ischemia-reperfusion (27). While there are several clear advantages to studying this disease process in rodents, including lower cost and larger litter size than other species, the inability to study premature animals limits the applicability of these models (20). Similar models have been developed using piglets (26, 28, 29) and non-human primates (30), but these species are more expensive and more difficult to care for. An additional limitation to these models of neonatal sepsis is the exclusion of antibiotic treatment and supportive care that would typically occur in human patients (20).

IMMUNOLOGY OF NEONATAL SEPSIS

Due to a limited exposure to environmental microbes, neonates rely on the innate immune system, which offers a rapid, short-term, and unspecified response to microorganisms (31). After a pathogen bypasses epithelial barriers, its pathogen associated molecular patterns (PAMPs) are detected by pathogen recognition receptors (PRRs), such as toll-like receptors (TLRs) (32, 33). Binding to TLRs stimulates a response through the release of cytokines, chemokines, complement proteins, and coagulation factors (34–36). While neonates and adults have similar expression levels of TLRs, the subsequent responses from PAMP-TLR binding differs (37). Septic neonates have decreased production of proinflammatory cytokines [TNF-α, IFN-γ, and IL-1β (38–40)], potentially due to decreased production of intracellular mediators of TLR signaling (41).

Several immune cells, including neutrophils, play a major role in the innate immune response (42). In rats, neonates have smaller baseline neutrophil reserves with higher risk of depletion of these reserves following sepsis as compared to adults (43). Additionally, neonatal neutrophils have lower expression of adhesion molecules (44, 45), which facilitate binding to the vascular endothelium, reducing neutrophil migration to the site of infection by 50% (45). Neonatal neutrophils also exhibit reduced deformability, which, when coupled with sepsis-induced hypotension, may lead to microvascular occlusion and successive organ dysfunction (46). Neonatal neutrophils also have impaired NET formation (47), reduced phagocytic capabilities (48), and decreased levels of bactericidal proteins (49). In addition, they are less efficient in responding to apoptotic stimuli (50, 51), which may prevent the resolution of inflammation and lead to excessive tissue damage (52). Overall, the combination of these changes in neutrophil functions may make neonates more susceptible to sepsis than adults.

Other key immune cells also demonstrate significant differences in the neonatal immune response. Neonates have low levels of antigen presenting cells (APCs), monocytes, and dendritic cells (53). While these cells have comparable cell surface TLR expression to adult cells (53), they express lower levels of costimulatory molecules (CD80, CD40) (54). Such factors contribute to a reduced ability of neonates to protect themselves from an infection. Another difference between adults and neonates is seen in mast cells, which release more histamine upon stimulation in neonates (55), potentially contributing to vasodilation and septic shock in this population.

In contrast to decreased numbers of other immune cells, neonates have larger populations of NK cells than adults (56). Neonatal NK cells have increased expression of inhibitory receptors (CD94/NKG2A), lower cytotoxic ability towards their targets, and decreased degranulation ability, when compared to adult NK cells (57). IFN-γ release by neonatal NK cells appears to differ based on type of *in vitro* stimulation, with some experiments showing increased IFN production (57) and others showing decreased levels (39) as compared to adults.

γδ-T cells, while lymphoid in lineage, are also innate immune cells that provide protection from microbial infection through the release of IFN-γ (58). γδ-T cells found in human cord blood have decreased cytotoxic capacity (59), decreased cytokine release (60), and lower levels of perforin and granzyme B effector molecules. Neonatal γδ-T cells are immature, reaching adult levels of maturity by 2 years of age (61), and have limited ability to respond to bacterial infection. In contrast, following infection with influenza, neonatal γδ-T cells rapidly produce IL-17A and contribute to improved survival as compared to neonatal mice lacking these cells (62).

iNKT-cells are adaptive immune cells with innate-like functions that have been shown to play a role in the neonatal immune response. While these cells do not appear to express TLRs as other innate immune cells do, they are activated by proinflammatory cytokines or lipid antigens and trigger further cytokine production and activation of other immune cell populations (63). In neonatal mice, loss of these cells leads to improved survival following sepsis as compared to WT neonates (64). iNKT-cells also migrate to the peritoneal cavity and are important for the mobilization of macrophages following sepsis in neonatal mice. These findings suggest that iNKT-cells play an important role in the neonatal response to sepsis.

ROLE OF CHECKPOINT PROTEINS IN SEPSIS

Two signals are required for T-cell activation to occur. First, an APC processes antigen and presents it to other cells *via* the MHC receptor (65). The T-cell receptor (TCR) binds to this antigen, creating the first signal. The second signal for activation is a co-stimulatory signal created by the binding of CD28 to B7, as an example (**Figure 1**). Concomitantly, co-inhibitory proteins, which can antagonize the second signal (66), are also present on various cell types, including APCs, T-cells, monocytes, macrophages, endothelial cells, tumor cells, etc. (67–70). These proteins allow for maintenance of self-tolerance in the body (71). The balance of co-stimulatory and co-inhibitory signals determines if the immune cell becomes activated or anergic/apoptotic (72).

During sepsis, the immune system generates simultaneous inflammatory and immunosuppressive responses (73), with balance of these responses necessary to prevent an overwhelming inflammatory response that could kill the host. While the inflammatory phase eventually peaks and returns toward baseline, many patients demonstrate profound long-term immunosuppression following sepsis (74). Immune checkpoint inhibitor proteins are often upregulated during the septic response and are thought to play a role in this immunosuppression (75). Here we will discuss the roles of several checkpoint inhibitors in sepsis and what is known about their involvement specifically in the neonatal immune response (**Table 1**).

PD-1 (Programmed Cell Death Protein 1)

PD-1 is a well-studied checkpoint inhibitor protein expressed on activated T-cells, NK cells, monocytes, dendritic cells, and γδ-T cells (67, 76). It is composed of an extracellular domain, transmembrane domain, and cytoplasmic tail containing an immunoreceptor tyrosine-based inhibitory motif (ITIM) and an immunoreceptor tyrosine-based switch motif (ITSM) domain (84, 85). Upon binding of PD-1 to its ligand (PD-L1 or PD-L2), PD-1 is phosphorylated and the SHP1/2 complex is recruited to the cytoplasmic tail (77) (**Figure 1**). This leads to inhibition of CD28-mediated activation of PI3K, blocking downstream activation of Akt and leading to decreased Bcl-xL, IL-2, and IFN-γ production (78). PD-1 also inhibits phosphorylation of CD3ζ, and ZAP70, PKCθ (79), though these effects can be reversed *in vitro* by administration of IL-2, IL-7, or IL-15 (86). To exert these inhibitory effects, PD-1 must be in close proximity to the antigen receptor. To facilitate this, PD-1 has been shown to translocate to form micro clusters with T-cell receptors on the surface of T-cells (87).

Following the induction of experimental sepsis in adult mice, increased PD-1 expression can lead to exhaustion of T-cells, characterized by decreased proliferation as well as decreased production of IL-2, IFN-γ, TNF-α, and chemokines (88) with the greatest level of inhibition seen at low levels of TCR stimulation (67). T-cells also demonstrate a shift toward the regulatory phenotype following PD-1 activation (88). These changes are thought to contribute to the immunosuppression seen after sepsis. Similar changes

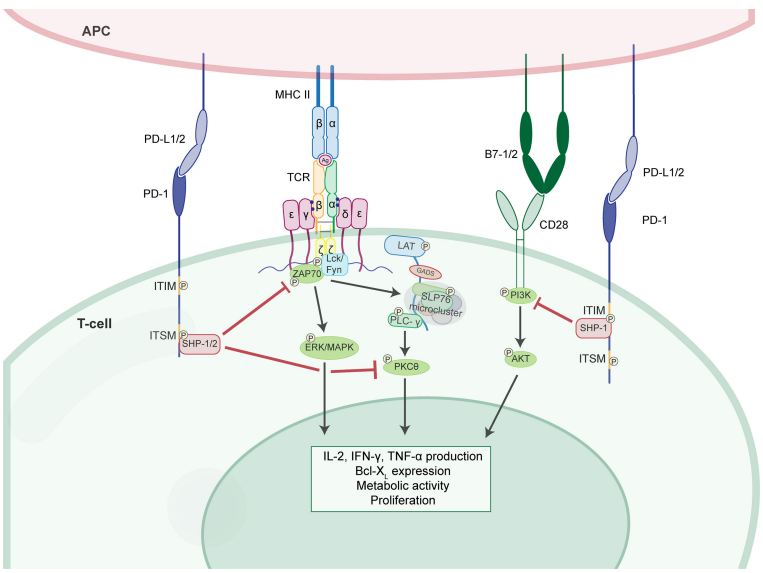

FIGURE 1 | PD-1 suppresses T-cell activation by inhibiting several kinase pathways. T-cell activation occurs when the TCR binds the antigen (Ag) presented by MHC II. This first signal results in ZAP70, Lck, and Fyn recruitment to the CD3-ζ chain proximal to the TCR. The first signal promotes the ERK/MAPK and PKC-θ activation. The second signal occurs when CD28 binds to B7-1/2 and results in PI3K recruitment and downstream AKT pathway activation. PD-1 intrinsically suppresses T-cell activation. Upon interaction with PD-L1/2 the ITSM domain of PD-1 recruits SHP-1/2. Activated SHP-1/2 inhibit ZAP70 and PKC-θ phosphorylation. The ITIM domain of PD-1 is also phosphorylated and recruits SHP-1. This activated SHP-1 inhibits PI3K phosphorylation resulting in suppression of the AKT pathway. These mechanisms of PD-1 induced suppression results in reduced cytokine production, metabolic activity, proliferation, and B-cell lymphoma-extra large (Bcl-X_L) mediated survival.

TABLE 1 | Brief summary of some selected checkpoint inhibitor ligands, expression, and signaling with relevance to the present discussion of neonatal sepsis.

Checkpoint Inhibitor	Ligands	Expression Pattern	Signaling Overview
PD-1	PD-L1 PD-L2	T-cells, NK cells, monocytes, dendritic cells (67), γδ-T cells (76)	SHP1/2 binds cytoplasmic tail -> inhibition of PI3K activation -> blocks Akt activation -> decreased Bcl-xL, IL-2, IFN-γ (77–79)
VISTA	VISTA VSIG3 PSGL-1	Spleen, thymus, bone marrow, leukocyte infiltrates, macrophages, monocytes, dendritic cells, T-cells, APCs (69)	SH2/SH3 binding -> STAT pathway activated -> inhibition of MAPK and NFκB pathways (80, 81)
HVEM	TNF LTα LIGHT BTLA CD160 HSV glycoprotein D	Fetal lung and kidney; adult spleen and peripheral blood leukocytes (70)	Recruitment of TRAF2 and TRAF5 -> transcription factor activation (eg NFκB and AP-1) (70)
BTLA	HVEM	Spleen, lymph nodes, $CD4^+$ T-cells, B-cells, dendritic cells (82)	Recruitment of SHP1/2 -> dephosphorylation of PI3K (83)

have been documented in human samples as well, with splenic T-cells from adult septic patients showing decreased capacity for IFN-γ and TNF-α production (89). Expression levels of PD-1 and its ligands also change in septic patients, with increased PD-1 expression on $CD4^+$ T-cells and increased PD-L1 expression on macrophages and endothelial cells.

$PD\text{-}1^{-/-}$ adult mice develop autoimmune glomerulonephritis (90) and dilated cardiomyopathy (91), demonstrating the important role of this checkpoint inhibitor in maintenance of self-tolerance. However, in the response to sepsis, PD-1 activity leads to increased morbidity and mortality. $PD\text{-}1^{-/-}$ adult mice have demonstrated improved survival following sepsis induced by CLP (92). Treatment of WT animals with anti-PD-1 or anti-PD-L1 antibodies similarly leads to improved survival in models of bacterial (93) and fungal (94) sepsis.

PD-L1 (Programmed Death-Ligand 1)

PD-L1 is one of two ligands for PD-1. It is a type 1 glycoprotein containing IgC and IgV domains (84). The intracellular portion of the protein has been found to be highly conserved across species (67). In addition to its well-studied interaction with PD-1, PD-L1 has been found to interact with B7 (CD80), which is a known receptor for other immune checkpoint proteins such as CTLA-4 and CD28 (95). When bound to B7, PD-L1 inhibits T-cell activation independent of PD-1 involvement.

PD-L1 is widely expressed on both immune cells (including T-cells, B-cells, monocytes, macrophages, dendritic cells, bone marrow-derived mast cells, neutrophils, mesenchymal stem cells) (67, 68) and in various tissues, such as the cardiac endothelium, placenta, pancreatic islets, liver, lung, and skin (68). Its expression pattern varies based on the activation state of the cell, with lower baseline expression on T-cells and macrophages and significant upregulation on activated cells, though no such upregulation is noted on activated B-cells (67). It has also been found to be overexpressed on various cancers. This pattern of expression is thought to allow for regulation of the peripheral immune response and maintenance of self-tolerance in biologically vital tissues, as well as a mechanism for tumors to evade immune control.

In mouse models, PD-L1 deficiency exacerbates autoimmune diabetes (96) and increases susceptibility to experimental autoimmune encephalomyelitis (EAE) (97), suggesting a role in the prevention of autoimmune conditions. In sepsis, PD-L1 expression is upregulated on monocytes, dendritic cells, and capillary endothelial cells in the spleen (88). Monocyte PD-L1 expression levels also correlate with severity of illness and mortality in adult septic patients (98), suggesting a potential role as a prognostic marker in this population.

VISTA (V-Domain Ig Suppressor of T-Cell Activation)

VISTA (PD-1H, VSIR, B7-H5, SISP1, Dies 1) (69, 99–101) is a relatively recent addition to the B7 family of checkpoint inhibitor proteins. It was identified *via* comparison of cell surface protein expression of resting vs activated T-regs and shares approximately 24% homology to PD-L1 (69). It is a type 1 transmembrane protein with an extracellular Ig-V domain, transmembrane segment, and cytoplasmic tail. It contains 2 invariant cysteine residues common to other B7 family members, plus an additional 4 cysteine residues that are unique to VISTA. These additional residues are highly preserved across species and are thought to allow for VISTA-VISTA interactions. In addition to self-binding, VISTA interacts with VSIG3, which is overexpressed on various GI cancers (102), and PSGL-1, an adhesion molecule involved in leukocyte rolling that is upregulated in inflammatory states (103).

VISTA's cytoplasmic tail contains SH2 and SH3 binding domains, allowing for signaling *via* STAT proteins (80). This leads to downstream inhibition of TLR-mediated activation of MAPKs and the NFκB pathway *via* a reduction in TRAF6 (81). Overall, VISTA activity has an inhibitory effect on naïve and memory T-cell proliferation without inducing apoptosis in these populations (69). It also leads to decreased production of IL-2 and IFN-γ.

VISTA is primarily expressed in hematopoietic tissues, including the spleen, thymus, and bone marrow, as well as in tissues with significant leukocyte infiltrates such as the lung (69). It has a lower level of baseline expression in the heart, kidney, brain, and ovary. VISTA expression is highly upregulated on

APCs during the inflammatory response and is also constitutively expressed on macrophages, monocytes, dendritic cells, and T-cells. Like PD-L1, VISTA deficiency has been found to exacerbate autoimmune conditions in mouse models, including EAE (104) and lupus (105). In addition, while many of these checkpoint inhibitor proteins have similar downstream effects on the immune response, VISTA and PD-1 have synergistic, non-redundant functions (106). This suggests that targeting a combination of these proteins may prove to be more beneficial than targeting them in isolation.

Adult VISTA$^{-/-}$ mice have significantly decreased survival following septic insult as compared to their WT counterparts (107). They also demonstrate elevated serum markers of end-organ damage in the liver, as well as higher serum levels of several cytokines (IL-6, IL-10, TNF-α, MCP-1, IL-17F and IL-23). VISTA also appears to play an important role in the T-reg response to sepsis. While WT adult mice have increased T-reg abundance after sepsis, no such change is seen in VISTA$^{-/-}$ mice. In addition, the survival of VISTA$^{-/-}$ mice following sepsis returns to the WT baseline if VISTA-expressing T-regs are given *via* adoptive transfer prior to septic insult.

HVEM (Herpesvirus Entry Mediator)

HVEM is a type 1 transmembrane receptor protein (108) containing 4 cysteine-rich domains that allow for ligand binding (70). Its cytoplasmic domain recruits TRAF2 and TRAF5, leading to downstream activation of various transcription factors, including NFκB and AP-1. HVEM is widely expressed throughout the body. High expression levels have been found at baseline in fetal lung and kidney, as well as adult spleen and peripheral blood leukocytes, with lower baseline expression in adult non-lymphoid tissues. HVEM is highly promiscuous in its interactions and can act as either ligand or receptor depending on its binding partner. It has several known ligands, including TNF, LTα, LIGHT, BTLA, CD160, and HSV glycoprotein D (83, 108–110).

LIGHT is a type II transmembrane protein (109) that is expressed in the spleen and lymph nodes, as well as on macrophages, T-cells, and immature dendritic cells (111). Its expression is inducible and its binding with HVEM stimulates proliferation of T-cells, induces IFN-γ production, and weakly stimulates NFκB-driven transcription (109). It also blocks proliferation of tumor cells *in vitro*. LIGHT also interacts with LTβR (112). This interaction produces a wide range of downstream effects, including cell apoptosis, lipid metabolism, and regulation of lymph node formation.

BTLA is a member of the Ig superfamily of proteins and contains 2 ITIM domains (113). BTLA is expressed in the spleen and lymph nodes, with low-level baseline expression on CD4$^+$ T-cells that significantly increases following T-cell activation (82). Its interaction with HVEM is unique in that it acts as a bidirectional switch, with opposing downstream effects depending on which protein acts as receptor and which as ligand, as well as the membrane conformation of the involved proteins (83, 114).

In adult mice after CLP, increased BTLA and HVEM-expressing macrophages, monocytes, dendritic cells, and neutrophils have been found in the peritoneal cavity (115), suggesting a role for these checkpoint proteins in local response to infection. BTLA knockout animals have increased survival, decreased indices of organ injury, and reduced peritoneal bacterial burden following CLP (115), while those treated with an agonistic BTLA antibody show increases in cytokine production, recruitment of inflammatory cells to the peritoneal cavity, and mortality (116).

Higher levels of soluble BTLA have also been found in septic patients, and these levels appear to correlate with severity of disease (117). BTLA expression on CD4$^+$ T-cells also correlates with severity of sepsis in ICU patients and is associated with increased risk of developing nosocomial infections (118). The immunosuppressed phenotype seen in these patients with higher BTLA expression may in part be explained by the increased apoptosis of T-cells seen following BTLA activation. These findings suggest a role for BTLA in prognostication and management of septic patients.

CHECKPOINT PROTEINS IN NEONATES

While the role of checkpoint inhibitor proteins has been extensively studied in adults, significantly less data exists in neonates. In mice, PD-1$^{-/-}$ neonates have been found to have a significant survival benefit following CS-induced sepsis as compared to WT neonates (119), mirroring the survival benefit seen in adult knockouts after CLP. These PD-1 knockouts also have increased production of cytokines following sepsis, specifically IL-6, IL-10, and TNF-α, as well as differences in the cell composition of peritoneal infiltrates. PD-1 also appears to play a role in modulating the response of neonatal iNKT-cells to sepsis, with both PD-1$^{-/-}$ and iNKT-cell$^{-/-}$ neonates showing similar effects on peritoneal macrophage populations that are distinct from those seen in WT neonates following CS (64).

PD-1 expression on monocytes has been studied in premature human infants, who have been found to have a lower baseline expression than their term counterparts (120). Premature infants with sepsis, however, have a significantly higher percentage of PD-1-expressing monocytes, with even higher expression levels seen in those who died of septic shock. PD-1 expression has also been studied in the context of inflammation due to biliary atresia. Infants diagnosed with biliary atresia have been found to have increased PD-1 expression on hepatic and circulating T-cells, as well as lower levels of IFN-γ in the liver (121). In a virus-induced biliary atresia model in mice, PD-1 blockade has been shown to lead to increased levels of AST, ALT, and IFN-γ, suggesting that PD-1 plays a role in mitigating liver injury in this disease process.

In humans, stimulation of CD4$^+$ T-cells isolated from neonates with *Staphylococcus aureus* leads to a conversion of those cells to FOXP3$^+$ regulatory T-cells (122). Blocking PD-L1 prevents this shift from occurring, suggesting that PD-L1 plays a role in controlling the immune response. BTLA expression has also been studied in human neonates, with higher levels of expression on dendritic cells of septic vs nonseptic patients (123). Samples from septic neonates also showed decreased T-

cell proliferation and decreased levels of maturation markers on $BTLA^+$ dendritic cells. The higher level of BTLA expression also correlated with decreased phagocytosis and bactericidal ability, as well as with the severity of sepsis in these patients.

Overall, these findings suggest that while there are significant differences in the neonatal immune response as compared to adults, checkpoint inhibitor proteins play an important role in the immune responses of both populations. These findings also suggest that checkpoint inhibitors play some of their most significant roles in 'innate' as opposed to simply 'adaptive' immune responses to sepsis. Other innate immune cells, such as neutrophils and γδ-T cells, are likely also affected by loss or blockade of checkpoint inhibition, but further research is needed to explore the effects of manipulating various checkpoint inhibitors on these cells. It is clear from the paucity of data in this specific and vulnerable population that much work remains to be done to understand the mechanisms by which checkpoint inhibitor proteins impact the neonatal immune response before they can be studied as potential therapeutic targets.

CLINICAL APPLICATIONS

While the roles of various checkpoint inhibitor proteins have been extensively studied in the setting of sepsis, their use as therapeutic targets in human patients is just beginning to be explored. Several phase 1b clinical trials have been undertaken to look at the safety of several compounds that target PD-1 and/or PD-L1 in septic patients (124, 125). These trials have not revealed any increase in cytokine levels or significant safety concerns, though they only include a small number of patients. Expanded trials will be necessary to quantify the risk of autoimmune side effects that could result from loss of checkpoint inhibition leading to impaired self-tolerance. These side effects have the potential to be especially concerning in the neonatal population as these patients have an underdeveloped immune system and are somewhat fragile as compared to adults. No trials have been performed using VISTA, HVEM, or any of their ligands as therapeutic targets and none have been performed in neonates. These provide areas of opportunity for further study and drug development.

Checkpoint inhibitor proteins are well-established therapeutic targets in oncology (**Figure 2**). Three medications have been developed and approved to target PD-1 [pembrolizumab (126), nivolumab (127), cemiplimab (128)], three for PD-L1 [atezolizumab (129), avelumab (130), durvalumab (131)], and one for CTLA-4 [ipilimumab (132)]. These medications are used to treat a wide variety of cancers, including breast, lymphoma, skin, lung, and GI tumors. Unfortunately, not all tumors respond to these medications due to different levels of expression of the checkpoint proteins (133). Combinatorial therapies have also been studied with success in reducing death and/or disease progression in several trials (134). While these medications have been used successfully in the setting of cancer immunotherapy, further trials will need to be done in septic patients to determine if the positive results seen in a chronic

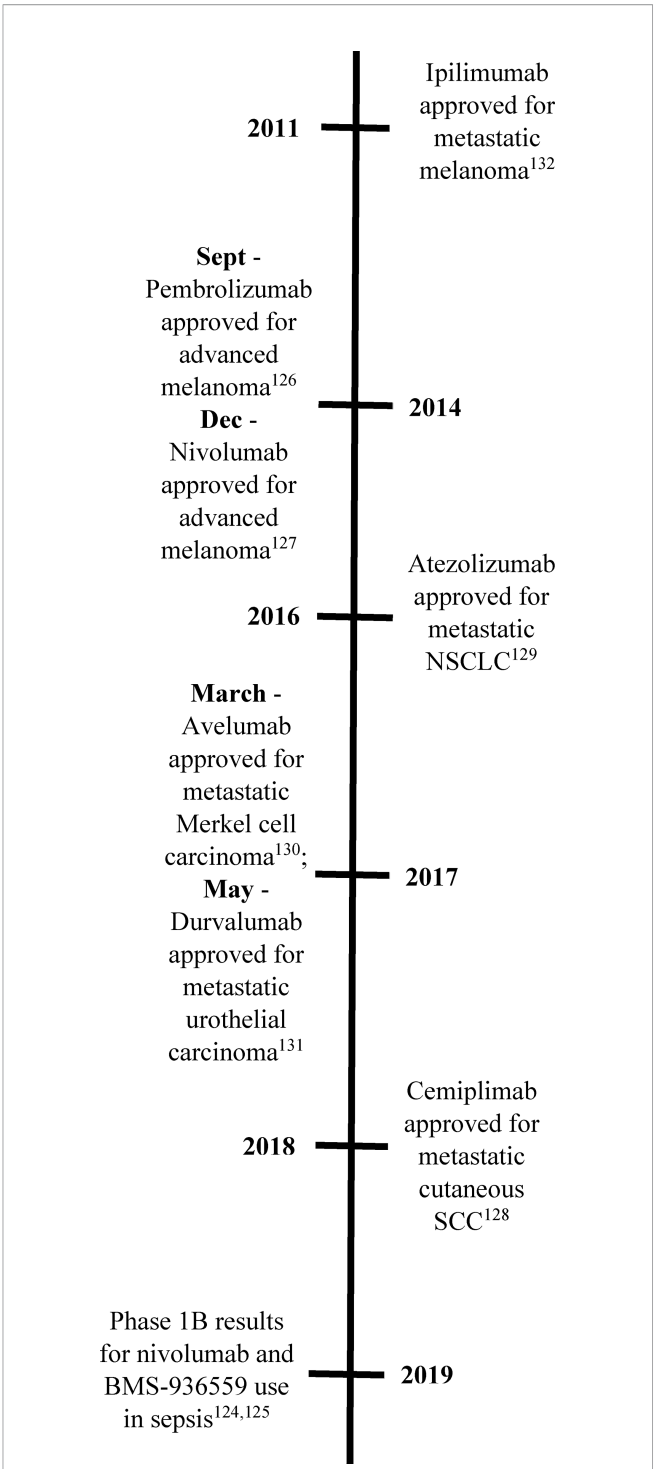

FIGURE 2 | Timeline of therapeutic applications of checkpoint inhibitor proteins. This timeline includes the initial FDA approval for each of the approved medications targeting checkpoint inhibitor proteins (PD-1, PD-L1, and CTLA-4), as well as the publications of phase 1 clinical trial results for two of these medications in septic patients.

process such as cancer will also be demonstrated in the more acute setting of sepsis.

CONCLUSIONS

Despite advances in knowledge about the mechanisms, diagnosis, and management of sepsis, significant gaps remain in the setting of neonatal sepsis, which continues to be a large burden on healthcare globally. The differences between the neonatal and adult immune response make it impossible to extrapolate findings in adult animals or patients to neonates, and further work needs to be done to understand how sepsis affects this population. Checkpoint inhibitor proteins, such as PD-1, PD-L1, VISTA, and HVEM, have been shown to play an important role in modulating the immune response to sepsis in adults. Significantly less data exists for neonates, providing an additional area for further research. Current data suggests that these proteins may prove to be useful for diagnosis, prognostication, and even treatment of septic patients, but there is still more work to be done before this can be applied in clinical practice.

AUTHOR CONTRIBUTIONS

EH conducted the majority of the literature search and writing of the manuscript, and also contributed to the preparation of the figures. HP contributed to the literature search and writing of the manuscript. C-SC provided revisions and conceptual feedback. CG contributed to the preparation of the figures and provided revisions and conceptual feedback. EF and AA, who contributed equally as senior authors to this work, provided the initial framework for the review and contributed substantial revisions and conceptual feedback for the manuscript and figures. All authors reviewed and approved the final manuscript.

FUNDING

This work was supported by the National Institutes of Health [R35 GM118097 (AA, C-SC), R25 GM083270 (CG), T32-HL134625 (CG) and T32 GM065085 (EH)].

REFERENCES

1. World Health Organization. *Newborn Mortality* (2022). Available at: https://www.who.int/news-room/fact-sheets/detail/levels-and-trends-in-child-mortality-report-2021.
2. Singer M, Deutschman CS, Seymour CW, Shankar-Hari M, Annane D, Bauer M, et al. The Third International Consensus Definitions for Sepsis and Septic Shock (Sepsis-3). *JAMA* (2016) 315(8):801–10. doi: 10.1001/jama.2016.0287
3. Liu L, Johnson HL, Cousens S, Perin J, Scott S, Lawn JE, et al. Global, Regional, and National Causes of Child Mortality: An Updated Systematic Analysis for 2010 With Time Trends Since 2000. *Lancet* (2012) 379 (9832):2151–61. doi: 10.1016/S0140-6736(12)60560-1
4. Zea-Vera A, Ochoa TJ. Challenges in the Diagnosis and Management of Neonatal Sepsis. *J Trop Pediatrics* (2015) 61(1):1–13. doi: 10.1093/tropej/fmu079
5. Fleischmann-Struzek C, Goldfarb DM, Schlattmann P, Schlapbach LJ, Reinhart K, Kissoon N. The Global Burden of Paediatric and Neonatal Sepsis: A Systematic Review. *Lancet Respir Med* (2018) 6(3):223–30. doi: 10.1016/S2213-2600(18)30063-8
6. Wynn JL. Defining Neonatal Sepsis. *Curr Opin Pediatr* (2016) 28(2):135–40. doi: 10.1097/MOP.0000000000000315
7. Angus DC, Linde-Zwirble WT, Lidicker J, Clermont G, Carcillo J, Pinsky MR. Epidemiology of Severe Sepsis in the United States: Analysis of Incidence, Outcome, and Associated Costs of Care. *Crit Care Med* (2001) 29(7):1303–10. doi: 10.1097/00003246-200107000-00002
8. Bone RC, Balk RA, Cerra FB, Dellinger RP, Fein AM, Knaus WA, et alDefinitions for sepsis and organ failure and guidlines for the use of innovative therapies in sepsis. The ACCP/SCCM Consensus Conference Committee. American College of Chest Physicians/Society of Critical Care Medicine. *Chest* (1992) 101(6):1644–55. doi: 10.1378/chest.101.6.1644
9. Weiss SL, Peters MJ, Alhazzani W, Agus MSD, Flori HR, Inwald DP, et al. Surviving Sepsis Campaign International Guidelines for the Management of Septic Shock and Sepsis-Associated Organ Dysfunction in Children. *Intensive Care Med* (2020) 46(Suppl 1):10–67. doi: 10.1007/s00134-019-05878-6
10. Molloy EJ, Wynn JL, Bliss J, Koenig JM, Keij FM, McGovern M, et al. Neonatal Sepsis: Need for Consensus Definition, Collaboration and Core Outcomes. *Pediatr Res* (2020) 88(1):2–4. doi: 10.1038/s41390-020-0850-5
11. Schlapbach LJ, Aebischer M, Adams M, Natalucci G, Bonhoeffer J, Latzin P, et al. Impact of Sepsis on Neurodevelopmental Outcome in a Swiss National Cohort of Extremely Premature Infants. *Pediatrics* (2011) 128(2):e348–57. doi: 10.1542/peds.2010-3338
12. Ortgies T, Rullmann M, Ziegelhöfer D, Bläser A, Thome UH. The Role of Early-Onset-Sepsis in the Neurodevelopment of Very Low Birth Weight Infants. *BMC Pediatr* (2021) 21(1):289. doi: 10.1186/s12887-021-02738-5
13. Hentges CR, Silveira RC, Procianoy RS, Carvalho CG, Filipouski GR, Fuentefria RN, et al. Association of Late-Onset Neonatal Sepsis With Late Neurodevelopment in the First Two Years of Life of Preterm Infants With Very Low Birth Weight. *J Pediatr (Rio J)* (2014) 90(1):50–7. doi: 10.1016/j.jped.2013.10.002
14. Blackburn ST. Renal Function in the Neonate. *J Perinat Neonatal Nurs* (1994) 8(1):37–47. doi: 10.1097/00005237-199406000-00006
15. Milsap RL, Jusko WJ. Pharmacokinetics in the Infant. *Environ Health Perspect* (1994) 102 Suppl 11(Suppl 11):107–10. doi: 10.1289/ehp.94102s11107
16. American Heart Association. *PALS Digital Reference Card*. (2020).
17. De Alarcon PA, Werner EJ. Normal Values and Laboratory Methods. In: EJ Werner and PA De Alarcon, editors. *Neonatal Hematology*. New York: Cambridge University Press (2005). p. 406–30.
18. Wichterman KA, Baue AE, Chaudry IH. Sepsis and Septic Shock–a Review of Laboratory Models and a Proposal. *J Surg Res* (1980) 29(2):189–201. doi: 10.1016/0022-4804(80)90037-2
19. Wynn JL, Scumpia PO, Delano MJ, O'Malley KA, Ungaro R, Abouhamze A, et al. Increased Mortality and Altered Immunity in Neonatal Sepsis Produced by Generalized Peritonitis. *Shock* (2007) 28(6):675–83. doi: 10.1097/shk.0b013e3180556d09
20. Nolan LS, Wynn JL, Good M. Exploring Clinically-Relevant Experimental Models of Neonatal Shock and Necrotizing Enterocolitis. *Shock* (2020) 53 (5):596–604. doi: 10.1097/SHK.0000000000001507
21. Giannoni E, Agyeman PKA, Stocker M, Posfay-Barbe KM, Heininger U, Spycher BD, et al. Neonatal Sepsis of Early Onset, and Hospital-Acquired and Community-Acquired Late Onset: A Prospective Population-Based Cohort Study. *J Pediatr* (2018) 201:106–14.e4. doi: 10.1016/j.jpeds.2018.05.048
22. Speer EM, Diago-Navarro E, Ozog LS, Raheel M, Levy O, Fries BC. A Neonatal Murine Escherichia Coli Sepsis Model Demonstrates That Adjunctive Pentoxifylline Enhances the Ratio of Anti- vs. Pro-

Inflammatory Cytokines in Blood and Organ Tissues. *Front Immunol* (2020) 11:577878. doi: 10.3389/fimmu.2020.577878
23. Fitzpatrick EA, You D, Shrestha B, Siefker D, Patel VS, Yadav N, et al. A Neonatal Murine Model of MRSA Pneumonia. *PLos One* (2017) 12(1): e0169273. doi: 10.1371/journal.pone.0169273
24. Hunter CJ, Singamsetty VK, Chokshi NK, Boyle P, Camerini V, Grishin AV, et al. Enterobacter Sakazakii Enhances Epithelial Cell Injury by Inducing Apoptosis in a Rat Model of Necrotizing Enterocolitis. *J Infect Dis* (2008) 198 (4):586–93. doi: 10.1086/590186
25. Lu J, Pierce M, Franklin A, Jilling T, Stafforini DM, Caplan M. Dual Roles of Endogenous Platelet-Activating Factor Acetylhydrolase in a Murine Model of Necrotizing Enterocolitis. *Pediatr Res* (2010) 68(3):225–30. doi: 10.1203/PDR.0b013e3181eb2efe
26. Good M, Sodhi CP, Ozolek JA, Buck RH, Goehring KC, Thomas DL, et al. Lactobacillus Rhamnosus HN001 Decreases the Severity of Necrotizing Enterocolitis in Neonatal Mice and Preterm Piglets: Evidence in Mice for a Role of TLR9. *Am J Physiol Gastrointest Liver Physiol* (2014) 306(11): G1021–32. doi: 10.1152/ajpgi.00452.2013
27. Lu P, Sodhi CP, Jia H, Shaffiey S, Good M, Branca MF, et al. Animal Models of Gastrointestinal and Liver Diseases. Animal Models of Necrotizing Enterocolitis: Pathophysiology, Translational Relevance, and Challenges. *Am J Physiol Gastrointest Liver Physiol* (2014) 306(11):G917–28. doi: 10.1152/ajpgi.00422.2013
28. Gibson RL, Berger JI, Redding GJ, Standaert TA, Mayock DE, Truog WE. Effect of Nitric Oxide Synthase Inhibition During Group B Streptococcal Sepsis in Neonatal Piglets. *Pediatr Res* (1994) 36(6):776–83. doi: 10.1203/00006450-199412000-00016
29. Lobe TE, Woodall DL, Griffin MP. Early Hemodynamic Indicators of Gram-Negative Sepsis and Shock in an Infant Pig Model. *J Pediatr Surg* (1991) 26 (9):1051–7. doi: 10.1016/0022-3468(91)90672-G
30. Hemming VG, London WT, Fischer GW, Curfman BL, Baron PA, Gloser H, et al. Immunoprophylaxis of Postnatally Acquired Group B Streptococcal Sepsis in Neonatal Rhesus Monkeys. *J Infect Dis* (1987) 156(4):655–8. doi: 10.1093/infdis/156.4.655
31. Levy O. Innate Immunity of the Newborn: Basic Mechanisms and Clinical Correlates. *Nat Rev Immunol* (2007) 7(5):379–90. doi: 10.1038/nri2075
32. Rittirsch D, Flierl MA, Ward PA. Harmful Molecular Mechanisms in Sepsis. *Nat Rev Immunol* (2008) 8(10):776–87. doi: 10.1038/nri2402
33. Kawai T, Akira S. The Roles of TLRs, RLRs and NLRs in Pathogen Recognition. *Int Immunol* (2009) 21(4):317–37. doi: 10.1093/intimm/dxp017
34. Kumagai Y, Takeuchi O, Akira S. Pathogen Recognition by Innate Receptors. *J Infect Chemother* (2008) 14(2):86–92. doi: 10.1007/s10156-008-0596-1
35. Hajishengallis G, Lambris JD. Crosstalk Pathways Between Toll-Like Receptors and the Complement System. *Trends Immunol* (2010) 31 (4):154–63. doi: 10.1016/j.it.2010.01.002
36. van Zoelen MA, Yang H, Florquin S, Meijers JC, Akira S, Arnold B, et al. Role of Toll-Like Receptors 2 and 4, and the Receptor for Advanced Glycation End Products in High-Mobility Group Box 1-Induced Inflammation *In Vivo*. *Shock* (2009) 31(3):280–4. doi: 10.1097/SHK.0b013e318186262d
37. Melvan JN, Bagby GJ, Welsh DA, Nelson S, Zhang P. Neonatal Sepsis and Neutrophil Insufficiencies. *Int Rev Immunol* (2010) 29(3):315–48. doi: 10.3109/08830181003792803
38. Levy O, Zarember KA, Roy RM, Cywes C, Godowski PJ, Wessels MR. Selective Impairment of TLR-Mediated Innate Immunity in Human Newborns: Neonatal Blood Plasma Reduces Monocyte TNF-Alpha Induction by Bacterial Lipopeptides, Lipopolysaccharide, and Imiquimod, But Preserves the Response to R-848. *J Immunol* (2004) 173(7):4627–34. doi: 10.4049/jimmunol.173.7.4627
39. Han P, Hodge G. Intracellular Cytokine Production and Cytokine Receptor Interaction of Cord Mononuclear Cells: Relevance to Cord Blood Transplantation. *Br J Haematol* (1999) 107(2):450–7. doi: 10.1046/j.1365-2141.1999.01696.x
40. Sharma AA, Jen R, Kan B, Sharma A, Marchant E, Tang A, et al. Impaired NLRP3 Inflammasome Activity During Fetal Development Regulates IL-1β Production in Human Monocytes. *Eur J Immunol* (2015) 45(1):238–49. doi: 10.1002/eji.201444707
41. Sadeghi K, Berger A, Langgartner M, Prusa AR, Hayde M, Herkner K, et al. Immaturity of Infection Control in Preterm and Term Newborns is Associated With Impaired Toll-Like Receptor Signaling. *J Infect Dis* (2007) 195(2):296–302. doi: 10.1086/509892
42. Mantovani A, Cassatella MA, Costantini C, Jaillon S. Neutrophils in the Activation and Regulation of Innate and Adaptive Immunity. *Nat Rev Immunol* (2011) 11(8):519–31. doi: 10.1038/nri3024
43. Erdman SH, Christensen RD, Bradley PP, Rothstein G. Supply and Release of Storage Neutrophils. A Developmental Study. *Biol Neonate* (1982) 41(3-4):132–7. doi: 10.1159/000241541
44. Kim SK, Keeney SE, Alpard SK, Schmalstieg FC. Comparison of L-Selectin and CD11b on Neutrophils of Adults and Neonates During the First Month of Life. *Pediatr Res* (2003) 53(1):132–6. doi: 10.1203/00006450-200301000-00022
45. Anderson DC, Rothlein R, Marlin SD, Krater SS, Smith CW. Impaired Transendothelial Migration by Neonatal Neutrophils: Abnormalities of Mac-1 (CD11b/CD18)-Dependent Adherence Reactions. *Blood* (1990) 76 (12):2613–21. doi: 10.1182/blood.V76.12.2613.2613
46. Linderkamp O, Ruef P, Brenner B, Gulbins E, Lang F. Passive Deformability of Mature, Immature, and Active Neutrophils in Healthy and Septicemic Neonates. *Pediatr Res* (1998) 44(6):946–50. doi: 10.1203/00006450-199812000-00021
47. Yost CC, Cody MJ, Harris ES, Thornton NL, McInturff AM, Martinez ML, et al. Impaired Neutrophil Extracellular Trap (NET) Formation: A Novel Innate Immune Deficiency of Human Neonates. *Blood* (2009) 113(25):6419–27. doi: 10.1182/blood-2008-07-171629
48. Miller ME. Phagocyte Function in the Neonate: Selected Aspects. *Pediatrics* (1979) 64(5 Pt 2 Suppl):709–12. doi: 10.1542/peds.64.5.709
49. Levy O, Martin S, Eichenwald E, Ganz T, Valore E, Carroll SF, et al. Impaired Innate Immunity in the Newborn: Newborn Neutrophils are Deficient in Bactericidal/Permeability-Increasing Protein. *Pediatrics* (1999) 104(6):1327–33. doi: 10.1542/peds.104.6.1327
50. Hanna N, Vasquez P, Pham P, Heck DE, Laskin JD, Laskin DL, et al. Mechanisms Underlying Reduced Apoptosis in Neonatal Neutrophils. *Pediatr Res* (2005) 57(1):56–62. doi: 10.1203/01.PDR.0000147568.14392.F0
51. Allgaier B, Shi M, Luo D, Koenig JM. Spontaneous and Fas-Mediated Apoptosis are Diminished in Umbilical Cord Blood Neutrophils Compared With Adult Neutrophils. *J Leukoc Biol* (1998) 64(3):331–6. doi: 10.1002/jlb.64.3.331
52. Koenig JM, Stegner JJ, Schmeck AC, Saxonhouse MA, Kenigsberg LE. Neonatal Neutrophils With Prolonged Survival Exhibit Enhanced Inflammatory and Cytotoxic Responsiveness. *Pediatr Res* (2005) 57 (3):424–9. doi: 10.1203/01.PDR.0000153945.49022.96
53. Willems F, Vollstedt S, Suter M. Phenotype and Function of Neonatal DC. *Eur J Immunol* (2009) 39(1):26–35. doi: 10.1002/eji.200838391
54. De Wit D, Tonon S, Olislagers V, Goriely S, Boutriaux M, Goldman M, et al. Impaired Responses to Toll-Like Receptor 4 and Toll-Like Receptor 3 Ligands in Human Cord Blood. *J Autoimmun* (2003) 21(3):277–81. doi: 10.1016/j.jaut.2003.08.003
55. Damsgaard TE, Nielsen BW, Henriques U, Hansen B, Herlin T, Schiøtz PO. Histamine Releasing Cells of the Newborn. Mast Cells From the Umbilical Cord Matrix and Basophils From Cord Blood. *Pediatr Allergy Immunol* (1996) 7(2):83–90. doi: 10.1111/j.1399-3038.1996.tb00111.x
56. Guilmot A, Hermann E, Braud VM, Carlier Y, Truyens C. Natural Killer Cell Responses to Infections in Early Life. *J Innate Immun* (2011) 3(3):280–8. doi: 10.1159/000323934
57. Le Garff-Tavernier M, Béziat V, Decocq J, Siguret V, Gandjbakhch F, Pautas E, et al. Human NK Cells Display Major Phenotypic and Functional Changes Over the Life Span. *Aging Cell* (2010) 9(4):527–35. doi: 10.1111/j.1474-9726.2010.00584.x
58. Skeen MJ, Ziegler HK. Activation of Gamma Delta T Cells for Production of IFN-Gamma is Mediated by Bacteria *via* Macrophage-Derived Cytokines IL-1 and IL-12. *J Immunol* (1995) 154(11):5832–41. PMID 7538532
59. Morita CT, Parker CM, Brenner MB, Band H. TCR Usage and Functional Capabilities of Human Gamma Delta T Cells at Birth. *J Immunol* (1994) 153 (9):3979–88. PMID 7930606

60. Engelmann I, Moeller U, Santamaria A, Kremsner PG, Luty AJ. Differing Activation Status and Immune Effector Molecule Expression Profiles of Neonatal and Maternal Lymphocytes in an African Population. *Immunology* (2006) 119(4):515–21. doi: 10.1111/j.1365-2567.2006.02466.x
61. van der Heiden M, Björkander S, Rahman Qazi K, Bittmann J, Hell L, Jenmalm MC, et al. Characterization of the γδ T-Cell Compartment During Infancy Reveals Clear Differences Between the Early Neonatal Period and 2 Years of Age. *Immunol Cell Biol* (2020) 98(1):79–87. doi: 10.1111/imcb.12303
62. Guo XJ, Dash P, Crawford JC, Allen EK, Zamora AE, Boyd DF, et al. Lung γδ T Cells Mediate Protective Responses During Neonatal Influenza Infection That Are Associated With Type 2 Immunity. *Immunity* (2018) 49(3):531–44.e6. doi: 10.1016/j.immuni.2018.07.011
63. Brennan PJ, Brigl M, Brenner MB. Invariant Natural Killer T Cells: An Innate Activation Scheme Linked to Diverse Effector Functions. *Nat Rev Immunol* (2013) 13(2):101–17. doi: 10.1038/nri3369
64. Fallon EA, Chun TT, Young WA, Gray C, Ayala A, Heffernan DS. Program Cell Death Receptor-1-Mediated Invariant Natural Killer T-Cell Control of Peritoneal Macrophage Modulates Survival in Neonatal Sepsis. *Front Immunol* (2017) 8:1469. doi: 10.3389/fimmu.2017.01469
65. Tai Y, Wang Q, Korner H, Zhang L, Wei W. Molecular Mechanisms of T Cells Activation by Dendritic Cells in Autoimmune Diseases. *Front Pharmacol* (2018) 9:642. doi: 10.3389/fphar.2018.00642
66. Linsley PS, Brady W, Urnes M, Grosmaire LS, Damle NK, Ledbetter JA. CTLA-4 is a Second Receptor for the B Cell Activation Antigen B7. *J Exp Med* (1991) 174(3):561–9. doi: 10.1084/jem.174.3.561
67. Keir ME, Butte MJ, Freeman GJ, Sharpe AH. PD-1 and its Ligands in Tolerance and Immunity. *Annu Rev Immunol* (2008) 26:677–704. doi: 10.1146/annurev.immunol.26.021607.090331
68. Chinai JM, Janakiram M, Chen F, Chen W, Kaplan M, Zang X. New Immunotherapies Targeting the PD-1 Pathway. *Trends Pharmacol Sci* (2015) 36(9):587–95. doi: 10.1016/j.tips.2015.06.005
69. Wang L, Rubinstein R, Lines JL, Wasiuk A, Ahonen C, Guo Y, et al. VISTA, a Novel Mouse Ig Superfamily Ligand That Negatively Regulates T-Cell Responses. *J Exp Med* (2011) 208(3):577–92. doi: 10.1084/jem.20100619
70. Marsters SA, Ayres TM, Skubatch M, Gray CL, Rothe M, Ashkenazi A. Herpesvirus Entry Mediator, a Member of the Tumor Necrosis Factor Receptor (TNFR) Family, Interacts With Members of the TNFR-Associated Factor Family and Activates the Transcription Factors NF-kappaB and AP-1. *J Biol Chem* (1997) 272(22):14029–32. doi: 10.1074/jbc.272.22.14029
71. Chikuma S. Basics of PD-1 in Self-Tolerance, Infection, and Cancer Immunity. *Int J Clin Oncol* (2016) 21(3):448–55. doi: 10.1007/s10147-016-0958-0
72. Zhang Q, Vignali DA. Co-Stimulatory and Co-Inhibitory Pathways in Autoimmunity. *Immunity* (2016) 44(5):1034–51. doi: 10.1016/j.immuni.2016.04.017
73. Tamayo E, Fernández A, Almansa R, Carrasco E, Heredia M, Lajo C, et al. Pro- and Anti-Inflammatory Responses are Regulated Simultaneously From the First Moments of Septic Shock. *Eur Cytokine Netw* (2011) 22(2):82–7. doi: 10.1684/ecn.2011.0281
74. Darden DB, Kelly LS, Fenner BP, Moldawer LL, Mohr AM, Efron PA. Dysregulated Immunity and Immunotherapy After Sepsis. *J Clin Med* (2021) 10(8):1742. doi: 10.3390/jcm10081742
75. Patil NK, Guo Y, Luan L, Sherwood ER. Targeting Immune Cell Checkpoints During Sepsis. *Int J Mol Sci* (2017) 18(11):2413. doi: 10.3390/ijms18112413
76. Hsu H, Boudova S, Mvula G, Divala TH, Mungwira RG, Harman C, et al. Prolonged PD1 Expression on Neonatal Vδ2 Lymphocytes Dampens Proinflammatory Responses: Role of Epigenetic Regulation. *J Immunol* (2016) 197(5):1884–92. doi: 10.4049/jimmunol.1600284
77. Latchman Y, Wood CR, Chernova T, Chaudhary D, Borde M, Chernova I, et al. PD-L2 is a Second Ligand for PD-1 and Inhibits T Cell Activation. *Nat Immunol* (2001) 2(3):261–8. doi: 10.1038/85330
78. Parry RV, Chemnitz JM, Frauwirth KA, Lanfranco AR, Braunstein I, Kobayashi SV, et al. CTLA-4 and PD-1 Receptors Inhibit T-Cell Activation by Distinct Mechanisms. *Mol Cell Biol* (2005) 25(21):9543–53. doi: 10.1128/MCB.25.21.9543-9553.2005
79. Sheppard KA, Fitz LJ, Lee JM, Benander C, George JA, Wooters J, et al. PD-1 Inhibits T-Cell Receptor Induced Phosphorylation of the ZAP70/CD3zeta Signalosome and Downstream Signaling to PKCtheta. *FEBS Lett* (2004) 574 (1-3):37–41. doi: 10.1016/j.febslet.2004.07.083
80. Nowak EC, Lines JL, Varn FS, Deng J, Sarde A, Mabaera R, et al. Immunoregulatory Functions of VISTA. *Immunol Rev* (2017) 276(1):66–79. doi: 10.1111/imr.12525
81. Xu W, Dong J, Zheng Y, Zhou J, Yuan Y, Ta HM, et al. Immune-Checkpoint Protein VISTA Regulates Antitumor Immunity by Controlling Myeloid Cell-Mediated Inflammation and Immunosuppression. *Cancer Immunol Res* (2019) 7(9):1497–510. doi: 10.1158/2326-6066.CIR-18-0489
82. Cai G, Freeman GJ. The CD160, BTLA, LIGHT/HVEM Pathway: A Bidirectional Switch Regulating T-Cell Activation. *Immunol Rev* (2009) 229(1):244–58. doi: 10.1111/j.1600-065X.2009.00783.x
83. Cheung TC, Steinberg MW, Oborne LM, Macauley MG, Fukuyama S, Sanjo H, et al. Unconventional Ligand Activation of Herpesvirus Entry Mediator Signals Cell Survival. *Proc Natl Acad Sci U S A* (2009) 106(15):6244–9. doi: 10.1073/pnas.0902115106
84. Qin W, Hu L, Zhang X, Jiang S, Li J, Zhang Z, et al. The Diverse Function of PD-1/PD-L Pathway Beyond Cancer. *Front Immunol* (2019) 10:2298. doi: 10.3389/fimmu.2019.02298
85. Chemnitz JM, Parry RV, Nichols KE, June CH, Riley JL. SHP-1 and SHP-2 Associate With Immunoreceptor Tyrosine-Based Switch Motif of Programmed Death 1 Upon Primary Human T Cell Stimulation, But Only Receptor Ligation Prevents T Cell Activation. *J Immunol* (2004) 173 (2):945–54. doi: 10.4049/jimmunol.173.2.945
86. Bennett F, Luxenberg D, Ling V, Wang IM, Marquette K, Lowe D, et al. Program Death-1 Engagement Upon TCR Activation has Distinct Effects on Costimulation and Cytokine-Driven Proliferation: Attenuation of ICOS, IL-4, and IL-21, But Not CD28, IL-7, and IL-15 Responses. *J Immunol* (2003) 170(2):711–8. doi: 10.4049/jimmunol.170.2.711
87. Yokosuka T, Takamatsu M, Kobayashi-Imanishi W, Hashimoto-Tane A, Azuma M, Saito T. Programmed Cell Death 1 Forms Negative Costimulatory Microclusters That Directly Inhibit T Cell Receptor Signaling by Recruiting Phosphatase SHP2. *J Exp Med* (2012) 209 (6):1201–17. doi: 10.1084/jem.20112741
88. Nakamori Y, Park EJ, Shimaoka M. Immune Deregulation in Sepsis and Septic Shock: Reversing Immune Paralysis by Targeting PD-1/PD-L1 Pathway. *Front Immunol* (2020) 11:624279. doi: 10.3389/fimmu.2020.624279
89. Boomer JS, To K, Chang KC, Takasu O, Osborne DF, Walton AH, et al. Immunosuppression in Patients Who Die of Sepsis and Multiple Organ Failure. *JAMA* (2011) 306(23):2594–605. doi: 10.1001/jama.2011.1829
90. Nishimura H, Nose M, Hiai H, Minato N, Honjo T. Development of Lupus-Like Autoimmune Diseases by Disruption of the PD-1 Gene Encoding an ITIM Motif-Carrying Immunoreceptor. *Immunity* (1999) 11(2):141–51. doi: 10.1016/S1074-7613(00)80089-8
91. Nishimura H, Okazaki T, Tanaka Y, Nakatani K, Hara M, Matsumori A, et al. Autoimmune Dilated Cardiomyopathy in PD-1 Receptor-Deficient Mice. *Science* (2001) 291(5502):319–22. doi: 10.1126/science.291.5502.319
92. Monaghan SF, Thakkar RK, Heffernan DS, Huang X, Chung CS, Lomas-Neira J, et al. Mechanisms of Indirect Acute Lung Injury: A Novel Role for the Coinhibitory Receptor, Programmed Death-1. *Ann Surg* (2012) 255 (1):158–64. doi: 10.1097/SLA.0b013e31823433ca
93. Zhang Y, Zhou Y, Lou J, Li J, Bo L, Zhu K, et al. PD-L1 Blockade Improves Survival in Experimental Sepsis by Inhibiting Lymphocyte Apoptosis and Reversing Monocyte Dysfunction. *Crit Care* (2010) 14(6):R220. doi: 10.1186/cc9354
94. Chang KC, Burnham CA, Compton SM, Rasche DP, Mazuski RJ, McDonough JS, et al. Blockade of the Negative Co-Stimulatory Molecules PD-1 and CTLA-4 Improves Survival in Primary and Secondary Fungal Sepsis. *Crit Care* (2013) 17(3):R85. doi: 10.1186/cc12711
95. Butte MJ, Keir ME, Phamduy TB, Sharpe AH, Freeman GJ. Programmed Death-1 Ligand 1 Interacts Specifically With the B7-1 Costimulatory

Molecule to Inhibit T Cell Responses. *Immunity* (2007) 27(1):111–22. doi: 10.1016/j.immuni.2007.05.016
96. Ansari MJ, Salama AD, Chitnis T, Smith RN, Yagita H, Akiba H, et al. The Programmed Death-1 (PD-1) Pathway Regulates Autoimmune Diabetes in Nonobese Diabetic (NOD) Mice. *J Exp Med* (2003) 198(1):63–9. doi: 10.1084/jem.20022125
97. Latchman YE, Liang SC, Wu Y, Chernova T, Sobel RA, Klemm M, et al. PD-L1-Deficient Mice Show That PD-L1 on T Cells, Antigen-Presenting Cells, and Host Tissues Negatively Regulates T Cells. *Proc Natl Acad Sci U S A* (2004) 101(29):10691–6. doi: 10.1073/pnas.0307252101
98. Shao R, Fang Y, Yu H, Zhao L, Jiang Z, Li CS. Monocyte Programmed Death Ligand-1 Expression After 3-4 Days of Sepsis is Associated With Risk Stratification and Mortality in Septic Patients: A Prospective Cohort Study. *Crit Care* (2016) 20(1):124. doi: 10.1186/s13054-016-1301-x
99. Flies DB, Wang S, Xu H, Chen L. Cutting Edge: A Monoclonal Antibody Specific for the Programmed Death-1 Homolog Prevents Graft-Versus-Host Disease in Mouse Models. *J Immunol* (2011) 187(4):1537–41. doi: 10.4049/jimmunol.1100660
100. Aloia L, Parisi S, Fusco L, Pastore L, Russo T. Differentiation of Embryonic Stem Cells 1 (Dies1) is a Component of Bone Morphogenetic Protein 4 (BMP4) Signaling Pathway Required for Proper Differentiation of Mouse Embryonic Stem Cells. *J Biol Chem* (2010) 285(10):7776–83. doi: 10.1074/jbc.M109.077156
101. Huang X, Zhang X, Li E, Zhang G, Wang X, Tang T, et al. VISTA: An Immune Regulatory Protein Checking Tumor and Immune Cells in Cancer Immunotherapy. *J Hematol Oncol* (2020) 13(1):83. doi: 10.1186/s13045-020-00917-y
102. Wang J, Wu G, Manick B, Hernandez V, Renelt M, Erickson C, et al. VSIG-3 as a Ligand of VISTA Inhibits Human T-Cell Function. *Immunology* (2019) 156(1):74–85. doi: 10.1111/imm.13001
103. Johnston RJ, Su LJ, Pinckney J, Critton D, Boyer E, Krishnakumar A, et al. VISTA is an Acidic pH-Selective Ligand for PSGL-1. *Nature* (2019) 574 (7779):565–70. doi: 10.1038/s41586-019-1674-5
104. Wang L, Le Mercier I, Putra J, Chen W, Liu J, Schenk AD, et al. Disruption of the Immune-Checkpoint VISTA Gene Imparts a Proinflammatory Phenotype With Predisposition to the Development of Autoimmunity. *PNAS* (2014) 111(41):14846–51. doi: 10.1073/pnas.1407447111
105. Ceeraz S, Sergent PA, Plummer SF, Schned AR, Pechenick D, Burns CM, et al. VISTA Deficiency Accelerates the Development of Fatal Murine Lupus Nephritis. *Arthritis Rheumatol* (2017) 69(4):814–25. doi: 10.1002/art.40020
106. Liu J, Yuan Y, Chen W, Putra J, Suriawinata AA, Schenk AD, et al. Immune-Checkpoint Proteins VISTA and PD-1 Nonredundantly Regulate Murine T-Cell Responses. *PNAS* (2015) 112(21):6682–7. doi: 10.1073/pnas.1420370112
107. Gray CC, Biron-Girard B, Wakeley ME, Chung CS, Chen Y, Quiles-Ramirez Y, et al. Negative Immune Checkpoint Protein, VISTA, Regulates the CD4 (+) T(reg) Population During Sepsis Progression to Promote Acute Sepsis Recovery and Survival. *Front Immunol* (2022) 13:861670. doi: 10.3389/fimmu.2022.861670
108. Montgomery RI, Warner MS, Lum BJ, Spear PG. Herpes Simplex Virus-1 Entry Into Cells Mediated by a Novel Member of the TNF/NGF Receptor Family. *Cell* (1996) 87(3):427–36. doi: 10.1016/S0092-8674(00)81363-X
109. Harrop JA, McDonnell PC, Brigham-Burke M, Lyn SD, Minton J, Tan KB, et al. Herpesvirus Entry Mediator Ligand (HVEM-L), a Novel Ligand for HVEM/TR2, Stimulates Proliferation of T Cells and Inhibits HT29 Cell Growth. *J Biol Chem* (1998) 273(42):27548–56. doi: 10.1074/jbc.273.42.27548
110. Mauri DN, Ebner R, Montgomery RI, Kochel KD, Cheung TC, Yu GL, et al. LIGHT, a New Member of the TNF Superfamily, and Lymphotoxin Alpha are Ligands for Herpesvirus Entry Mediator. *Immunity* (1998) 8(1):21–30. doi: 10.1016/S1074-7613(00)80455-0
111. Tamada K, Shimozaki K, Chapoval AI, Zhai Y, Su J, Chen SF, et al. LIGHT, a TNF-Like Molecule, Costimulates T Cell Proliferation and is Required for Dendritic Cell-Mediated Allogeneic T Cell Response. *J Immunol* (2000) 164 (8):4105–10. doi: 10.4049/jimmunol.164.8.4105
112. Liu W, Chou TF, Garrett-Thomson SC, Seo GY, Fedorov E, Ramagopal UA, et al. HVEM Structures and Mutants Reveal Distinct Functions of Binding to LIGHT and BTLA/Cd160. *J Exp Med* (2021) 218(12)e20211112. doi: 10.1084/jem.20211112
113. Watanabe N, Gavrieli M, Sedy JR, Yang J, Fallarino F, Loftin SK, et al. BTLA is a Lymphocyte Inhibitory Receptor With Similarities to CTLA-4 and PD-1. *Nat Immunol* (2003) 4(7):670–9. doi: 10.1038/ni944
114. Murphy TL, Murphy KM. Slow Down and Survive: Enigmatic Immunoregulation by BTLA and HVEM. *Annu Rev Immunol* (2010) 28:389–411. doi: 10.1146/annurev-immunol-030409-101202
115. Shubin NJ, Chung CS, Heffernan DS, Irwin LR, Monaghan SF, Ayala A. BTLA Expression Contributes to Septic Morbidity and Mortality by Inducing Innate Inflammatory Cell Dysfunction. *J Leukoc Biol* (2012) 92 (3):593–603. doi: 10.1189/jlb.1211641
116. Cheng T, Bai J, Chung CS, Chen Y, Biron BM, Ayala A. Enhanced Innate Inflammation Induced by Anti-BTLA Antibody in Dual Insult Model of Hemorrhagic Shock/Sepsis. *Shock* (2016) 45(1):40–9. doi: 10.1097/SHK.0000000000000479
117. Lange A, Sundén-Cullberg J, Magnuson A, Hultgren O. Soluble B and T Lymphocyte Attenuator Correlates to Disease Severity in Sepsis and High Levels Are Associated With an Increased Risk of Mortality. *PLos One* (2017) 12(1):e0169176. doi: 10.1371/journal.pone.0169176
118. Shubin NJ, Monaghan SF, Heffernan DS, Chung CS, Ayala A. B and T Lymphocyte Attenuator Expression on CD4+ T-Cells Associates With Sepsis and Subsequent Infections in ICU Patients. *Crit Care* (2013) 17(6):R276. doi: 10.1186/cc13131
119. Young WA, Fallon EA, Heffernan DS, Efron PA, Cioffi WG, Ayala A. Improved Survival After Induction of Sepsis by Cecal Slurry in PD-1 Knockout Murine Neonates. *Surgery* (2017) 161(5):1387–93. doi: 10.1016/j.surg.2016.11.008
120. Zasada M, Lenart M, Rutkowska-Zapała M, Stec M, Durlak W, Grudzień A, et al. Analysis of PD-1 Expression in the Monocyte Subsets From non-Septic and Septic Preterm Neonates. *PLos One* (2017) 12(10):e0186819. doi: 10.1371/journal.pone.0186819
121. Guo X, Xu Y, Luo W, Fang R, Cai L, Wang P, et al. Programmed Cell Death Protein-1 (PD-1) Protects Liver Damage by Suppressing IFN-γ Expression in T Cells in Infants and Neonatal Mice. *BMC Pediatr* (2021) 21(1):317. doi: 10.1186/s12887-021-02794-x
122. Rabe H, Nordström I, Andersson K, Lundell AC, Rudin A. Staphylococcus Aureus Convert Neonatal Conventional CD4(+) T Cells Into FOXP3(+) CD25(+) CD127(low) T Cells *via* the PD-1/PD-L1 Axis. *Immunology* (2014) 141(3):467–81. doi: 10.1111/imm.12209
123. Wang WD, Yang XR, Guo MF, Pan ZF, Shang M, Qiu MJ, et al. Up-Regulation of BTLA Expression in Myeloid Dendritic Cells Associated With the Treatment Outcome of Neonatal Sepsis. *Mol Immunol* (2021) 134:129–40. doi: 10.1016/j.molimm.2021.03.007
124. Hotchkiss RS, Colston E, Yende S, Crouser ED, Martin GS, Albertson T, et al. Immune Checkpoint Inhibition in Sepsis: A Phase 1b Randomized Study to Evaluate the Safety, Tolerability, Pharmacokinetics, and Pharmacodynamics of Nivolumab. *Intensive Care Med* (2019) 45(10):1360–71. doi: 10.1007/s00134-019-05704-z
125. Hotchkiss RS, Colston E, Yende S, Angus DC, Moldawer LL, Crouser ED, et al. Immune Checkpoint Inhibition in Sepsis: A Phase 1b Randomized, Placebo-Controlled, Single Ascending Dose Study of Antiprogrammed Cell Death-Ligand 1 Antibody (BMS-936559). *Crit Care Med* (2019) 47(5):632–42. doi: 10.1097/CCM.0000000000003685
126. US Food and Drug Administration and Center for Drug Evaluation and Research. *Keytruda BLA 125514/0 Approval Letter* . Available at: https://www.accessdata.fda.gov/drugsatfda_docs/appletter/2014/125514Orig1s000ltr.pdf.
127. US Food and Drug Administration and Center for Drug Evaluation and Research. *Opdivo NDA 125554Orig1s000 Approval Letter* . Available at: https://www.accessdata.fda.gov/drugsatfda_docs/nda/2014/125554Orig1s000Approv.pdf.
128. US Food and Drug Administration and Center for Drug Evaluation and Research. *Libtayo BLA 761097 Approval Letter* . Available at: https://www.accessdata.fda.gov/drugsatfda_docs/nda/2018/761097Orig1s000Approv.pdf.

129. US Food and Drug Administration and Center for Drug Evaluation and Research. *Tecentriq BLA 761041 Approval Letter* . Available at: https://www.accessdata.fda.gov/drugsatfda_docs/nda/2016/761041Orig1s000Approv.pdf.
130. US Food and Drug Administration and Center for Drug Evaluation and Research. *Bavencio BLA 761049 Approval Letter* . Available at: https://www.accessdata.fda.gov/drugsatfda_docs/appletter/2017/761049Orig1s000ltredt.pdf.
131. US Food and Drug Administration and Center for Drug Evaluation and Research. *Imfinzi BLA 761069 Approval Letter* . Available at: https://www.accessdata.fda.gov/drugsatfda_docs/nda/2017/761069Orig1s000Approv.pdf.
132. US Food and Drug Administration and Center for Drug Evaluation and Research. *Yervoy BLA 125377/0 Approval Letter* . Available at: https://www.accessdata.fda.gov/drugsatfda_docs/nda/2011/125377Orig1s000Approv.pdf.
133. Rotte A, Jin JY, Lemaire V. Mechanistic Overview of Immune Checkpoints to Support the Rational Design of Their Combinations in Cancer Immunotherapy. *Ann Oncol* (2018) 29(1):71–83. doi: 10.1093/annonc/mdx686
134. Rotte A. Combination of CTLA-4 and PD-1 Blockers for Treatment of Cancer. *J Exp Clin Cancer Res* (2019) 38(1):255. doi: 10.1186/s13046-019-1259-z

Conflict of Interest: The authors declare that the research was conducted in the absence of any commercial or financial relationships that could be construed as a potential conflict of interest.

frontiers | Frontiers in Pharmacology

ORIGINAL RESEARCH
published: 04 July 2022
doi: 10.3389/fphar.2022.923814

Nanoparticle-Induced Augmentation of Neutrophils' Phagocytosis of Bacteria

Kathryn M. Rubey[1], Alexander R. Mukhitov[2], Jia Nong[2,3], Jichuan Wu[2,3], Vera P. Krymskaya[2], Jacob W. Myerson[3], G. Scott Worthen[1]* and Jacob S. Brenner[2]*,[3]*

[1]Department of Pediatrics, Children's Hospital of Philadelphia, Philadelphia, PA, United States, [2]Department of Medicine, University of Pennsylvania, Philadelphia, PA, United States, [3]Department of Pharmacology, University of Pennsylvania, Philadelphia, PA, United States

Despite the power of antibiotics, bacterial infections remain a major killer, due to antibiotic resistance and hosts with dysregulated immune systems. We and others have been developing drug-loaded nanoparticles that home to the sites of infection and inflammation via engineered tropism for neutrophils, the first-responder leukocytes in bacterial infections. Here, we examined how a member of a broad class of neutrophil-tropic nanoparticles affects neutrophil behavior, specifically questioning whether the nanoparticles attenuate an important function, bacterial phagocytosis. We found these nanoparticles actually *augment* phagocytosis of non-opsonized bacteria, increasing it by ~50%. We showed this augmentation of phagocytosis is likely co-opting an evolved response, as opsonized bacteria also augment phagocytosis of non-opsonized bacteria. Enhancing phagocytosis of non-opsonized bacteria may prove particularly beneficial in two clinical situations: in hypocomplementemic patients (meaning low levels of the main bacterial opsonins, complement proteins, seen in conditions such as neonatal sepsis and liver failure) or for bacteria that are largely resistant to complement opsonization (e.g., *Neisseria*). Additionally, we observe that; 1) prior treatment with bacteria augments neutrophil uptake of neutrophil-tropic nanoparticles; 2) neutrophil-tropic nanoparticles colocalize with bacteria inside of neutrophils. The observation that neutrophil-tropic nanoparticles enhance neutrophil phagocytosis and localize with bacteria inside neutrophils suggests that these nanoparticles will serve as useful carriers for drugs to ameliorate bacterial diseases.

Keywords: nanoparticle, nanomedicine, neutrophil, phagocytosis, opsonization, complement

OPEN ACCESS

Edited by:
Alexey Victorovich Sokolov, Institute of Experimental Medicine (RAS), Russia

Reviewed by:
Milankumar Prajapati, Brown University, United States
Yuan Tang, University of Toledo, United States

****Correspondence:***
Jacob W. Myerson myerson@pennmedicine.upenn.edu
G. Scott Worthen worthen@chop.edu
Jacob S. Brenner jacob.brenner@pennmedicine.upenn.edu

Specialty section:
This article was submitted to Inflammation Pharmacology, a section of the journal Frontiers in Pharmacology

Received: *19 April 2022*
Accepted: *31 May 2022*
Published: *04 July 2022*

Citation:
Rubey KM, Mukhitov AR, Nong J, Wu J, Krymskaya VP, Myerson JW, Worthen GS and Brenner JS (2022) Nanoparticle-Induced Augmentation of Neutrophils' Phagocytosis of Bacteria. Front. Pharmacol. 13:923814. doi: 10.3389/fphar.2022.923814

1 INTRODUCTION

The introduction of antibiotics last century has left the lay public thinking that bacterial infections are a relatively solved problem, but the clinical reality is that these diverse diseases still cause a huge number of deaths and severe illnesses, even when antibiotics are used (File and Marrie, 2010; Xu et al., 2020; Rubey and Brenner, 2021; WHO, 2021). The reasons for incomplete effectiveness include at least 3 major factors: First, the "host response" to bacteria is often deleterious, epitomized by sepsis-induced organ failure (Pechous, 2017; Lelubre and Vincent, 2018). Second, bacterial resistance to antibiotics is rising precipitously (Boucher et al., 2009; Reardon, 2015; Centers for Disease Control and Prevention, 2019). Third, many hosts, by virtue of age, underlying condition, or therapeutic

regimen, are immunocompromised and unable to clear bacteria even in the presence of antibiotics (Grant and Hung, 2013; Tosi et al., 2018). All of these problems are compounded by a lack of innovation in therapies compared to other fields (Silver, 2011).

To solve this problem, we and others have been developing nanoparticles that can deliver drugs directly to the site of infection (Rubey and Brenner, 2021). This approach may address each of the 3 problems listed above, depending on whether the cargo drug is an antibiotic, whose therapeutic index can be improved by localization, or an immunomodulator. A particularly promising method for targeting these nanoparticles to acute infections is directing the nanoparticles to neutrophils. Neutrophils are "first responder" leukocytes for most acute bacterial infections, and massively accumulate in sites of infection (Yipp et al., 2017). By delivering antibiotics to neutrophils, nanoparticles could improve bacterial killing. This may be especially useful for antibiotics that cannot cross neutrophil membranes, such as aminoglycosides. Alternatively, neutrophil-tropic nanoparticles could deliver anti-inflammatories to modulate some of the neutrophils' more deleterious responses (part of the dysregulated host defense of sepsis (Zemans, Colgan and Downey, 2009)), such as production of tissue damaging mediators such as neutrophil extracellular traps (NETs) (Yipp and Kubes, 2013), reactive oxygen species (ROS), and proteases (Moraes, Zurawska and Downey, 2006). Nanoparticles with tropism for neutrophils have potential to greatly improve most key aspects of acute bacterial infections, and even non-bacterial inflammatory diseases, such as acute respiratory distress syndrome (ARDS), the highly neutrophilic lung inflammation that kills in COVID-19 (Sinha et al., 2022).

We recently reported a nanomaterials screen to identify nanoparticles with strong tropism to the neutrophils that accumulate in the capillaries of the lungs during inflammation and play a major role in pneumonia, COVID-19, and ARDS (Myerson et al., 2022). We found a broad class of nanoparticles with neutrophil-tropism: "nanoparticles with agglutinated proteins" (NAPs). NAPs have surface-accessible proteins arranged in a non-crystalline pattern (meaning agglutinated/amorphous). By contrast, crystalline protein nanoparticles (viral capsids, ferritin, etc), which have their surface proteins arranged in a fixed and regular pattern, do not have neutrophil tropism. We showed this tropism is due to the fact that NAPs rapidly bind the serum proteins, including C3b and other complement proteins, suggesting complement activation, while non-NAPs do not. Complement is an important component of the immune system that aids phagocytic cells in recognizing particulate matter to be phagocytosed. Previous studies have been dedicated to further understanding of complement binding and activation caused by nanoparticles as it can be a barrier to a nanocarrier's therapeutic potential (Scieszka et al., 1991; Inturi et al., 2015; Chen et al., 2017; Moghimi and Simberg, 2017; Betker et al., 2018; Vu et al., 2019). We have chosen to use this property to our advantage as serum-opsonization of NAPs is essential for their strong neutrophil tropism.

To develop NAPs for targeted delivery to neutrophils in infectious diseases, such as pneumonia, we aim here to ensure that NAPs coordinate with the key beneficial functions of neutrophils, and do not negatively impact their function. Previous studies have shown that nanoparticle phagocytosis may decrease neutrophil adhesion and migration (Fromen et al., 2017). Probably the most essential function of neutrophils during infections like pneumonia is phagocytosis of bacteria, since phagocytosis is necessary for killing of certain bacteria (Lee, Harrison and Grinstein, 2003). Here, we tested neutrophil phagocytosis of NAPs before and after neutrophil phagocytosis of the common bacterial pathogen, *E. coli*. We found that NAPs do not negatively impact neutrophil phagocytosis of bacteria and NAPs localize to neutrophils that have also taken up bacteria. Quite surprisingly, NAPs, given *after* bacteria, enhance efficiency of neutrophils' phagocytosis of bacteria that have not been opsonized by serum proteins. This effect, termed here *second particle augmentation factor (2PAF)* was illustrated in both: flow cytometry and microscopy. Our results suggest applicability of NAPs to two important clinical situations: hypocomplementemic states (e.g., the neonate (Wolach et al., 1994; Kemp and Campbell, 1996; Schelonka and Infante, 1998; McGreal et al., 2012; Zimmermann and Jones, 2021) and liver failure) and bacteria that have strong complement-defense mechanisms (Flannagan, Cosío and Grinstein, 2009) (e.g., *Neisseria* coats itself in the complement inhibitor Factor H). In such clinical situations, NAPs' augmentation of bacterial phagocytosis and colocalization with bacteria in neutrophils could provide a major benefit, beyond the benefits of cargo drugs themselves.

2 RESULTS AND DISCUSSION

We recently developed a diverse class of nanoparticles with neutrophil-tropism: NAPs(Myerson et al., 2022). In the present study, we focus on a prototypical member of this class, lysozyme-dextran nanogels (hereafter referred to as "nanogels" or NGs). NGs have the benefit for antibiotic delivery of prolonged nanoparticle shelf-life (years at 4C) and a very high drug-to-carrier mass ratio (Myerson et al., 2018, 2019).

In these experiments with nanogels, we again confirmed our previous findings that particle uptake is enhanced by opsonization by complement proteins present in serum (Myerson et al., 2022). When complement protein C3 is depleted from serum via cobra venom factor (CVF) (Haihua et al., 2018), we see a significant decrease in the percent of neutrophils that take up nanogels (**Supplemental Figure S1**). The green serum nanogels (second green bar) showed ~80% positivity, as compared to the green CVF nanogels (third and fifth green bars) which had ~30% positivity. It has been well established that complement binding to *E. coli* is necessary for neutrophil phagocytosis of the bacteria (Horwitz and Silverstein, 1980; Brekke et al., 2007). We utilized serum-opsonization of both NAPs and *E. coli* bioparticles for these experiments.

One of the first tests of whether these nanocarriers can be used to augment bacterial killing is whether neutrophils will take up the nanocarriers after having been exposed to bacteria. In this experiment, diagrammed in **Figure 1A**, neutrophils were

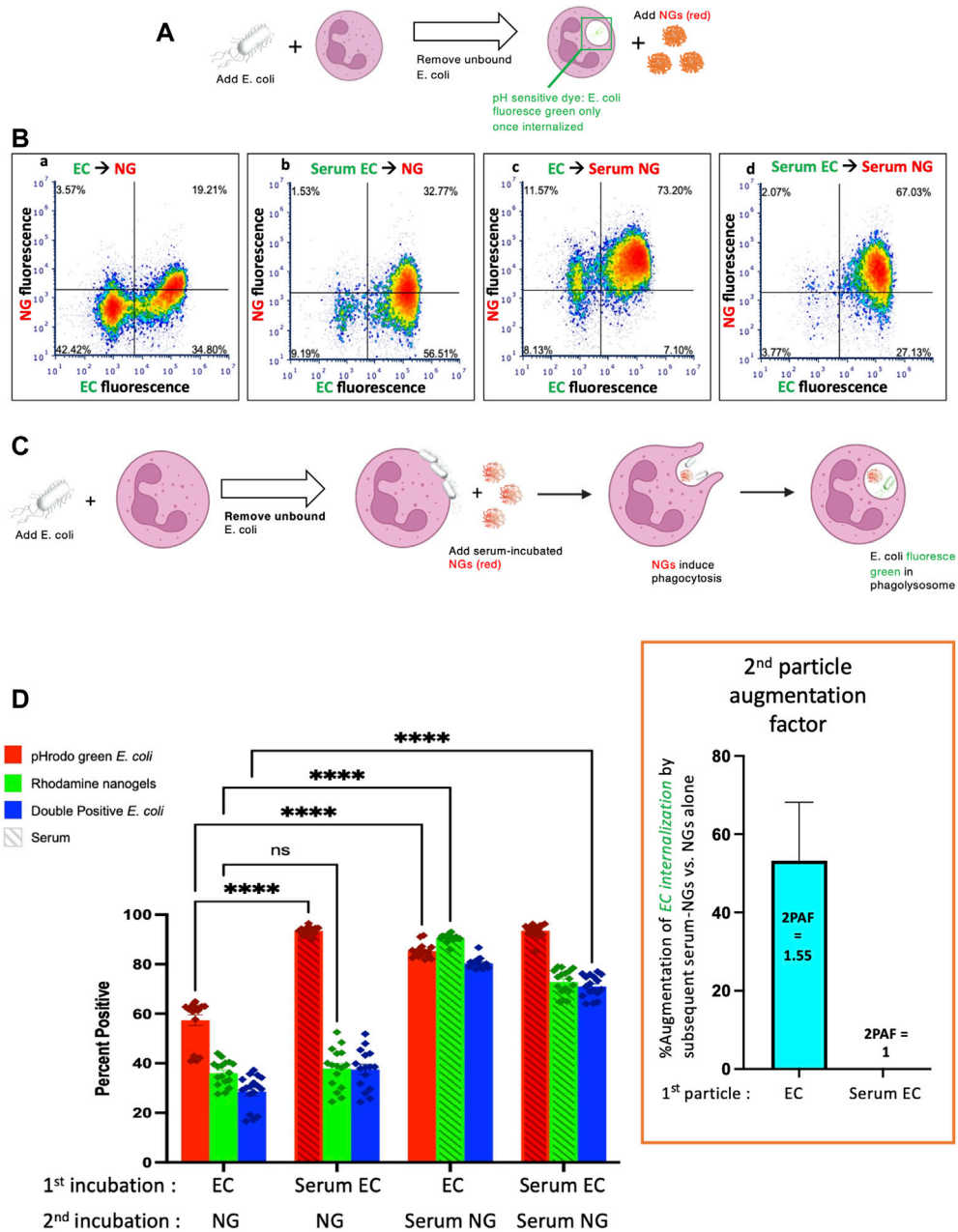

FIGURE 1 | Nanogels augment phagocytosis of E. coli. **(A)** Neutrophils were incubated with pH-sensitive fluorescent E. coli that only fluoresce in the low pH of the phagosome, thus allowing detection of their phagocytosis. Notably, E. coli that bind to the exterior of neutrophils but are not internalized do *not* fluoresce. First neutrophils were exposed to green E. coli, thoroughly washed to remove unbound E. coli, and then incubated with red nanogels ("NG"). Importantly, before exposure to the neutrophils, select aliquots of nanogels and E. coli were opsonized by serum and thoroughly washed before exposure to neutrophils. **(B)** Representative dot-plots of the neutrophils subjected to flow cytometry *after* the second incubation, examining for green fluorescence (x-axis, indicating phagocytosis of the E. coli) and red (y-axis, nanogels). At the top of each subpanel, we indicate whether the E. coli (EC) were not exposed to serum (simply "EC") or were serum-opsonized ("Serum EC"); similar notation is used for nanogels without serum exposure (simply "NG") or those that were serum-opsonized ("Serum NG"). Neutrophils positive for uptake of green E. coli are represented as dots to the right of the vertical bar in the middle of the plot, with that threshold determined by measuring fluorescence of E. coli not exposed to any E. coli. Similarly, neutrophils represented as dots above the horizontal line are positive for red nanogels **(C)** Diagram of the proposed mechanism underlying this 2PFE of 1.5. Some E. coli remain bound to the neutrophil surface even after thoroughly washing the cells (second neutrophil image), but these surface-bound E. coli do not fluoresce since buffer pH of ~7 prevents their pH-sensitive dye from fluorescing. When these neutrophils encounter Serum NG, they phagocytose not just the nanogels, but also the E. coli (third neutrophil image), causing the E. coli to fluoresce in the low pH of the phagosome (fourth neutrophil). **(D)** Quantification of the flow cytometry experiments with n = 6 biological replicates for each sample. The bottom axis lists for the first and second incubations whether the E. coli and nanogels were first exposed to serum or not. The y-axis lists the % of neutrophils that were positive for phagocytosed E. coli (recalling that pH-sensitive E.coli on the *surface* of neutrophils will *not* fluoresce). Among the many bars to compare, the most important is comparing the first vs. third red bars, which both measure the % of neutrophils that phagocytosed

(*Continued*)

FIGURE 1 | non-serum-opsonized E. coli (EC). When the second incubation was with NG (not serum exposed), only 55% of neutrophils were positive for the EC presented during the first incubation. However, when the second incubation was with *Serum* NG, 85% of neutrophils were positive for the EC presented during the first incubation. This important ratio (first vs. third red bar), which we call the "second particle augmentation factor (2PAF)" was ~1.55 (*inset in box*, red), and *measures the fold-increase in phagocytosis of ECs induced by Serum NG (compared to non-serum-exposed NG, which serves as an internal control)*. Notably, while Serum NG augment uptake of (non-opsonized) EC by 50% (2PAF of 1.5), Serum NG do not significantly augment neutrophil uptake of Serum EC (second vs. fourth red bar, 2PAF = 1.0, blue bar in inset). Thus, Serum NG only augment phagocytosis of non-opsonized E. coli.

incubated with heat-killed *E. coli* bioparticles which have surface conjugated pHrodo green, a pH-sensitive dye that fluoresces green only when in the low pH environment of the phagosome. After this 60-min 37°C incubation, the neutrophils were pelleted and washed to remove free bacteria. The neutrophils were then incubated with nanogels for 15 min, and subjected to flow cytometry. Before exposure to neutrophils, half the samples of *E. coli* were serum-opsonized (hereafter referred to as "Serum EC"), while the other half were not exposed to serum (simply labeled as "EC" in **Figure 1**). Similarly, nanogels were divided into serum-opsonized ("Serum NG") and not (simply "NG").

Flow cytometry was gated to analyze neutrophils exclusively (**Supplemental Figure S2**). Representative flow cytometry dot-plots are depicted in **Figure 1B** and quantified in n = 6 biological replicates in **Figure 1D**. We compared the summary statistic of the percentage of neutrophils positive for *E. coli* and/or nanogel fluorescence. Among the numerous comparisons that can be made in this dataset, a surprising finding is demonstrated by comparing the first and third *E. coli* uptake values (red bars) in **Figure 1D**. These conditions measure the fraction of neutrophils that are positive for phagocytosis of *E. coli* that had not been exposed to serum ("EC"). When these neutrophils were incubated with nanogels that had not been exposed to serum (first red bar), 55% of the neutrophils were positive for *E. coli* phagocytosis. This percentage of neutrophils positive for *E. coli* went up to 85% if the nanogels had been pre-opsonized by serum. This means that serum-opsonized nanogels are able to augment *E. coli* phagocytosis. This augmentation occurred even though the nanogels were delivered *after* free *E. coli* had been washed away from the neutrophils.

We term this enhancement the "second particle augmentation factor" (2PAF) and define it for this particular experiment (**Figure 1**) as the following ratio: (% neutrophils positive for EC phagocytosis when the second delivered particle is Serum NG)/[% neutrophils positive for EC phagocytosis when the second delivered particle is (non-serum-exposed) NG]. 2PAF can be more generally defined as: (% neutrophils positive for particle #1 phagocytosis, given that particle #2 is serum-opsonized)/(% neutrophils positive for particle #1 phagocytosis, given that particle #2 was not exposed to serum); where particle #1 refers to the particle (or microbe) neutrophils are exposed to in the first incubation, and particle #2 refers to the second incubation. Thus, a 2PAF >1 indicates that serum-opsonized particle #2 are able to augment phagocytosis of particle #1 (as compared to the control condition, which uses particle #2 that was not exposed to serum). Calculating the 2PAF for non-serum exposed *E. coli* (EC), we thus get 2PAF = 85%/55% = 1.55, meaning that serum-opsonized nanogels increase neutrophil phagocytosis of these *E. coli* by 50% (**Figure 1D**, inset, blue bar). A 2PAF >1 is only found when the *E. coli* have not been serum opsonized: 2PAF = 1 when using serum-opsonized *E. coli*, a 0% increase (**Figure 1D**, inset). Thus, serum-opsonized nanogels are able to augment uptake of non-opsonized bacteria, but not opsonized bacteria, the latter of which are already phagocytosed so extensively (~100%) that we cannot detect improvement within the dynamic range of this assay. These findings that serum-opsonized nanogels would be most effective in augmenting phagocytosis of bacteria that are not complement-opsonized, such as bacteria that evade complement by covering themselves with Factor H (*Neisseria*, etc), or bacterial infections in hypocomplementemic hosts (e.g., neonatal sepsis). The mechanism by which serum enhances NAP phagocytosis is through coating the particles with complement proteins (e.g., C3), as shown previously (Myerson et al., 2022), and in **Supplemental Figure S1**. While complement opsonization is necessary for enhanced phagocytosis of NAPs, it is not known whether the 2PAF augmentation effect is also complement-dependent, a question that warrants future investigation.

A hypothesis to explain this enhancement is outlined in **Figure 1C**. The neutrophils are first incubated with green *E. coli* that fluoresce only when in the phagosome, since the *E. coli* is conjugated to the pH-sensitive dye pHrodo green. After incubating the *E. coli* with the neutrophils, free *E. coli* are removed by pelleting and thoroughly washing the neutrophils. However, some *E. coli* remain bound to the surface of the neutrophils (depicted in the second neutrophil of **Figure 1C**), but they will fluoresce minimally in subsequent flow cytometry unless they are internalized into an acidic compartment. Upon addition of serum-opsonized NGs, these surface-bound *E. coli* become phagocytosed as bystanders when the NGs are phagocytosed (third neutrophil of **Figure 1C**). This leads to the *E. coli* particles accumulating in the low-pH phagosome, where they fluoresce during flow cytometry. Thus, the use of *E. coli* that fluoresce only in the phagosome allowed detection of a 2PAF >1. As the free, unbound *E. coli* was removed prior to exposure to NGs, the *E. coli* present for the second exposure (NG) was neutrophil-bound. Thus, the mechanism of the 2PAF likely represents NG-facilitated phagocytosis of previously bound *E. coli* rather than a non-specific enhancement of phagocytosis.

Having made the finding that nanogels can augment phagocytosis of bacteria, we tested whether this was a phenomenon unique to NGs. We performed experiments with NGs replaced as a "second particle" by a second *E coli* particle, checking whether the second bacterial particles could enhance uptake of bacteria that were delivered during a first incubation. The experimental protocol was the same as **Figure 1A**, except that particle #1 was pHrodo green *E. coli*, and particle #2 was pHrodo red *E. coli* (**Figure 2A**). Here, the relevant conditions to compare

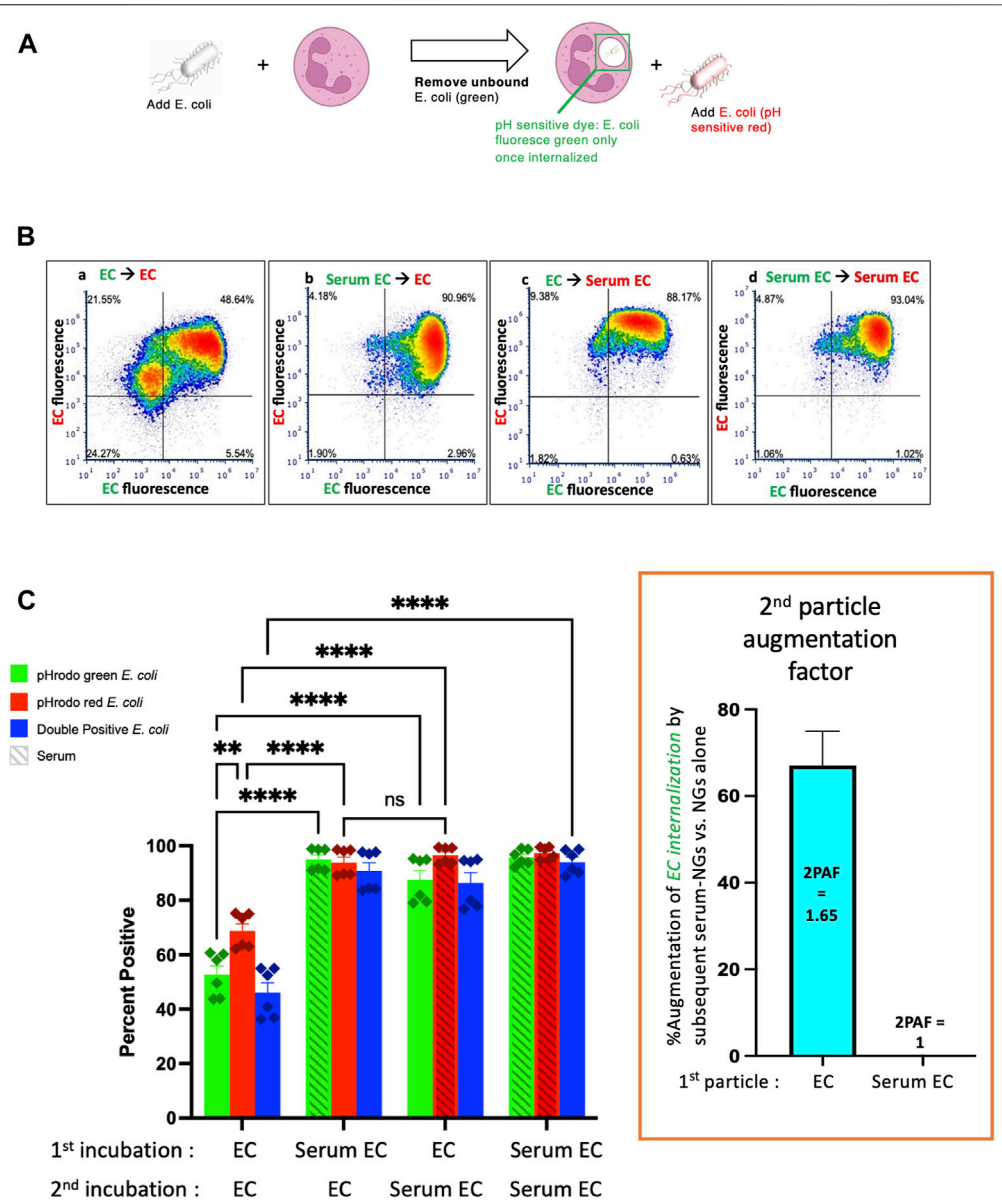

FIGURE 2 | Similarly to serum-opsonized nanogels, serum-opsonized E. coli augment internalization of non-opsonized E. coli. **(A)** Experimental scheme, similar to **Figure 1A**, but the second incubation was with E. coli. Note the first incubation was green E. coli, while the second was red E. coli. This experiment tests if, similar to serum-opsonized nanogels, E. coli can augment phagocytosis of previously delivered E. coli. **(B)** Representative dot-plots of the neutrophils, using the same notation as **Figure 1**. **(C)** Quantification of flow cytometry experiments (n = 6 biological replicates). Analogous to **Figure 1**, the most important comparison is the first vs. third green bars, which both measure the % of neutrophils that phagocytosed non-serum-opsonized green E. coli (EC) which were present during the first incubation. When the second incubation was also with EC, only 50% of neutrophils were positive for the green EC presented during the first incubation. However, when the second incubation was with Serum EC, 85% of neutrophils were positive for the green EC presented during the first incubation. Thus, when the first particle is EC, the "second particle augmentation factor (2PAF)" was ~1.65 (inset, red). While Serum EC augment uptake of (non-opsonized) EC by 65%, Serum EC do not significantly augment phagocytosis of Serum EC that were present in the first incubation (2PAF = 1.0, blue bar in inset). Also notable is that Serum EC delivered as the first particle augments the uptake of EC delivered second (second red bar vs. first red bar), showing the 2PAF effect does not depend on other order in which particles are delivered.

are **Figure 2C**'s first vs third green bars. This shows that phagocytosis of EC (non-serum exposed *E. coli*) is augmented by subsequent delivery of Serum EC (serum-opsonized *E. coli*). Indeed, the 2PAF = 1.65, or a 65% increase, (**Figure 2C**, inset, blue bar), is very similar to the 2PAF = 1.55 achieved with nanogels as particle # 2 (**Figure 1C**, inset, blue bar). Once again, the 2PAF is >1 only when the first-delivered particle (EC) had not been opsonized. Thus, the NGs' ability to augment uptake of bacteria is not unique to NGs, but is recapitulated in the neutrophil response to bacterial pathogens given in sequence. Our prior work shows that NGs, like bacteria, have tropism for neutrophils due to their rapid opsonization by

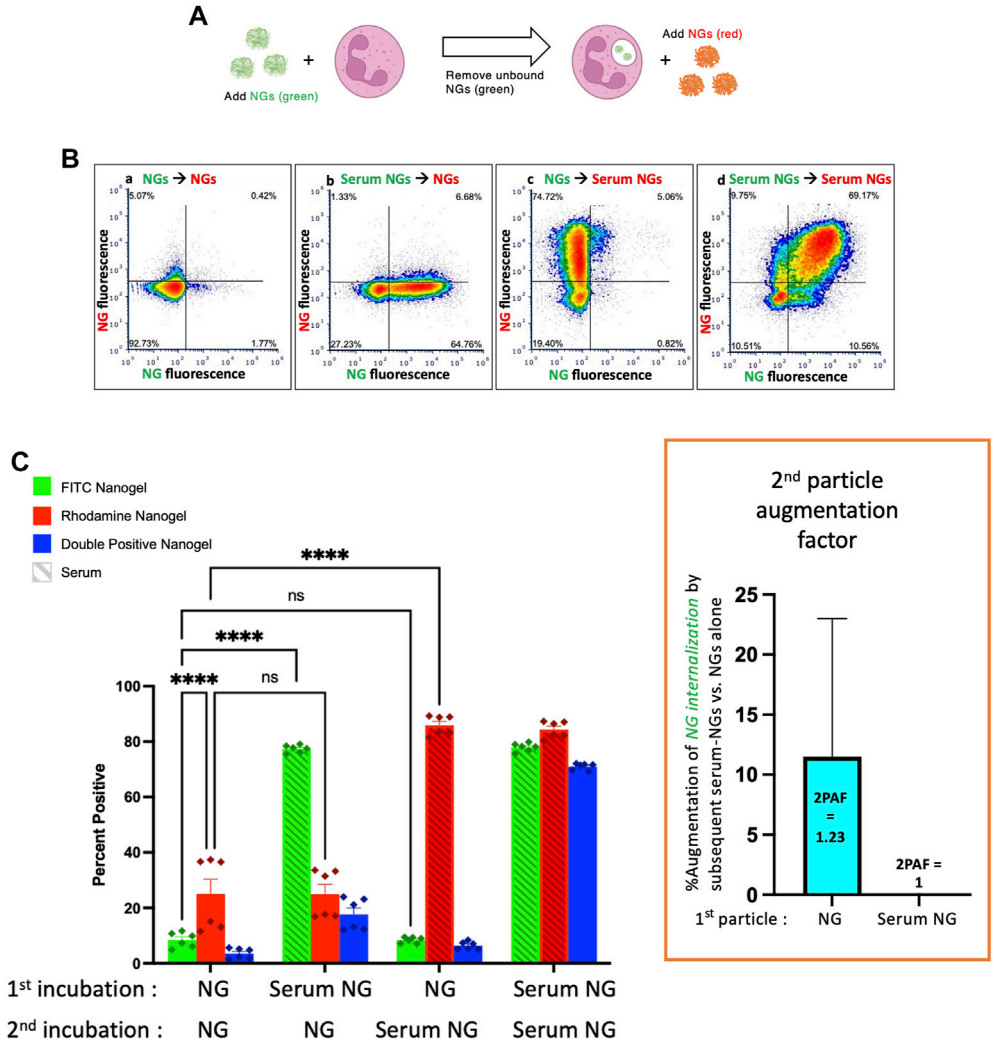

FIGURE 3 | Serum-opsonized nanogels do not augment neutrophil association with previously delivered nanogels. **(A)** Similar to the paradigm described in **Figure 1**, neutrophils were exposed to green nanogels, followed by washing to remove unbound neutrophils, then exposed to red nanogels, washed, and then the neutrophils were subjected to flow cytometry. **(B)** Representative flow cytometry dot-plots. **(C)** Quantification of n = 6 biological replicates. The most notable comparison is the first and third green bars, which indicate that serum-opsonized nanogels ("Serum NGs") do not augment the fraction of neutrophils that are positive for binding to non-serum-exposed nanogels ("NGs"). Notably, unlike the pH-sensitive E. coli used in **Figures 1**, **2**, nanogels fluoresce both when bound to the neutrophil surface and when in the phagosome. Thus, it is possible that some NGs are bound to the neutrophil surface and then internalized after exposure to Serum NGs, but this assay cannot detect such internalization events. Another major result of this set of conditions is that Serum NGs have uniformly high uptake into neutrophils regardless of whether the neutrophils were first exposed to other nanogels (NGs or Serum NGs), suggesting the neutrophils do not saturate their uptake of Serum NGs in this dynamic range (they do not "get full").

complement (Myerson et al., 2022). The parallel 2PAF effects for NGs and *E. coli* coincide with these similar uptake mechanisms.

Having established that both serum-opsonized NGs and serum-opsonized bacteria can augment phagocytosis of non-opsonized bacteria, we questioned whether NG uptake could be similarly enhanced. We used the same protocol as above, except with particle #1 as NGs (green), and particle #2 as a separate sample of NGs (red) (**Figure 3A**). Comparing the first and third green bars in **Figure 3C**, we see that serum-opsonized NGs are *minimally* able to augment phagocytosis of *previously* delivered NGs. Thus, 2PAF = 1.23. These results may be attributed to difference in fluorophores of the *E. coli* bioparticles and NGs, as NGs fluoresce equally well on the surface of neutrophils (pH 7) and in phagosomes (pH 4–5). More likely though, the low levels of first incubation NG fluorescence observed in the first and third green bars suggest that neutrophils do not retain nanogels on their surface after washing, which would thus prevent augmentation by nanogels delivered during the second incubation. **Figure 3C** also shows that non-opsonized particle #2 NG uptake (the first red bar) is higher than non-opsonized particle #1 NG uptake (the first green bar). Under certain circumstances, such as these, exposure of neutrophils to a first particle (even one that is mostly washed away) may increase the phagocytic efficiency of the neutrophils

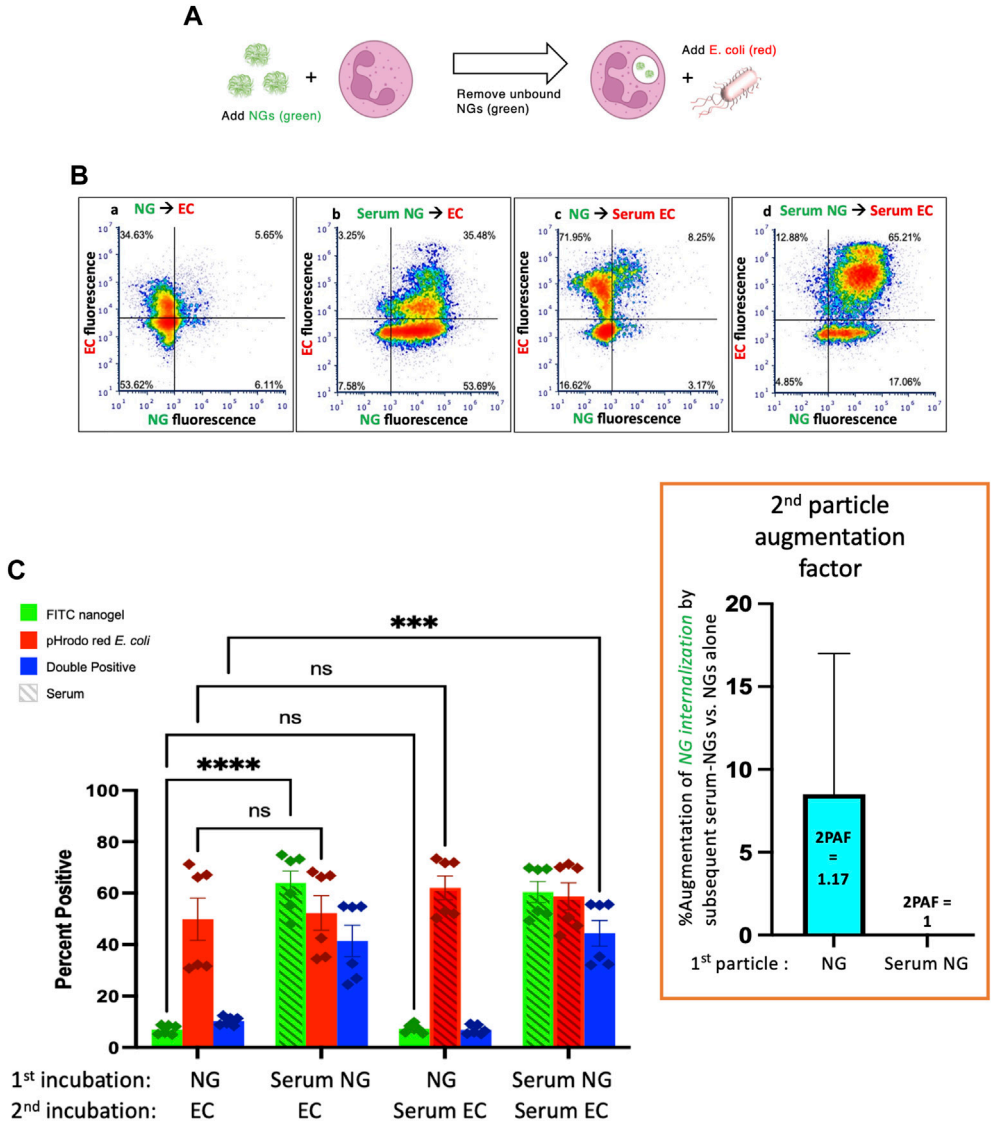

FIGURE 4 | Serum-opsonized E. coli are also unable to augment neutrophil association with previously delivered nanogels. **(A)** Here the first particle is nanogels, while the second particle is E. coli. Thus, this tests if EC can augment neutrophil association with nanogels. **(B)** Representative flow cytometry dot-plots. **(C)** Quantification of n = 6 biological replicate. The most notable comparison again is the first and third green bars, which indicate that serum-opsonized E. coli ("Serum ECs") do not augment the fraction of neutrophils that are positive for binding to non-serum-exposed nanogels ("NGs"). A second important result is that nanogels do *not* decrease neutrophil phagocytosis of E. coli (all red bars are equal). This is clinically relevant because it means that if a neutrophil phagocytoses a nanogel and then later encounters a bacterium, the nanogel will not reduce the likelihood of uptake of the bacterium. Thus, the nanogels do not induce immunosuppression by this metric.

for nanoparticles that are delivered later. This finding is consistent with previous studies showing neutrophils are known to change their activity state after phagocytosis (Bazzoni et al., 1991). **Figure 3** suggests that the order and timing of particle delivery matter significantly.

Finally, we administered *E. coli* as particle #2 after NGs as particle #1 (**Figure 4A**). As in **Figure 3**, when NGs are delivered first, their uptake is minimally augmented by a second particle with 2PAF = 1.17, even when the second particle is highly stimulatory serum-opsonized *E. coli* (**Figure 4C**, first vs. third green bars).

Figure 4 also shows that delivery of NGs *before E. coli* does not impair neutrophils' uptake of *E. coli*: levels of *E. coli* uptake were identical for all conditions tested in **Figure 4C**. This is an important result in the path to clinical translation of neutrophil-tropic nanoparticles, as such nanoparticles might compromise therapy if they inhibited subsequent phagocytosis of bacteria.

Taken together, the data presented here strongly indicate that serum-opsonized nanogels and *E. coli* augment phagocytosis of non-opsonized bacteria. We sought to confirm and extend these flow cytometry results with a complementary approach. Therefore, we performed a similar protocol of exposing neutrophils to nanogels and bacteria, but this time we analyzed the cells using microscopy. Not only could this serve as a confirmation of the flow cytometry results,

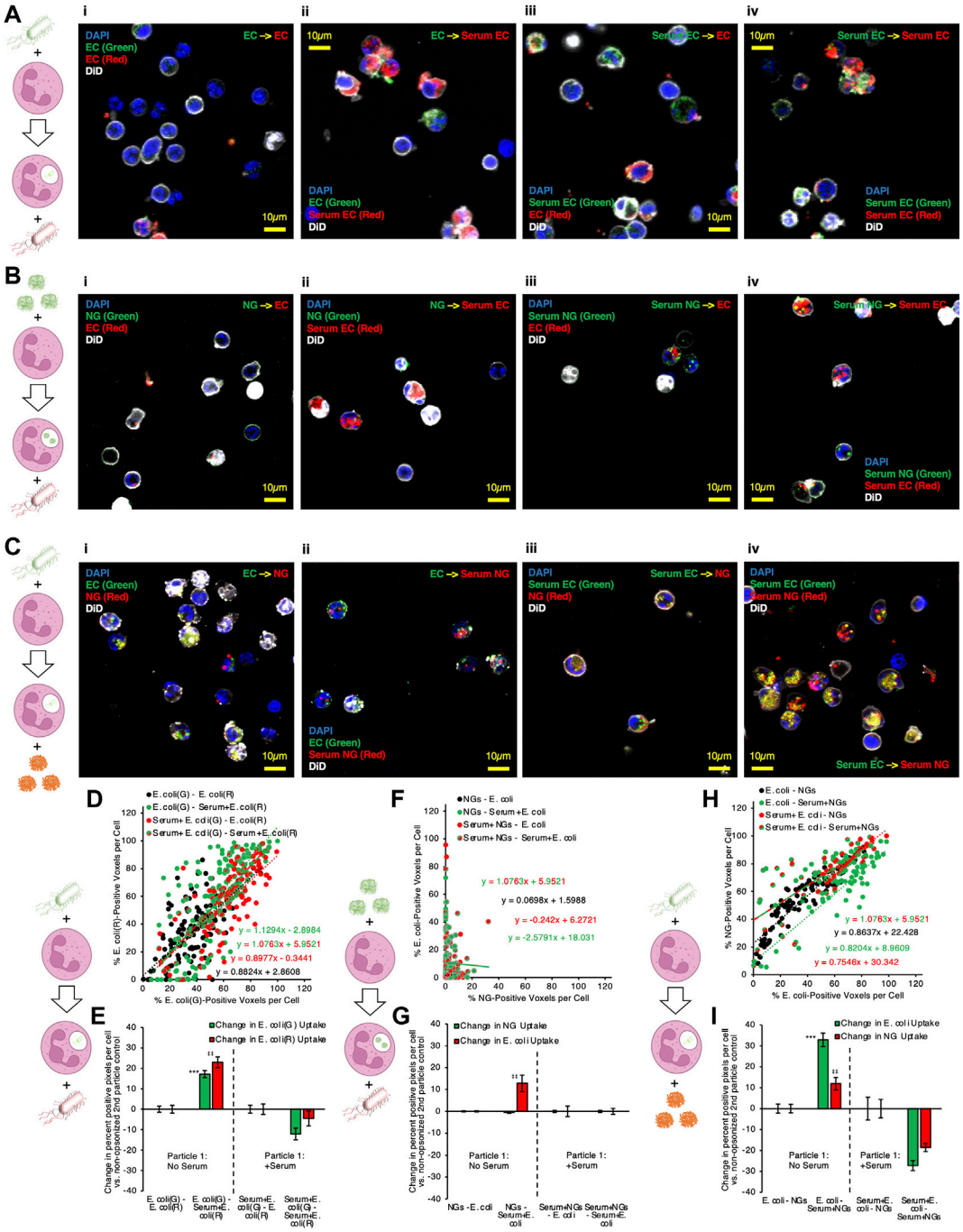

FIGURE 5 | Microscopy confirms that serum-opsonized nanogels improve internalization of non-opsonized E. coli, and that they then share significant colocalization within neutrophils. **(A)** Example images of neutrophils given two different labeled E. coli doses in sequence, for different serum pretreatment conditions applied to the E. coli. **(B)** Example images of neutrophils given lysozyme-dextran nanogels (NGs) prior to E. coli, for different serum pretreatment conditions applied to the NGs and E. coli. **(C)** Example images of neutrophils given E. coli prior to NGs, for different serum pretreatment conditions applied to the NGs and E. coli. Each point depicted in **(D)** indicates data for 1 cell, in imaging experiments as in **(A)**. The horizontal coordinate indicates quantity of green E. coli signal and the vertical coordinate indicates quantity of red E. coli signal. Higher slope indicates that cells generally have more red E. coli, relative to quantity of green E. coli. All conditions showed strong positive correlation between red and green signal, indicating that cells taking up green E. coli, given first, were likely to take up red E. coli, given subsequently. **(E)** 2PAF enhancement of first particle (green) E. coli by addition of serum to second particle (red) E. coli., in imaging experiments as in **(A)**. Bars three to four and seven to eight in **(E)** show the per-cell average difference in uptake of each color E. coli induced by serum treatment of second particle (red) E. coli. Green bars >0 indicate serum treatment of second particle (red) E. coli increases the average per cell uptake of first particle (green) E. coli. **(F–G)** Data is as presented in **(D–E)**, but for imaging experiments as in **(B)**, wherein NGs were given to neutrophils before E. coli. There was poor correlation between per-cell NG signal and E. coli signal, for all serum pretreatment conditions, indicating that neutrophil uptake of NGs does not predict subsequent uptake of E. coli. **(G)** indicates no 2PAF effect exerted by second particle

(*Continued*)

FIGURE 5 | E. coli on NGs. **(H–I)** Data is as presented in **(D–E)** and **(F–G)**, but for imaging experiments as in **(C)**, wherein E. coli was given to neutrophils before NGs. In **(H)**, there was strong correlation between NG and E. coli uptake in any given cell, when E. coli was taken up before neutrophil exposure to NGs. In **(I)**, bar 3 indicates that opsonized second particle NGs enhance uptake of non-opsonized first particle E. coli.

but imaging data additionally can determine if the particles #1 and #2 co-localize with each other within the cell, which gives further insight into the 2PAF phenomenon.

We began this line of experiments by performing the same sequential delivery protocol used in flow cytometry experiments, but instead of flow cytometry, cells were fixed in suspension with paraformaldehyde and adhered to glass for microscopy imaging. **Figure 5A–C** provide representative microscopy data. **Figure 5A** shows data where both particle #1 and particle #2 are *E. coli*. We found the same result as in flow cytometry: Serum EC delivered as particle #2 augmented neutrophil phagocytosis of (non-opsonized) EC delivered as particle #1 (compare green and yellow signals in **Figure 5Aii** vs. **Figure 5Ai**). Yellow signal in **Figure 5A** indicates intracellular overlap between green (particle #1) and red (particle #2) *E. coli* inside of neutrophils, consistent with a large fraction of particle #1 being phagocytosed at the same time and into the same compartment as particle #2. **Figure 5B** shows data where particle #1 is NGs (green) and particle #2 is *E. coli* (red). In this data, we observe minimal colocalization between the two particles, consistent with flow cytometry data in **Figure 4** showing no 2PAF effect when NGs are given before *E. coli*. **Figure 5C** shows data where particle #1 is *E. coli* (green) and particle #2 is NGs (red). The condition for which flow cytometry yielded 2PAF = 1.55 [EC - Serum NG; (**Figure 5Cii**)], yielded imaging data with a high degree of intracellular overlap between *E. coli* (particle #1) and NGs (particle #2). These imaging data qualitatively support a key conclusion from our quantitative flow cytometry data: opsonized NGs or *E. coli* not only augment uptake of previously delivered, non-opsonized bacteria, but also show localization into similar intracellular compartments. The observation that particles localize to similar intracellular compartments under conditions of 2PAF augmentation suggests the possibility that after augmented uptake the neutrophil has preserved, and possibly increased, bactericidal activity. However, that hypothesis requires further investigations beyond the scope of the current study.

To quantify the data from these microscopy experiments, images of each particle were thresholded via Renyi entropic filtering to identify the portions of each image that were positive for either particle #1 or particle #2. Guided by DiO membrane staining, we identified regions of interest encompassing each cell in each obtained image. Overlaying the thresholded images on the regions of interest corresponding to individual cells allowed us to determine the fraction of pixels in each cell that contained either particle #1 or particle #2. In panels 5D, 5F, and 5H, each point in the presented scatter plots represents the results of this analysis for one neutrophil. The y-axis value for each point represents the percentage of pixels in the neutrophil containing particle #2 and the x-axis value represents the percentage of pixels in the neutrophil containing particle #1. A line was fitted to the data for each condition. Lines with slope = 1 indicate that each neutrophil took up equal quantities of particle #1 and particle #2. Lines with slope >1 indicate a tendency to take up more of particle #2 than particle #1. Lines with slope <1 indicate a tendency to take up more of particle #1 than particle #2. We therefore used percentage of positive pixels as a metric for levels of particle #1 and particle #2 uptake in each neutrophil. To derive 2PAF values from the imaging data, we subtracted from our uptake values for each cell the average uptake values for the 2PAF baseline conditions (conditions where particle #2 is not opsonized). We therefore determined our 2PAF value in imaging experiments as the percent *increase* in either particle #1 or particle #2 uptake for each imaged cell vs the expected level of uptake when particle #2 is not opsonized. These findings are depicted in panels 5E, 5G, and 5I.

Panels 5D and 5E depict quantitative analysis of imaging data where particles #1 and #2 were both *E. coli*. All serum treatment conditions in these experiments showed strong positive correlation between signal from particles #1 and #2, indicating that cells taking up green *E. coli*, given first, were very likely to take up red *E. coli*, delivered second. This confirms this assay behaves as expected: cells do not saturate their *E. coli* uptake in this dosing regimen; cells with more uptake of one *E. coli* have more uptake of the second; green and red fluorophores perform equally. As with flow cytometry data in **Figure 2C**, data in **Figure 5E** show a clear 2PAF effect exerted by particle #2 *E. coli* on particle #1 *E. coli*. When particle #1 *E. coli* is not opsonized, uptake of particle #1 increases by ~20% if particle #2 *E. coli* is opsonized, compared to data where particle #2 *E. coli* is not opsonized.

Panels 5F and 5G depict analysis of imaging data where particle #1 is NGs and particle #2 is *E. coli*. R-squared values were less than 0.1 for all lines in panel 5F except that for Serum + NGs–Serum + *E. coli*, indicating poor linear correlation between particle #1 and particle #2 uptake for the conditions in this data. This indicates that, when a given neutrophil takes up NGs as particle #1, improved uptake of *E. coli* as particle #2 cannot be predicted for that same cell. Similarly, analysis of imaging-based 2PAF also indicates no 2PAF effect exerted by particle #2 *E. coli* on particle #1 NGs. All imaging-based 2PAF calculations showed no change in particle #1 NG uptake induced by opsonized particle #2 *E. coli* vs 2PAF baseline conditions with non-opsonized particle #2 *E. coli*. These data suggest that co-localization is compromised under these conditions, consistent with our understanding that multiple pathways can lead to phagocytosis, not all necessarily leading to accumulation in the identical intracellular compartment (Sahay, Alakhova and Kabanov, 2010).

Finally, panels 5H and 5I depict analysis of imaging data where particle #1 is E. *coli* and particle #2 is NGs. As with data in panel

5D, panel 5H shows strong positive correlation between particle #1 *E. coli* uptake and particle #2 NG uptake. For all serum treatment conditions, particle #2 NGs were more likely to be taken up in neutrophils that had already taken up particle #1 *E. coli*. This finding contrasts with the data in panel 5F, where, when NGs are given as particle #1, there was no positive correlation between NG uptake and *E. coli* uptake in any given cell. These findings match with analysis of the double-positive (*E. coli*-positive and NG-positive) cell counts in flow cytometry data in the blue bars in **Figure 1C**, **Figure 4C**. Panel 5I shows imaging-based 2PAF values for conditions where *E. coli* is particle #1 and NGs are particle #2. Again, these image analysis findings agree with our flow cytometry data: When non-opsonized *E. coli* is particle #1, we observe a 33% increase in *E. coli* uptake per neutrophil when particle #2 NGs are serum-treated vs when particle #2 NGs are not serum-treated. In imaging data, NGs as particle #2 exert a clear 2PAF effect enhancing uptake of *E. coli* as particle #1.

For conditions where we observed 2PAF effects (with *E. coli* as both particles #1 and #2 or with *E. coli* as particle #1 and NGs as particle #2), neutrophils were also examined with three-dimensional confocal imaging (**Supplemental Figure S4, S5**). For our confocal imaging analysis, we computed quantities of NGs and E. coli in each cell as in **Figure 5**, but quantities of NGs and *E. coli* reflected fluorescent voxels, rather than pixels. Additionally, we quantified voxels that contained both particle #1 and particle #2, directly assessing three-dimensional colocalization of particles #1 and #2 in the confocal images.

For experiments where both particles #1 and #2 were *E. coli*, ~80% of *E. coli* particle #1 signal was spatially colocalized with *E. coli* particle #2 signal when *E. coli* particle #2 was opsonized (panels B–C, green bars 1 and 3 in panel C). Only ~50% of *E. coli* particle #1 signal was spatially colocalized with E. coli particle #2 signal when *E. coli* particle #2 was not opsonized (green bar 2 in **Supplemental Figure S4**, panel C). This finding fits well with a central part of our hypothesis as to the 2PAF mechanism: When there is a 2PAF effect, delayed phagocytosis of particle #1 is driven by coincident uptake of particle #2. In our confocal data, we find that particle #1 *E. coli* is mostly found colocalized with opsonized particle #2 *E. coli* inside neutrophils. This colocalization is diminished under conditions where 2PAF is diminished, when particle #2 *E. coli* is not opsonized. Under conditions with 2PAF effects, particle #2 colocalization with particle #1 (**Supplemental Figure S4**, panel A, red bars in panel C) was less than particle #1 colocalization with particle #2 (**Supplemental Figure S4**, panel A, green bars in panel C). This can be attributed to; 1) opsonized particle #2 *E. coli* being phagocytosed independently of particle #1 at a higher frequency than events where particle #1 was phagocytosed independently of particle #2; 2) opsonized particle #2 *E. coli* being taken up in neutrophils to a greater degree than particle #1 *E. coli*. Panel D in **Supplemental Figure S4** indeed indicates higher average uptake values for *E. coli* particle #2 vs *E. coli* particle #1, especially in 2PAF-affected conditions.

Our prototypical 2PAF conditions, where *E. coli* were particle #1 and NGs were particle #2, were also examined in confocal imaging data. Here particle #1 *E. coli* colocalized with particle #2 NGs at ~50–60% frequency when particle #2 NGs were opsonized (**Supplemental Figure S5**, panels B–C, green bars 1 and 3 in panel C). In comparison, *E. coli* colocalized with NGs at only ~35% frequency under non-2PAF conditions, where particle #2 NGs were not opsonized (**Supplemental Figure S5**, panels B–C, green bar 2 in panel C). As with data for 2PAF-affected conditions with double *E. coli* treatments, *E. coli*-NG 2PAF-affected conditions featured augmented colocalization of particle #1 (*E. coli*) with particle #2 (NGs), implying phagocytosis of particle #1 *E. coli* and particle #2 NGs in the same subcellular locations in neutrophils. Particle #2 NG colocalization with particle #1 *E. coli* (**Supplemental Figure S5**, panel A, red bars in panel C) was greater than particle #1 *E. coli* localization with NGs (**Supplemental Figure S5**, panel B, green bars in panel C). This may reflect generally higher uptake of *E. coli* vs NGs (**Supplemental Figure S5**, panel D), where *E. coli* likely has a higher chance of being taken up in neutrophils independently of NGs, compared to lower quantities of NG uptake meaning NGs have a lower chance of being taken up independently of *E. coli*. Colocalization of particle #2 NGs with particle #1 *E. coli* bodes well for proposed NG drug delivery to neutrophils designed to help augment neutrophil killing of bacteria: When NGs are given after neutrophils have been exposed to bacteria, the NGs end up in the same places as bacteria inside neutrophils. Our proposed mechanism of the 2PAF effect and co-localization of particles can be seen in **Supplemental Figure S6**.

This study has several limitations. First, the data presented here are all derived from *in vitro* studies. Neutrophil isolation may modify neutrophil function, thus imposing constraints on interpretation. Of note, however, our previous study suggested a good correlation between *in vitro* and *in vivo* observations of NAP uptake in neutrophils (Myerson et al., 2022). Similarly, the *in vivo* environment may contain neutrophil stimuli not seen *in vitro*. Opsonization with normal mouse serum also may not include all of the opsonins that might be present during an inflammatory process, although we have not detected any significantly different effect using acute phase sera (data not shown). While it is promising that phagocytosis is preserved with particle exposure, and under certain conditions increased, there are several other neutrophil functions that will need to be investigated. We plan to conduct future studies aimed at evaluation of other key neutrophil functions, including: NETosis, cytokine and reactive oxygen species generation, and bacteria killing. Additionally, neutrophils represent one of several immune lineages that should be investigated for the 2PAF effect, such as macrophages. Finally, neutrophils are significantly heterogeneous both within and between donors. Accordingly, use of multiple donors reduces this effect, and flow cytometry permits observation of potential heterogeneity, thus mitigating this concern.

3 MATERIALS AND METHODS

3.1 Lysozyme-Dextran Nanogel Synthesis

Lysozyme-dextran nanogels (LDNGs) were synthesized as previously described (Li et al., 2008; Coll Ferrer et al., 2014; Myerson et al., 2018, 2022). Rhodamine-dextran or FITC-dextran

(Sigma) and lysozyme from hen egg white (Sigma) were dissolved in deionized and filtered water at a 1:1 or 2:1 mol:mol ratio. Then pH was adjusted to 7.1 and solution was lyophilized. For Maillard reaction, the lyophilized product was heated for 18 h at 60°C, with 80% humidity maintained via saturated KBr solution in the heating vessel. Dextran-lysozyme conjugates were dissolved in deionized and filtered water to a concentration of 5 mg/ml. Solutions were stirred at 80°C for 30 min. Diameter of LDNGs was evaluated with dynamic light scattering (DLS, Malvern) after heat gelation. Particle suspensions were stored at 4°C.

3.2 Murine Serum

Blood was obtained through the inferior vena cava as previously described (Mei et al., 2010; Parasuraman et al., 2010) from B6 wild type mice and pooled. Blood was allowed to clot for 30 min at room temperature, and serum was separated by centrifugation of 1,500 rpm × 10 min at 4°C. Complement proteins were depleted from serum via Cobra Venom Factor as previously described (Haihua et al., 2018).

3.3 Murine Neutrophils

Femurs were harvested from B6 wild type mice, and bone marrow was collected and pooled. Neutrophils were isolated from bone marrow via negative selection (Stemcell EasySep™ Mouse Neutrophil Enrichment Kit cat #19762). Neutrophils were suspended in DMEM media at a concentration of 2×10^6 neutrophils/mL. Isolated neutrophils were 95% viable by trypan blue, and 80% pure using Ly6g staining and flow cytometry (See **Supplemental Figure S1**).

3.4 Nanogel Preparation

FITC-labelled lysozyme-dextran NGs were synthesized as above. Stock NGs were brought to a concentration of 5×10^{11} particles/mL. To serum-treat prior to neutrophil incubation, NGs were incubated in 50% serum in DMEM for 1 h at 37°C.

3.5 E. Coli BioParticles

For bacterial particles, both pHrodo™ red and green *E. coli* BioParticles™ conjugates (Invitrogen, Thermo Fisher cat #P35361 and #P35366) were used. BioParticles were brought to a concentration of 2 mg/ml in PBS. To serum-treat *E. coli* BioParticles prior to neutrophil incubation, BioParticles were incubated in equal volume serum for 1 h at 37°C.

3.6 Prototypical Experiment

3.6.1 Sequential Particle Analysis

Neutrophils were isolated and prepared as above. 500uL of neutrophils were incubated with 20uL of either particle while rotating at 37°C. First particle incubation time was 15 min for NGs and 1 h for *E. coli* BioParticles, with exception of the conditions with two color *E. coli* BioParticles. In those conditions the first *E. coli* BioParticles incubation was done at 15 min to recapitulate the initial NG incubation. Samples were then washed and pelleted 300 g × 6 min to remove unbound particles. The neutrophils were then resuspended in 500uL DMEM media. The second particle was then incubated with the neutrophils while rotation at 37°C. Second particle incubation time was 15 min for NGs and 1 h for *E. coli* BioParticles, with exception of the conditions with two color NGs. In those conditions the second NG incubation was incubated for 60 min to recapitulate the second exposure *E. coli* incubation. Samples were then washed and pelleted again, then resuspended in FACS buffer. For flow cytometry samples, they were stained with anti-Ly6G antibody prior to analysis. For microscopy samples, they were suspended in solution with 2% paraformaldehyde for 30 min at room temperature, then pelleted and resuspended at a concentration of 1×10^6/ml.

3.6.2 Sample Preparation and Confocal Microscopy

90 µl of paraformaldehyde fixed cells was incubated with 5×10^{-7} M DAPI and 1:100 Vybrant™ DiD Cell-Labeling Solution (Invitrogen) at 37°C for 20 min. Samples were centrifuged at 2000 g × 1 min. They were washed with 1 ml PBS and sprun at 2000RPM x 3 min twice. Finally, they were resuspended in 80 µl PBS then dropped on cavity slides (Eisco), covered with coverslips (FisherScientific), and analyzed with Leica TCS SP8 Laser confocal microscope. Visualization of neutrophils was performed with water immersion objective HC PL APO CS2 40x/1.10. Images were obtained in sequential scanning mode using Diode 405, OPSL 488, OPSL 552 and Diode 638 lasers. We used scan speed 200 Hz and pixel size 0.223 µm for flat images. Z-stacks were obtained with scan speed 600 Hz, XY pixel size 0.223 µm and voxel size 0.424 µm. Images and Z-stacks were processed with LASX (Leica microsystems). Images and Z-stacks were converted to TIFF images for analysis in ImageJ (FIJI distribution 2.1.0/1.53q). Processing and analysis, including image thresholding, fluorescence colocalization, and per-cell analysis of fluorescence signals, employed custom ImageJ macros, code for which is provided in full in the supplement. For per-cell analyses, regions of interest were drawn manually around each imaged cell, using images of DiD membrane stain to define the edges of individual cells.

3.6.3 Animal Study Protocols

All animal studies were carried out in strict accordance with Guide for the Care and Use of Laboratory Animals as adopted by National Institutes of Health and approved by Children's Hospital of Philadelphia Institutional Animal Care and Use Committee. All animal experiments used male B6 mice, 6–8 weeks old, purchased from Jackson Laboratories. Mice were maintained at 20–25°C, 50 ± 20% humidity, and on a 12/12 h dark/light cycle with food and water *ad libitum*.

3.6.4 Statistical Analysis

Error bars indicate the standard error of the mean throughout. Significance tests are described in captions. Statistical power was determined for statements of statistical significance and tabulated in the supplementary materials.

4 CONCLUSION

The data presented here are consistent with a model of neutrophil phagocytosis in which a non-opsonized bacteria, that is poorly

phagocytosed, is nonetheless still available in a compartment (likely the surface plasma membrane) from which it can be subsequently taken up in response to a more phagocytic-stimulatory particle, whether it be an opsonized bacteria or an opsonized nanogel. Similarly, initial exposure to a bacterial-like particle further enhances subsequent uptake of nanogels, even non-opsonized ones. Thus, the nanogel might be used in its opsonized form, even without incorporated drugs, to enhance uptake of poorly-opsonized bacteria. Furthermore, under these circumstances, the bacteria and nanoparticles are found in similar intracellular compartments, suggesting that delivery to specific compartments of the phagocytosing neutrophil might be possible.

DATA AVAILABILITY STATEMENT

The raw data supporting the conclusions of this article will be made available by the authors, without undue reservation.

ETHICS STATEMENT

The animal study was reviewed and approved by INSTITUTIONAL ANIMAL CARE AND USE COMMITTEE, Children's Hospital of Philadelphia.

AUTHOR CONTRIBUTIONS

KR, JB, and GW contributed to conception and design of the study. KR performed all experiments and analyzed the flow cytometry. JW provided mouse femurs for neutrophil isolation. AM and JN performed the microscopy imaging. KR, AM, JM, GW, and JB wrote sections of the manuscript. All authors contributed to manuscript revision, read, and approved the submitted version.

ACKNOWLEDGMENTS

We are grateful for the support by the grants from the National Institutes of Health F32-HL-151026 (KR), RO1-HL-151467 and RO1-HL-158737 (VK), R01-HL-157189 (VM/GW), K08-HL-138269, R01-HL-153510 and R01-HL-160694 (JB), and UH3-TR-002198 (GW), as well as, the Job Research Foundation Grant (VK). The schematics in this manuscript were created with biorender.com.

SUPPLEMENTARY MATERIAL

The Supplementary Material for this article can be found online at: https://www.frontiersin.org/articles/10.3389/fphar.2022.923814/full#supplementary-material

REFERENCES

Bazzoni, F., Cassatella, M. A., Rossi, F., Ceska, M., Dewald, B., and Baggiolini, M. (1991). Phagocytosing Neutrophils Produce and Release High Amounts of the Neutrophil-Activating Peptide 1/interleukin 8. *J. Exp. Med.* 173 (3), 771–774. doi:10.1084/jem.173.3.771

Betker, J. L., Jones, D., Childs, C. R., Helm, K. M., Terrell, K., Nagel, M. A., et al. (2018). Nanoparticle Uptake by Circulating Leukocytes: A Major Barrier to Tumor Delivery. *J. Control Release* 286, 85–93. doi:10.1016/j.jconrel.2018.07.031

Boucher, H. W., Talbot, G. H., Bradley, J. S., Edwards, J. E., Gilbert, D., Rice, L. B., et al. (2009). Bad Bugs, No Drugs: No ESKAPE! an Update from the Infectious Diseases Society of America. *Clin. Infect. Dis.* 48 (1), 1–12. doi:10.1086/595011

Brekke, O. L., Christiansen, D., Fure, H., Fung, M., and Mollnes, T. E. (2007). The Role of Complement C3 Opsonization, C5a Receptor, and CD14 in E. Coli-Induced Up-Regulation of Granulocyte and Monocyte CD11b/CD18 (CR3), Phagocytosis, and Oxidative Burst in Human Whole Blood. *J. Leukoc. Biol.* 81, 1404–1413. doi:10.1189/jlb.0806538

Centers for Disease Control and Prevention (2019). *Antibiotic Resistance Threats in the United States*. Washington: U.S Department of Health and Human services, 1–113. doi:10.15620/cdc:82532

Chen, F., Wang, G., Griffin, J. I., Brenneman, B., Banda, N. K., Holers, V. M., et al. (2017). Complement Proteins Bind to Nanoparticle Protein Corona and Undergo Dynamic Exchange *in Vivo*. *Nat. Nanotechnol.* 12 (4), 387–393. doi:10.1038/nnano.2016.269

Ferrer, M. C., Shuvaev, V. V., Zern, B. J., Composto, R. J., Muzykantov, V. R., and Eckmann, D. M. (2014). ICAM-1 Targeted Nanogels Loaded with Dexamethasone Alleviate Pulmonary Inflammation. *PLoS ONE* 9 (7), e102329. doi:10.1371/journal.pone.0102329

File, T. M., and Marrie, T. J. (2010). Burden of Community-Acquired Pneumonia in North American Adults. *Postgrad. Med.* 122 (2), 130–141. doi:10.3810/pgm.2010.03.2130

Flannagan, R. S., Cosío, G., and Grinstein, S. (2009). Antimicrobial Mechanisms of Phagocytes and Bacterial Evasion Strategies. *Nat. Rev. Microbiol.* 7, 355–366. doi:10.1038/nrmicro2128

Fromen, C. A., Kelley, W. J., Fish, M. B., Adili, R., Noble, J., Hoenerhoff, M. J., et al. (2017). Neutrophil-Particle Interactions in Blood Circulation Drive Particle Clearance and Alter Neutrophil Responses in Acute Inflammation. *ACS Nano* 11 (11), 10797–10807. doi:10.1021/acsnano.7b03190

Grant, S. S., and Hung, D. T. (2013). Persistent Bacterial Infections, Antibiotic Tolerance, and the Oxidative Stress Response. *Virulence* 4, 273–283. doi:10.4161/viru.23987

Haihua, C., Wei, W., Kun, H., Yuanli, L., and Fei, L. (2018). Cobra Venom Factor-Induced Complement Depletion Protects against Lung Ischemia Reperfusion Injury through Alleviating Blood-Air Barrier Damage. *Sci. Rep.* 8 (1), 10346–10348. Springer US. doi:10.1038/s41598-018-28724-z

Horwitz, M. A., and Silverstein, S. C. (1980). Influence of the *Escherichia coli* Capsule on Complement Fixation and on Phagocytosis and Killing by Human Phagocytes. *J. Clin. Invest.* 65 (1), 82–94. doi:10.1172/JCI109663

Inturi, S., Wang, G., Chen, F., Banda, N. K., Holers, V. M., Wu, L., et al. (2015). Modulatory Role of Surface Coating of Superparamagnetic Iron Oxide Nanoworms in Complement Opsonization and Leukocyte Uptake. *ACS Nano* 9 (11), 10758–10768. doi:10.1021/acsnano.5b05061

Kemp, A. S., and Campbell, D. E. (1996). The Neonatal Immune System. *Seminars Neonatol.* 1 (2), 67–75. W.B. Saunders. doi:10.1016/S1084-2756(05)80002-8

Lee, W. L., Harrison, R. E., and Grinstein, S. (2003). Phagocytosis by Neutrophils. *Microbes Infect.* 5, 1299–1306. doi:10.1016/j.micinf.2003.09.014

Lelubre, C., and Vincent, J. L. (2018). Mechanisms and Treatment of Organ Failure in Sepsis. *Nat. Rev. Nephrol.* 14, 417–427. doi:10.1038/s41581-018-0005-7

Li, J., Yu, S., Yao, P., and Jiang, M. (2008). Lysozyme-dextran Core-Shell Nanogels Prepared via a Green Process. *Langmuir* 24 (7), 3486–3492. PDF. doi:10.1021/LA702785B/SUPPL_FILE/LA702785B-FILE003

McGreal, E. P., Hearne, K., and Spiller, O. B. (2012). Off to a Slow Start: Under-development of the Complement System in Term Newborns Is More Substantial Following Premature Birth. *Immunobiology* 217 (2), 176–186. doi:10.1016/j.imbio.2011.07.027

Mei, J., Liu, Y., Dai, N., Favara, M., Greene, T., Jeyaseelan, S., et al. (2010). CXCL5 Regulates Chemokine Scavenging and Pulmonary Host Defense to Bacterial Infection. *Immunity* 33 (1), 106–117. doi:10.1016/J.IMMUNI.2010.07.009

Moghimi, S. M., and Simberg, D. (2017). Complement Activation Turnover on Surfaces of Nanoparticles. *Nano Today* 15, 8–10. doi:10.1016/j.nantod.2017.03.001

Moraes, T. J., Zurawska, J. H., and Downey, G. P. (2006). Neutrophil Granule Contents in the Pathogenesis of Lung Injury. *Curr. Opin. Hematol.* 13 (1), 21–27. doi:10.1097/01.moh.0000190113.31027.d5

Myerson, J. W., Braender, B., Mcpherson, O., Glassman, P. M., Kiseleva, R. Y., Shuvaev, V. V., et al. (2018). Flexible Nanoparticles Reach Sterically Obscured Endothelial Targets Inaccessible to Rigid Nanoparticles. *Adv. Mater* 30 (32), e1802373. doi:10.1002/adma.201802373

Myerson, J. W., McPherson, O., DeFrates, K. G., Towslee, J. H., Marcos-Contreras, O. A., Shuvaev, V. V., et al. (2019). Cross-linker-Modulated Nanogel Flexibility Correlates with Tunable Targeting to a Sterically Impeded Endothelial Marker. *ACS Nano* 13 (10), 11409–11421. doi:10.1021/acsnano.9b04789

Myerson, J. W., Patel, P. N., Rubey, K. M., Zamora, M. E., Zaleski, M. H., Habibi, N., et al. (2022). Supramolecular Arrangement of Protein in Nanoparticle Structures Predicts Nanoparticle Tropism for Neutrophils in Acute Lung Inflammation. *Nat. Nanotechnol.* 17 (1), 86–97. doi:10.1038/s41565-021-00997-y

Parasuraman, S., Raveendran, R., and Kesavan, R. (2010). Blood Sample Collection in Small Laboratory Animals. *J. Pharmacol. Pharmacother.* 1 (2), 87–93. doi:10.4103/0976-500X.72350

Pechous, R. D. (2017). With Friends like These: The Complex Role of Neutrophils in the Progression of Severe Pneumonia. *Front. Cell. Infect. Microbiol.* 7, 160. doi:10.3389/fcimb.2017.00160

Reardon, S. (2015). Spread of Antibiotic-Resistance Gene Does Not Spell Bacterial Apocalypse - yet. *Nature*. doi:10.1038/nature.2015.19037

Rubey, K. M., and Brenner, J. S. (2021). Nanomedicine to Fight Infectious Disease. *Adv. Drug Deliv. Rev.* 179, 113996. doi:10.1016/j.addr.2021.113996

Sahay, G., Alakhova, D. Y., and Kabanov, A. V. (2010). Endocytosis of Nanomedicines. *J. Control Release* 145, 182–195. doi:10.1016/j.jconrel.2010.01.036

Schelonka, R. L., and Infante, A. J. (1998). Neonatal Immunology. *Semin. Perinatol.* 22 (1), 2–14. doi:10.1016/S0146-0005(98)80003-7

Scieszka, J. F., Maggiora, L. L., Wright, S. D., and Cho, M. J. (1991). Role of Complements C3 and C5 in the Phagocytosis of Liposomes by Human Neutrophils. *Pharm. Res.* 8 (1), 65–69. doi:10.1023/A:1015830306839

Silver, L. L. (2011). Challenges of Antibacterial Discovery. *Clin. Microbiol. Rev.* 24 (1), 71–109. doi:10.1128/CMR.00030-10

Sinha, S., Rosin, N. L., Arora, R., Labit, E., Jaffer, A., Cao, L., et al. (2022). Dexamethasone Modulates Immature Neutrophils and Interferon Programming in Severe COVID-19. *Nat. Med.* 28 (1), 201–211. doi:10.1038/s41591-021-01576-3

Tosi, M., Roat, E., De Biasi, S., Munari, E., Venturelli, S., Coloretti, I., et al. (2018). Multidrug Resistant Bacteria in Critically Ill Patients: a Step Further Antibiotic Therapy. *J. Emerg. Crit. Care Med.* 2, 103. doi:10.21037/jeccm.2018.11.08

Vu, V. P., Gifford, G. B., Chen, F., Benasutti, H., Wang, G., Groman, E. V., et al. (2019). Immunoglobulin Deposition on Biomolecule Corona Determines Complement Opsonization Efficiency of Preclinical and Clinical Nanoparticles. *Nat. Nanotechnol.* 14 (3), 260–268. doi:10.1038/s41565-018-0344-3

WHO (2021). Pneumonia (No Date). Available at: https://www.who.int/news-room/fact-sheets/detail/pneumonia (Accessed: March 4, 2021).

Wolach, B., Carmi, D., Gilboa, S., Satar, M., Segal, S., Dolfin, T., et al. (1994). Some Aspects of the Humoral Immunity and the Phagocytic Function in Newborn Infants. *Isr. J. Med. Sci.* 30 (5–6), 331–335. Available at: http://www.ncbi.nlm.nih.gov/pubmed/8034475.

Xu, J., Murphy, S. L., Kockanek, K. D., and Arias, E. (2020). Mortality in the United States, 2018. *NCHS data Brief.* (355), 1

Yipp, B. G., Kim, J. H., Lima, R., Zbytnuik, L. D., Petri, B., Swanlund, N., et al. (2017). The Lung Is a Host Defense Niche for Immediate Neutrophil-Mediated Vascular Protection. *Sci. Immunol.* 2 (10), 8929. doi:10.1126/sciimmunol.aam8929

Yipp, B. G., and Kubes, P. (2013). NETosis: How Vital Is it? *Blood* 122 (16), 2784–2794. doi:10.1182/BLOOD-2013-04-457671

Zemans, R. L., Colgan, S. P., and Downey, G. P. (2009). Transepithelial Migration of Neutrophils: Mechanisms and Implications for Acute Lung Injury. *Am. J. Respir. Cell Mol. Biol.* 40, 519–535. doi:10.1165/rcmb.2008-0348TR

Zimmermann, P., and Jones, C. E. (2021). Factors That Influence Infant Immunity and Vaccine Responses. *Pediatr. Infect. Dis. J. NLM (Medline)* 40 (5), S40–S46. doi:10.1097/INF.0000000000002773

Conflict of Interest: The authors declare that the research was conducted in the absence of any commercial or financial relationships that could be construed as a potential conflict of interest.

Publisher's Note: All claims expressed in this article are solely those of the authors and do not necessarily represent those of their affiliated organizations, or those of the publisher, the editors and the reviewers. Any product that may be evaluated in this article, or claim that may be made by its manufacturer, is not guaranteed or endorsed by the publisher.

frontiers | Frontiers in Pharmacology

ORIGINAL RESEARCH
published: 08 July 2022
doi: 10.3389/fphar.2022.891889

Network Pharmacology and Experimental Validation to Explore the Mechanism of Qing-Jin-Hua-Tan-Decoction Against Acute Lung Injury

Shunli Xiao[1†], Lu Liu[1†], Zhengxiao Sun[1], Xiaoqian Liu[1], Jing Xu[1], Zhongyuan Guo[2], Xiaojie Yin[1], Fulong Liao[1], Jun Xu[3], Yun You[1] and Tiejun Zhang[3]**

[1]Institute of Chinese Materia Medica, China Academy of Chinese Medical Sciences, Beijing, China, [2]College of Pharmacy, Henan University of Chinese Medicine, Zhengzhou, China, [3]National and Local United Engineering Laboratory of Modern Preparation and Quality Control Technology of Traditional Chinese Medicine, Tianjin Institute of Pharmaceutical Research, Tianjin, China

OPEN ACCESS

Edited by:
Tsong-Long Hwang,
Chang Gung University, Taiwan

Reviewed by:
Po-Jen Chen,
E-Da Hospital, Taiwan
Hua Yu,
University of Macau, China

***Correspondence:**
Yun You
yyou@icmm.ac.cn
Tiejun Zhang
zhangtj@tjipr.com.cn

[†]These authors have contributed equally to this work

Specialty section:
This article was submitted to Inflammation Pharmacology, a section of the journal Frontiers in Pharmacology

Received: 08 March 2022
Accepted: 24 May 2022
Published: 08 July 2022

Citation:
Xiao S, Liu L, Sun Z, Liu X, Xu J, Guo Z, Yin X, Liao F, Xu J, You Y and Zhang T (2022) Network Pharmacology and Experimental Validation to Explore the Mechanism of Qing-Jin-Hua-Tan-Decoction Against Acute Lung Injury. Front. Pharmacol. 13:891889. doi: 10.3389/fphar.2022.891889

Qing-Jin-Hua-Tan-Decoction (QJHTD), a classic famous Chinese ancient prescription, has been used for treatment of pulmonary diseases since Ming Dynasty. A total of 22 prototype compounds of QJHTD absorbed into rat blood were chosen as candidates for the pharmacological network analysis and molecular docking. The targets from the intersection of compound target and ALI disease targets were used for GO and KEGG enrichment analyses. Molecular docking was adopted to further verify the interactions between 22 components and the top 20 targets with higher degree values in the component–target–pathway network. *In vitro* experiments were performed to verify the results of network pharmacology using SPR experiments, Western blot experiments, and the PMA-induced neutrophils to produce neutrophil extracellular trap (NET) model. The compound–target–pathway network includes 176 targets and 20 signaling pathways in which the degree of MAPK14, CDK2, EGFR, F2, SRC, and AKT1 is higher than that of other targets and which may be potential disease targets. The biological processes in QJHTD for ALI mainly included protein phosphorylation, response to wounding, response to bacterium, regulation of inflammatory response, and so on. KEGG enrichment analyses revealed multiple signaling pathways, including lipid and atherosclerosis, HIF-1 signaling pathway, renin–angiotensin system, and neutrophil extracellular trap formation. The molecular docking results showed that baicalin, oroxylin A-7-glucuronide, hispidulin-7-O-β-D-glucuronide, wogonoside, baicalein, wogonin, tianshic acid, and mangiferin can be combined with most of the targets, which might be the core components of QJHTD in treatment of ALI. Direct binding ability of baicalein, wogonin, and baicalin to thrombin protein was all micromolar, and their K_D values were 11.92 μM, 1.303 μM, and 1.146 μM, respectively, revealed by SPR experiments, and QJHTD could inhibit Src phosphorylation in LPS-activated neutrophils by Western blot experiments. The experimental results of PMA-induced neutrophils to produce NETs indicated that QJHTD could inhibit the production of NETs. This study revealed the active compounds, effective targets, and potential pharmacological mechanisms of QJHTD acting on ALI.

Keywords: Qing-Jin-Hua-Tan-Decoction, acute lung injury, neutrophil extracellular traps, thrombin, network pharmacology

INTRODUCTION

Acute lung injury (ALI) and its most severe form, acute respiratory distress syndrome (ARDS), are still the main causes of acute respiratory failure in critically ill patients, with high morbidity and mortality in the past 20 years (Wood et al., 2020). The pathophysiological processes of ALI are believed to involve epithelial and endothelial dysfunction, excessive accumulation, and activation of immune cells, inflammation, oxidative stress, apoptosis, and activation of clotting pathways (Matthay and Zemans, 2011; Matthay et al., 2012; Nadon and Schmidt, 2014). There is currently no specific and effective treatment for ALI. However, there is growing interest in alternative and natural treatments for ALI (Patel et al., 2018).

Qing-Jin-Hua-Tan-Decoction (QJHTD), a classic ancient prescription, listed in the Catalog of Ancient Classical Formulas (first batch released by State Administration of TCM in 2018), which is constituted by 11 Chinese herbal medicines, namely, *Scutellariae Radix*, *Gardeniae Fructus*, *Fritillariae Thunbergii Bulbus*, *Mori Cortex*, *Trichosanthis Semen Tostum*, *Citri Exocarpium Rubrum*, *Platycodonis Radix*, *Ophiopogonis Radix*, *Anemarrhenae Rhizoma*, *Poria*, *and Glycyrrhizae Radix* et Rhizoma. It was first recorded in the ancient book of *Yixue Tongzhi* written by YE Wen-ling in Ming dynasty for treating pulmonary disease with phlegm-heat obstructing lung syndrome, with the significant functions of clearing heat and moistening the lung, reducing phlegm, and relieving cough (Zhang et al., 2021). Previous studies have shown that the pharmacological effects of QJHTD are mainly focused on relieving cough and removing phlegm (Chen et al., 2016), anti-inflammation (Wu et al., 2019), and regulating immune function (Li and Jiang, 2018) in the treatment of pulmonary diseases. It has been reported that QJHTD inhibits LPS-induced ALI (Zhang, 2021). Nevertheless, its exact mechanism of QJHTD on ALI is still unknown.

Network pharmacology is an emerging discipline developed on the network computer platform integrating systematic biology, multi-pharmacology, and computational biology. It helps reveal the mechanism of action of traditional Chinese medicine (TCM) with multicomponent, multitarget, and multisignaling pathways (Hopkins, 2008; Li and Zhang, 2013). Molecular docking is a computational technology that functions through the interaction and affinity between the receptor and drug micromolecules (Chen et al., 2014; Saikia and Bordoloi, 2019), and this method can quickly and effectively screen out the

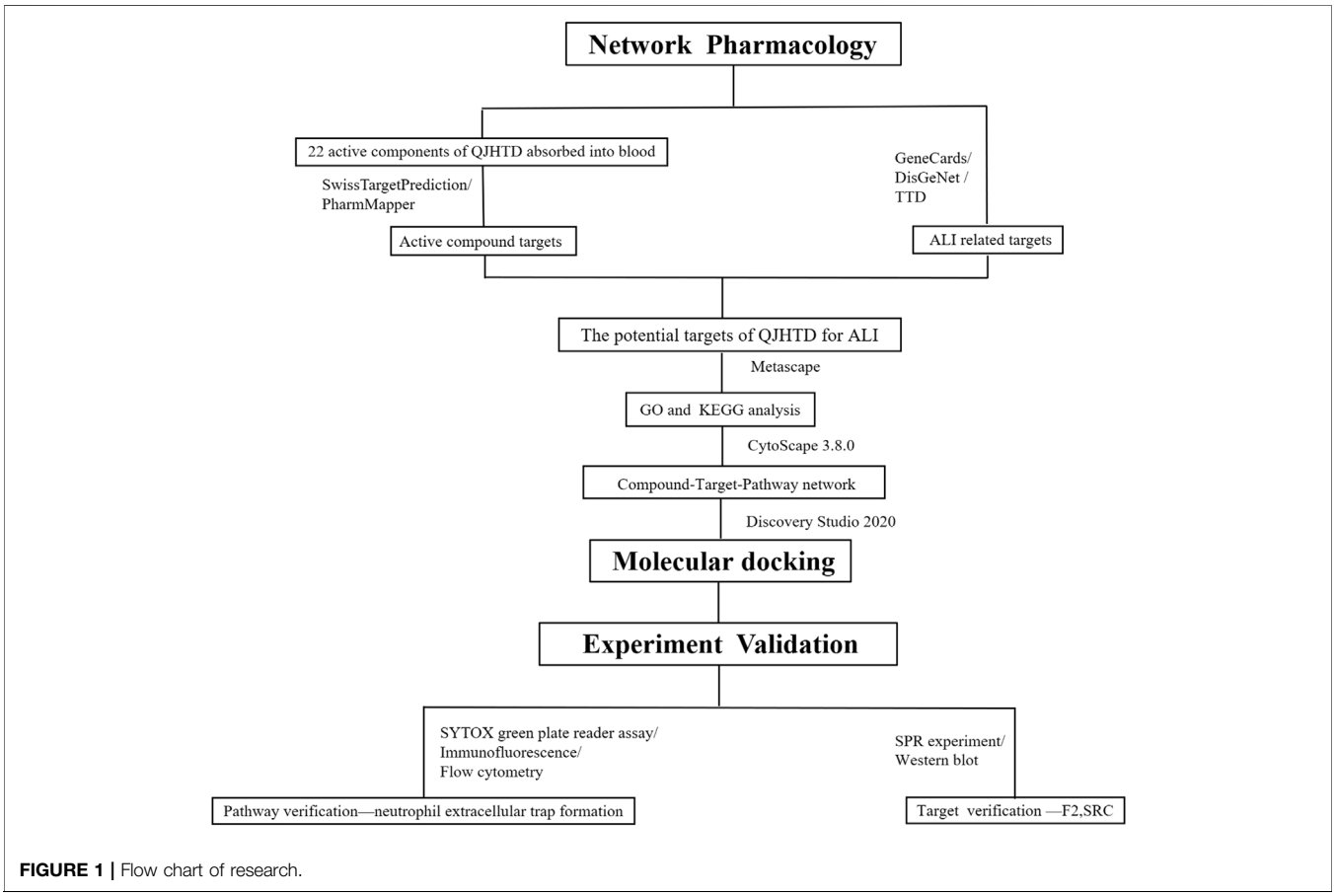

FIGURE 1 | Flow chart of research.

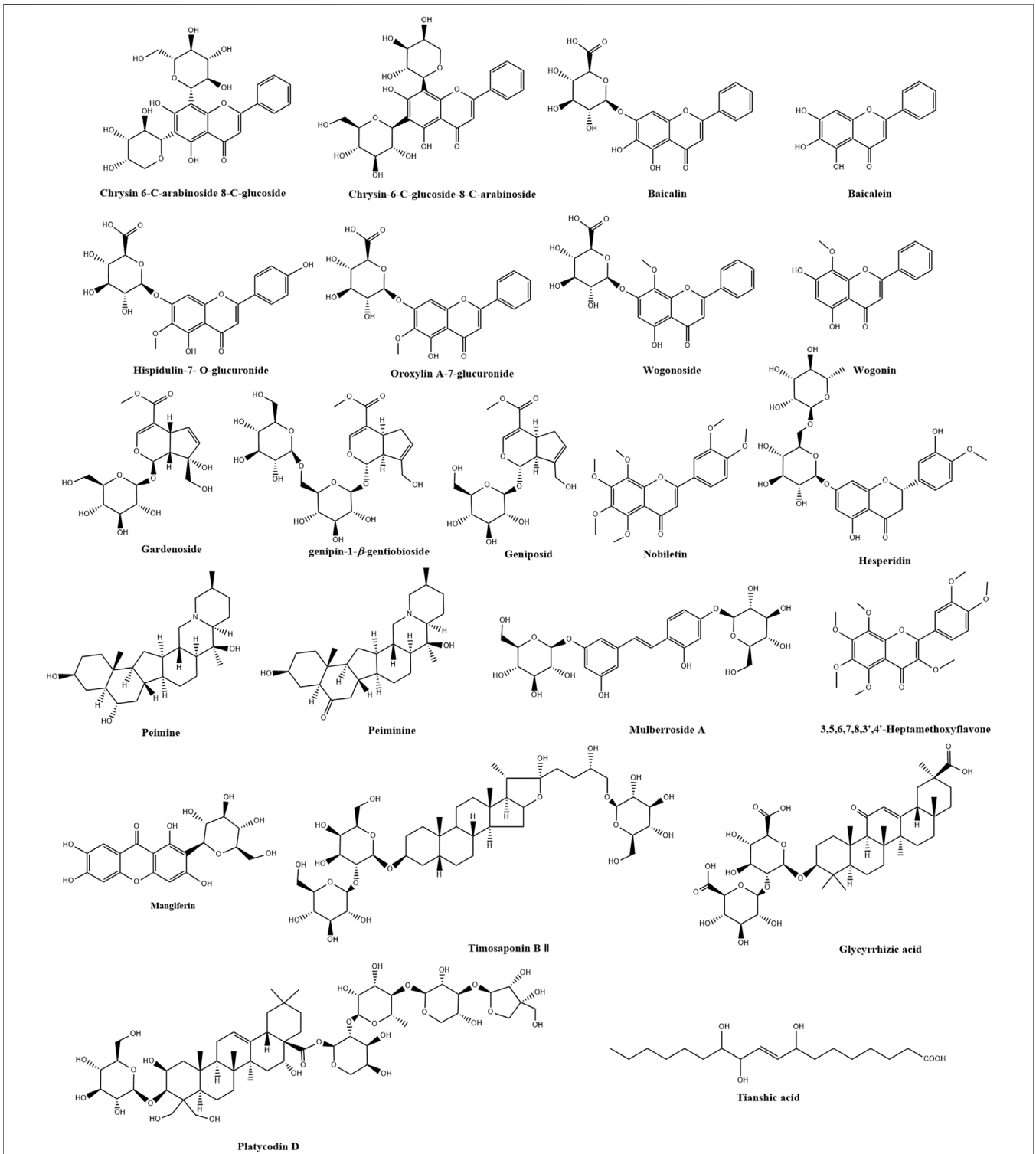

FIGURE 2 | Twenty-two active components of QJHTD and their chemical structures.

active ingredients. Surface plasmon resonance (SPR) technology has become one of the important means for analysis of small molecules and target proteins, with remarkable features of providing high-precision results and real-time, label-free measurements (Patching, 2014; Nguyen et al., 2015; Olaru et al., 2015; Prabowo et al., 2018).

In this research, we adopted the method of network pharmacology combined with molecular docking to screen the

possible targets, active components, and signaling pathways of QJHTD against ALI and verified them by SPR technology and cell experiments to further clarify the pharmacological mechanism of QJHTD against ALI. The flow chart of the research is shown in **Figure 1**. This work provides experimental basis and new mechanisms for the therapy of ALI with QJHTD.

MATERIALS AND METHODS

Identification of Active Components of QJHTD and Their Target Retrieval

A total of 22 prototype components were identified in the rat plasma and are referred to in the previous published literature by the research group (Liu et al., 2022). Chemical characterization analysis and quantitative analysis of QJHTD are shown in **Supplementary Material**. The chemical structure of 22 active components is shown in **Figure 2**, and their chemical information is shown in **Supplementary Table S1**. The SDF format file of the QJHTD components was downloaded from PubChem (https://pubchem.ncbi.nlm.nih.gov/) (Kim, 2016) and uploaded to PharmMapper databases (Liu X. et al., 2010; Wang et al., 2016; Wang et al., 2017) and SwissTargetPrediction. The targets with norm fit ≥0.6 in the output of PharmMapper and convert protein names to official gene symbols (*Homo sapiens*) using UniProt Knowledgebase (http://www.uniprot.org/) (UniProt Consortium, 2018). The potential drug targets predicted by the two databases were selected for further verification.

Screening Targets of ALI Disease

The information of the therapeutic target was searched by using "acute lung injury" as the keyword. The databases used in this study are GeneCards (https://www.genecards.org/), DisGeNet https://www.disgenet.org/home/), and TTD (http://db.idrblab.net/ttd/). Then, the components and disease overlap proteins are used as candidate targets for the treatment of ALI.

GO and KEGG Enrichment Analysis

Metascape combines functional enrichment, interactome analysis, gene annotation, and membership search to leverage over 40 independent knowledge bases within one integrated portal (Zhou et al., 2019). The core target proteins of QJHTD for ALI were inputted into Metascape, after which we set $p < 0.01$ to analyze GO and KEGG pathway enrichment. The first 20 KEGG and GO clusters pathway information were screened and included, and the results were saved and visualized by R software.

Construction of the Compound–Target–Pathway Network

The top 20 clusters obtained from the previous KEGG pathway enrichment analysis correspond to 22 active compounds and the core targets of QJHTD in the treatment ALI and construct the network of "compounds–targets–pathways" using CytoScape 3.8.0 to analyze the network topology parameters of the targets, including degree, betweenness, and closeness.

Molecular Docking

The virtual docking of key proteins and active components was performed using Discovery Studio 2020 software (College of Pharmacy, Henan University of Chinese Medicine) to study their interaction. For the top 20 targets with a higher degree value in the compound–target–pathway network, the corresponding 3D structure was downloaded in the RSCB PDB database (https://www.rcsb.org/) (Richardson et al., 2021), and 22 component structures were obtained from the PubChem database, and the components were prepared using the "Prepare Ligands" module to obtain the 3D structure. For protein preparation, crystallographic water molecules were removed and then used in the "Prepare Protein" module. Subsequently, CDOCKER was performed for molecular docking (Wu et al., 2003). To enable this mechanism, all default parameters were taken into account, allowing 10 poses to be generated for each ligand. Docking estimation was performed by the CDOCKER energy, which was used to assess the affinity of the proteins and ingredients. 80% of -CDOCKER ENERGY of the target protein and its corresponding prototype ligand was viewed as the threshold, and the components with higher scores were regarded as the active ingredients that interacted with the protein.

EXPERIMENTAL VALIDATION

Materials

QJHTD was prepared by Tianjin Pharmaceutical Research Institute Co., Ltd. (Tianjin, China). The preparation process of QJHTD is shown in **Supplementary Figure S1**. Thrombin (Cat No: HY-114164), dihydrorhodamine 123 (DHR123) (Cat No: HY-101894/CS-7988), and diphenyleneiodonium chloride (DPI) (Cat No: HY-100965) were purchased from MedChemExpress LLC (Monmouth Junction, NJ, United States). Baicalin (CAS No. 21967-41-9), baicalein (CAS No. 491-67-8), and wogonin (CAS No. 632-85-9) were obtained from Shanghai Yuanye Biological Co., Ltd (Shanghai, China), and the purity of all compounds was higher than 98%. The Amino Coupling Kit (Cat No: BR-1000-50), HBS-EP buffer solution (Cat No: BR-1001-88), CM5 Sensor Chip (Cat No: BR-1003-99), and Percoll (Cat No: 17-0891-01) were purchased from GE Healthcare (Braunschweig, Germany). Hoechest 33342 (Cat No: H1399) and SYTOX™ Green Nucleic Acid Stain (Cat No: S7020) were purchased from Invitrogen (Carlsbad, CA, United States). PMA (Cat No: P1585) and LPS (from *Escherichia coli* O111: B4) were obtained from Sigma (St. Louis, MO, United States). Fetal bovine serum (FBS) (Cat No: BR-1003-99) was obtained from Gemini (Woodland, CA, United States). RPMI 1640 medium (Cat No: 10,491), Wright-Giemsa Stain solution (Cat No: G1020), Red Blood Cell Lysis Buffer (Cat No: R1010), Dilution Buffer (Cat No: R1017), Normal Goat Serum (Cat No: SL038), and BCA protein assay kit (Cat No: PC0020) were obtained from Solarbio Life Science (Beijing, China). The ROS detection kit (Cat No: S0033S) and Poly-L-lysine (Cat No: C0313) were obtained from Beyotime (Shanghai, China). Rabbit monoclonal to Src (ab133283), rabbit monoclonal to Src (phospho Y419) (ab185617), rabbit monoclonal to Myeloperoxidase (ab208670), and Alexa Fluor® 488 Goat

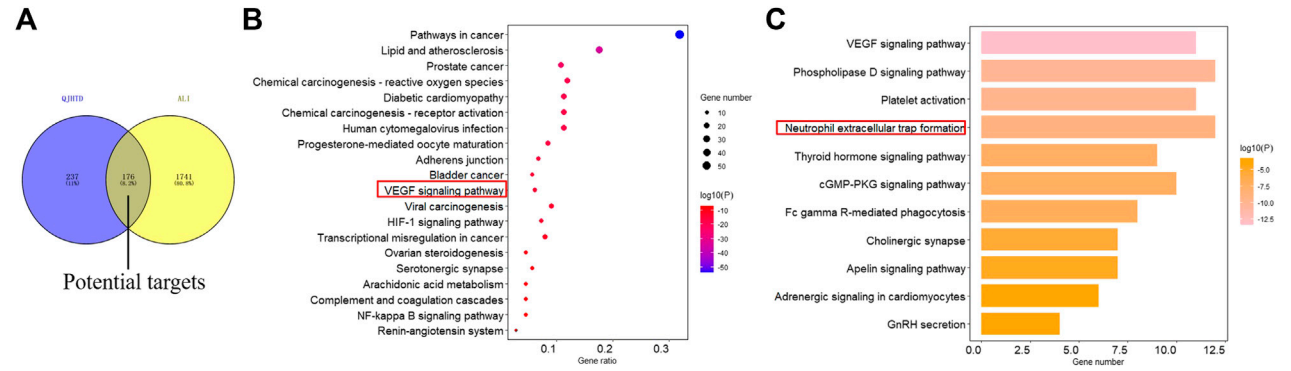

FIGURE 3 | Venn diagram of overlapping targets of QJHTD and ALI; **(A)** top 20 cluster pathways for KEGG enrichment analysis; **(B)** and the 11th clustering pathway expansion diagram **(C)**.

polyclonal Secondary Antibody to rabbit IgG - H&L (ab150077) were obtained from Abcam (Cambridge, MA, United States). HRP-conjugated goat anti-rabbit IgG antibody (Cat No:bs-40295G-HRP) was obtained from Bioss (Beijing, China). PE anti-rat CD11b/c Antibody (Cat No: B339537) was obtained from BioLegend (San Diego, CA, United States).

Surface Plasmon Resonance (SPR)

CM5 Sensor Chip was esterified with the crosslinking agents EDC and NHS. The thrombin protein at a concentration of 5 μg/ml in sodium acetate at pH 4.5 was coupled to the surface of the chip, and then the remaining reactive carboxyl on the matrix were blocked using 1 M ethanolamine, at pH 8.5. The compound of baicalin, baicalein, and wogonin were dissolved in DMSO to 10 mM, was diluted with HBS-EP buffer solution to 500 μM, and then diluted successively to 50 μM, 25 μM, 12.5 μM, 6.25 μM, 3.125 μM, 1.5625 μM, 0.7813 μM (baicalin), 12.5 μM, 6.25 μM, 3.125 μM, 1.5625 μM, and 0.7813 μM (baicalein) and 12.5 μM, 6.25 μM, 3.125 μM, 0.7813 μM, and 0.3906 μM (wogonin) using 5% DMSO HBS-EP buffer. The SPR experiment was performed using the Biacore T200 SPR instrument. The injection sample time and velocity were 120s and 20 μl/min, respectively. The protein dissociation time was 300 s.

Rat Peripheral Blood Neutrophil Isolation

Male Sprague–Dawley rats (220–240 g) were obtained from the Weitonglihua Experimental Animal Technology Co. (Beijing, China) [SCXK 2016–0,006], and housed at 25–28 °C and humidity of 45–55%, with free access to food and drink for 7 days before use.

Rat neutrophils were isolated from the whole blood of healthy rats by gradient centrifugation using Percoll. Briefly, blood was collected from the abdominal aorta of rats and anticoagulated with 109 mM sodium citrate (1:9 blood v/v), and the whole blood was diluted with an equal volume of dilution buffer. Diluted blood was smeared on the interface of the two layers of 82% Percoll and 69% Percoll, and centrifugation was carried out at 710 *g* for 30 min. Neutrophils were collected in the cell layer between the two layers and washed with PBS. Then, red blood cell lysis buffer was added, gently blown for 3–5 min, and incubated at 4°C for 15 min. Centrifugation was carried out at 290 g for 10 min. The supernatant was discarded, and the pellet was washed with PBS and centrifuged again at 250 g for 10 min. The pellet obtained at this point contains the neutrophils. The purity of neutrophil was determined by the flow cytometry and Wright-Giemsa Stain.

SYTOX Green Plate Reader Assay for NETosis Analysis

Sytox Green dye was used to observe and measure the release of NETs under different conditions (Shi et al., 2019). To quantify the amount of PMA-induced formation of NETs *in vitro*, neutrophils isolated from rat blood (8×10^4 cells/well in 200 μl of medium with 1 μM SytoxGreen) were seeded into 96-well plates. These neutrophils were activated with the media (control), QJHTD at different concentrations (0.125, 0.25, and 0.50 g/L), 50 nM PMA, and 50 nM PMA with QJHTD at different concentrations (0.125, 0.25, and 0.50 g/L), respectively. The plate was placed in a 37°C, 5% CO_2 incubator for 4 h. Fluorescence was monitored 0 and 4 h using a SpectraMax i3x plate reader (Molecular Devices, San Jose, CA) with excitation at 488 nm and emission at 525 nm. Fluorescence intensity (extracellular DNA) was calculated as (Fluorescence intensity at 4 h) - (Fluorescence intensity at 0 h). The cell status of each group was observed by Axio Observer Z1 (Carl Zeiss AG, Oberkochen, Germany) after the detection with fluorescence microplate.

NET Induction and Immunofluorescence Staining

Rat peripheral blood neutrophils (1.6×10^5 cells) were seeded on poly-L-lysine-coated coverslips in 48-well plates and cultured for 4 h in RPMI medium containing media (control), 50 nM PMA, or 50 nM PMA with QJHTD at different concentrations (0.125, 0.25, and 0.5 g/L). Subsequently, the cells were fixed with 4% paraformaldehyde for 20 min and permeabilized with 0.2% Triton-X-100 for 20 min. After blocking with 5% normal goat serum for 1 h, it was incubated with rabbit anti-MPO overnight (1:100 dilutions) at 4°C, followed by Alexa Fluor® 488 -conjugated

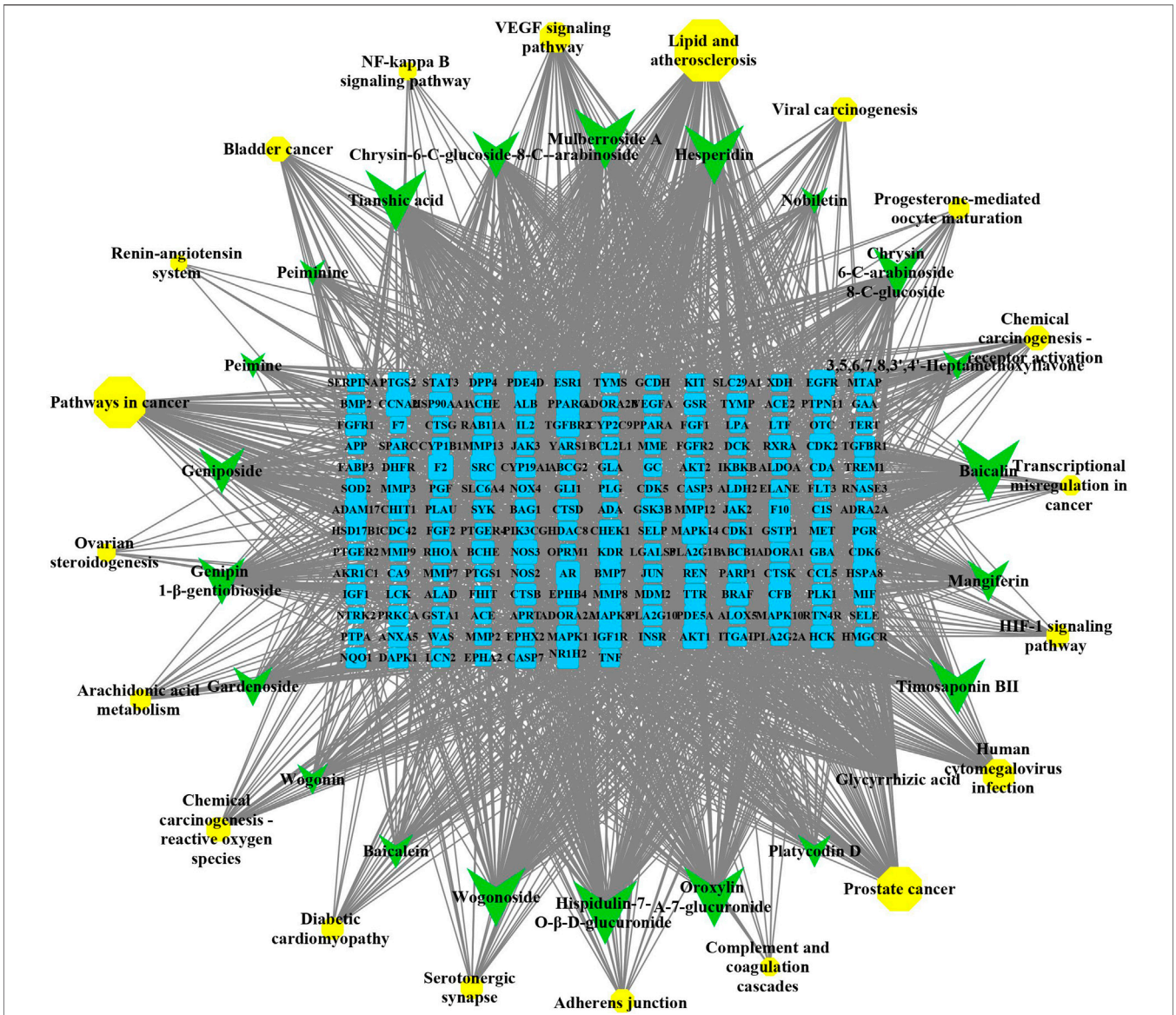

FIGURE 4 | Compound–target–pathway network of QJHTD in the treatment for ALI. The yellow circles, green V shape, and blue square represent the pathway, active components, and targets, respectively.

goat antirabbit IgG antibody (1:200 dilutions) for 3 h in the dark. The DNA was counterstained with Hoechst 33342 for 10 min. The images were acquired using Axio Observer Z1 (Carl Zeiss AG, Oberkochen, Germany) and a C11440-42U30 digital camera (Hamamatsu Photonics, Shizuoka, Japan) and processed with BioFlux Montage software (Fluxion Biosciences, Alameda, CA, United States).

Quantification of ROS Production

The neutrophils were preloaded with DCFH-DA and were diluted at 1:1,000 with PBS. After the extracellular DCFH-DA dye was washed, the cells were resuspended in fresh RPMI medium (8×10^4 cells) and were seeded in a 96-well plate. The fluorescence intensity was detected by a SpectraMax i3x plate reader (Molecular Devices, San Jose, CA) at 0, 1, 2, 3, and 4 h, and the excitation wavelength was 488 nm, and the emission wavelength was 525 nm.

Neutrophils were preloaded with 10 μM dihydrorhodamine 123 (DHR123) at 37°C for 20 min. After washing the extracellular DHR123, the cells were resuspended in fresh RPMI medium containing media (control), 50 nM PMA, or 50 nM PMA with QJHTD at different concentrations (0.125, 0.25, and 0.50 g/L) and 50 nM PMA with 20 μM diphenyleneiodonium (DPI) for 1 h. After PBS washing, ROS production was determined using a BD FACSAria II flow cytometer (BD Bioscience, New Jersey, United States).

TABLE 1 | Related information of molecular docking models and molecular docking results of the top 20 targets with 22 active components of QJHTD.

Targets	PDB ID	Radius Å	Active pocket coordinates	RMSD Å	-CDOCKER ENERGY (kcal/mol) of the original ligand	The number of successful components	The number of -CDOCKER ENERGY higher than 80% of the original ligand
MAPK14	1W83	10.040	4.9556, 13.0505, 35.9238	0.6596	41.645	16 (72.23%)	1 (4.55%)
EGFR	5UG9	8.275	−13.8137, 15.0141, −26.6268	1.9704	27.8811	19 (86.36%)	5 (22.73%)
CDK2	1PXK	9.200	12.4244, 45.2819, 24.0306	1.1059	26.7258	17 (77.27%)	6 (27.27%)
SRC	2H8H	9.940	21.0350, 20.1995, 58.5490	1.123	5.4287	20 (90.91%)	13 (59.09%)
CCNA2	4FX3	8.195	−9.7242, 3.4762, 37.1244	0.8398	21.8394	19 (86.36%)	10 (45.45%)
F2	3QWC	7.750	16.8398, −12.7995, 22.4897	0.4607	25.636	19 (86.36%)	3 (13.64%)
AKT1	4EKL	9.495	28.2195, 5.26228, 11.3812	0.702	31.6881	19 (86.36%)	4 (18.18%)
ESR1	5AAV	8.852	31.4186, 12.7432, 11.4012	0.4013	27.683	17 (77.27%)	3 (13.64%)
AR	2PIX	7.500	27.7039, 2.0436, 4.6478	0.2254	6.2037	17 (77.27%)	3 (13.64%)
NOS3	6POV	9.132	−32.2287, −38.6579, −184.9843	0.6297	3.26707	20 (90.91%)	13 (59.09%)
PGR	3HQ5	8.880	−3.0303, −7.6424, 24.3050	0.3023	22.4897	17 (77.27%)	3 (13.64%)
GSK3B	4PTC	7.568	−3.5261, 0.78590, −35.4591	0.4392	35.275	19 (86.36%)	2 (9.09%)
TGFBR2	5E91	10.000	14.9144, −1.0736, 5.5120	1.0171	36.3647	19 (86.36%)	3 (13.64%)
HSPA8	6B1I	8.275	−13.8137, 15.0141, −26.6268	0.7064	58.539	18 (81.82%)	0 (0.00%)
HSP90AA1	6U9A	8.854	3.5789, 9.2703, 26.5332	0.8465	21.1237	20 (90.91%)	5 (22.73%)
IGF1R	1JQH	7.896	28.9641, 58.5570, −8.2719	1.7115	84.4747	22 (100.00%)	0 (0.00%)
PPARG	3OSI	6.610	15.3645, 18.2322, 11.2332	0.3888	32.9185	19 (86.36%)	3 (13.64%)
MMP3	4G9L	7.947	21.6653, 68.3753, 106.167	1.1247	51.0165	20 (90.91%)	1 (4.55%)
PDE4D	1XOQ	11.000	14.0064, 29.3300, 53.1901	0.4731	25.4934	19 (86.36%)	10 (45.45%)
BRAF	3C4C	9.182	0.4785, −2.1111, −19.74544	0.5851	17.0889	18 (81.82%)	6 (27.27%)

Western Blot

According to the network pharmacology and molecular docking results, we selected SRC activity for Western blot verification. The neutrophils were activated using LPS (1 μg/ml), following incubation with or without QJHTD (0.125, 0.25, and 0.5 g/L) at 37°C for 1 h. After 1 h, the cells were added with ice-cold lysis buffer containing protein phosphatase inhibitor mixture, lysed on ice for 30 min, and centrifuged (12,000 rpm, 4°C, 20 min) to obtain the supernatant. Protein concentrations were determined by the BCA protein assay kit. After denaturation by boiling, the proteins were separated by SDS-PAGE and transferred to PVDF membranes. Then, the membranes were blocked with 5% BSA at room temperature for 1.5 h and then incubated with anti-Src (1:1,000 dilution) and anti-Src (phospho Y419) (1:5,000) overnight at 4°C. Subsequently, the membranes were incubated with HRP-linked secondary antibody (1:2,000) at room temperature for 1 h. The results of Western blot were visualized by using an ECL detection system (Syngene, Cambridge, United Kingdom) and analyzed by ImageJ software.

Statistical Analysis

All data were expressed as the mean ± SD of three independent experiments. The comparison between *multiple* groups was performed by *one-way ANOVA* followed by the *LSD* test when the variances were homogeneous or Dunnetts T3 test when the variances were non-homogeneous. All data were analyzed statistically using the SPSS version 23.0 (IBM, Armonk, NY, United States). $p < 0.05$ was considered statistically significant.

RESULTS

The Potential Targets of QJHTD for ALI

A total of 413 potential QJHTD-related targets were predicted by PharmMapper and SwissTargetPrediction (**Supplementary Table S2**), and 1,917 disease targets were finally summarized and obtained by removing the duplicate targets by searching the disease databases including GeneCards, DisGeNet, and TTD (**Supplementary Table S3**). The intersection of the QJHTD-related targets and ALI-related targets has 176 targets (**Figure 3A**, **Supplementary Table S4)**, which include AKT1, MAPK1, F2, PPARG, and so on. The 176 targets were considered the potential therapeutic targets of QJHTD for ALI.

GO and KEGG Pathway Enrichment Analysis of QJHTD for ALI

Metascape was used to analyze the signal pathways of QJHTD-related targets in improving ALI. The results of GO enrichment analysis are shown in **Supplementary Figure S4**. The biological processes in QJHTD for ALI mainly involved included protein phosphorylation, response to wounding, response to bacterium,

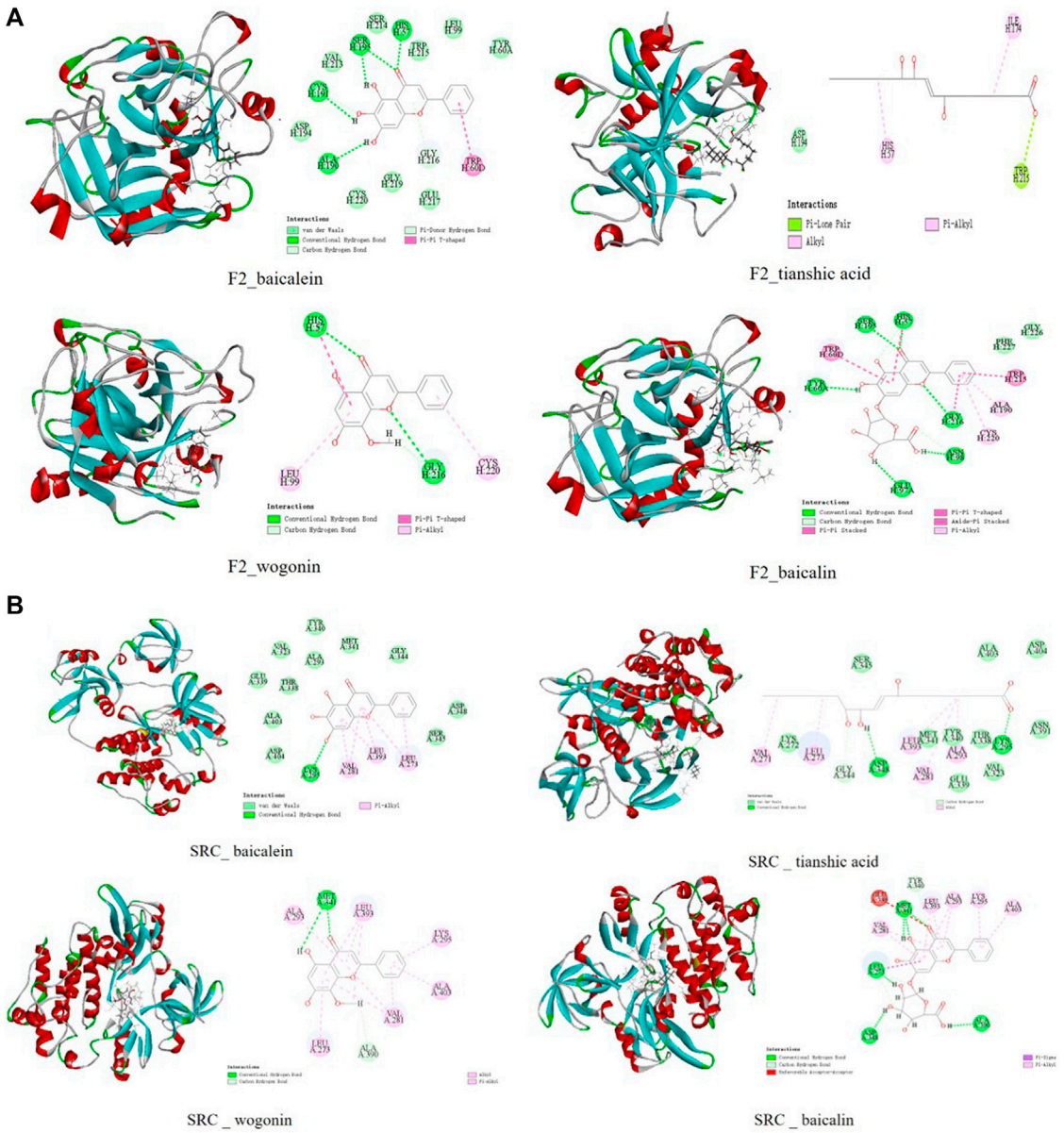

FIGURE 5 | Two- and three-dimensional ligand–protein interactions of baicalein, tianshic acid, wogonin, and baicalin with F2 **(A)** and SRC**(B)**.

regulation of inflammatory response, and so on. Cellular components were related to vesicle lumen, extracellular matrix, platelet alpha granule, and extrinsic component of the plasma membrane. Molecular functions analysis revealed protein serine/threonine/tyrosine kinase activity, endopeptidase activity, nitric-oxide synthase regulator activity, and phosphatase binding. The GO enrichment analysis may be related to the pathogenesis of ALI.

For each given gene list, pathway and process enrichment analysis has been carried out with the following ontology sources: KEGG pathway. All genes in the genome have been used as the enrichment background. Terms with a p-value < 0.01, a minimum count of 3, and an enrichment factor >1.5 are collected and grouped into clusters based on their membership similarities. The most statistically significant term within a cluster is chosen to represent the cluster. The first 20 clusters were selected according to their p-values to generate the bubble chart for visualization (**Figure 3B**). It is involved with lipid and atherosclerosis, HIF-1 signaling pathway, transcriptional misregulation in cancer, renin–angiotensin system, VEGF signaling pathway, and so on. From cluster 11, the VEGF signaling pathway expanded, and we can see that it contains

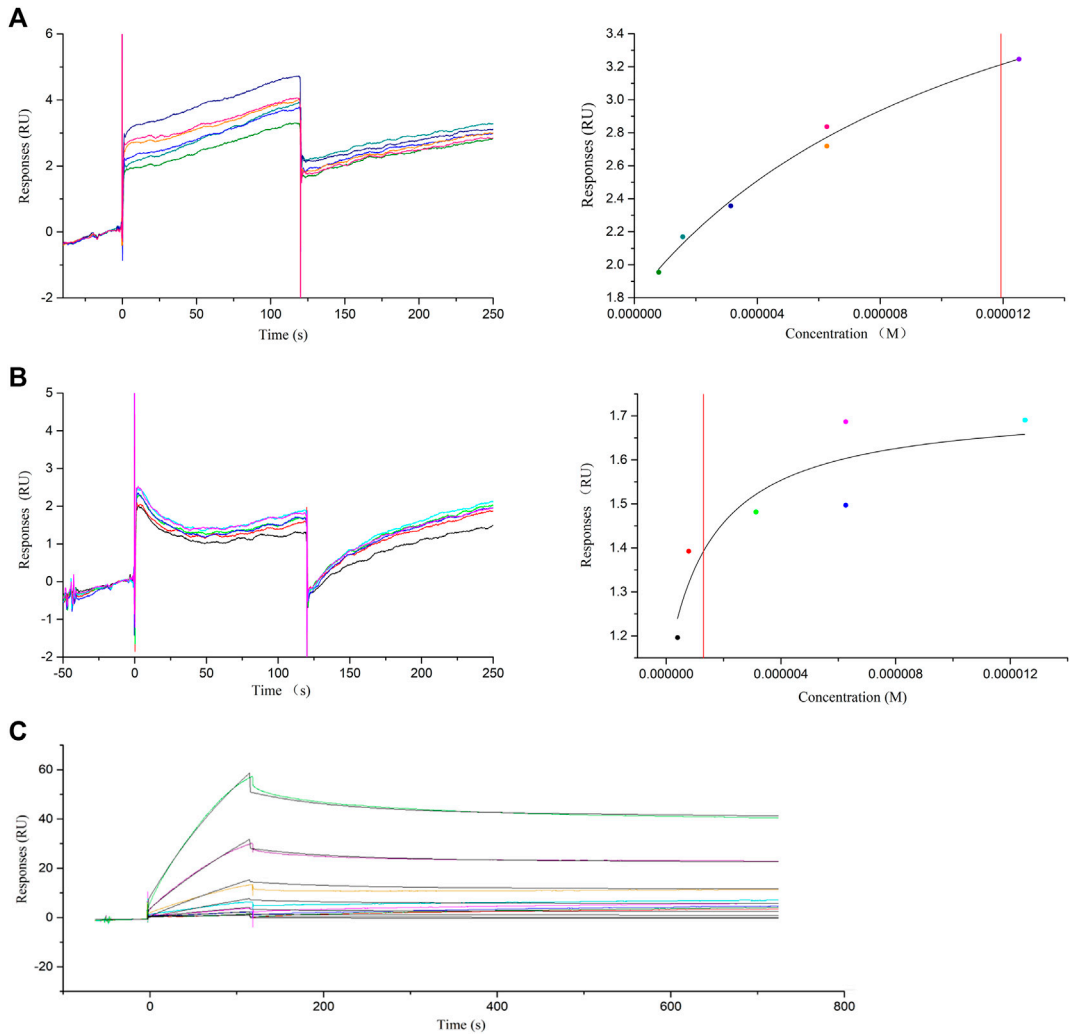

FIGURE 6 | SPR assay of the interaction of baicalein, wogonin, baicalin, and thrombin protein. **(A)** SPR assay of baicalein binding to thrombin (left) and the representative binding curve (right). **(B)** SPR assay of wogonin binding to thrombin (left) and the representative binding curve (right). **(C)** SPR titration curve of baicalin with thrombin protein.

VEGF signaling pathway, phospholipase D signaling pathway, platelet activation, neutrophil extracellular trap formation, and so on (**Figure 3C**). Neutrophils are the host's first line of defense against microbial infection and play an important role in innate immune response (Nauseef and Borregaard, 2014; Leiding, 2017). Neutrophils survive for a short time in the blood, and they can resist pathogenic microorganisms by phagocytosis, degranulation, and formation of NETs (Kolaczkowska and Kubes, 2013). In recent years, it has been found that in ALI, neutrophil adhesion aggregation and continuous activation lead to an inflammatory cascade, during which a large number of NETs are produced (Saffarzadeh et al., 2012; Luo et al., 2014). Therefore, based on the results of network pharmacology and literature review, we adopted the PMA-induced neutrophil production NET model to verify whether QJHTD treats ALI by inhibiting NETs.

Compound–Target–Pathway Network

CytoScape 3.8.0 software was used to construct a component–target–pathway network of QJHTD in treating ALI and was used to calculate and sort the topological parameters (degree) of the nodes in the abovementioned network (**Figure 4**). The network has 218 nodes, including 22 components, 176 targets, 20 pathways, and 2,044 edges. The larger the node, the greater the degree, and the more nodes connected to it. It was surprised that the degree of MAPK14, CDK2, EGFR, F2, SRC, and AKT1 were higher in the compound–target–pathway network. It was concluded that the 22 active ingredients acted on 176 targets by relevant pathways in lipid and atherosclerosis, renin–angiotensin system, HIF-1 signaling pathway, and so on. Multiple pathways are linked to each other by common targets, indicating the synergistic action of QJHTD in treating ALI.

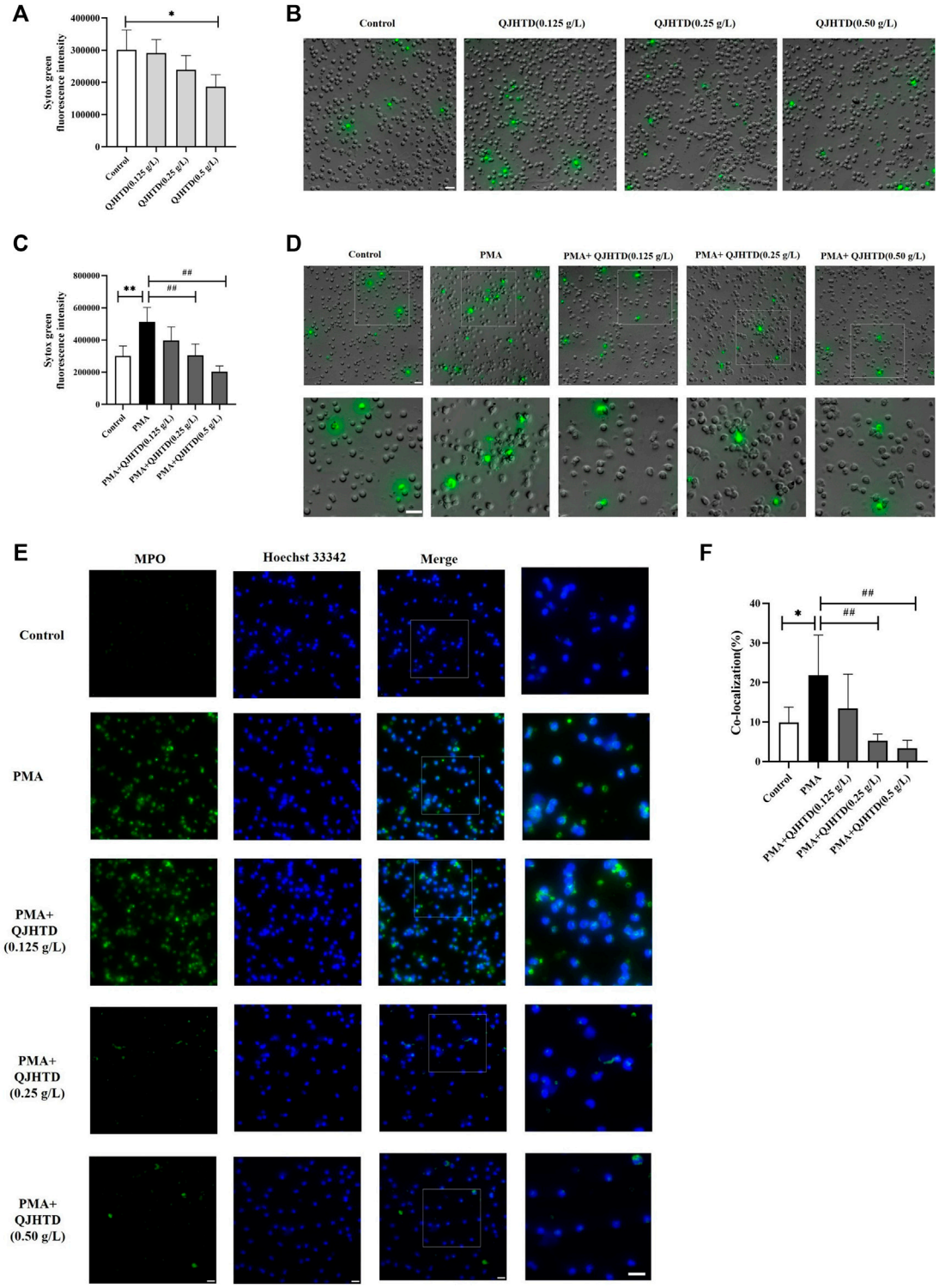

FIGURE 7 | QJHTD inhibited NET formation. **(A)** Effect of different concentrations of QJHTD (0.125, 0.25, and 0.5 g/L) on neutrophils. **(B)** Images of A, scale bar = 20 μm. **(C)** Levels of extracellular DNA released by neutrophils, which were cultured with media, PMA (50 nM), or PMA (50 nM) plus 0.125,0.25, and 0.5 g/L QJHTD. **(D)** Images of C, scale bar = 20 μm. **(E)** Representative images of immunofluorescent staining showed PMA-induced NET formation. Hoechst 33342 (blue), MPO (green), scale bar = 20 μm. **(F)** Quantification data of **(E)**. Data presented as the mean ± SD of three independent experiments (*$p < 0.05$ and **$p < 0.01$ compared with control group, $^{\#}p < 0.05$ and $^{\#\#}p < 0.01$ compared with PMA group).

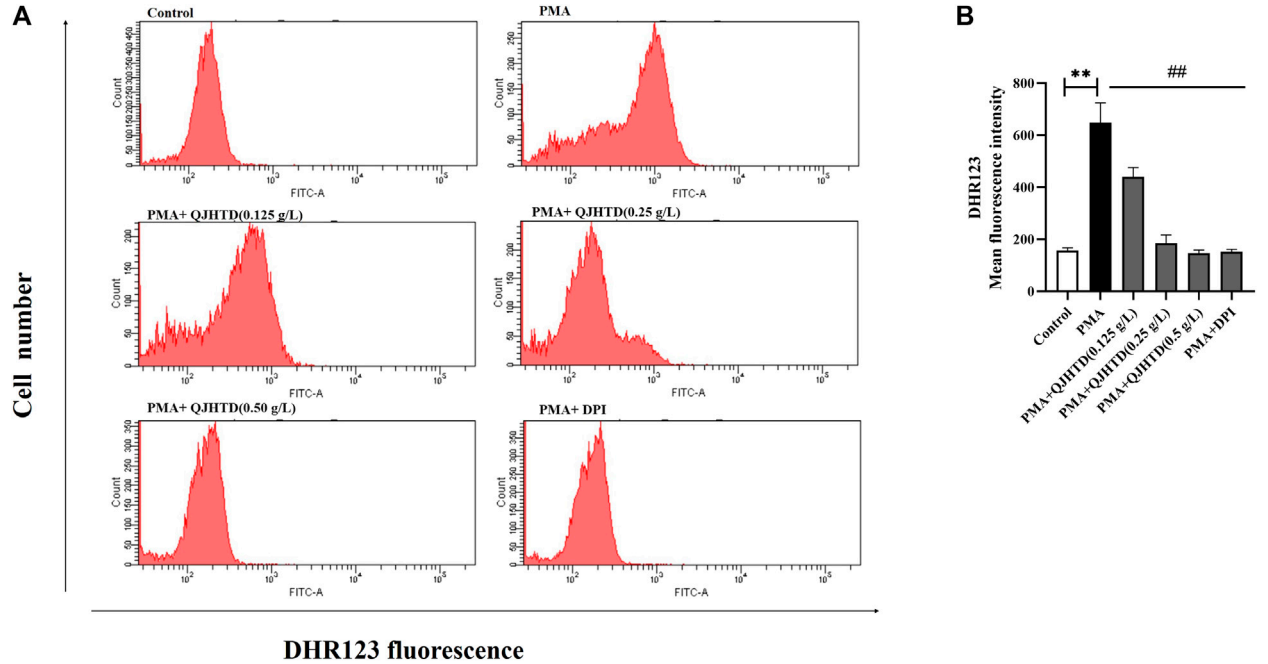

FIGURE 8 | QJHTD could reduce the generation of ROS during the formation of NETs. **(A)** ROS was monitored by flow cytometry using cell-permeable DHR123. **(B)** Quantification data of **(A)** data presented as the mean ± SD of three independent experiments (**$p < 0.01$ compared with control group, $^{\#\#}p < 0.01$ compared with PMA group).

Molecular Docking Results

The 22 active components of QJHTD were used as candidate docking components. By analyzing the degree value of the targets in the component–target–pathway network, the first 20 targets (**Supplementary Table S5**) with higher degree values were selected for molecular docking experiments. The initial compounds of the protein were extracted from the active pockets and redocked and RMSD≤2 evaluated that the docking algorithm could reproduce the receptor-ligand binding mode (Huang et al., 2010).

The original ligands of the selected crystal structures of 20 targets were used to define the active pockets. The original ligands were taken out, and the CDOCKER method was used. Re-dock to the set active pocket, calculate its RMSD and scoring value and its active pocket information, and calculation results are shown in **Table 1**. It can be seen from the table that the RMSD of the 20 targets are all less than 2 Å, indicating that the selected docking method and parameter settings are reasonable and can be used for further molecular docking research. Molecular docking results in the top 20 target proteins with 22 chemicals and are shown in **Supplementary Table S6** and **Table 1**. The higher -CDOCKER ENERGY is, the more likely the chemical and target are to interact with each other. The results showed that most chemical components had good interaction and binding activities with the targets. Components such as baicalin, oroxylin A-7-glucuronide, hispidulin-7-O-β-D-glucuronide, wogonoside, baicalein, wogonin, tianshic acid, and mangiferin are bound to most of the target proteins, which may be the core components of QJHTD for ALI.

Studies have shown that the inflammation of ALI depends on tissue factors and thrombin (Lou et al., 2019). Plasma and lavage fluid thrombin elevated evidently in the animal models of ALI, and thrombin has been found as a key molecule linking coagulation and inflammation (Lou et al., 2019; Arroyo et al., 2021; Kaspi et al., 2021). The results of molecular docking experiments showed that the docking scores of baicalein, wogonin, tianshic acid, and baicalin to F2 (thrombin) reached the effective binding scores. Two- and three-dimensional ligand–protein interactions of baicalein, tianshic acid, wogonin, and baicalin with F2 (PDB ID: 3QWC) are shown in **Figure 5A**. Both baicalin and wogonin inhibited thrombin-catalyzed fibrin polymerization and platelet functions and inhibited the activities of thrombin (Ku and Bae, 2014; Lee, et al., 2015b). Affinity capillary electrophoresis (ACE) is one of the predominant methods for interaction studies, and baicalein had the greatest affinity with thrombin in comparison with the Kb values of other flavonoid compounds (Li et al., 2018), and it has indicated more OH groups in the A-ring and more thrombin inhibitory activity (Liu L. et al., 2010). Taking into account all these, we thus selected baicalin, wogonin, and baicalein for the experiment of SPR.

The results of molecular docking experiments showed that the docking scores of 13 compounds including baicalein and wogonin to SRC reached the effective binding scores (**Supplementary Table S6**). Two- and three-dimensional ligand–protein interactions of baicalein, tianshic acid, wogonin, and baicalin with SRC (PDB ID: 2H8H) are shown in **Figure 5B**. The Src kinase family plays an important role in

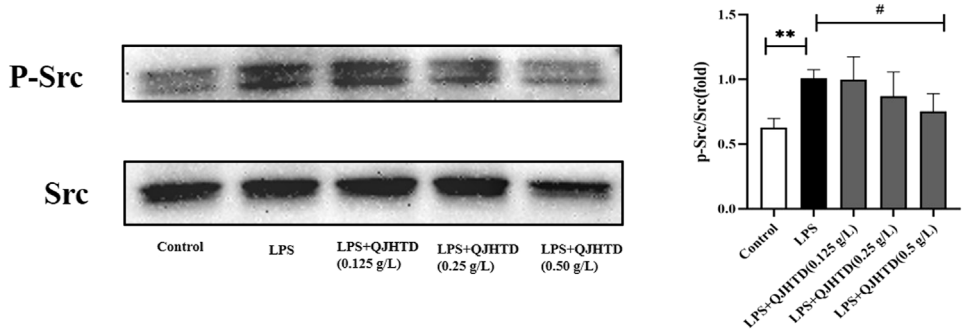

FIGURE 9 | QJHTD suppresses SRC phosphorylation in the LPS-activated neutrophils. Data presented as the mean ± SD of three independent experiments (**p < 0.01 compared with control group, $^{\#}p$ < 0.05 compared with LPS group).

LPS-induced ALI, and studies have shown that bletinib and resveratrol ameliorates neutrophil inflammation and lung injury *via* inhibition of Src family kinases (Tsai et al., 2019; Kao et al., 2021).

SPR Experiment Results

In the SPR experiment, baicalein, wogonin, and baicalin were screened out as *in vitro* validation molecular models, and small-molecule and macromolecular interaction experiments with thrombin protein were performed. The binding affinity (K_D) describes the strength of the binding between the ligand and the analyzing molecule. K_D can be obtained by either "steady-state" or "kinetic" methods. The steady-state method was used in the "fast-up and fast-down" binding mode to obtain affinity, such as baicalein (**Figure 6A**) and wogonin (**Figure 6B**). Kinetic analysis K_D was obtained from the association rate constant (Ka) and dissociation rate constant (Kd), which was the combined result of the two processes of association and dissociation, such as baicalin (**Figure 6C**). The results showed that the direct binding ability of baicalein, wogonin, and baicalin to thrombin protein was all micromolar, and their K_D values were 11.92 μM , 1.303 μM , and 1.146 μM, respectively (**Figure 6**). Therefore, it was speculated that baicalein, wogonin, and baicalin bind to the thrombin protein and inhibit its activities and might exert thrombosis prevention in ALI to some extent.

Rat Peripheral Blood Neutrophil Purity

The purity of neutrophils is >80% with PE Mouse anti-rat CD11b/c antibody was used to label neutrophils (**Supplementary Figure S5A**). By Wright-Giemsa staining, it was further confirmed that the purity of neutrophils was >80%. At the same time, it could be observed that the neutrophils had complete morphology, the cytoplasm was light red, and the nucleus was purple and lobulated, divided into two–five leaves (**Supplementary Figure S5B**).

QJHTD Significantly Inhibited PMA-Induced NETs Formation

Phorbol 12-myristate 13-acetate (PMA) is most widely used as an inducer of NETosis. Sytox Green dye is a high-affinity nucleic acid stain that readily cross-damaged cell membranes but does not penetrate the membranes of living cells. At the same time, it could be used to observe and measure the release of NETs (Shi et al., 2019). QJHTD (0.125, 0.25 g/L) showed no significant difference compared with that of the control group (p > 0.05), and the immunofluorescence intensity of the QJHTD (0.50 g/L) group was significantly lower than that of the control group (p < 0.05), suggesting that the QJHTD group has no cytotoxic effect on neutrophils, and the QJHTD (0.50 g/L) group may play a protective role (**Figure 7A**). Meanwhile, as shown in **Figure 7B**, QJHTD (0.125, 0.25, and 0.50 g/L) did not change the morphology of neutrophils.

The immunofluorescence intensity values of the PMA + QJHTD group with different concentrations (0.25 and 0.50 g/L) were significantly decreased compared with those of the PMA group (p < 0.01), indicating that QJHTD could inhibit PMA-induced neutrophil releasing NETs (**Figure 7C**). From **Figure 7D**, the result was consistent with the fluorescence intensity of each well detected by the fluorescence microplate. It was found that 4 h after PMA stimulation of neutrophils, compared with the control group, the morphology of neutrophils in the PMA group had changed, the cells were flattened, and neutrophils released a large number of green fluorescent filament-like and reticular NETs. Compared with the PMA group, the PMA + QJHTD group with different concentrations (0.25 and 0.50 g/L) did not change the flattened morphology of neutrophils, but the green fluorescent filamentous structures and NETs were significantly reduced, suggesting that QJHTD inhibits the release of NETs from the PMA-stimulated neutrophils.

We measured the release of NETs by detecting the release of MPO-DNA complexes. Immunofluorescent staining of MPO (neutrophil marker) and Hoechst-33342 (nucleic staining) further confirmed the inhibitory effect of QJHTD (**Figure 7E**). Compared with the control group, neutrophils lost their original structure after PMA stimulation, and their nuclear morphology also showed depolymerization and expansion. There was no significant difference between the PMA + QJHTD group (0.125 g/L) and the PMA group, but the PMA + QJHTD group (0.25 and 0.5 g/L) released

significantly less NETs to the extracellular network and filamentous structures ($p < 0.01$) (**Figure 7E**, **Figure 7F**). These experiments documented that QJHTD inhibited the formation of PMA-stimulated NETs.

QJHTD Could Reduce the Generation of ROS During the Formation of NETs

NETosis is a multifactorial process, but the detailed molecular mechanisms are not fully understood. The formation of PMA-induced NETs is closely related to ROS generation by nicotinamide adenine dinucleotide phosphate (NADPH) oxidase (Fuchs et al., 2007; De Bont et al., 2018; Fousert et al., 2020). DPI, an NADPH inhibitor, was used as a positive control for the inhibition of ROS production. In the PMA-stimulated neutrophils, the ROS production increased with longer time and the neutrophils were stimulated by PMA (**Supplementary Figure S6**). As can be seen from **Figure 8** and **Supplementary Figure S6**, QJHTD treatment at concentrations of 0.125, 0.25, and 0.5 g/L significantly inhibited PMA induced ROS production ($p < 0.01$), suggesting that the inhibitory effect of QJHTD on NET formation is mediated by ROS inhibition.

QJHTD Suppresses Src Phosphorylation in LPS-Activated Neutrophils

The Src kinase family plays an important role in the systemic inflammatory response induced by LPS (Lee et al., 2007; Toumpanakis et al., 2017). Neutrophils have a key role in innate immunity and the development of infections and inflammation, and activation of the Src-dependent Smad3 signaling pathway mediates neutrophil inflammation and oxidative stress (Li et al., 2015). In this study, QJHTD (0.5 g/L) was shown to inhibit the phosphorylation of Src in the LPS-activated neutrophils (**Figure 9**).

DISCUSSION

ALI is a diffuse inflammatory response of the lung caused by various internal and external pathogenic factors, which is clinically characterized by respiratory distress and refractory hypoxemia followed by respiratory failure, and with a mortality of approximately 40% (Kallet and Haas, 2003; Matthay and Zemans, 2011). Uncontrolled inflammatory response caused by various immune cells, inflammatory mediators, and cytokines is the main pathophysiological basis of ALI (Tang et al., 2009). Neutrophils play a significant role in the innate immune system. They can quickly migrate to the inflammatory site and digest and destroy the invading pathogenic microorganisms (Nauseef and Borregaard, 2014; Leiding, 2017). Some studies have demonstrated neutrophils exert an important part in the pathogenesis of ALI (Chen et al., 2018; Tsai et al., 2018; Kinnare et al., 2022). Neutrophils play a core role in the initiation, propagation, and resolution of this complex inflammatory environment by migrating to the lungs and performing various proinflammatory functions. These include release of threshing and bactericidal proteins, release of cytokines and ROS, and production of NETs (Potey et al., 2019; Yang et al., 2021).

QJHTD is a classic prescription for the treatment of pulmonary inflammation, and its beneficial effects have been clinically proven. Studies have demonstrated that QJHTD has an obvious effect in the treatment of ALI (Zhang, 2021). Major components of QJHTD such as baicalin (Ding et al., 2016), baicalein (Jiang et al., 2022), wogonin (Takagi et al., 2014), wogonoside (Zhang et al., 2014), geniposide (Xiaofeng et al., 2012), glycyrrhizic acid (Zhao et al., 2016), and platycodin D (Tao et al., 2015) showed good therapeutic effects on ALI. Furthermore, baicalein has been found to inhibit neutrophil respiratory burst activity and its ROS production (Reina et al., 2013). In neutrophils, activated by *N*-Formyl-Met-Leu-Phe (fMLF) or PMA, both baicalein and baicalin effectively blocked the assembly of NADPH oxidase and inhibit the activity of MPO and downregulated the expression of Mac-1, thereby reducing neutrophil adhesion (Shen et al., 2003). Wogonin and wogonoside have also been shown to effectively suppress neutrophil inflammatory activity by inhibiting neutrophil entry into the airways (Takagi et al., 2014) and lung tissue (Zhang et al., 2014; Yeh et al., 2016).

Based on the network pharmacology results, the key targets with higher degree values of the compound–target–pathway network included MAPK14, CDK2, EGFR, F2, SRC, AKT1, and so on. The p38 MAPKs signaling pathway plays an important role in regulating neutrophil activation, especially endotoxin stimulation (Li et al., 2021). In addition, it was demonstrated that MAPK14 was highly expressed in the tissues of ALI mice, and silencing MAPK14 could alleviate ALI symptoms by downregulating inflammatory cytokines (Pan et al., 2019). Inhibition of CDK2 could be used to control neutrophil numbers at the sites of infection or injury, potentially preventing neutrophil-mediated excessive inflammation (Hsu et al., 2019). In lung tissue, EGFR is widely expressed in epithelial cells, and EGFR activation can recruit neutrophils, promoting the secretion of antibacterial peptides and elimination of pathogenic microorganisms (Burgel and Nadel, 2008). EGFR is also involved in regulating the expression of IL-8, thereby promoting the adhesion of neutrophils (Hamilton et al., 2003). Treatment with EGFR inhibitors, such as erlotinib, AG1478, and 451 effectively reduced inflammatory cell infiltration and relieved lung injury in the ALI animal models (Shan et al., 2017; Tao et al., 2019). The Src family consists of non-receptor tyrosine kinases with nine members in total, namely, Src, Fyn, Yes, Yrk, Blk, Fgr, Hck, Lck, and Lyn (Okutani et al., 2006). Several key neutrophil functions are regulated by Src kinases, such as adhesion-dependent degranulation of neutrophils requires the Fgr and Hck (Mócsai et al., 1999). Activation of Src-dependent Smad3 signaling mediates neutrophilic inflammation and oxidative stress in hyperoxia-augmented ventilator-induced lung injury (Li et al., 2015). Studies have shown that bletinib and resveratrol ameliorate neutrophil inflammation and lung injury *via* inhibition of Src family kinases (Tsai et al., 2019; Kao et al., 2021). AKT1 gene deletion can promote neutrophil apoptosis,

attenuate neutrophil influx into the lungs of mice, and diminish the expression of proinflammatory factors in bronchoalveolar lavage fluid after intratracheal administration of low-molecular-mass hyaluronan (Zhao et al., 2018). It has also been reported that AKT1 expressed by neutrophils is downregulated during bacterial infection and neutrophil activation, and in the mouse models of ALI and *S. aureus* infection, AKT1 deficiency resulted in severe disease progression with concomitant neutrophil recruitment and enhanced antimicrobial activity, and the AKT1-STAT1 signaling axis may negatively regulate neutrophil recruitment and activation in these ALI mice (Liu et al., 2013). CLLV-1, an AKT inhibitor targeting AKT Cys310, showed potent anti-inflammatory activity in human neutrophils and LPS-induced mouse ALI (Chen et al., 2019).

The top 20 targets with higher degree values of the compound–target–pathway network were selected for molecular docking experiments. The result of molecular docking showed that baicalin, oroxylin A-7-glucuronide, hispidulin-7-O-β-D-glucuronide, wogonoside, baicalein, wogonin, and mangiferin bound with most target proteins. These flavonoids might be the main effective ingredients of QJHTD in the treatment of ALI. The anti-inflammatory mechanism and much more biological activities of baicalein, baicalin, wogonoside, wogonin, and mangiferin have been reported (Chen et al., 2009; Ku and Bae, 2015; Lee et al., 2015a; Qu et al., 2017), such as mangiferin anti-inflammatory by inhibiting the MAPK pathways (Jeong et al., 2014; Suchal et al., 2016; Liu et al., 2019). Wogonin protects against endotoxin-induced ALI *via* reduction of p38 MAPK and JNK phosphorylation (Wei et al., 2017). Components such as baicalin, oroxylin A-7-glucuronide, wogonoside, baicalein, and wogonin are characterized by potential pharmacologically activity in the treatment of virus related to lung inflammation (Li et al., 2011). Meanwhile, both baicalin and wogonin inhibited thrombin-catalyzed fibrin polymerization and platelet functions, prolonged PTT and PT significantly, and inhibited the activities and production of thrombin and FXa (Ku and Bae, 2014; Lee et al., 2015b). The result of molecular docking and SPR experiments suggested that compounds of baicalein, wogonin, and baicalin have a strong affinity with thrombin protein. In the animal models of ALI, plasma and lavage fluid thrombin content elevated evidently (Lou et al., 2019; Arroyo et al., 2021; Kaspi et al., 2021). Neutrophils were shown to be effector cells mediating lung vascular injury after thrombin-induced intravascular coagulation (Malik and Horgan, 1987). Meanwhile, neutrophils were found in large numbers in thrombi within thrombi in injured mice, suggesting that neutrophils are crucial for pathological thrombosis (Brill et al., 2012; Martinod et al., 2013). Moreover, neutrophil binding to endothelial cells was inhibited by ICAM-1 or LFA-1 inhibitors; thus, thrombosis was reduced in mice (Darbousset et al., 2012). In particular, extracellular DNA and histones have been reported to induce thrombin activation *in vitro* (Fuchs et al., 2010; Semeraro et al., 2011), and NETs have been identified in the experimental models of deep-vein thrombosis (De Boer et al., 2013). In *E. coli* induced sepsis, inhibition of NETs attenuates intravascular coagulation and end-organ damage, and blocking NET-induced intravascular coagulation restores microvascular perfusion (McDonald et al., 2017). As mentioned previously, there is a close correlation between thrombin and neutrophils, especially NETs.

GO enrichment analysis of the interactive targets has shown that the biological processes engaged in QJHTD for ALI mainly involved protein phosphorylation, response to wounding, response to bacterium, regulation of inflammatory response, and so on. Molecular functions analysis revealed protein serine/threonine/tyrosine kinase activity, endopeptidase activity, nitric-oxide synthase regulator activity, and phosphatase binding. In terms of cellular components, GO enrichment analysis involved vesicle lumen, extracellular matrix, and platelet alpha granule. More and more studies implicated the potential role of platelet mediators in the pathogenesis and progression of ALI (Looney et al., 2009; Lê et al., 2015; Yasui et al., 2016).

The result of KEGG pathway analysis included neutrophil extracellular trap formation. NETs are a network structure comprising DNA backbone, granule components, histones, and neutrophil elastase and other bactericidal proteins that are released into the extracellular space after neutrophils are stimulated and activated and named this process NETosis (Brinkmann et al., 2004). NETs are a double-edged sword. On the one hand, they can immobilize or trap and kill invading pathogens, exert antimicrobial effects, and facilitate inflammation subsidence, and it is an innate response against pathogen invasion and plays an important role in host defense (Brinkmann, 2018; Petretto et al., 2019; Hilscher and Shah, 2020). However, excessive formation or insufficient clearance can not only directly cause tissue damage but also recruit other proinflammatory cells or proteins, promote the release of inflammatory factors, and further expand inflammatory response (Luo et al., 2014).

For the past few years, NETs have been well-documented in the ALI (Saffarzadeh et al., 2012; Luo et al., 2014; Liu et al., 2016; Gan et al., 2018). Studies have found that NETs are closely related to the damage degree of alveolar epithelial and endothelial cells and the concentration of inflammatory mediators, suggesting that NETs may play an important role in the pathological process of ALI (Saffarzadeh et al., 2012; Luo et al., 2014). Bacteria, viruses, fungi, activated platelets, PMA, and IL-8 can activate neutrophils to generate NETs (Narasaraju et al., 2011; Carestia et al., 2016). We isolated neutrophils from rat peripheral blood, induced neutrophils by PMA, and verified that QJHTD inhibited the formation of NETs by SYTOX Green plate reader assay, fluorescence microscopy, and immunofluorescence stain. These experiments documented that QJHTD inhibited the formation of PMA-stimulated NETs. There are two main pathways for the formation of NETs: pyrolysis NET formation dependent on NADPH oxidase and non-pyrolysis NET formation independent of NADPH oxidase (Chen et al., 2021). PMA activates protein kinase C, which in turn stimulates the production of ROS by activating NADPH oxidase (Fuchs et al., 2007; De Bont et al., 2018; Fousert et al., 2020). DCFH-DA and DHR123 were used as a probe to quantify ROS production, and it was found that QJHTD reduced ROS production during the formation of NETs. Based on the result of *in vitro* experiments, we can speculate that QJHTD plays a crucial role in the treatment of ALI by inhibiting NETs.

CONCLUSION

In this study, 22 prototype compounds of QJHTD absorbed into rat blood were combined with the network pharmacology investigation, molecular docking, and experimental validation to elucidate the mechanism of QJHTD against ALI. According to the results, baicalin, oroxylin A-7-glucuronide, hispidulin-7-O-β-D-glucuronide, wogonoside, baicalein, wogonin, tianshic acid, and mangiferin were identified as the vital active compounds, and CDK2, EGFR, AKT1, F2, SRC, and MAPK14 were considered the major targets. SPR experiments also confirmed that baicalein, wogonin, and baicalin have a strong affinity with thrombin protein and might exert thrombosis prevention in ALI to some extent. Western blot experiments demonstrated that QJHTD inhibited Src phosphorylation in LPS-activated neutrophils evidently. Sytox green plate reader assay, fluorescence microscopy, and immunofluorescence stain validated that QJHTD inhibited the formation of PMA-stimulated NETs. This study revealed the active compounds, effective targets, and potential pharmacological mechanisms of QJHTD acting on ALI.

DATA AVAILABILITY STATEMENT

The original contributions presented in the study are included in the article/**Supplementary Material**. Further inquiries can be directed to the corresponding authors.

ETHICS STATEMENT

The animal study was reviewed and approved by the Animal Care and Use Committee of Institute of Chinese Materia Medica, China Academy of Chinese Medical Sciences (No. 2020B114).

AUTHOR CONTRIBUTIONS

YY, TZ, and SX contributed conception and design of the study; SX, LL, XL, JX, XY, ZG, XY, and FL performed the experiments; SX, LL, and ZS analyzed and interpreted the data; YY and SX wrote the manuscript. All authors contributed to manuscript revision and approved the submission.

FUNDING

This work was supported by Scientific and Technological Innovation Project of China Academy of Chinese Medical Sciences (CI 2021A04616), TCM the Belt and Road Cooperation Project (GH201918), and State Major Projects on New Drug Innovation (No. 2018ZX09721004-006-003).

SUPPLEMENTARY MATERIAL

The Supplementary Material for this article can be found online at: https://www.frontiersin.org/articles/10.3389/fphar.2022.891889/full#supplementary-material

REFERENCES

Arroyo, A. B., Fernández-Pérez, M. P., Del Monte, A., Águila, S., Méndez, R., Hernández-Antolín, R., et al. (2021). miR-146a Is a Pivotal Regulator of Neutrophil Extracellular Trap Formation Promoting Thrombosis. *Haematologica* 106, 1636–1646. doi:10.3324/haematol.2019.240226

Brill, A., Fuchs, T. A., Savchenko, A. S., Thomas, G. M., Martinod, K., De Meyer, S. F., et al. (2012). Neutrophil Extracellular Traps Promote Deep Vein Thrombosis in Mice. *J. Thromb. Haemost.* 10, 136–144. doi:10.1111/j.1538-7836.2011.04544.x

Brinkmann, V. (2018). Neutrophil Extracellular Traps in the Second Decade. *J. Innate Immun.* 10, 414–421. doi:10.1159/000489829

Brinkmann, V., Reichard, U., Goosmann, C., Fauler, B., Uhlemann, Y., Weiss, D. S., et al. (2004). Neutrophil Extracellular Traps Kill Bacteria. *Science* 303 (5663), 1532–1535. doi:10.1126/science.1092385

Burgel, P. R., and Nadel, J. A. (2008). Epidermal Growth Factor Receptor-Mediated Innate Immune Responses and Their Roles in Airway Diseases. *Eur. Respir. J.* 32, 1068–1081. doi:10.1183/09031936.00172007

Carestia, A., Kaufman, T., and Schattner, M. (2016). Platelets: New Bricks in the Building of Neutrophil Extracellular Traps. *Front. Immunol.* 7, 271. doi:10.3389/fimmu.2016.00271

Chen, C. Y., Tsai, Y. F., Huang, W. J., Chang, S. H., and Hwang, T. L. (2018). Propofol Inhibits Endogenous Formyl Peptide-Induced Neutrophil Activation and Alleviates Lung Injury. *Free Radic. Biol. Med.* 129, 372–382. doi:10.1016/j.freeradbiomed.2018.09.048

Chen, K., Shao, L. H., Wang, F., Shen, X. F., Xia, X. F., Kang, X., et al. (2021). Netting Gut Disease: Neutrophil Extracellular Trap in Intestinal Pathology. *Oxid. Med. Cell Longev.* 2021, 5541222. doi:10.1155/2021/5541222

Chen, L., Du, J., Dai, Q., Zhang, H., Pang, W., and Hu, J. (2014). Prediction of Anti-tumor Chemical Probes of a Traditional Chinese Medicine Formula by HPLC Fingerprinting Combined with Molecular Docking. *Eur. J. Med. Chem.* 83, 294–306. doi:10.1016/j.ejmech.2014.06.037

Chen, P. J., Ko, I. L., Lee, C. L., Hu, H. C., Chang, F. R., Wu, Y. C., et al. (2019). Targeting Allosteric Site of AKT by 5,7-Dimethoxy-1,4-Phenanthrenequinone Suppresses Neutrophilic Inflammation. *EBioMedicine* 40, 528–540. doi:10.1016/j.ebiom.2019.01.043

Chen, Y., Lu, N., Ling, Y., Gao, Y., Wang, L., Sun, Y., et al. (2009). Wogonoside Inhibits Lipopolysaccharide-Induced Angiogenesis *In Vitro* and *In Vivo* via Toll-like Receptor 4 Signal Transduction. *Toxicology* 259, 10–17. doi:10.1016/j.tox.2009.01.010

Chen, Y., Feng, C. L., Li, G. M., Ge, D. Y., Wang, J., Li, C. Y., et al. (2016). Qingjinhuatan Decoction Adjusting Chronic Obstructive Pulmonary Model Rat in Airway Mucus Hypersecretion by Neutrophil Elastase and Mucin 5AC. *Jilin J. Tradit. Chin. Med.* 36 (1), 65–71. doi:10.13463/j.cnki.jlzyy.2016.01.018

Darbousset, R., Thomas, G. M., Mezouar, S., Frère, C., Bonier, R., Mackman, N., et al. (2012). Tissue Factor-Positive Neutrophils Bind to Injured Endothelial Wall and Initiate Thrombus Formation. *Blood* 120, 2133–2143. doi:10.1182/blood-2012-06-437772

De Boer, O. J., Li, X., Teeling, P., Mackaay, C., Ploegmakers, H. J., Van Der Loos, C. M., et al. (2013). Neutrophils, Neutrophil Extracellular Traps and Interleukin-17 Associate with the Organisation of Thrombi in Acute Myocardial Infarction. *Thromb. Haemost.* 109, 290–297. doi:10.1160/TH12-06-0425

De Bont, C. M., Koopman, W. J. H., Boelens, W. C., and Pruijn, G. J. M. (2018). Stimulus-dependent Chromatin Dynamics, Citrullination, Calcium Signalling and ROS Production during NET Formation. *Biochim. Biophys. Acta Mol. Cell Res.* 1865, 1621–1629. doi:10.1016/j.bbamcr.2018.08.014

Ding, X. M., Pan, L., Wang, Y., and Xu, Q. Z. (2016). Baicalin Exerts Protective Effects against Lipopolysaccharide-Induced Acute Lung Injury by Regulating the Crosstalk between the CX3CL1-CX3CR1 axis and NF-κB Pathway in CX3CL1-Knockout Mice. *Int. J. Mol. Med.* 37 (3), 703–715. doi:10.3892/ijmm.2016.2456

Fousert, E., Toes, R., and Desai, J. (2020). Neutrophil Extracellular Traps (NETs) Take the Central Stage in Driving Autoimmune Responses. *Cells* 9 (4), 915. doi:10.3390/cells9040915

Fuchs, T. A., Abed, U., Goosmann, C., Hurwitz, R., Schulze, I., Wahn, V., et al. (2007). Novel Cell Death Program Leads to Neutrophil Extracellular Traps. *J. Cell Biol.* 176 (2), 231–241. doi:10.1083/jcb.200606027

Fuchs, T. A., Brill, A., Duerschmied, D., Schatzberg, D., Monestier, M., Myers, D. D., et al. (2010). Extracellular DNA Traps Promote Thrombosis. *Proc. Natl. Acad. Sci. U. S. A.* 107 (36), 15880–15885. doi:10.1073/pnas.1005743107

Gan, T., Yang, Y., Hu, F., Chen, X., Zhou, J., Li, Y., et al. (2018). TLR3 Regulated Poly I:C-Induced Neutrophil Extracellular Traps and Acute Lung Injury Partly through P38 MAP Kinase. *Front. Microbiol.* 9, 3174. doi:10.3389/fmicb.2018.03174

Hamilton, L. M., Torres-Lozano, C., Puddicombe, S. M., Richter, A., Kimber, I., Dearman, R. J., et al. (2003). The Role of the Epidermal Growth Factor Receptor in Sustaining Neutrophil Inflammation in Severe Asthma. *Clin. Exp. Allergy* 33 (2), 233–240. doi:10.1046/j.1365-2222.2003.01593.x

Hilscher, M. B., and Shah, V. H. (2020). Neutrophil Extracellular Traps and Liver Disease. *Semin. Liver Dis.* 40 (2), 171–179. doi:10.1055/s-0039-3399562

Hopkins, A. L. (2008). Network Pharmacology: the Next Paradigm in Drug Discovery. *Nat. Chem. Biol.* 4 (11), 682–690. doi:10.1038/nchembio.118

Hsu, A. Y., Wang, D., Liu, S., Lu, J., Syahirah, R., Bennin, D. A., et al. (2019). Phenotypical microRNA Screen Reveals a Noncanonical Role of CDK2 in Regulating Neutrophil Migration. *Proc. Natl. Acad. Sci. U. S. A.* 116 (37), 18561–18570. doi:10.1073/pnas.1905221116

Huang, S. Y., Grinter, S. Z., and Zou, X. (2010). Scoring Functions and Their Evaluation Methods for Protein-Ligand Docking: Recent Advances and Future Directions. *Phys. Chem. Chem. Phys.* 12 (40), 12899–12908. doi:10.1039/c0cp00151a

Jeong, J. J., Jang, S. E., Hyam, S. R., Han, M. J., and Kim, D. H. (2014). Mangiferin Ameliorates Colitis by Inhibiting IRAK1 Phosphorylation in NF-κB and MAPK Pathways. *Eur. J. Pharmacol.* 740, 652–661. doi:10.1016/j.ejphar.2014.06.013

Jiang, C., Zhang, J., Xie, H., Guan, H., Li, R., Chen, C., et al. (2022). Baicalein Suppresses Lipopolysaccharide-Induced Acute Lung Injury by Regulating Drp1-dependent Mitochondrial Fission of Macrophages. *Biomed. Pharmacother.* 145, 112408. doi:10.1016/j.biopha.2021.112408

Kallet, R. H., Liu, K., and Tang, J. (2003). Management of Acidosis during Lung-Protective Ventilation in Acute Respiratory Distress Syndrome. *Respir. Care Clin. N. Am.* 9, 437–456. xvii-xviii. doi:10.1016/s1078-5337(03)00034-0

Kao, T. I., Chen, P. J., Wang, Y. H., Tseng, H. H., Chang, S. H., Wu, T. S., et al. (2021). Bletinib Ameliorates Neutrophilic Inflammation and Lung Injury by Inhibiting Src Family Kinase Phosphorylation and Activity. *Br. J. Pharmacol.* 178 (20), 4069–4084. doi:10.1111/bph.15597

Kaspi, H., Semo, J., Abramov, N., Dekel, C., Lindborg, S., Kern, R., et al. (2021). MSC-NTF (NurOwn®) Exosomes: a Novel Therapeutic Modality in the Mouse LPS-Induced ARDS Model. *Stem Cell Res. Ther.* 12 (1), 72. doi:10.1186/s13287-021-02143-w

Kim, S. (2016). Getting the Most Out of PubChem for Virtual Screening. *Expert Opin. Drug Discov.* 11 (9), 843–855. doi:10.1080/17460441.2016.1216967

Kinnare, N., Hook, J. S., Patel, P. A., Monson, N. L., and Moreland, J. G. (2022). Neutrophil Extracellular Trap Formation Potential Correlates with Lung Disease Severity in COVID-19 Patients. *Inflammation* 45 (2), 800–811. doi:10.1007/s10753-021-01585-x

Kolaczkowska, E., and Kubes, P. (2013). Neutrophil Recruitment and Function in Health and Inflammation. *Nat. Rev. Immunol.* 13 (3), 159–175. doi:10.1038/nri3399

Ku, S. K., and Bae, J. S. (2014). Antithrombotic Activities of Wogonin and Wogonoside via Inhibiting Platelet Aggregation. *Fitoterapia* 98, 27–35. doi:10.1016/j.fitote.2014.07.006

Ku, S. K., and Bae, J. S. (2015). Baicalin, Baicalein and Wogonin Inhibits High Glucose-Induced Vascular Inflammation *In Vitro* and *In Vivo*. *BMB Rep.* 48 (9), 519–524. doi:10.5483/bmbrep.2015.48.9.017

Lê, V. B., Schneider, J. G., Boergeling, Y., Berri, F., Ducatez, M., Guerin, J. L., et al. (2015). Platelet Activation and Aggregation Promote Lung Inflammation and Influenza Virus Pathogenesis. *Am. J. Respir. Crit. Care Med.* 191 (7), 804–819. doi:10.1164/rccm.201406-1031OC

Lee, H. S., Moon, C., Lee, H. W., Park, E. M., Cho, M. S., and Kang, J. L. (2007). Src Tyrosine Kinases Mediate Activations of NF-kappaB and Integrin Signal during Lipopolysaccharide-Induced Acute Lung Injury. *J. Immunol.* 179, 7001–7011. doi:10.4049/jimmunol.179.10.7001

Lee, W., Ku, S. K., and Bae, J. S. (2015a). Anti-inflammatory Effects of Baicalin, Baicalein, and Wogonin *In Vitro* and *In Vivo*. *Inflammation* 38 (1), 110–125. doi:10.1007/s10753-014-0013-0

Lee, W., Ku, S. K., and Bae, J. S. (2015b). Antiplatelet, Anticoagulant, and Profibrinolytic Activities of Baicalin. *Arch. Pharm. Res.* 38 (5), 893–903. doi:10.1007/s12272-014-0410-9

Leiding, J. W. (2017). Neutrophil Evolution and Their Diseases in Humans. *Front. Immunol.* 8, 1009. doi:10.3389/fimmu.2017.01009

Li, C., Lin, G., and Zuo, Z. (2011). Pharmacological Effects and Pharmacokinetics Properties of Radix Scutellariae and its Bioactive Flavones. *Biopharm. Drug Dispos.* 32 (8), 427–445. doi:10.1002/bdd.771

Li, C., Liu, J. H., Su, J., Lin, W. J., Zhao, J. Q., Zhang, Z. H., et al. (2021). LncRNA XIST Knockdown Alleviates LPS-Induced Acute Lung Injury by Inactivation of XIST/miR-132-3p/MAPK14 Pathway: XIST Promotes ALI via miR-132-3p/MAPK14 axis. *Mol. Cell Biochem.* 476 (12), 4217–4229. doi:10.1007/s11010-021-04234-x

Li, L. F., Lee, C. S., Liu, Y. Y., Chang, C. H., Lin, C. W., Chiu, L. C., et al. (2015). Activation of Src-Dependent Smad3 Signaling Mediates the Neutrophilic Inflammation and Oxidative Stress in Hyperoxia-Augmented Ventilator-Induced Lung Injury. *Respir. Res.* 16 (1), 112. doi:10.1186/s12931-015-0275-6

Li, L. Q., and Jiang, C. C. (2018). Influence of Qingjin Huatan Decoction Combined with Levofloxacin on White Blood Cell Count, C Reactive Protein Level and Immune Function in Patients with Klebsiellar Pneumonia. *J. Emerg. Tradit. Chin. Med.* 27 (03), 429–431. doi:10.3969/j.issn.1004-745X.2018.03.015

Li, Q. Q., Yang, Y. X., Qv, J. W., Hu, G., Hu, Y. J., Xia, Z. N., et al. (2018). Investigation of Interactions between Thrombin and Ten Phenolic Compounds by Affinity Capillary Electrophoresis and Molecular Docking. *J. Anal. Methods Chem.* 2018, 4707609. doi:10.1155/2018/4707609

Li, S., and Zhang, B. (2013). Traditional Chinese Medicine Network Pharmacology: Theory, Methodology and Application. *Chin. J. Nat. Med.* 11 (2), 110–120. doi:10.1016/S1875-5364(13)60037-0

Liu, G., Bi, Y., Wang, R., Shen, B., Zhang, Y., Yang, H., et al. (2013). Kinase AKT1 Negatively Controls Neutrophil Recruitment and Function in Mice. *J. Immunol.* 191 (5), 2680–2690. doi:10.4049/jimmunol.1300736

Liu, J. T., Zhao, H. P., Zhu, Q., Zhang, H. B., Li, X. Y., Han, Y. Q., et al. (2022). Study on Critical Quality Attributes of Qingjin Huatan Tang Based on Serum Pharmacochemistry. *China J. Chin. Materia Med.* 47 (05), 1392–1402. doi:10.19540/j.cnki.cjcmm.20211122.201

Liu, K., Wang, F., Wang, S., Li, W. N., and Ye, Q. (2019). Mangiferin Attenuates Myocardial Ischemia-Reperfusion Injury via MAPK/Nrf-2/HO-1/NF-*κB In Vitro* and *In Vivo*. *Oxid. Med. Cell Longev.* 2019, 7285434. doi:10.1155/2019/7285434

Liu, L., Ma, H., Yang, N., Tang, Y., Guo, J., Tao, W., et al. (2010). A Series of Natural Flavonoids as Thrombin Inhibitors: Structure-Activity Relationships. *Thromb. Res.* 126 (5), e365–78. doi:10.1016/j.thromres.2010.08.006

Liu, S., Su, X., Pan, P., Zhang, L., Hu, Y., Tan, H., et al. (2016). Neutrophil Extracellular Traps Are Indirectly Triggered by Lipopolysaccharide and Contribute to Acute Lung Injury. *Sci. Rep.* 6, 37252. doi:10.1038/srep37252

Liu, X., Ouyang, S., Yu, B., Liu, Y., Huang, K., Gong, J., et al. (2010). PharmMapper Server: a Web Server for Potential Drug Target Identification Using Pharmacophore Mapping Approach. *Nucleic Acids Res.* 38, W609–W614. doi:10.1093/nar/gkq300

Looney, M. R., Nguyen, J. X., Hu, Y., Van Ziffle, J. A., Lowell, C. A., and Matthay, M. A. (2009). Platelet Depletion and Aspirin Treatment Protect Mice in a Two-Event Model of Transfusion-Related Acute Lung Injury. *J. Clin. Invest.* 119 (11), 3450–3461. doi:10.1172/JCI38432

Lou, J., Hu, Y., Wu, M. D., Che, L. Q., Wu, Y. F., Zhao, Y., et al. (2019). Endothelial Cell-specific Anticoagulation Reduces Inflammation in a Mouse Model of Acute Lung Injury. *Acta Pharmacol. Sin.* 40 (6), 769–780. doi:10.1038/s41401-018-0175-7

Luo, L., Zhang, S., Wang, Y., Rahman, M., Syk, I., Zhang, E., et al. (2014). Proinflammatory Role of Neutrophil Extracellular Traps in Abdominal Sepsis. *Am. J. Physiol. Lung Cell Mol. Physiol.* 307 (7), L586–L596. doi:10.1152/ajplung.00365.2013

Malik, A. B., and Horgan, M. J. (1987). Mechanisms of Thrombin-Induced Lung Vascular Injury and Edema. *Am. Rev. Respir. Dis.* 136 (2), 467–470. doi:10.1164/ajrccm/136.2.467

Martinod, K., Demers, M., Fuchs, T. A., Wong, S. L., Brill, A., Gallant, M., et al. (2013). Neutrophil Histone Modification by Peptidylarginine Deiminase 4 Is Critical for Deep Vein Thrombosis in Mice. *Proc. Natl. Acad. Sci. U. S. A.* 110 (21), 8674–8679. doi:10.1073/pnas.1301059110

Matthay, M. A., Ware, L. B., and Zimmerman, G. A. (2012). The Acute Respiratory Distress Syndrome. *J. Clin. Invest.* 122 (8), 2731–2740. doi:10.1172/JCI60331

Matthay, M. A., and Zemans, R. L. (2011). The Acute Respiratory Distress Syndrome: Pathogenesis and Treatment. *Annu. Rev. Pathol.* 6, 147–163. doi:10.1146/annurev-pathol-011110-130158

McDonald, B., Davis, R. P., Kim, S. J., Tse, M., Esmon, C. T., Kolaczkowska, E., et al. (2017). Platelets and Neutrophil Extracellular Traps Collaborate to Promote Intravascular Coagulation during Sepsis in Mice. *Blood* 129 (10), 1357–1367. doi:10.1182/blood-2016-09-741298

Mócsai, A., Ligeti, E., Lowell, C. A., and Berton, G. (1999). Adhesion-dependent Degranulation of Neutrophils Requires the Src Family Kinases Fgr and Hck. *J. Immunol.* 162 (2), 1120–1126. doi:10.0000/PMID9916742

Nadon, A. S., and Schmidt, E. P. (2014). "Pathobiology of the Acute Respiratory Distress Syndrome," in *Pathobiology of Human Disease*, 2665–2676. doi:10.1016/B978-0-12-386456-7.05309-0

Narasaraju, T., Yang, E., Samy, R. P., Ng, H. H., Poh, W. P., Liew, A. A., et al. (2011). Excessive Neutrophils and Neutrophil Extracellular Traps Contribute to Acute Lung Injury of Influenza Pneumonitis. *Am. J. Pathol.* 179 (1), 199–210. doi:10.1016/j.ajpath.2011.03.013

Nauseef, W. M., and Borregaard, N. (2014). Neutrophils at Work. *Nat. Immunol.* 15 (7), 602–611. doi:10.1038/ni.2921

Nguyen, H. H., Park, J., Kang, S., and Kim, M. (2015). Surface Plasmon Resonance: a Versatile Technique for Biosensor Applications. *Sensors (Basel)* 15 (5), 10481–10510. doi:10.3390/s150510481

Okutani, D., Lodyga, M., Han, B., and Liu, M. (2006). Src Protein Tyrosine Kinase Family and Acute Inflammatory Responses. *Am. J. Physiol. Lung Cell Mol. Physiol.* 291 (2), L129–L141. doi:10.1152/ajplung.00261.2005

Olaru, A., Bala, C., Jaffrezic-Renault, N., and Aboul-Enein, H. Y. (2015). Surface Plasmon Resonance (SPR) Biosensors in Pharmaceutical Analysis. *Crit. Rev. Anal. Chem.* 45 (2), 97–105. doi:10.1080/10408347.2014.881250

Pan, W., Wei, N., Xu, W., Wang, G., Gong, F., and Li, N. (2019). MicroRNA-124 Alleviates the Lung Injury in Mice with Septic Shock through Inhibiting the Activation of the MAPK Signaling Pathway by Downregulating MAPK14. *Int. Immunopharmacol.* 76, 105835. doi:10.1016/j.intimp.2019.105835

Patching, S. G. (2014). Surface Plasmon Resonance Spectroscopy for Characterisation of Membrane Protein-Ligand Interactions and its Potential for Drug Discovery. *Biochim. Biophys. Acta* 1838, 43–55. doi:10.1016/j.bbamem.2013.04.028

Patel, V. J., Biswas Roy, S., Mehta, H. J., Joo, M., and Sadikot, R. T. (2018). Alternative and Natural Therapies for Acute Lung Injury and Acute Respiratory Distress Syndrome. *Biomed. Res. Int.* 2018, 2476824. doi:10.1155/2018/2476824

Petretto, A., Bruschi, M., Pratesi, F., Croia, C., Candiano, G., Ghiggeri, G., et al. (2019). Neutrophil Extracellular Traps (NET) Induced by Different Stimuli: A Comparative Proteomic Analysis. *PLoS One* 14 (7), e0218946. doi:10.1371/journal.pone.0218946

Potey, P. M., Rossi, A. G., Lucas, C. D., and Dorward, D. A. (2019). Neutrophils in the Initiation and Resolution of Acute Pulmonary Inflammation: Understanding Biological Function and Therapeutic Potential. *J. Pathol.* 247 (5), 672–685. doi:10.1002/path.5221

Prabowo, B. A., Purwidyantri, A., and Liu, K. C. (2018). Surface Plasmon Resonance Optical Sensor: A Review on Light Source Technology. *Biosens. (Basel)* 8 (3), 80. doi:10.3390/bios8030080

Qu, S., Wang, W., Li, D., Li, S., Zhang, L., Fu, Y., et al. (2017). Mangiferin Inhibits Mastitis Induced by LPS via Suppressing NF-κB and NLRP3 Signaling Pathways. *Int. Immunopharmacol.* 43, 85–90. doi:10.1016/j.intimp.2016.11.036

Reina, E., Al-Shibani, N., Allam, E., Gregson, K. S., Kowolik, M., and Windsor, L. J. (2013). The Effects of Plantago Major on the Activation of the Neutrophil Respiratory Burst. *J. Tradit. Complement. Med.* 3 (4), 268–272. doi:10.4103/2225-4110.119706

Richardson, J. S., Richardson, D. C., and Goodsell, D. S. (2021). Seeing the PDB. *J. Biol. Chem.* 296, 100742. doi:10.1016/j.jbc.2021.100742

Saffarzadeh, M., Juenemann, C., Queisser, M. A., Lochnit, G., Barreto, G., Galuska, S. P., et al. (2012). Neutrophil Extracellular Traps Directly Induce Epithelial and Endothelial Cell Death: a Predominant Role of Histones. *PLoS One* 7 (2), e32366. doi:10.1371/journal.pone.0032366

Saikia, S., and Bordoloi, M. (2019). Molecular Docking: Challenges, Advances and its Use in Drug Discovery Perspective. *Curr. Drug Targets* 20 (5), 501–521. doi:10.2174/1389450119666181022153016

Semeraro, F., Ammollo, C. T., Morrissey, J. H., Dale, G. L., Friese, P., Esmon, N. L., et al. (2011). Extracellular Histones Promote Thrombin Generation through Platelet-dependent Mechanisms: Involvement of Platelet TLR2 and TLR4. *Blood* 118 (7), 1952–1961. doi:10.1182/blood-2011-03-343061

Shan, X., Zhang, Y., Chen, H., Dong, L., Wu, B., Xu, T., et al. (2017). Inhibition of Epidermal Growth Factor Receptor Attenuates LPS-Induced Inflammation and Acute Lung Injury in Rats. *Oncotarget* 8 (16), 26648–26661. doi:10.18632/oncotarget.15790

Shen, Y. C., Chiou, W. F., Chou, Y. C., and Chen, C. F. (2003). Mechanisms in Mediating the Anti-inflammatory Effects of Baicalin and Baicalein in Human Leukocytes. *Eur. J. Pharmacol.* 465, 171–181. doi:10.1016/s0014-2999(03)01378-5

Shi, Y., Shi, H., Nieman, D. C., Hu, Q., Yang, L., Liu, T., et al. (2019). Lactic Acid Accumulation during Exhaustive Exercise Impairs Re Lease of Neutrophil Extracellular Traps in Mice. *Front. Physiol.* 10, 709. doi:10.3389/fphys.2019.00709

Suchal, K., Malik, S., Gamad, N., Malhotra, R. K., Goyal, S. N., Ojha, S., et al. (2016). Mangiferin Protect Myocardial Insults through Modulation of MAPK/TGF-beta Pathways. *Eur. J. Pharmacol.* 776, 34–43. doi:10.1016/j.ejphar.2016.02.055

Takagi, R., Kawano, M., Nakagome, K., Hashimoto, K., Higashi, T., Ohbuchi, K., et al. (2014). Wogonin Attenuates Ovalbumin Antigen-Induced Neutrophilic Airway Inflammation by Inhibiting Th17 Differentiation. *Int. J. Inflam.* 2014, 571508. doi:10.1155/2014/571508

Tang, B. M., Craig, J. C., Eslick, G. D., Seppelt, I., and Mclean, A. S. (2009). Use of Corticosteroids in Acute Lung Injury and Acute Respiratory Distress Syndrome: a Systematic Review and Meta-Analysis. *Crit. Care Med.* 37 (5), 1594–1603. doi:10.1097/CCM.0b013e31819fb507

Tao, H., Li, N., Zhang, Z., Mu, H., Meng, C., Xia, H., et al. (2019). Erlotinib Protects LPS-Induced Acute Lung Injury in Mice by Inhibiting EGFR/TLR4 Signaling Pathway. *Shock* 51 (1), 131–138. doi:10.1097/SHK.0000000000001124

Tao, W., Su, Q., Wang, H., Guo, S., Chen, Y., Duan, J., et al. (2015). Platycodin D Attenuates Acute Lung Injury by Suppressing Apoptosis and Inflammation *In Vivo* and *In Vitro*. *Int. Immunopharmacol.* 27 (1), 138–147. doi:10.1016/j.intimp.2015.05.005

Toumpanakis, D., Vassilakopoulou, V., Sigala, I., Zacharatos, P., Vraila, I., Karavana, V., et al. (2017). The Role of Src & ERK1/2 Kinases in Inspiratory Resistive Breathing Induced Acute Lung Injury and Inflammation. *Respir. Res.* 18, 209. doi:10.1186/s12931-017-0694-7

Tsai, Y. F., Chen, C. Y., Chang, W. Y., Syu, Y. T., and Hwang, T. L. (2019). Resveratrol Suppresses Neutrophil Activation via Inhibition of Src Family Kinases to Attenuate Lung Injury. *Free Radic. Biol. Med.* 145, 67–77. doi:10.1016/j.freeradbiomed.2019.09.021

Tsai, Y. F., Yang, S. C., Chang, W. Y., Chen, J. J., Chen, C. Y., Chang, S. H., et al. (2018). Garcinia Multiflora Inhibits FPR1-Mediated Neutrophil Activation and Protects against Acute Lung Injury. *Cell Physiol. Biochem.* 51 (6), 2776–2793. doi:10.1159/000495970

Uniprot Consortium (2018). UniProt: the Universal Protein Knowledgebase. *Nucleic Acids Res.* 46 (5), 2699. doi:10.1093/nar/gky092

Wang, X., Pan, C., Gong, J., Liu, X., and Li, H. (2016). Enhancing the Enrichment of Pharmacophore-Based Target Prediction for the Polypharmacological Profiles of Drugs. *J. Chem. Inf. Model* 56 (6), 1175–1183. doi:10.1021/acs.jcim.5b00690

Wang, X., Shen, Y., Wang, S., Li, S., Zhang, W., Liu, X., et al. (2017). PharmMapper 2017 Update: a Web Server for Potential Drug Target Identification with a Comprehensive Target Pharmacophore Database. *Nucleic Acids Res.* 45 (W1), W356–W360. doi:10.1093/nar/gkx374

Wei, C. Y., Sun, H. L., Yang, M. L., Yang, C. P., Chen, L. Y., Li, Y. C., et al. (2017). Protective Effect of Wogonin on Endotoxin-Induced Acute Lung Injury via Reduction of P38 MAPK and JNK Phosphorylation. *Environ. Toxicol.* 32 (2), 397–403. doi:10.1002/tox.22243

Wood, C., Kataria, V., and Modrykamien, A. M. (2020). The Acute Respiratory Distress Syndrome. *Proc. (Bayl Univ. Med. Cent.* 33 (3), 357–365. doi:10.1080/08998280.2020.1764817

Wu, G., Robertson, D. H., Brooks, C. L., 3rd., and Vieth, M. (2003). Detailed Analysis of Grid-Based Molecular Docking: A Case Study of CDOCKER—A CHARMm-Based MD Docking Algorithm. *J. Comput. Chem.* 24 (13), 1549–1562. doi:10.1002/jcc.10306

Wu, L. A., Zhao, M., and Xu, G. L. (2019). Effect of Qingjin Huatan Tang on COPD of Rat Inflammatory Response by Regulating Autophagy. *Chin. J. Exp. Tradit. Med. Formulae* 25 (18), 30–35. doi:10.13422/j.cnki.syfjx.20191801

Xiaofeng, Y., Qinren, C., Jingping, H., Xiao, C., Miaomiao, W., Xiangru, F., et al. (2012). Geniposide, an Iridoid Glucoside Derived from Gardenia Jasminoides, Protects against Lipopolysaccharide-Induced Acute Lung Injury in Mice. *Planta Med.* 78 (6), 557–564. doi:10.1055/s-0031-1298212

Yang, S. C., Tsai, Y. F., Pan, Y. L., and Hwang, T. L. (2021). Understanding the Role of Neutrophils in Acute Respiratory Distress Syndrome. *Biomed. J.* 44 (4), 439–446. doi:10.1016/j.bj.2020.09.001

Yasui, H., Donahue, D. L., Walsh, M., Castellino, F. J., and Ploplis, V. A. (2016). Early Coagulation Events Induce Acute Lung Injury in a Rat Model of Blunt Traumatic Brain Injury. *Am. J. Physiol. Lung Cell Mol. Physiol.* 311 (1), L74–L86. doi:10.1152/ajplung.00429.2015

Yeh, Y. C., Yang, C. P., Lee, S. S., Horng, C. T., Chen, H. Y., Cho, T. H., et al. (2016). Acute Lung Injury Induced by Lipopolysaccharide Is Inhibited by Wogonin in Mice via Reduction of Akt Phosphorylation and RhoA Activation. *J. Pharm. Pharmacol.* 68 (2), 257–263. doi:10.1111/jphp.12500

Zhang, L., Ren, Y., Yang, C., Guo, Y., Zhang, X., Hou, G., et al. (2014). Wogonoside Ameliorates Lipopolysaccharide-Induced Acute Lung Injury in Mice. *Inflammation* 37 (6), 2006–2012. doi:10.1007/s10753-014-9932-z

Zhang, Q. L. (2021). *Biological Activity Evaluation of the Famous Classical Formulae Qing-Jin-Hua-Tan-Decoction*. Beijing: China Academy of Chinese Medical Sciences. Master's thesis. doi:10.27658/d.cnki.gzzyy.2021.000188

Zhang, Q. L., Li, Y., Xiao, S. P., and You, Y. (2021). Advance in Study on Classic Prescription Qingjin Huatantang. *Chin. J. Exp. Tradit. Med. Formulae* 27 (3), 198–207. doi:10.13422/j.cnki.syfjx.20202301

Zhao, H., Ma, Y., and Zhang, L. (2018). Low-molecular-mass Hyaluronan Induces Pulmonary Inflammation by Up-Regulation of Mcl-1 to Inhibit Neutrophil Apoptosis via PI3K/Akt1 Pathway. *Immunology* 155 (3), 387–395. doi:10.1111/imm.12981

Zhao, H., Zhao, M., Wang, Y., Li, F., and Zhang, Z. (2016). Glycyrrhizic Acid Prevents Sepsis-Induced Acute Lung Injury and Mortality in Rats. *J. Histochem Cytochem* 64 (2), 125–137. doi:10.1369/0022155415610168

Zhou, Y., Zhou, B., Pache, L., Chang, M., Khodabakhshi, A. H., Tanaseichuk, O., et al. (2019). Metascape Provides a Biologist-Oriented Resource for the Analysis of Systems-Level Datasets. *Nat. Commun.* 10 (1), 1523. doi:10.1038/s41467-019-09234-6

Conflict of Interest: The authors declare that the research was conducted in the absence of any commercial or financial relationships that could be construed as a potential conflict of interest.

Publisher's Note: All claims expressed in this article are solely those of the authors and do not necessarily represent those of their affiliated organizations, or those of the publisher, the editors and the reviewers. Any product that may be evaluated in this article, or claim that may be made by its manufacturer, is not guaranteed or endorsed by the publisher.

frontiers | Frontiers in Immunology

TYPE Original Research
PUBLISHED 26 July 2022
DOI 10.3389/fimmu.2022.943554

OPEN ACCESS

EDITED BY
Tsong-Long Hwang,
Chang Gung University, Taiwan

REVIEWED BY
Heng Chi,
Ocean University of China, China
Matthias Bartneck,
University Hospital RWTH Aachen, Germany

*CORRESPONDENCE
Sangwoon Chung
Sangwoon.chung@osumc.edu

SPECIALTY SECTION
This article was submitted to Inflammation, a section of the journal Frontiers in Immunology

RECEIVED 13 May 2022
ACCEPTED 01 July 2022
PUBLISHED 26 July 2022

CITATION
Kim JY, Stevens P, Karpurapu M, Lee H, Englert JA, Yan P, Lee TJ, Pabla N, Pietrzak M, Park GY, Christman JW and Chung S (2022) Targeting ETosis by miR-155 inhibition mitigates mixed granulocytic asthma lung Inflammation. *Front. Immunol.* 13:943554. doi: 10.3389/fimmu.2022.943554

Targeting ETosis by miR-155 inhibition mitigates mixed granulocytic asthmatic lung inflammation

Ji Young Kim[1,2], Patrick Stevens[3], Manjula Karpurapu[1], Hyunwook Lee[1], Joshua A. Englert[1], Pearlly Yan[4], Tae Jin Lee[5], Navjot Pabla[2], Maciej Pietrzak[3], Gye Young Park[6], John W. Christman[1] and Sangwoon Chung[1]*

[1]Division of Pulmonary, Critical Care, and Sleep Medicine, Department of Internal Medicine, Ohio State University Wexner Medical Center, Davis Heart and Lung Research Institute, Columbus, OH, United States, [2]Division of Pharmaceutics and Pharmacology, College of Pharmacy and Comprehensive Cancer Center, The Ohio State University, Columbus, OH, United States, [3]Comprehensive Cancer Center, Biomedical Informatics Shared Resources, The Ohio State University College of Medicine, Columbus, OH, United States, [4]Comprehensive Cancer Center, Division of Hematology, Department of Internal Medicine, The Ohio State University College of Medicine, Columbus, OH, United States, [5]Department of Neurosurgery, McGovern Medical School, University of Texas Health Science Center at Houston, Houston, TX, United States, [6]Section of Pulmonary, Critical Care, and Sleep Medicine, Department of Medicine, University of Illinois at Chicago, Chicago, IL, United States

Asthma is phenotypically heterogeneous with several distinctive pathological mechanistic pathways. Previous studies indicate that neutrophilic asthma has a poor response to standard asthma treatments comprising inhaled corticosteroids. Therefore, it is important to identify critical factors that contribute to increased numbers of neutrophils in asthma patients whose symptoms are poorly controlled by conventional therapy. Leukocytes release chromatin fibers, referred to as extracellular traps (ETs) consisting of double-stranded (ds) DNA, histones, and granule contents. Excessive components of ETs contribute to the pathophysiology of asthma; however, it is unclear how ETs drive asthma phenotypes and whether they could be a potential therapeutic target. We employed a mouse model of severe asthma that recapitulates the intricate immune responses of neutrophilic and eosinophilic airway inflammation identified in patients with severe asthma. We used both a pharmacologic approach using miR-155 inhibitor-laden exosomes and genetic approaches using miR-155 knockout mice. Our data show that ETs are present in the bronchoalveolar lavage fluid of patients with mild asthma subjected to experimental subsegmental bronchoprovocation to an allergen and a severe asthma mouse model, which resembles the complex immune responses identified in severe human asthma. Furthermore, we show that miR-155 contributes to the extracellular release of dsDNA, which exacerbates allergic lung inflammation, and the inhibition of miR-155 results in therapeutic benefit in severe asthma mice. Our findings show that targeting dsDNA release represents an attractive therapeutic target for

mitigating neutrophilic asthma phenotype, which is clinically refractory to standard care.

KEYWORDS

asthmatic inflammation, neutrophilic asthma phenotype, extracellular trap, miR-155, exosome delivery

Introduction

Over the last two decades, asthma incidence in the United States has increased from 5.5% to 7.8% of the general population and is a major health concern for patients and medical professionals (CDC, Most Recent National Asthma Data, 2019). Asthma is the most common chronic inflammatory disease with several characterized endotypes and phenotypes (1–3). Pathophysiologic mechanisms in asthma and treatment strategies are determined by inflammatory phenotypes (4). Unlike the relatively well-defined mechanisms that result in type 2 high eosinophilic asthma inflammation, those leading to non-type 2 high mixed neutrophilic/eosinophilic asthma are poorly understood, and the specific treatments based on molecular pathogenesis are yet to be developed. Although only 10% of asthmatics are categorized as mixed cellular (5), they account for nearly 200,000 hospitalizations and 3,500 deaths per year in the United States (6). Non-type 2 severe asthma is poorly responsive to corticosteroid therapy, compared to the highly steroid-responsive type 2 eosinophilic asthma (7). Recent evidence indicates that asthma exacerbations resulting from excessive activation of the innate immune responses are manifested as airway neutrophilia, although details of the mechanism are not fully elucidated (8–10). Given the frequency, severity, and disability associated with the neutrophilic or mixed cellular asthma phenotypes, it is crucial to identify molecular mechanisms that contribute to mixed cellular asthma that is poorly responsive to conventional therapy.

Although several mediators have been implicated in neutrophil recruitment to the airways (9, 11, 12), these have not proven to be pivotal in the pathogenesis of neutrophilic and/or mixed neutrophilic/eosinophilic asthma, indicating that there are gaps in our knowledge of the immune response in the airways of those with severe asthma. Therefore, it is important to identify critical factors contributing to increased neutrophils in asthmatic airways of these refractory phenotypes. To understand the complex immune responses of severe human asthma, it is imperative to develop a mouse model of severe asthma that displays mixed granulocytic infiltrates in the airways (7). Although no ideal mouse model provides a comprehensive nature of severe human asthma (13), our model is characterized by mixed eosinophilic and neutrophilic inflammation, which is ideal for determining mechanisms and potential therapeutic targets in corticosteroid-refractory severe asthma.

Neutrophils have an important role in innate defense mechanisms. However, in asthma, airway neutrophils have been associated with disease severity and acute exacerbations (14). Elevated sputum eosinophils and neutrophils are associated with the lowest lung function in asthma (15–17). Specifically, the interaction of eosinophils and neutrophils is associated with a greater decline in lung function compared to any single inflammatory pathway in severe asthma (17). Th1/IFN-γ and Th17/IL-17 pathways play critical roles in neutrophil recruitment to the lungs in both neutrophilic and mixed neutrophilic/eosinophilic severe asthma (18–20). The bacterial second messenger cyclic (c)-di-GMP has been shown to be a mucosal adjuvant that induces a Th1–Th17 response (21, 22). Upon activation, neutrophils release chromatin fibers, referred to as extracellular traps (ETs), consisting of host double-stranded (ds)DNA, histones, and granule contents (23). Web-like structure ETs have antimicrobial defense activity by ensnaring microbes in a sticky matrix of extracellular chromatin and bactericidal proteins (24) but also have physiologic and pathologic roles in asthmatic airways (25–27). Although multiple lines of evidence showed that ETs released by activated neutrophils and eosinophils increase asthma severity (26, 28, 29), the mechanisms by which ETs influence the progression of mixed neutrophilic/eosinophilic severe asthma have not yet been defined.

Our study shows that ETs were released in the bronchoalveolar lavage fluid (BALF) of patients with asthma who underwent subsegmental bronchoprovocation with allergen (SBP-AG) challenge. In a murine asthma model that resembles the complex immune responses identified in severe human asthma, we observed that microRNA (miR)-155 regulates the release of ETs, which is associated with the severity of allergic immune responses. Using a serum-derived exosome-based oligonucleotide delivery system, we blocked the release of ETs *in vivo* and attenuated the severity of allergic lung inflammation in the mouse model. Our results provide strong pre-clinical evidence that targeting host dsDNA release is an effective therapeutic approach for mitigating mixed neutrophilic/

eosinophilic asthma lung inflammation and alleviating severe airway hyperresponsiveness.

Materials and methods

Detailed methods are described in the Supplementary Material.

Subsegmental bronchoprovocation with allergen bronchoscopy protocol

This protocol was approved by the Institutional Review Board (IRB) of the University of Illinois (Chicago, IL, USA), and an investigational new drug (IND) was obtained from the Food and Drug Administration (FDA) for bronchoscopic administration of allergens to volunteers. The details of the protocol were described in our previous publication (30, 31). In brief, we recruited study subjects who are on step 1 asthma therapy according to the National Asthma Education and Prevention Program (NAEPP) Asthma Guidelines. After informed consent was obtained, subjects underwent screening for inclusion and exclusion criteria, which included skin prick testing for dust mite, short ragweed, and cockroach allergens. Once the screening was complete, BAL was performed per standard research guidelines approved by the IRB. Pre-challenge BAL samples were obtained right before SBP-AG. At 48 h after the SBP-AG, post-challenge BAL samples were obtained from the allergen exposed, at the adjacent and contralateral subsegment. The maximum challenge dose for SBP-AG was 5 ml of 100 binding antibody units (BAU)/ml or 1:2,000 wt/vol concentration of allergen. The mean age of the UIC was 24 (range 18–36), and the male-to-female ratios were 2:4.

Mice

C57BL/6, miR-155KO (007745), and PAD4KO mice (030315) were purchased from the Jackson Laboratories (Bar Harbor, ME, USA). Myeloid miR-155 knockout mice and miR-$155^{fl/fl}$ mice (026700) were crossed with LysM-cre mice (004781, Jackson Laboratories, Bar Harbor, ME, USA) to homozygosity (miR-$155^{fl/fl}$LysMcre). Littermates were used as controls. DNA extraction and genotyping were performed as described previously (32). Unless otherwise stated, mice at age-matched 8 to 12 weeks were used in this study.

Induction of murine asthma model

We used the published triple-allergen (DRA)-induced mouse asthma model with minor modifications (30, 33, 34). DRA mixture includes extracts of dust mite (*Dermatophagoides farina*, 830 μg/ml), ragweed (*Ambrosia artemisiifolia*, 8.34 mg/ml), and *Aspergillus fumigatus* (830 μg/ml; Stallergenes Greer, Lenoir, NC, USA). Mice were sensitized with the DRA allergen mixture on days 0 and 5 by intranasal (i.n.) injection. Seven days later (day 12), mice were challenged with DRA mixture (200 μg) at the same concentration used for sensitization in 20 μl of saline once daily for 3 days/week for 4 weeks. Twenty-four hours following the final challenge, mice were sacrificed, and BALF and lung tissues were collected for further analysis. All sensitized animals had elevated levels of total IgE.

In the severe asthma model, mice were sensitized with DRA (100 μg) and cyclic-di-GMP (c-di-GMP) (5 μg; Tocris, Minneapolis, MN, USA) intranasally on days 0 and 5. Seven days later (day 12), mice were subjected to three challenge sets involving three consecutive challenges with DRA (100 μg) and c-di-GMP (0.5 μg) with a rest of 4 days in between challenge sets (7). Mice were then euthanized, and features of allergic airway inflammation were assessed, 24 h following the final challenge. The schematic of this model is shown in Figure 1A.

Delivery of small RNA-loaded exosomes *in vivo*

Serum exosomes were isolated according to the manufacturer's protocol (Thermo Fisher Scientific, Waltham, MA, USA). Nanoparticle tracking analysis was performed to determine the size and concentration of serum exosomes (NanoSight NS300). Modified calcium-mediated transfection was used to introduce small RNAs, including the miR-155 inhibitor (catalog no. MSTUD0080, Sigma, St. Louis, MO, USA) and inhibitor control (catalog no. NCSTUD001, Sigma) into serum exosomes (35). To deliver small RNAs into serum exosomes, 100 pmol of small RNA was loaded into 100 μg of serum EXOs quantified by protein content (36). For *in vivo* experiments, small RNA-loaded exosomes in 30 μl of saline were i.n. instilled into the mouse lung 30 min before the challenge at 3 weeks. One day after the last instillation, mice were sacrificed, and the cellular profile in the BALF was evaluated.

Measurements of airway hyperresponsiveness

Mechanical properties of the mouse lung were assessed in mice anesthetized with ketamine/xylazine using the forced oscillation technique as previously described (34). Anesthetized mice were mechanically ventilated on a FlexiVent computer-controlled ventilator (SCIREQ, Montreal, QC, Canada) with 8 ml/kg tidal volume at a frequency of 150 breaths/min and 2–3 cmH_2O positive end-expiratory pressure. Continuous EKG and pulse oximetry monitoring (Starr Life Sciences, Oakmont, PA, USA) was performed. Pressure and flow

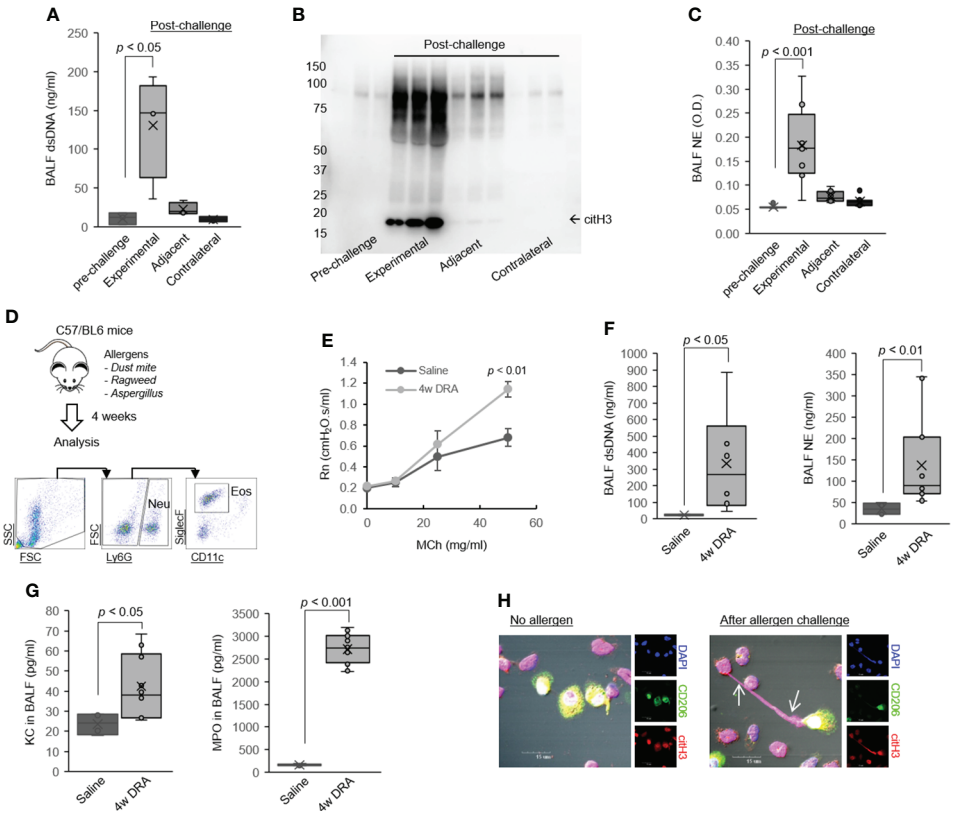

FIGURE 1
Leukocytes released ET-derived host dsDNA in asthma. **(A)** PicoGreen assays of extracellular dsDNA in the BALF samples obtained pre- and post-allergen challenge in the subsegmental bronchoprovocation with allergen (SBP-AG) protocol (N = 3). **(B)** Western immunoblot for citH3 in BALF samples obtained pre- and post–allergen challenge in the SBP-AG protocol. **(C)** NE from BALF in the SBP-AG protocol. **(D)** Mice were sensitized and challenged by daily intranasal (i.n.) administration of DRA or saline, 3 days a week for 4 weeks. Cell staining for markers of neutrophils ($CD45^+Ly6G^+$) and eosinophils ($CD45^+Ly6G^-SiglecF^+CD11c^-$). **(E)** Airway hyperresponsiveness (AHR) in mice subjected to the 4 weeks triple allergen asthma model. Shown are central airway resistance (Newtonian resistance, Rn) values. **(F)** Concentration of extracellular dsDNA and NE in the BALF of mice subjected to triple allergen asthma model (N = 6). **(G)** The level of neutrophil chemokine KC and MPO in BALF from DRA-induced asthmatic mice (N = 6). **(H)** Representative confocal microscopy images of lung macrophages from allergen-exposed mice producing ETs with co-expression of citH3 (arrow). Blue, staining for DNA; red, citH3; green, macrophages. Graphs were plotted as mean ± SE. p-Values were obtained using a two-tailed Student's t-test. BALF, bronchoalveolar lavage fluid; ET, extracellular trap; NE, neutrophil elastase; MPO, myeloperoxidase.

data (reflective of the airway and tissue dynamics) were used to calculate lung resistance, static lung compliance, and dynamic lung compliance at baseline with the use of the single-compartment and constant phase model. Standardized recruitment maneuvers were performed prior to each physiologic measurement to prevent atelectasis and standardize volume history. Maximal airway responsiveness was measured following exposure to increasing doses of nebulized methacholine (MCh) (0–50 mg/ml).

DsDNA measurement in bronchoalveolar lavage fluid

DsDNA was measured in the acellular fraction of the BALF, which was obtained after a double centrifugation and supernatant collection. Levels of dsDNA were determined with Quant-iT PicoGreen dsDNA reagent (Invitrogen, Carlsbad, CA, USA) according to the manufacturer's protocol. For immunoblot analysis for citH3 to detect ETs, anti-citH3 (ab5103, Abcam, Cambridge, UK) was used.

Single-cell RNA sequencing

Single cells were obtained from asthma lung tissues by mechanical and enzymatic dissociation (33). After enzymatic digestion, the cells were placed in an inactivation buffer (Roswell Park Memorial Institute (RPMI) 1640 + 10% fetal bovine serum (FBS)) and filtered to remove any remaining tissue, the filtrate was centrifuged at 300*g*, the cell pellet was suspended in red blood cell (RBC) lysis buffer and resuspended in inactivation

buffer, and viability was determined to be 85%–95% before submitting for approximately 0.75 to 1 × 10^5 cells for single-cell RNA sequencing (scRNA-seq) analysis. Library preparation was carried out using 10x Genomics Chromium controller (10x Genomics). Chromium 10x Genomics single-cell library was sequenced as 150 base pair single-end reads on an Illumina NovaSeq 6000 (Illumina, Inc., San Diego, CA, USA), with cells from each of the two microchips sequenced across three flow cell lanes.

Bioinformatics analysis for next-generation sequencing data

Single-cell data in feature-barcode matrices were processed using Cell Ranger 6.0.0 (37) using the GRCm38 (mm10) genome (downloaded March 2021 refdata-gex-mm10-2020-A build from10x) to identify unsupervised cell clusters. The data were natural log transformed and normalized for scaling the sequencing depth to a total of 1e4 molecules per cell, followed by regressing out the number of UMI using Seurat 4.0.4 (38). Briefly, cells were selected based on RNA content thresholds: greater than 300 RNA features, less than 2,000 unique expressed genes (nFeature_RNA), and mitochondrial gene content less than 25% using the "subset" function. Preprocessed data from the six samples were integrated using the Seurat function, the FindIntegrationAnchors function, and IntegrateData using 20 principal components as default parameters normalized with NormalizeData function. The variable features were found with FindVariableFeatures function using 2,000 features. After scaling and principal component analysis (PCA) normalization with default parameters, clustering was performed using Seurat functions FindNeighbors and FindClusters functions using 20 PCs at resolution of 0.8 with the Louvain algorithm. The identified clusters were then visualized using Uniform Manifold Approximation and Projection (UMAP) embedding using 20 PCs. The feature plots were generated using Seurat function FeaturePlot using the RNA assay. Module score was calculated from inputting genes using the Seurat-implemented function AddModuleScore and generated using the FeaturePlot function as described (38). The average expression levels of each cluster at the single-cell level are subtracted by the aggregated expression of random control feature sets (200 by default). For dot plot figures, normalized expression values were generated using NormalizeData function from the RNA assay after splitting clusters by condition. This would create a matrix of natural log-normalized gene expression with a scaling factor of 10,000. The size of the circle represents the number of cells in the cluster when the gene was detected. z-Score dot plots were generated using raw expression data using the scale function in Seurat dot plot function. Pathway enrichment analysis for lymphocyte clusters was performed using Ingenuity Pathway Analysis (IPA) (39). Raw data for IPA analysis was found using Seurat implemented function FindAllMarkers using parameters: only.pos = FALSE, min.pct = 0.2, thresh.use = 0.2. IPA pathway z-score of greater than 2 is considered activated, while a score of less than −2 is considered an inhibited pathway. Canonical Pathway figures were generated using ggplot2 [https://cran.r-project.org/web/packages/ggplot2/citation.html] in R. Functional enrichment analysis by cluster was performed using enrichR [https://maayanlab.cloud/Enrichr/] DEenrichRPlot function using the Gene ontology (GO) 2021 pathways and Kyoto Encyclopedia of Genes and Genomes (KEGG) 2019 mouse databases [https://www.genome.jp/kegg/kegg1.html].

Statistical analysis

Data were represented as box-and-whisker plots unless otherwise noted. Results were expressed as means ± SE. A comparison between two groups was performed with Student's *t*-test for unpaired variables. Statistical significance is indicated in figure legends. A $p < 0.05$ was considered statistically significant.

Results

Leukocytes release extracellular trap-derived dsDNA in asthma

ETs have been shown to be present in the airways of asthmatics (25, 26). High expression of ETs-derived dsDNA correlates with airway neutrophilia and epithelial cell damage and is related to mucus production (5, 9). Consistent with these findings, our data show that leukocyte-released ET-derived dsDNA presents in BALF of volunteers with asthma who were experimentally challenged with allergens (Figure 2A). As illustrated, there was a dramatic increase in extracellular dsDNA in the allergen-challenged site compared with the pre-challenge or contralateral post-challenge sites, with a significantly lower level in the immediate subsegment adjacent to the allergen-challenged site. To confirm that the extracellular dsDNA is derived from ETosis, we measured hyper-citrullinated histone H3 (citH3), a characteristic of ETs. CitH3 was present in the post-challenged sites, the highest at the experimental site (Figure 2B). Consistent with this finding, neutrophil elastase (NE) was also higher in the allergen-challenged site (Figure 2C).

We also observed an increase in BALF dsDNA and NE levels in a murine model of chronic asthma (Figure 2F), in which mice were challenged with the common triple allergen DRA (dust mite, ragweed, and *Aspergillus*) for 4 weeks as our group previously reported (Figure 2D) (33). As shown, neutrophils (Neu, $CD45^+Ly6G^+$) and eosinophils (Eos, $CD45^+Ly6G^-SiglecF^+CD11c^-$) were detected in the airways of allergen-challenged mice (Figure 2D), with was associated with accentuated MCh-induced airway

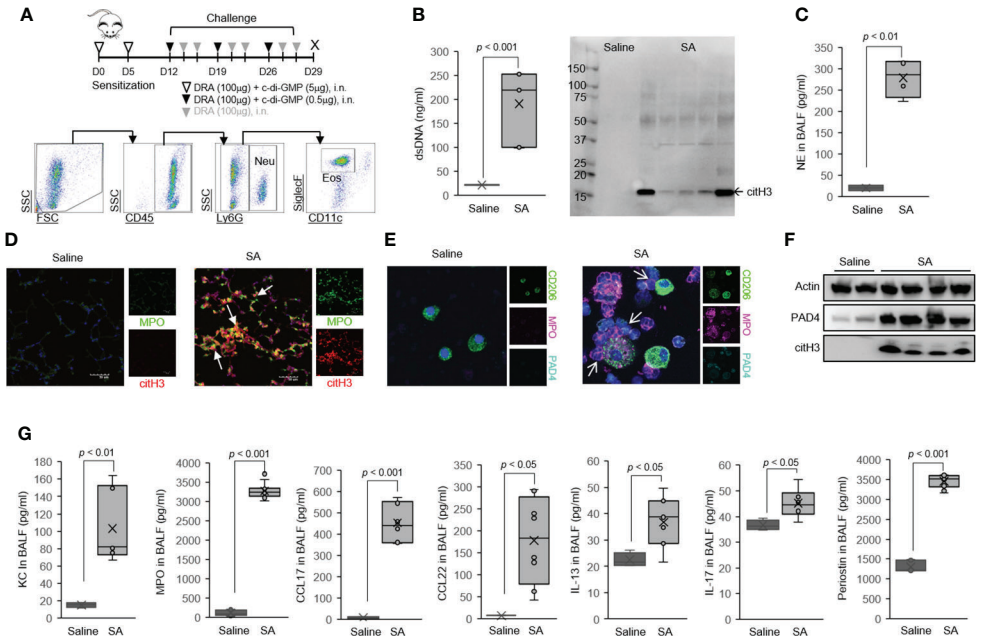

FIGURE 2
Host dsDNA release was greatly increased in the airways of severe asthma (SA) mice. **(A)** Schematics of the mouse model of SA used in the study. Mice were sensitized and challenged with c-di-GMP and DRA for 3 weeks, and BALF was collected on day 29. Representative gating strategy outlining airway neutrophils and eosinophils in SA mice. **(B)** PicoGreen assay and Western immunoblot for citH3 showing ET-associated DNA present in BALF. **(C)** NE in the BALF of mice in the SA model. **(D)** We observed amorphous, unshaped, extracellular DNA structures that colocalized with citH3 (red) and MPO (green) in severe asthma mouse lungs, as identified by immunofluorescence. **(E)** Representative confocal microscopy images of BAL cells from SA mice producing MPO with co-expression of PAD4 (arrow). Blue, staining for DNA; purple, MPO; green, macrophages; cyan, PAD4. **(F)** Expression of PAD4 as determined by Western immunoblot. **(G)** The level of neutrophil chemokine chemokines and cytokines in BALF from SA mice (N = 6). Graphs were plotted as mean ± SE. p-Values were obtained using a two-tailed Student's t-test. ET, extracellular trap; BALF, bronchoalveolar lavage fluid; NE, neutrophil elastase.

responsiveness (Figure 2E). Notably, the levels of neutrophil chemokine CXCL1 (also known as Gro-α in humans and KC in mice) and myeloperoxidase (MPO), a surrogate marker of increased neutrophils, were significantly increased in BALF from the allergen-challenged mice compared to saline-challenged control (Figure 2G). Finally, we detected extracellular DNA structures that prominently colocalized with citH3 in pulmonary macrophages and granulocytes from the mouse model of asthma (Figure 1H, arrows). These data indicate that recruited leukocytes, neutrophils and eosinophils, are the major cellular source of dsDNA in the asthmatic airways in humans and mice.

Host dsDNA release is significantly increased in the airways of severe asthma mice

Airway neutrophilia is one of the hallmarks of acute exacerbation or severe subgroups of asthma (14). In order to address this important clinically relevant issue, we employed a mouse model of severe asthma that recapitulates the intricate immune responses of neutrophilic and eosinophilic airway inflammation identified in patients with severe asthma (16, 17, 40). In this severe asthma model (hereafter, SA model), mice are sensitized to the three allergens (DRA) along with c-di-GMP followed by 1 week of rest and then 3 weeks of intranasal challenge (Figure 1A) (7). A key feature of this model is increased numbers of eosinophils and neutrophils in BAL samples that were characterized by flow cytometry. In this model, the recruited neutrophils underwent ETosis in the lung, as evidenced by increased BALF dsDNA, citH3, and NE (Figures 1B, C). Using immunofluorescence microscopy, we observed amorphous and unshaped structures colocalized with citH3 and MPO in severe asthma mouse lungs (Figure 1D). Peptidyl arginine deiminase 4 (PAD4) has been shown to be involved in ETosis by hyper-citrullination of histones (5). Notably, high-resolution confocal microscopy indicated the presence of MPO/PAD4-positive neutrophils in the BAL cells of the severe asthma mice (Figure 1E), indicating that recruited neutrophils are a cellular source of dsDNA and citH3 in severe asthmatic airways. The level of PAD4 protein was much higher in the whole lung tissue of the severe asthma mice than in the

saline-treated control (Figure 1F) along with high levels of BAL-KC and BAL-MPO in the severe asthma mice (Figure 1G).

Neutrophils and eosinophils were increased in BAL fluids of the mice subjected to the SA model, compared with saline-challenged control (Supplementary Figures 1A, B), but the SA model had fewer BAL eosinophils compared to the triple allergen (DRA)-only model (Supplementary Figure 2). The DRA/c-di-GMP challenge significantly induced the expression of genes associated with Th2 and Th17 immune responses (including *Il13*, *Il17*, *Ifng*, *Kc*, and *Muc5a/c*) compared to the saline-treated control (Supplementary Figure 1C). Periodic acid-Schiff (PAS) staining detected that mucus glycol conjugates of goblet cells were also increased in the severe asthma mice (Supplementary Figure 1D). Of note, the severe asthma mice had highly increased bronchial hyper-reactivity to MCh (Supplementary Figure 1E), compared to that of the triple allergen (DRA)-only model (Figure 2E). Total serum IgE and the levels of BALF Th2 cytokines/chemokines such as CCL17, CCL22, IL-13, IL-17, and periostin were elevated in the severe asthma mice compared to the saline-treated control (Figure 1G).

MiR-155 is involved in extracellular trap formation in severe asthma

Recent studies indicate that miR-155 plays an indispensable role in Th1/Th2/Th17 immune responses (41, 42). In this study, we hypothesized that miR-155 is involved in ETs formation and related cellular functions in macrophages. We observed that lungs and sorted alveolar macrophages (AMs) from the severe asthma mice contained higher levels of miR-155 than those derived from the saline-treated control (Figure 3A and Supplementary Figure 2B). Of interest, the myeloid cell-specific miR-155-deficient mice (miR-155$^{fl/fl}$LysM-cre) showed a reduction in extracellular dsDNA level in BALF as compared to control littermates (miR-155$^{fl/fl}$) at a steady state (Supplementary Figures 3A–C). However, there was no difference in BAL cell numbers (Supplementary Figure 3D).

When mice were subjected to the SA model, miR-155 whole-body deficiency (miR-155KO mice) significantly decreased the total number of BAL cells (Figure 3B) with a marked reduction in BAL eosinophil and neutrophil counts compared with that in

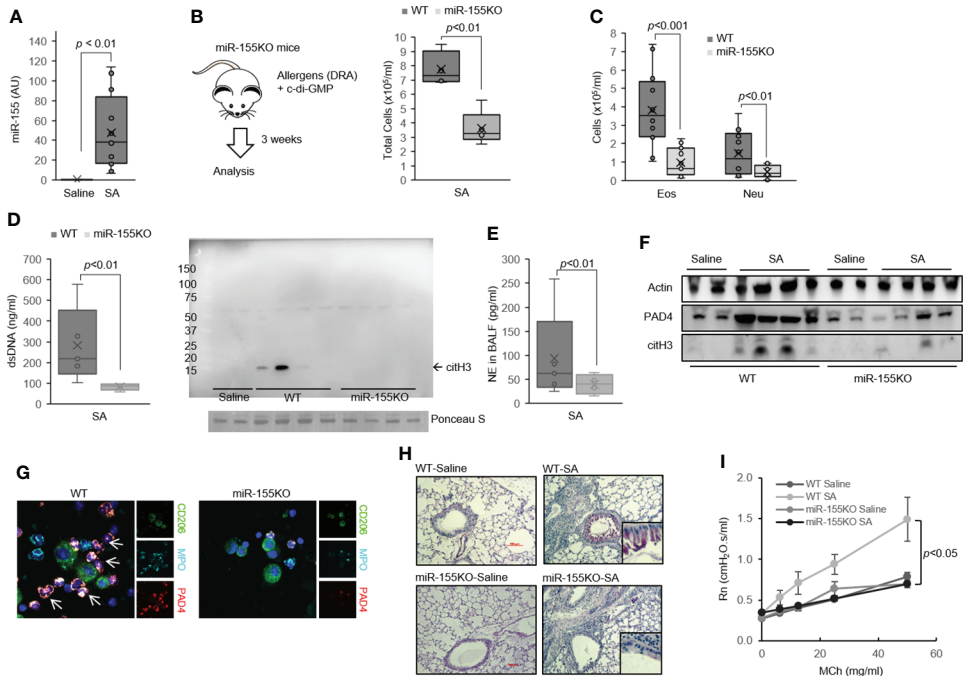

FIGURE 3
MiR-155 is involved in ET formation in severe asthma (SA). **(A)** Expression of miR-155 in lung from SA mice (N = 3–5). **(B)** Total cells and **(C)** leukocyte differentials were counted in the BALF of the mouse model of SA used in the study (N = 6-8). **(D)** PicoGreen assay and Western immunoblot for citH3 showing ET-associated DNA present in BALF. **(E)** NE in the BALF from WT and miR-155KO mice (N = 5). **(F)** PAD4 and citH3 proteins as determined by Western immunoblotting from SA mouse lung. **(G)** Representative confocal microscopy images of BAL cells from SA mice producing MPO with co-expression of PAD4 (arrow). Blue, staining for DNA; cyan, MPO; green, macrophages; red, PAD4. **(H)** PAS-stained sections from WT (top) and miR-155KO (bottom) mouse lungs subjected to the SA model. Boxed regions are shown enlarged at right. **(I)** Airway hyperresponsiveness (AHR) in WT and miR-155KO mice subjected to the SA model. Graphs were plotted as mean ± SE. p-Values were obtained using a two-tailed Student's t-test. ET, extracellular trap; BALF, bronchoalveolar lavage fluid; NE, neutrophil elastase; MPO, myeloperoxidase; PAS, periodic acid-Schiff; WT, wild type.

wild-type (WT) mice (Figure 3C). Furthermore, the miR-155KO mice had markedly reduced cell-free dsDNA (Figure 3D) and NE (Figure 3E) in BAL fluids, which are characteristics of ETosis. Consistent with these findings, miR-155KO mouse lungs subjected to the SA model had decreased PAD4 and citH3 expressions (Figure 3F). This lower propensity of the miR-155KO mice to ETosis in severe asthma seems to be associated with a decreased number of PAD4-positive neutrophils in BALF (Figure 3G). Together, these findings indicate that miR-155 regulates ETosis and is pivotal to neutrophilic lung inflammation such as severe asthma.

The miR-155KO mice subjected to the SA model had significantly decreased mRNA levels of characteristic genes involved in eosinophilic (*Il4*, *Il13*, *Ccl17*, and *Muc5a/c*) and neutrophilic (*Il17*, *Mmp12*, and *Kc*) inflammation compared to the WT counterparts (Supplementary Figure 4A). Similarly, the miR-155KO mice subjected to the SA model had decreased PAS staining (Figure 3H) and blunted MCh-induced airway responsiveness (Figure 3I) as well as marked deficiency in Th2 and Th17 cytokine productions (Supplementary Figure 4B). Consistent with these findings, BAL Th2 and Th17 cytokines were also significantly decreased in the miR-155KO mice (Supplementary Figure 4C). Collectively, these data indicate that miR-155 regulates Th2 and Th17 allergic lung inflammation *via* ETosis process.

Inhibition of miR-155 alters eosinophilic and neutrophilic inflammation in the mouse model of severe asthma

Next, we examined whether miR-155 could be targeted to decrease allergic lung inflammation by inducing defective ETosis. Emerging evidence indicates that exosomes can serve as vehicles for therapeutic drug delivery (43, 44). We established a protocol using serum-derived exosomes to deliver the specific inhibitor against miR-155 into the lung *in vivo*, as previously described (35). We purified exosomes from mouse serum and determined the size of serum-derived exosomes and inflammatory lung response *in vivo*. Nanoparticle tracking analysis measurement (NanoSight) showed that the purified serum-derived exosomes were ~78 nm in diameter, as expected from the previous study (45) (Supplementary Figure 5A). Incubation of serum-derived exosomes with primary alveolar macrophages showed no cytotoxic effect (Supplementary Figure 5B). Serum-derived exosome treatment on mouse lungs did not alter the number of BAL inflammatory cells (Supplementary Figure 5C). To evaluate the efficiency of miR-155 inhibition *in vivo*, a synthetic miR-155 inhibitor (mmu-miR-155-5p, Sigma-Aldrich) was loaded into exosomes using modified calcium-mediated transfection and delivered to the lung *via* intranasal instillation (Supplementary Figure 5D). As shown, exosome-mediated delivery of the specific miR-155 inhibitor decreased the miR-155 level in the lung, compared with the group treated with a control vector (Supplementary Figure 5E).

In the SA model, the neutrophil influx into BAL was significantly decreased in miR-155 inhibitor/exosome-treated mice compared with control/exosome-treated mice (Figure 4A, 19.3% vs. 34%). The exosome-mediated delivery of miR-155 inhibitor significantly decreased the total number of BAL cells with a marked reduction in BAL eosinophil and neutrophil numbers, compared with control/exosome-treated mice (Figures 4B, C), although both groups were equally sensitized to the allergens because total serum IgE levels were identical in the SA model (Figure 4D). Moreover, BAL-dsDNA and citH3 were markedly decreased in BALF of the miR-155 inhibitor/exosome-treated mice subjected to the SA model as compared with their counterpart control (Figure 4E), indicating the critical roles of miR-155 in ETosis. Concordant with the decrease of ETosis, the miR-155 inhibitor/exosome-treated mice had attenuated levels of BAL-NE (Figure 4F).

Next, we examined the asthma features of the SA model with the exosome-mediated delivery of a miR-155 inhibitor. The treatment with a miR-155 inhibitor in the lung in the SA model induced a marked reduction in the expression of *Il13*, *Il17*, *Ifng*, *Kc*, and *Ccl17* genes in the lung (Figure 5A); decreased goblet cell hyperplasia (Figure 5B); and lowered PAD4 protein expression in the lung as compared to the control group (Figure 5C). Airway hyperresponsiveness (AHR) was also markedly lower in the miR-155 inhibitor/exosome-treated mice (Figure 5D). Similarly, there was a significant deficiency in Th2 and Th17 cytokine production (Supplementary Figure 5F) and the secretion of BAL-cytokines such as KC, IL-17, IL-13, IL-5, and CCL17 in the miR-155 inhibitor-treated group (Figure 5E). Together, these data indicate that miR-155 has a pivotal role in promoting ETosis, and miR-155 could be a target to decrease mixed Th1/Th2/Th17 immune responses.

MiR-155 deficiency alters heterogeneity of lung immune cells in a mouse model of severe asthma

Next, we performed scRNA-seq to investigate the transcriptional profiles of lungs affected by miR-155. Single-cell suspensions of whole lungs were generated from the WT and miR-155KO mice subjected to the SA model (N = 3 each). Consistent with our previous data (Figure 3C), the miR-155KO mice had decreased inflammatory cell influx (Supplementary Figures 6A–C). Cells were immediately encapsulated and barcoded for library preparation using a 10x Genomics microfluidics system, followed by sequencing. We recovered approximately 10,000 individual cells, which were annotated based on established cell markers (38, 46, 47). Unsupervised clustering analysis revealed 27 different clusters corresponding to distinct cell types of the lung, including epithelial, stromal,

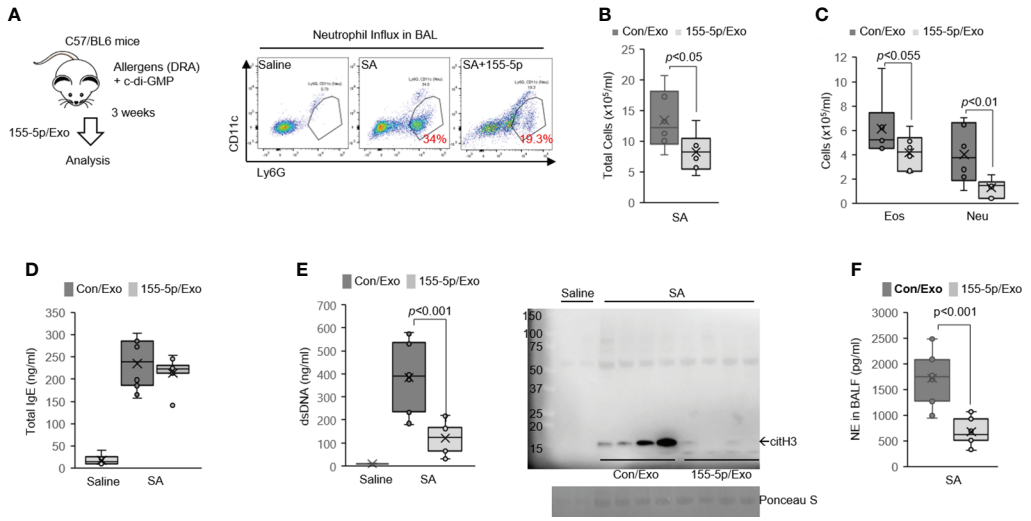

FIGURE 4
Delivery of miR-155 inhibitor has broad immunosuppressive potential in severe asthma (SA) mice. **(A)** Delivery of miRNA inhibitor *via* serum-derived exosomes into the lung macrophages *in vivo*. Serum exosomes measuring 100 μg transfected with 100 pmol of inhibitor control or miR-155 inhibitor (miR-155-5p) were given. Mice were sensitized and challenged with c-di-GMP and DRA and treated with miR-155 inhibitor or control on days 25, 26, and 27. Neutrophil influx in BAL from SA mice is analyzed by flow cytometry (N = 5-7). **(B)** Total cells and **(C)** leukocyte differentials were counted in the BALF. **(D)** All SA animals had elevated levels of total IgE. **(E)** PicoGreen assay and Western immunoblot for citH3 showing ET-associated DNA present in BALF. **(F)** NE in the BALF of mice to the SA model. Graphs were plotted as mean ± SE. p-Values were obtained using a two-tailed Student's t-test. BAL, bronchoalveolar lavage; BALF, bronchoalveolar lavage fluid; ET, extracellular trap; NE, neutrophil elastase.

endothelial, and leukocyte lineages with specific molecular markers (Figure 6A). The miR-155KO mice subjected to the SA model showed a decrease in lung immune cells, whereas the numbers of structural cells such as epithelial and endothelial cells were slightly increased compared to their WT counterparts (Figure 6B and Supplementary Figure 6D). We evaluated the expression of genes associated with asthma-related responses and airway remodeling per cell clusters (10, 47). Several genes were among the most highly expressed factors, including *Egr1*, *Il1b*, *Stat1*, *Rel*, *Tcf4*, and *Nfkb1* (Supplementary Figure 6E).

Next, we examined ETs formation-related genes in the identified lung cell clusters. By using dot plots, we showed that the transcripts of ET formation-related genes were substantially downregulated in the miR-155KO mice subjected to the SA model (Supplementary Figure 6F). We evaluated the expression of genes associated with ETosis (48–52) including *Atf3*, *Atf4*, *Bax*, *Ptgs2*, *Arg2*, *Il1b*, *Rps3*, *Prdx6*, *Jun*, *Cd74*, *C3*, and *Hmgb1* in leukocyte clusters of the SA model (Figure 6C). We also detected low-level expression of several genes in the miR-155KO mice subjected to the SA model. Gene module scores for these signature genes were compared between the miR-155KO and WT mice. The miR-155KO mice subjected to the SA model have less enriched gene module scores of these signature genes compared to their counterpart control (Figure 6D). Among these genes, *Il1b* and *Ptgs2* were differentially expressed in granulocyte clusters between the WT and miR-155KO mice. *Rps3* was predominantly expressed in T-cell clusters, whereas *Arg2* was expressed in macrophage clusters (Figure 6E). Gene set enrichment analysis using IPA presented the lung leukocyte clusters, which showed decreased activation of pathways of RHOGDI (Rho GDP-dissociation inhibitor) signaling, apoptosis signaling, TWEAK (TNF-related weak inducer of apoptosis) signaling, IL-17 signaling, and PAK signaling, which regulate cellular function including stress-related response and allergic airway diseases 10, 18, 41), during severe asthma in the miR-155KO mice. In contrast, PPAR signaling, PPARα/RXRα signaling, and PTEN signaling pathways in miR-155KO leukocyte clusters were higher than those of the WT counterparts (Supplementary Figure 6G).

PAD4 inhibition results in decreased dsDNA with no effect on granulocytes influx in severe asthma

To further address the functional impact of ETosis on asthma, we used PAD4 knockout mice (PAD4KO) that have defective ETosis (53). PAD4KO mice had a markedly lower level of BALF dsDNA, although inflammatory cells infiltrating the lungs were higher than those of their WT counterpart (Supplementary Figures 7A–C). Similarly, the specific inhibitor for PAD4, GSK484 (10 mg/kg, i.p., three times), decreased PAD4

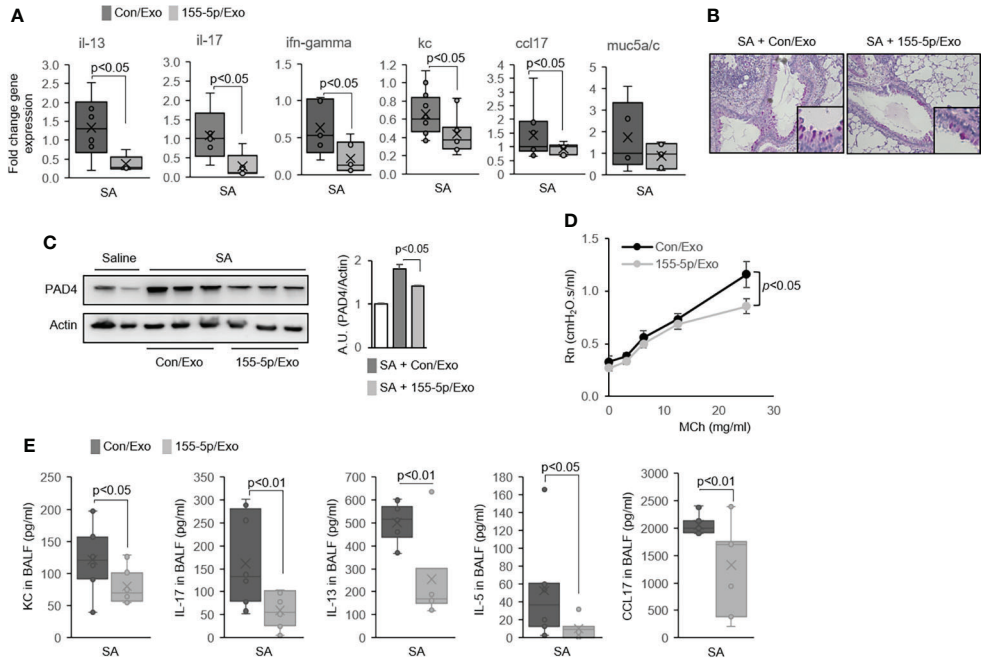

FIGURE 5
MiR-155 inhibition alters eosinophilic and neutrophilic inflammation in the airways of severe asthma (SA) mice. **(A)** The mRNA expression in lung tissues from Con/Exo- and 155-5p/Exo-treated mouse lungs subjected to the SA model (N = 5–7). **(B)** Representative histologic lung sections stained with PAS. Boxed regions are shown enlarged at right. **(C)** Expression of PAD4 as determined by Western immunoblot. **(D)** Airway hyperresponsiveness (AHR) in Con/Exo- and 155-5p/Exo-treated mice subjected to the SA model. **(E)** The level of cytokines in BALF (N = 5–7). Graphs were plotted as mean ± SE. p-Values were obtained using a two-tailed Student's t-test. PAS, periodic acid-Schiff.

activity in the lung and reduced dsDNA release and NE productions in BALF (Supplementary Figures 7D, E). However, PAD4 inhibition had no change in the number of total cells or granulocyte counts in the lung (Supplementary Figures 7F, G) and did not alter miR-155 expression in the SA model (Supplementary Figure 7H). These data indicate that PAD4 is downstream of miR-155 with a limited function in dsDNA releases, and miR-155 has a broader impact on asthma phenotypes along with regulating ETosis.

Intranasal instillation of deoxyribonuclease reduces airway eosinophils but has no effect on airway inflammation in a mouse model of severe asthma

We also tested the potential impact of naked dsDNA on asthma phenotypes with deoxyribonuclease (DNase) I treatment (200 U, i.n., three times) (Supplementary Figure 8A). DNase I treatment modestly decreased BAL eosinophils in the SA model, whereas BAL neutrophils remained unchanged (Supplementary Figures 8A, B). DNase I had a similar partial decrease in airway mucus cell metaplasia and decreased IL-13 and muc5a/c in the lung, suggesting that DNase I did not affect neutrophil response to allergen challenge (Supplementary Figures 8C, D).

Discussion

Asthma is a consequence of complex gene–environment interactions, with heterogeneity in clinical presentation (54). Based on the development of relevant biological therapies, type 2-high is the most well-defined endotype of asthma (55). The more severe form of asthma, the mixed granulocytic phenotype, has few endotype-specific therapeutic options, and therefore, further study of its underlying mechanisms is needed. The severe asthma endotype with airway eosinophils and neutrophils is associated with asthma exacerbations and is resistant to inhaled and systemic corticosteroids. To address this important clinically relevant issue, we developed a severe asthma mouse model that recapitulates the immune response that has been identified in the airways of patients with mixed granulocytic asthma. Abundant neutrophils infiltrate the lung, and mixed neutrophilic/eosinophilic inflammation was greatly increased in our severe asthma mouse model, which is consistent with the literature (5, 7, 21, 22). Our data indicate that ETosis is involved directly and indirectly in regulating neutrophil and eosinophil accumulation,

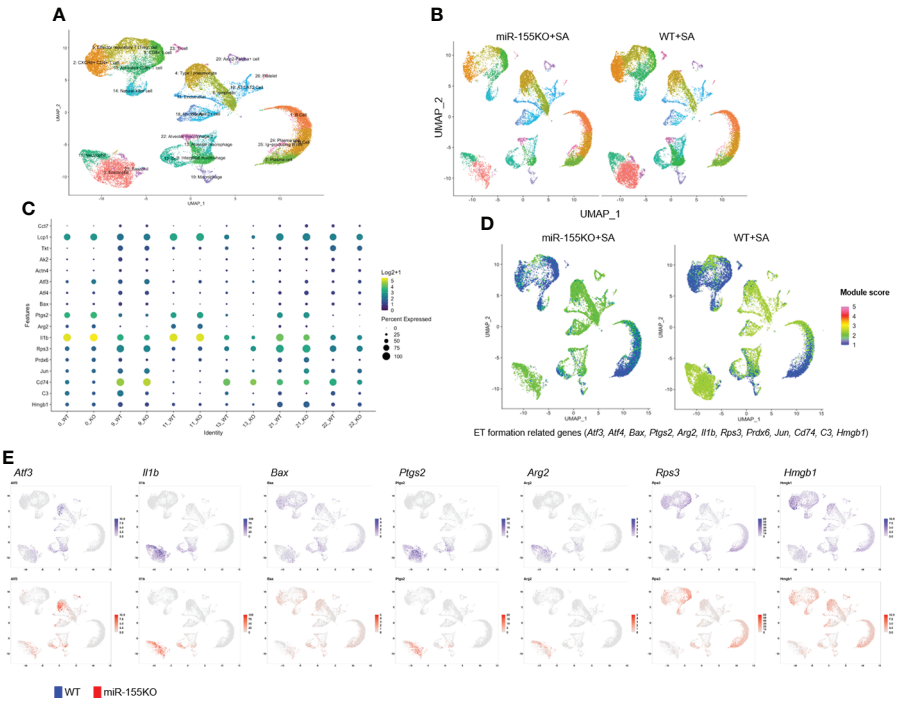

FIGURE 6
Single-cell RNA-seq analysis of the lung cells in severe asthma (SA) mice. **(A)** Single-cell RNA-seq was performed on single-cell suspensions from whole lungs of mice. Cells were clustered using a graph-based shared nearest-neighbor clustering approach plotted by a UMAP plot. UMAP plot of all scRNA-seq data showing a total of 27 distinct cellular populations that were identified. **(B)** UMAP plots of lung cells from the miR-155KO and WT SA groups (N = 3 per group). All cells were analyzed using canonical correlation analysis with the Seurat R package. **(C)** The expression levels of ET formation-related *Ccl7*, *Lpc1*, *Tkt*, *Ak2*, *Actn4*, *Atf3*, *Atf4*, *Bax*, *Ptgs2*, *Arg2*, *Il1b*, *Rps3*, *Prdx6*, *Jun*, *Cd74*, *C3*, and *Hmgb1* genes are shown. Each dot size corresponds to the percentage of cells in the cluster expressing a gene, and dot color corresponds to the mean expression level for the gene in the cluster. **(D)** UMAP plots compare gene module scores between miR-155KO and WT SA mouse lungs using ET formation-related genes (*Atf3*, *Atf4*, *Bax*, *Ptgs2*, *Arg2*, *Il1b*, *Rps3*, *Prdx6*, *Jun*, *Cd74*, *C3*, and *Hmgb1*). **(E)** UMAP plots show the expression of the indicated ET-related genes in each cluster. UMAP, Uniform Manifold Approximation and Projection; WT, wild type; ET, extracellular trap.

which have a pathophysiological role in promoting excessive inflammation and tissue damage. We identified a marked increase in lung eosinophils/neutrophils and extracellular dsDNA in animals exposed to allergens with c-di-GMP. We also discovered that short non-coding miR-155 acts as an early regulator of the release of host dsDNA and ETosis in severe asthma. The severity of the disease is reduced in miR-155-deficient mice compared to their WT counterparts. The neutrophil influx in BAL was decreased in miR-155 inhibitor/exosome-treated severe asthma mice. There was a significantly reduced BALF dsDNA in PAD4 deficient; however, the infiltration of lung immune cells was not decreased. DNase I instillation decreased the intensity of airway inflammation but did not impact miR-155-derived neutrophilia. Together, these findings indicate that miR-155 promotes the release of host dsDNA that contributes to airway damage and mixed granulocytic inflammation.

Outside of the original observation of ETs antimicrobial activity, recent studies have described an assortment of ET-associated immunologic processes and pathologies. ETs contain histones and granular proteins such as NE and MPO. Soluble ET components prime other immune cells to induce sterile inflammation or immune cell recruitment. The released extracellular DNA acts as a danger signal and triggers cytokine production for additional immune response (24). A novel perspective has emerged in light of recent reports, which showed that ETs are generated by both eosinophils and neutrophils in human atopic asthmatic airways (25, 26). Patients with mixed neutrophils and eosinophils in their lungs have more severe airflow obstruction and a higher frequency of exacerbations and are resistant to treatment with corticosteroids (15). Both neutrophils and eosinophils undergo ETosis to promote inflammation and tissue damage in response to many pathogens and pro-inflammatory stimuli. Therefore, key aspects of ETs in the immune response are sufficient to recapitulate many features of asthma pathophysiology. In this study, we focused on the role of ETs in regulating asthmatic airway inflammation directly or indirectly by modulating other immune cell recruitments. Our severe asthma mouse results unequivocally indicate that there is a substantial level of

biologically active ETs present in the airways of asthmatics with neutrophil/eosinophil-enriched inflammatory response. It is important to note that increased ETosis associated with mild asthma as well, suggesting that an imbalance of ET formation in the lung may also contribute to enhanced Th2 response in asthma pathogenesis.

MicroRNAs are dynamic post-transcriptional regulators of gene networks. Profiling studies of miRNAs in human biopsy specimens and mouse models of asthma showed differential expression in ~10%–20% of miRNAs (56). MiR-155 is one of the first identified and most studied miRNAs up to date. It is thought to play a role in the functioning of the human immune system (57, 58). MiR-155 is essential for Th2-mediated eosinophilic inflammation through the transcription factor PU.1 (59). Additionally, ILC2 and IL-33 signaling are regulated by miR-155 in Th2 eosinophilic allergic airway inflammation (42). Thus, miR-155 is of considerable interest for understanding immune regulation in allergic asthma conditions. Herein, we showed that host dsDNA release from ETosis in mixed neutrophilic and eosinophilic asthma phenotypes is dependent on miR-155 expression levels. Many neutrophils infiltrated into the lungs, and increased NE productions were significantly reduced in the miR-155KO mice compared to the WT mice. We made the novel observation that the miR-155KO mice were unable to induce both neutrophil and eosinophil influx in the lung in response to severe asthma conditions, which suggests another role for miR-155 in neutrophilic inflammation in severe asthma. MiR-155-deficient mice also showed decreased PAD4 expression levels as compared to the WT mice, which is consistent with the results of *in vitro* study (60). Our data confirm previous *in vitro* data indicating that after stimulation, activation of PAD4 occurs but is regulated by miR-155 in exaggerated ETs generation. These observations predict that miR-155 functions as a positive regulator of ETosis *via* regulation of PAD4 gene expression. We first asked if myeloid-specific miR-155 deficiency is sufficient to recapitulate the phenotype observed in global miR-155 knockout mice, as well as to gauge the effectiveness of inhibitor delivery to rescue the phenotype. However, we show that myeloid-specific deletion of miR-155 in miR-155$^{fl/fl}$LysMCre mice leads to a reduction of BALF dsDNA without affecting macrophage, neutrophil, or eosinophil numbers in a model of severe asthma. This might explain the myeloid lineage in miR-155$^{fl/fl}$LysMCre mice with residual miR-155 in the lungs since in a model of severe asthma, inflammatory cell influx is completely blunted in whole-body miR-155KO mice. Future studies should identify the role of myeloid miR-155 and their associated phenotypes in neutrophilic severe asthma in the lung.

Various clinical trials using miRNA mimetics or anti-miRNAs as therapeutic targets are currently underway and show promising results (61). Our therapeutic approach involving a miR-155 inhibitor has informed the concept to deliver small RNA molecules using serum-derived exosomes into the lung *in vivo*. An exosome-based drug delivery system has recently attracted increasing attention (36). Notably, exosome-mediated drug delivery has the following advantages in comparison with other approaches, such as nanoparticles, liposomes, and viruses. Nanoparticles and liposomes delivered into the lung *via* the i.t. route usually forms aggregate (35). Exosomes are potentially less toxic and less immunogenic compared with exogenous delivery vehicles (62). They also have been shown to be a mode of transport across the blood–brain barrier (63). However, the delivery of exosome-based therapeutics to the lungs *via* i.n. or i.t. remains unexplored. Our results indicate that the exosome-loaded miR-155 inhibitor is successfully delivered *via* i.n. instillation and exerted functions in lungs *in vivo*. Nonetheless, the correct timing of miR-155 inhibition is critical to be functional in the lungs while limiting inflammatory cell influx and tissue damages. A partial targeting miR-155 after severe asthma onset did not produce salutary effects on reducing BALF dsDNA and lung injury.

In the model tested herein, we used DNase I and PAD4 inhibitors to assess the functional importance of ETs in severe allergic asthma. None of these approaches are fully specified for suppression of the heightened Th2/Th17 response. It is important to note that the biological activity of the inhibitors may not be optimal in the lung tissue and could be influenced by factors that are inherent to the experimental models used (64). Treatment with DNase I and PAD4 inhibitor reduced dsDNA release in BALF; however, it had the same global outcome on the development of severe asthma compared to vehicle severe asthma mice, suggesting that ETs could mediate the onset of severe asthmatic airway inflammation in the models tested here.

Single-cell profiling of lung immune cells and identification of molecular pathways in asthma pathogenesis are critical fields of interest in asthma research. This also provides a vital information resource for the immune cellular network in the lung during an asthma exacerbation. Here, our results provide data-driven different transcriptional profiles present in the immune cells of the lung at the single-cell level that contribute to the pathogenesis of asthma and decode the network by using gene set enrichment analysis. In our established severe asthma mouse model, we identified 27 major cell clusters by using SingleR. While numerous immune cells are present in the lungs of severe asthma mice, eosinophils, T lymphocytes, neutrophils, and macrophages are the most abundant cells, whose levels are consistent across different phenotypes of asthma. The profile of the identified cell clusters in miR-155-deficient and WT mice in the presence of c-di-GMP with DRA challenge was not altered, although miR-155KO suppressed c-di-GMP/DRA-induced increased levels of eosinophils and neutrophils. Detailed analysis revealed distinct transcriptional modulation in heightened Th2/Th17 response when compared in mice lacking miR-155. Inflammatory factors and innate/adaptive immune responses are essential in driving the development and exacerbation of asthma. We were able to

find the expression of multiple key factors of persistent inflammation, adaptive immune response, and ETosis pathway in our experimental model. These factors critically regulate exaggerated inflammatory responses, inducing asthma exacerbation (10). The pathway analysis supports that miR-155 influences ETosis, at least in part, through significant modulation of neutrophil, eosinophil, and macrophage responses. ET-derived DNA and granule proteins from these myeloid linage cells are key components in driving the pathogenesis of asthma exacerbation in this model. It has become clear that uncontrolled ET formation or their insufficient removal can have serious consequences; however, ET formation pathway is still under investigation.

There are several limitations of this study, which might serve as directions for future studies. Excessive release of a serine protease NE can damage surrounding tissues and contribute to lung dysfunction (65). Neutrophils are the dominant cellular source of NE, but it is also produced by macrophages (66–68). Our group has reported that a majority of the resident cells in the human BALF from our SBP-AG protocol were CD163-positive AMs (30). In the allergen-challenged experimental site, the newly recruited eosinophils appeared to have co-existed with recruited monocyte-derived AMs (but not neutrophils) (69). We reported that the newly recruited macrophage population in the airway is a very different phenotype from these resident macrophages. Remarkably, elevated NE was observed in BALF obtained from human subjects with asthma after SBP-AG protocol without any neutrophil influx. This phenomenon was speculated to occur due to increased innate immune cells (i.e., monocyte-derived AMs) in a mild intermittent allergic asthma model. Further work is required to address the precise role of macrophage-derived NE in allergic lung inflammation. Second, our experiments using mice treated with PAD4 inhibitor and DNase I did not fully reveal miR-155 regulation pathways. Independent evaluation of miR-155 regulation pathways including the PAD4 axis in the global outcome of the development of severe asthma is further needed. Next, although we found that miR-155$^{fl/fl}$LysMCre mice had reduction of BALF dsDNA, the role of myeloid miR-155 and their associated phenotypes in neutrophilic severe asthma in the lung needs to be further studied. Besides, our next study should address how miR-155 modulates cellular function in specific cell subsets in both innate and adaptive immune responses by scRNA-seq in the future.

In summary, ETosis and associated host dsDNA are cardinal features of mixed granulocytic inflammation in severe asthma. Our data indicate that short non-coding miR-155 contributes to the release of extracellular dsDNA, which exacerbates many features of allergic inflammation. We developed a novel therapeutic tool using serum-derived exosomes as oligonucleotide delivery vehicles, leading to the control of the release of ETs *in vivo*. Our single-cell transcriptional analysis of mouse lung immune cells provides an insightful framework for understanding the distinct expression patterns of ET-related genes at the individual cell level. These findings provide pre-clinical evidence that targeting host dsDNA release represents an attractive therapeutic approach for mitigating the inflammatory asthma features for mixed granulocytic severe asthma patients.

Data availability statement

The datasets presented in this study can be found in online repositories. The name of the repository and accession number can be found below: NCBI Gene Expression Omnibus; GSE203656.

Ethics statement

The studies involving human participants were reviewed and approved by University of Illinois Center for Clinical and Translational Science. The patients/participants provided their written informed consent to participate in this study.

Author contributions

JK and SC performed the experiments, analyzed data, and drafted the manuscript. MK, HL, JE, and TL assisted in the mouse and cellular experiments. PS, MP, and PY obtained and analyzed the scRNA-seq data. NP, GP, and JC served as consultants for this project. GP and JC supported the SBP-AG protocol and assisted with data analyses. SC supervised the project. All authors contributed to the writing of the final manuscript.

Acknowledgments

This work was supported by grants from the National Institutes of Health (R01HL137224 and R01HL153170), the American Lung Association (RG-416620 and CA-699246), and Internal Medicine at the Ohio State University (Junior Investigator Award). The authors thank the subjects with asthma who volunteered for the SBP-AG protocol and the staff of the Clinical Interface Core at the University of Illinois Center for Clinical and Translational Science (UIC-CCTS) for assistance with patient recruitment, screening, and performing bronchoscopy. In addition, we would like to thank Flow Cytometry Shared Resource, Comparative Pathology and Digital Imaging Shared Resource, Microscopy Resource, Genomics Shared Resource, and Biomedical Informatics Shared Resource (P30CA016058) for their technical assistance.

Conflict of interest

The authors declare that the research was conducted in the absence of any commercial or financial relationships that could be construed as a potential conflict of interest.

Publisher's note

All claims expressed in this article are solely those of the authors and do not necessarily represent those of their affiliated organizations, or those of the publisher, the editors and the reviewers. Any product that may be evaluated in this article, or claim that may be made by its manufacturer, is not guaranteed or endorsed by the publisher.

Supplementary material

The Supplementary Material for this article can be found online at: https://www.frontiersin.org/articles/10.3389/fimmu.2022.943554/full#supplementary-material

References

1. Fanta CH. "Asthma.". *N Engl J Med* (2009) 360(10):1002–14. doi: 10.1056/NEJMra0804579

2. Woodruff PG, Modrek B, Choy DF, Jia G, Abbas AR, Ellwanger A, et al. "T-helper type 2-driven inflammation defines major subphenotypes of asthma.". *Am J Respir Crit Care Med* (2009) 180(5):388–95. doi: 10.1164/rccm.200903-0392OC

3. Wenzel SE. "Asthma phenotypes: the evolution from clinical to molecular approaches.". *Nat Med* (2012) 18(5):716–25. doi: 10.1038/nm.2678

4. Taylor SL, Leong LEX, Choo JM, Wesselingh S, Yang IA, Upham JW, et al. "Inflammatory phenotypes in patients with severe asthma are associated with distinct airway microbiology.". *J Allergy Clin Immunol* (2018) 141(1):94–103.e115. doi: 10.1016/j.jaci.2017.03.044

5. Krishnamoorthy N, Douda DN, Brüggemann TR, Ricklefs I, Duvall MG, Abdulnour RE, et al. "Neutrophil cytoplasts induce TH17 differentiation and skew inflammation toward neutrophilia in severe asthma.". *Sci Immunol* (2018) 3(26). doi: 10.1126/sciimmunol.aao4747

6. Nurmagambetov TA, Krishnan JA. "What will uncontrolled asthma cost in the united states?". *Am J Respir Crit Care Med* (2019) 200(9):1077–8. doi: 10.1164/rccm.201906-1177ED

7. Raundhal M, Morse C, Khare A, Oriss TB, Milosevic J, Trudeau J, et al. "High IFN-gamma and low SLPI mark severe asthma in mice and humans.". *J Clin Invest* (2015) 125(8):3037–50. doi: 10.1172/JCI80911

8. Wood LG, Baines KJ, Fu J, Scott HA, Gibson PG. "The neutrophilic inflammatory phenotype is associated with systemic inflammation in asthma.". *Chest* (2012) 142(1):86–93. doi: 10.1378/chest.11-1838

9. Moore WC, Hastie AT, Li X, Li H, Busse WW, Jarjour NN, et al. "Sputum neutrophil counts are associated with more severe asthma phenotypes using cluster analysis.". *J Allergy Clin Immunol* (2014) 133(6):1557–63.e1555. doi: 10.1016/j.jaci.2013.10.011

10. Wang L, Netto KG, Zhou L, Liu X, Wang M, Zhang G, et al.). "Single-cell transcriptomic analysis reveals the immune landscape of lung in steroid-resistant asthma exacerbation.". *Proc Natl Acad Sci USA* (2021) 118(2). doi: 10.1073/pnas.2005590118

11. Jatakanon A, Uasuf C, Maziak W, Lim S, Chung KF, Barnes PJ. "Neutrophilic inflammation in severe persistent asthma.". *Am J Respir Crit Care Med* (1999) 160(5 Pt 1):1532–9. doi: 10.1164/ajrccm.160.5.9806170

12. Norzila MZ, Fakes K, Henry RL, Simpson J, Gibson PG. "Interleukin-8 secretion and neutrophil recruitment accompanies induced sputum eosinophil activation in children with acute asthma.". *Am J Respir Crit Care Med* (2000) 161(3 Pt 1):769–74. doi: 10.1164/ajrccm.161.3.9809071

13. Maltby S, Tay HL, Yang M, Foster PS. "Mouse models of severe asthma: Understanding the mechanisms of steroid resistance, tissue remodelling and disease exacerbation.". *Respirology* (2017) 22(5):874–85. doi: 10.1111/resp.13052

14. Ray A, Kolls JK. "Neutrophilic inflammation in asthma and association with disease severity.". *Trends Immunol* (2017) 38(12):942–54. doi: 10.1016/j.it.2017.07.003

15. Hastie AT, Moore WC, Meyers DA, Vestal PL, Li H, Peters SP, et al. "Analyses of asthma severity phenotypes and inflammatory proteins in subjects stratified by sputum granulocytes.". *J Allergy Clin Immunol* (2010) 125(5):1028–36.e1013. doi: 10.1016/j.jaci.2010.02.008

16. Demarche S, Schleich F, Henket M, Paulus V, Van Hees T, Louis R. "Detailed analysis of sputum and systemic inflammation in asthma phenotypes: are paucigranulocytic asthmatics really non-inflammatory?". *BMC Pulm Med* (2016) 16:46. doi: 10.1186/s12890-016-0208-2

17. Hastie AT, Mauger DT, Denlinger LC, Coverstone A, Castro M, Erzurum S, et al. "Mixed sputum granulocyte longitudinal impact on lung function in the severe asthma research program.". *Am J Respir Crit Care Med* (2021) 203(7):882–92. doi: 10.1164/rccm.202009-3713OC

18. McKinley L, Alcorn JF, Peterson A, Dupont RB, Kapadia S, Logar A, et al. "TH17 cells mediate steroid-resistant airway inflammation and airway hyperresponsiveness in mice. " *J Immunol* (2008) 181(6):4089–97. doi: 10.4049/jimmunol.181.6.4089

19. Ray A, Raundhal M, Oriss TB, Ray P, Wenzel SE. "Current concepts of severe asthma.". *J Clin Invest* (2016) 126(7):2394–403. doi: 10.1172/JCI84144

20. Wadhwa R, Dua K, Adcock IM, Horvat JC, Kim RY, Hansbro PM. "Cellular mechanisms underlying steroid-resistant asthma.". *Eur Respir Rev* (2019) 28(153). doi: 10.1183/16000617.0096-2019

21. Oriss TB, Raundhal M, Morse C, Huff RE, Das S, Hannum R, et al. "IRF5 distinguishes severe asthma in humans and drives Th1 phenotype and airway hyperreactivity in mice.". *JCI Insight* (2017) 2(10). doi: 10.1172/jci.insight.91019

22. Lewis BW, Jackson D, Amici SA, Walum J, Guessas M, Guessas S, et al.). "Corticosteroid insensitivity persists in the absence of STAT1 signaling in severe allergic airway inflammation.". *Am J Physiol Lung Cell Mol Physiol* (2021) 321(6):L1194–205. doi: 10.1152/ajplung.00244.2021

23. Boe DM, Curtis BJ, Chen MM, Ippolito JA, Kovacs EJ. "Extracellular traps and macrophages: new roles for the versatile phagocyte.". *J Leukoc Biol* (2015) 97(6):1023–35. doi: 10.1189/jlb.4RI1014-521R

24. Yousefi S, Simon D, Stojkov D, Karsonova A, Karaulov A, Simon HU. "*In vivo* evidence for extracellular DNA trap formation.". *Cell Death Dis* (2020) 11(4):300. doi: 10.1038/s41419-020-2497-x

25. Dworski R, Simon HU, Hoskins A, Yousefi S. "Eosinophil and neutrophil extracellular DNA traps in human allergic asthmatic airways.". *J Allergy Clin Immunol* (2011) 127(5):1260–6. doi: 10.1016/j.jaci.2010.12.1103

26. Lachowicz-Scroggins ME, Dunican EM, Charbit AR, Raymond W, Looney MR, Peters MC, et al. "Extracellular DNA, neutrophil extracellular traps, and inflammasome activation in severe asthma.". *Am J Respir Crit Care Med* (2019) 199(9):1076–85. doi: 10.1164/rccm.201810-1869OC

27. Granger V, Taille C, Roach D, Letuve S, Dupin C, Hamidi F, et al. "Circulating neutrophil and eosinophil extracellular traps are markers of severe asthma.". *Allergy* (2020) 75(3):699–702. doi: 10.1111/all.14059

28. Imanishi T, Ishihara C, Badr Mel S, Hashimoto-Tane A, Kimura Y, Kawai T, et al. "Nucleic acid sensing by T cells initiates Th2 cell differentiation.". *Nat Commun* (2014) 5:3566. doi: 10.1038/ncomms4566

29. Toussaint M, Jackson DJ, Swieboda D, Guedan A, Tsourouktsoglou TD, Ching YM, et al.). "Host DNA released by NETosis promotes rhinovirus-induced type-2 allergic asthma exacerbation.". *Nat Med* (2017) 23(6):681–91. doi: 10.1038/nm.4332

30. Park GY, Lee YG, Berdyshev E, Nyenhuis S, Du J, Fu P, et al. "Autotaxin production of lysophosphatidic acid mediates allergic asthmatic inflammation.". *Am J Respir Crit Care Med* (2013) 188(8):928–40. doi: 10.1164/rccm.201306-1014OC

31. Moon HG, Kim SJ, Jeong JJ, Han SS, Jarjour NN, Lee H, et al. "Airway epithelial cell-derived colony stimulating factor-1 promotes allergen sensitization.". *Immunity* (2018) 49(2):275–87.e275. doi: 10.1016/j.immuni.2018.06.009

32. Chung S, Lee TJ, Reader BF, Kim JY, Lee YG, Park GY, et al. "FoxO1 regulates allergic asthmatic inflammation through regulating polarization of the macrophage inflammatory phenotype.". *Oncotarget* (2016) 7(14):17532–46. doi: 10.18632/oncotarget.8162

33. Chung S, Kim JY, Song MA, Park GY, Lee YG, Karpurapu M, et al. "FoxO1 is a critical regulator of M2-like macrophage activation in allergic asthma.". *Allergy* (2019) 74(3):535–48. doi: 10.1111/all.13626

34. Chung S, Lee YG, Karpurapu M, Englert JA, Ballinger MN, Davis IC, et al. "Depletion of microRNA-451 in response to allergen exposure accentuates asthmatic inflammation by regulating Sirtuin2.". *Am J Physiol Lung Cell Mol Physiol* (2020) 318(5):L921–30. doi: 10.1152/ajplung.00457.2019

35. Zhang D, Lee H, Wang X, Rai A, Groot M, Jin Y. "Exosome-mediated small RNA delivery: A novel therapeutic approach for inflammatory lung responses.". *Mol Ther* (2018) 26(9):2119–30. doi: 10.1016/j.ymthe.2018.06.007

36. Zhang D, Lee H, Zhu Z, Minhas JK, Jin Y. "Enrichment of selective miRNAs in exosomes and delivery of exosomal miRNAs *in vitro* and *in vivo*.". *Am J Physiol Lung Cell Mol Physiol* (2017) 312(1):: L110–L121. doi: 10.1152/ajplung.00423.2016

37. Zheng GX, Terry JM, Belgrader P, Ryvkin P, Bent ZW, Wilson R, et al. "Massively parallel digital transcriptional profiling of single cells.". *Nat Commun* (2017) 8:14049. doi: 10.1038/ncomms14049

38. Hao Y, Hao S, Andersen-Nissen E, Mauck WM, Zheng S, Butler A, et al. "Integrated analysis of multimodal single-cell data.". *Cell* (2021) 184(13):3573–87.e3529.0000. doi: 10.1016/j.cell.2021.04.048

39. Kramer A, Green J, Pollard JJr., Tugendreich S. "Causal analysis approaches in ingenuity pathway analysis.". *Bioinformatics* (2014) 30(4):523–30. doi: 10.1093/bioinformatics/btt703

40. Fahy JV. "Eosinophilic and neutrophilic inflammation in asthma: insights from clinical studies.". *Proc Am Thorac Soc* (2009) 6(3):256–9. doi: 10.1513/pats.200808-087RM

41. Escobar TM, Kanellopoulou C, Kugler DG, Kilaru G, Nguyen CK, Nagarajan V, et al. "miR-155 activates cytokine gene expression in Th17 cells by regulating the DNA-binding protein Jarid2 to relieve polycomb-mediated repression.". *Immunity* (2014) 40(6):865–79. doi: 10.1016/j.immuni.2014.03.014

42. Johansson K, Malmhall C, Ramos-Ramirez P, Radinger M.). "MicroRNA-155 is a critical regulator of type 2 innate lymphoid cells and IL-33 signaling in experimental models of allergic airway inflammation.". *J Allergy Clin Immunol* (2017) 139(3):1007–16.e1009. doi: 10.1016/j.jaci.2016.06.035

43. Lamichhane TN, Raiker RS, Jay SM. "Exogenous DNA loading into extracellular vesicles *via* electroporation is size-dependent and enables limited gene delivery.". *Mol Pharm* (2015) 12(10):3650–7. doi: 10.1021/acs.molpharmaceut.5b00364

44. Zhang H, Liu J, Qu D, Wang L, Wong CM, Lau CW, et al. "Serum exosomes mediate delivery of arginase 1 as a novel mechanism for endothelial dysfunction in diabetes.". *Proc Natl Acad Sci U.S.A.* (2018) 115(29):E6927–36. doi: 10.1073/pnas.1721521115

45. Zhao F, Cheng L, Shao Q, Chen Z, Lv X, Li J, et al. "Characterization of serum small extracellular vesicles and their small RNA contents across humans, rats, and mice.". *Sci Rep* (2020) 10(1):4197. doi: 10.1038/s41598-020-61098-9

46. Zhang X, Lan Y, Xu J, Quan F, Zhao E, Deng C, et al. "CellMarker: a manually curated resource of cell markers in human and mouse.". *Nucleic Acids Res* (2019) 47(D1):D721–8. doi: 10.1093/nar/gky900

47. Li H, Wang H, Sokulsky L, Liu S, Yang R, Liu X, et al. "Single-cell transcriptomic analysis reveals key immune cell phenotypes in the lungs of patients with asthma exacerbation.". *J Allergy Clin Immunol* (2021) 147(3):941–54. doi: 10.1016/j.jaci.2020.09.032

48. Boespflug ND, Kumar S, McAlees JW, Phelan JD, Grimes HL, Hoebe K, et al. "ATF3 is a novel regulator of mouse neutrophil migration.". *Blood* (2014) 123(13):2084–93. doi: 10.1182/blood-2013-06-510909

49. Vaibhav K, Braun M, Alverson K, Khodadadi H, Kutiyanawalla A, Ward A, et al. "Neutrophil extracellular traps exacerbate neurological deficits after traumatic brain injury.". *Sci Adv 6(22)* (2020) 6(22):eaax8847. doi: 10.1126/sciadv.aax8847

50. Yang LY, Luo Q, Lu L, Zhu WW, Sun HT, Wei R, et al. "Increased neutrophil extracellular traps promote metastasis potential of hepatocellular carcinoma *via* provoking tumorous inflammatory response.". *J Hematol Oncol* (2020) 13(1):3. doi: 10.1186/s13045-019-0836-0

51. Surolia R, Li FJ, Wang Z, Kashyap M, Srivastava RK, Traylor AM, et al. "NETosis in the pathogenesis of acute lung injury following cutaneous chemical burns.". *JCI Insight* (2021) 6(10). doi: 10.1172/jci.insight.147564

52. Zhan Y, Ling Y, Deng Q, Qiu Y, Shen J, Lai H, et al. "HMGB1-mediated neutrophil extracellular trap formation exacerbates intestinal Ischemia/Reperfusion-induced acute lung injury.". *J Immunol* (2022) 208(4):968–78. doi: 10.4049/jimmunol.2100593

53. Claushuis TAM, van der Donk LEH, Luitse AL, van Veen HA, van der Wel NN, van Vught LA, et al. "Role of peptidylarginine deiminase 4 in neutrophil extracellular trap formation and host defense during klebsiella pneumoniae-induced pneumonia-derived sepsis.". *J Immunol* (2018) 201(4):1241–52. doi: 10.4049/jimmunol.1800314

54. Papi A, Brightling C, Pedersen SE, Reddel HK. Asthma. *Lancet* (2018) 391(10122):783–800. doi: 10.1016/S0140-6736(17)33311-1

55. Kyriakopoulos C, Gogali A, Bartziokas K, Kostikas K. "Identification and treatment of T2-low asthma in the era of biologics.". *ERJ Open Res* (2021) 7(2). doi: 10.1183/23120541.00309-2020

56. Garbacki N, Di Valentin E, Huynh-Thu VA, Geurts P, Irrthum A, Crahay C, et al. "MicroRNAs profiling in murine models of acute and chronic asthma: a relationship with mRNAs targets.". *PloS One* (2011) 6(1):e16509. doi: 10.1371/journal.pone.0016509

57. Zhou H, Li J, Gao P, Wang Q, Zhang J. miR-155: A novel target in allergic asthma.". *Int J Mol Sci* (2016) 17(10). doi: 10.3390/ijms17101773

58. Ekiz HA, Huffaker TB, Grossmann AH, Stephens WZ, Williams MA, Round JL, et al. "MicroRNA-155 coordinates the immunological landscape within murine melanoma and correlates with immunity in human cancers.". *JCI Insight* (2019) 4(6). doi: 10.1172/jci.insight.126543

59. Malmhall C, Alawieh S, Lu Y, Sjostrand M, Bossios A, Eldh M, et al.). "MicroRNA-155 is essential for T(H)2-mediated allergen-induced eosinophilic inflammation in the lung.". *J Allergy Clin Immunol* (2014) 133(5):1438.e1421–1427. doi: 10.1016/j.jaci.2013.11.008

60. Hawez A, Al-Haidari A, Madhi R, Rahman M, Thorlacius H. "MiR-155 regulates PAD4-dependent formation of neutrophil extracellular traps.". *Front Immunol* (2019) 10:2462. doi: 10.3389/fimmu.2019.02462

61. Shah MY, Ferrajoli A, Sood AK, Lopez-Berestein G, Calin GA. "microRNA therapeutics in cancer - an emerging concept.". *EBioMedicine* (2016) 12:34–42. doi: 10.1016/j.ebiom.2016.09.017

62. Wood MJ, O'Loughlin AJ, Samira L. "Exosomes and the blood-brain barrier: implications for neurological diseases.". *Ther Delivery* (2011) 2(9):1095–9. doi: 10.4155/tde.11.83

63. Matsumoto J, Stewart T, Banks WA, Zhang J. "The transport mechanism of extracellular vesicles at the blood-brain barrier.". *Curr Pharm Des* (2017) 23(40):6206–14. doi: 10.2174/1381612823666170913164738

64. Radermecker C, Sabatel C, Vanwinge C, Ruscitti C, Marechal P, Perin F, et al. "Locally instructed CXCR4(hi) neutrophils trigger environment-driven allergic asthma through the release of neutrophil extracellular traps.". *Nat Immunol* (2019) 20(11):1444–55. doi: 10.1038/s41590-019-0496-9

65. Domon H, Nagai K, Maekawa T, Oda M, Yonezawa D, Takeda W, et al. "Neutrophil elastase subverts the immune response by cleaving toll-like receptors and cytokines in pneumococcal pneumonia.". *Front Immunol* (2018) 9:732. doi: 10.3389/fimmu.2018.00732

66. Dollery CM, Owen CA, Sukhova GK, Krettek A, Shapiro SD, Libby P. "Neutrophil elastase in human atherosclerotic plaques: production by macrophages". *Circulation* (2003) 107(22):2829–36. doi: 10.1161/01.CIR.0000072792.65250.4A

67. Doster RS, Sutton JA, Rogers LM, Aronoff DM, Gaddy JA. "Streptococcus agalactiae induces placental macrophages to release extracellular traps loaded with tissue remodeling enzymes *via* an oxidative burst-dependent mechanism.". *mBio* (2018) 9(6). doi: 10.1128/mBio.02084-18

68. Taylor S, Dirir O, Zamanian RT, Rabinovitch M, Thompson AAR. "The role of neutrophils and neutrophil elastase in pulmonary arterial hypertension.". *Front Med (Lausanne)* (2018) 5:217. doi: 10.3389/fmed.2018.00217

69. Lee YG, Jeong JJ, Nyenhuis S, Berdyshev E, Chung S, Ranjan R, et al. "Recruited alveolar macrophages, in response to airway epithelial-derived monocyte chemoattractant protein 1/CCL2, regulate airway inflammation and remodeling in allergic asthma.". *Am J Respir Cell Mol Biol* (2015) 52(6):772–84. doi: 10.1165/rcmb.2014-0255OC

frontiers | Frontiers in Immunology

TYPE Review
PUBLISHED 28 July 2022
DOI 10.3389/fimmu.2022.922377

OPEN ACCESS

EDITED BY
Galina Sud'ina,
Lomonosov Moscow State University, Russia

REVIEWED BY
Viviana Marin-Esteban,
Université Paris-Saclay, France
Nina Victor Vorobjeva
Lomonosov Moscow State University, Russia

*CORRESPONDENCE
Kehinde Adebayo Babatunde
kehinde.babatunde@ucalgary.ca

SPECIALTY SECTION
This article was submitted to Inflammation, a section of the journal Frontiers in Immunology

RECEIVED 17 April 2022
ACCEPTED 01 July 2022
PUBLISHED 28 July 2022

CITATION
Babatunde KA and Adenuga OF (2022) Neutrophils in malaria: A double-edged sword role.
Front. Immunol. 13:922377.
doi: 10.3389/fimmu.2022.922377

Neutrophils in malaria: A double-edged sword role

Kehinde Adebayo Babatunde[1,2*] and Oluwadamilola Fatimat Adenuga[3]

[1]Department of Physiology and Pharmacology, University of Calgary, Calgary, AB, Canada, [2]Department of Pathology & Laboratory Medicine, University of Wisconsin, Madison, WI, United States, [3]Department of Pathobiological Sciences, University of Wisconsin-Madison, Madison, WI, United States

Neutrophils are the most abundant leukocytes in human peripheral blood. They form the first line of defense against invading foreign pathogens and might play a crucial role in malaria. According to World Health Organization (WHO), malaria is a globally significant disease caused by protozoan parasites from the *Plasmodium* genus, and it's responsible for 627,000 deaths in 2020. Neutrophils participate in the defense response against the malaria parasite *via* phagocytosis and reactive oxygen species (ROS) production. Neutrophils might also be involved in the pathogenesis of malaria by the release of toxic granules and the release of neutrophil extracellular traps (NETs). Intriguingly, malaria parasites inhibit the anti-microbial function of neutrophils, thus making malaria patients more susceptible to secondary opportunistic *Salmonella* infections. In this review, we will provide a summary of the role of neutrophils during malaria infection, some contradicting mouse model neutrophil data and neutrophil-related mechanisms involved in malaria patients' susceptibility to bacterial infection.

KEYWORDS

neutrophil, malaria, *plasmodium*, *salmonella typhimurium*, neutrophil extracellular traps (NETs)

Introduction

According to the WHO, malaria is a globally significant disease caused by protozoan parasites from the *Plasmodium* genus. There are five species of the protozoan genus *Plasmodium* known to infect humans: *P. falciparum*, *P. vivax*, *P. malariae*, *P. ovale*, and *P. knowlesi*, of which *P. falciparum* is responsible for most cases of severe malaria and death (1). The parasites caused over 241 million clinical cases and 627,000 deaths in 2020; this represents about 14 million more cases in 2020 compared to 2019 and 69 000 more deaths. Sub-Saharan Africa continues to carry the heaviest malaria burden, accounting for about 95% of all malaria cases and 96% of all deaths in 2020 (2). There are three clinical presentations of malaria identified: severe or complicated, mild or uncomplicated

(3) and asymptomatic (4). The host immune response to malaria infection varies depending on factors. Factors like the genetic make-up of parasite proteins, co-infections, host genetics, host ethnic background, and geographical locations (5, 6). The response starts with physical barriers, progresses to an innate immune response, and leads to more adaptive responses.

Brief overview of the *Plasmodium* life cycle

The malaria parasites have a complex life cycle requiring a human and mosquito host (7). During the blood meal of the female Anopheles mosquito, sporozoites are transmitted into the human hosts (8). The pre-erythrocytic developmental stage is initiated when the released sporozoites migrate to the host liver. In the liver, the released sporozoites infect the hepatocytes (liver cells) in a process known as the liver stage. Within the hepatocytes the parasites grow and replicate as hepatic schizonts over a period of 10–12 days after which they are released as merozoites. The blood stage of the parasite starts when the merozoites rapidly invades the red blood cells (RBCs) in the bloodstream. During the blood stage, the merozoites replicates to produce more daughter parasites which are then released from the host cell upon parasite egress and subsequently re-invade RBCs to start a new asexual replication cycle (9). A small proportion of the malaria parasites will eventually differentiate into gametocytes to begin the sexual cycle which are subsequently taken up by mosquitos during the next blood meal (10).

Neutrophil functions

Neutrophils are the most abundant white blood cell accounting for up to 70% of all blood leukocytes (11). They are also known as polymorphonuclear cells (PMNs) and are terminally differentiated leukocytes. Neutrophils are professional phagocytes, which use receptor mediated phagocytosis to internalize pathogens into phagolysosomes (12). Cytoplasmic granules include cathepsins, elastases, and myeloperoxidases that fuse with the phagolysosome to digest phagocytosed pathogens, in a process known as degranulation (12). Release of reactive oxygen species (ROS), produced *via* an NADPH oxidase-dependent process is a crucial bactericidal mechanism. Neutrophils can also kill extracellular pathogens by degranulation, secretion of ROS, or the release of neutrophil extracellular traps (NETs). NETs is the release of decondensed chromatin laced with granular proteins and histones to prevent the spread of pathogens (13).

Neutrophils are crucial for the body's innate immune response (14, 15) and are involved in various disease processes, including pathogen infection (16), pulmonary diseases (17), cardiovascular diseases (18), inflammatory disorders (19) and cancer (20). They are challenging to study because they are short-lived effector cells of the innate immune system. Upon sensing infection, neutrophils are the first cells to migrate to the infection site (21). At the affected tissues, neutrophils use multiple antimicrobial functions such as engulfing foreign matter for internal digestion, reactive oxygen species (ROS) production and releasing NETs. The immune system plays a vital role in controlling the parasite's growth (22). Clinical data has shown that the number of circulating neutrophils is high in patients with acute uncomplicated malaria (23), in contrast to circulating lymphocytes, which decrease during *P. falciparum* infections. During *Plasmodium* infection, parasites components and cytokines are produced and might activate circulating neutrophils. Activated neutrophils are equipped with several weapons to mount an immune defense against the parasite. While on the other hand, these neutrophil weapons might also be involved in the pathogenesis of severe malaria, though the underlying mechanism is still unclear.

During malaria infection, the immune system is overwhelmed resulting in immune suppression thereby making malaria patients to be at risk of developing secondary infections. One well-documented risk factor for invasive bacterial infection is *Plasmodium falciparum* malaria (24, 25). In Sub-Saharan Africa countries, bacterial infection in children is highly associated with malaria infection (26–28). In this review, we assess the literature examining the role of neutrophils during malaria infection and the neutrophil related mechanism involved in malaria patients' susceptibility to bacterial infection.

The role of neutrophils in response to *Plasmodium* parasite

One of the ways by which neutrophil play a role in the clearance of malaria parasites is by phagocytosis. Neutrophils express immunoglobulin (Ig) binding receptors Fcγ receptors and complement receptor 1 (CR1) and complement receptor 3 (CR3) (29). Phagocytosis of the released sporozoites during malaria infection are facilitated by the FcγR-receptors and by the presence of antibodies against the circum-sporozoite protein, one of the main surface antigens on sporozoites (30). Phagocytosis of parasite infected red blood cells (iRBC) *in vivo* has been observed in children with malaria (31) and in bone marrow aspirates which show neutrophils with internalized merozoites and trophozoites (32). The interaction between neutrophils and iRBCs is mediated by PfEMP1 on the iRBC surface and ICAM-1 expressed on neutrophils (33).

Neutrophil phagocytosis of free merozoites could be in an antibody dependent manner or *via* a complement mediated opsonization manner (23, 34) and can be enhanced in the

presence of immune sera or when cytokines such as interferon gamma and tumor necrosis factor was added (35, 36). Recently, it was demonstrated that at high antibody levels, neutrophils are more effective *via* the action of FcγRIIA and FcγRIIIB (37). This may suggest that neutrophils are responsible for the phagocytosis of parasites in immune patients. In addition, neutrophil uptake of serum opsonized merozoites has been demonstrated *in vitro* and *ex vivo* (38). In contrast to complement dependent merozoites phagocytosis, phagocytosis of iRBC in neutrophil is largely dependent on the presence of IgG (39). Neutrophils phagocytose gametes *in vitro* in conditions similar to those of the mosquito gut when immune sera is present especially IgG (40). However, *ex vivo* evidence of the specific role of neutrophil phagocytosis of intra erythrocytic gametes in human is still lacking.

Neutrophils can clear pathogens by producing ROS by converting oxygen to superoxide *via* nicotinamide adenine dinucleotide phosphate oxidase (NADPH) oxidase (NOX). This superoxide is converted into hydrogen peroxide (H_2O_2) and hydroxyl radicals (-OH), collectively known as ROS (41). Neutrophils may also be involved in the control of parasite growth through antibody-dependent respiratory burst (ADRB) (35). Neutrophils isolated from malaria patients have been shown to exhibit higher ADRB activity *in vitro* and promote parasite clearance by inhibiting parasite growth (42). ROS related parasite inhibition occurs during the parasite intra-erythrocytic development stage (43) rather than during the merozoite stage. This was further demonstrated by Dasari et al. that ROS production from stimulated neutrophils does not inhibit merozoite growth *in vitro* (34). Though the mechanism underlying the observed impaired ROS production in neutrophils during malaria is unclear but released hemozoins (23) and digestive vacuoles (DV) (34) from iRBC have been suggested to be responsible.

Evidence of NETs in Malaria

Neutrophil extracellular trap (NET) formation is an essential innate strategy for immobilizing and killing foreign pathogens by neutrophils. It occurs when activated neutrophils degranulate and release their antimicrobial factors into the extracellular environment. Several factors might induce NET formation during *Plasmodium* infections such as crystal uric acid is a potent inducer of NETosis (44) (*Plasmodium* cannot synthesize purines and imports hypoxanthine as a purine source (45). Upon erythrocyte rupture and release, xanthine dehydrogenase, which is normally present in the blood (46) will efficiently degrade it into uric acid and are released into circulation during malaria. *Plasmodium*-infected erythrocytes accumulate hypoxanthine, a precursor for uric acid), pro-inflammatory cytokines like TNF and IL8 increase during *Plasmodium* infections (47), H2O2 is secreted by immune cells stimulated by the malaria parasite and *Plasmodium* antigens induce NETosis *in vitro* (48). NETs may contribute to the host defense against sporozoites and merozoites (35). Studies have shown that in the peripheral blood of children with complicated and uncomplicated *P. falciparum* infections, NETs like structures are present (49, 50). The release of NETs might play a crucial role in controlling parasite dissemination, but on the other hand, it may also contribute to the development of severe complications. Few studies have reported the possible role of NETs in controlling parasite growth during malaria. For example, Kho and colleagues reported that NET formation was inversely associated with parasitemia levels in patients with asymptomatic malaria (51). Another study by Rodrigues et al. showed that Pulmozyme (active molecule: DNase 1) treatment to inhibit NETosis resulted in increased parasitemia levels in *P. berghei* infected mice and subsequently decreased survival rate (49). However, the group also reported that the same observation was not recorded when *P. chabaudi*-infected mice were treated with Pulmozyme. Interestingly, *Plasmodium* parasites express TatD-like DNases to cleave NETs. *In vivo* mouse data have shown that treatment of mice with recombinant TatD resulted in low parasitemia and ultimately increased survival rate (52). Knackstedt et al. demonstrated that NETs might be driving inflammatory pathogenesis in malaria (53). However, evidences that NETs released in response to malaria parasite and proof that NETs are present in tissues is still debatable. For example, Feintuch and colleagues reported that brain tissue sections from children with fatal cerebral malaria (CM) and associated retinopathy were stained with NET markers, neutrophil elastase, and citrullinated histones, with no evidence of NETs was observed (54). In contrast, a recent study by Knackstedt et al. examined and analyzed retinal tissue from fatal pediatric cases who had died of cerebral malaria. The authors showed the image of NETs by colocalizing citrullinated histone H3, elastase, and DAPI (53).

The role of neutrophils in the pathogenesis of malaria

Neutrophils may also contribute to the pathophysiology of malaria complications. Studies have associated high number of neutrophils with severe malaria cases (51, 53). The association between plasma levels of MPO, lysozyme and neutrophil lipocalin and malaria severity has been reported by several studies (35, 51, 53). In patients with severe malaria, neutrophil granule proteins such as neutrophil elastase and defensin have been observed to be increased compared to uncomplicated malaria patients (55). Another study also reported that during CM, neutrophil proteins in plasma are associated with CM and may contribute to CM pathology (endothelium damage *via* neutrophil elastase) (56) (Figure 1). Another indication for

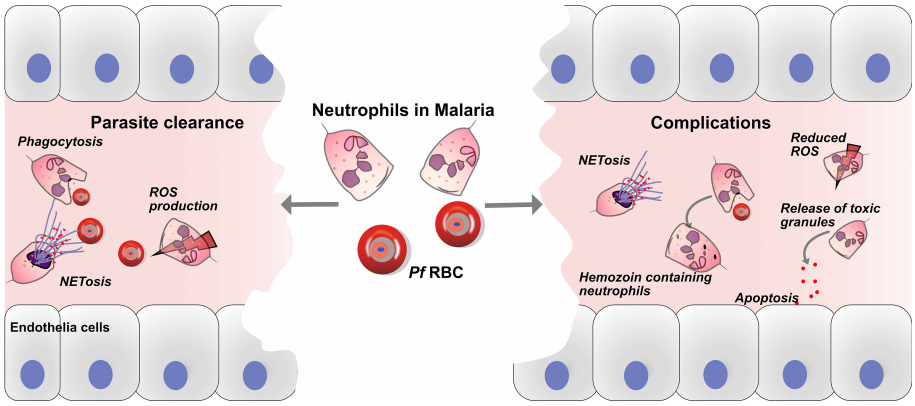

FIGURE 1
Roles of neutrophils in defense and pathology of malaria. Neutrophils play crucial roles in the immune defense against malaria, through parasite clearance *via* neutrophil phenotypic functions such as phagocytosis, reactive oxygen species (ROS) production and NETs release. On the other hand, neutrophils might play a role in the development of malaria complications, and haemozoin-containing neutrophils are associated with malaria severity. In addition, the release of toxic granules, such as myeloperoxidase (MPO), neutrophil elastase (NE) and matrix metalloproteinase-8 (MMP-8), causes endothelial cell damage *via* apoptosis. Finally, the release of NETs may aggravate complications during malaria infection.

neutrophil activation is the release of matrix metalloproteinase (MMP)-8 and 9. For example, increased levels of plasma protein MMP-8 was reported in malaria patient, but no significant difference between uncomplicated and severe malaria. Furthermore, in Sub Saharan African children with CM, immunohistochemical staining revealed the presence of MMP-8 in the retina tissue accompanied with oedema, thus suggesting the role of MMP-8 in vascular endothelial barrier disruption (57). In addition, *in vivo* data further demonstrated that knocking out MMP-9 had no significant effect on CM development and survival in mice (58). Chemokines such as CXCLI and CXCL8 are known neutrophil chemoattractants, were at an increased level in the plasma of severe malaria patients (59). Furthermore, studies have associated a link between hemozoin laden neutrophils and disease severity has been reported in several malaria patients (60–62). In conclusion, these studies suggest a link between neutrophil activation and malaria severity.

Murine malaria model to understand the role of neutrophils in malaria pathogenesis

Animal models have been used to study the role of neutrophils in malaria complications including lung injury, CM and liver injury (17, 63, 64). Murine models have demonstrated the association of accumulated neutrophils in the lungs with lung injury. Murine models of CM have demonstrated that neutrophils express cytokines such as IL2, IL12, IL18, IFNγ, and TNF and chemoattractive-chemokines (65) suggesting a role for neutrophils in cytokine and chemokine secretion during CM. Nacer and colleagues reported that neutrophils in murine CM are detected in the vasculature (66) and their depletion prevented CM development (67). Using chimeric mice, Ioannidis and colleagues identified neutrophils as the main cellular sources of CXCL10, a CXCR3 binding chemokine which is essential for the attraction of pathogenic CD8+ T cells to the brain in murine CM (68). In addition, studies revealed that circulating levels of CXCL10 is the most accurate predictor of CM mortality (69) (70) and its neutralization with specific mAbs, significantly prevents brain intravascular inflammation and protects infected animals from CM by reducing peripheral parasitemia level (71–73).

Murine malaria models: Neutrophil contradicting data

Murine models have over the years played a valuable role in understanding the role of neutrophils in malaria (Table 1) however, there are contradicting data on the role of neutrophils using the mouse model, and as such, neutrophils' role in malaria is still unclear. For example, Schumak et al. (74) suggested that the number of circulating neutrophils in the blood and brain increased in *P. berghei* ANKA infected mice, while in contrast, Pai et al. reported no increase in the number of circulating neutrophils in the brain (79) though the experimental approach to count neutrophils were different in the two studies. In Schumak study, brain tissue was fixed in buffered formalin and quantification of neutrophils in tissue

TABLE 1 Showing studies on neutrophil in murine malaria.

Mouse strain	Parasite strain/Load/ route of infection	Procedure for neutrophil depletion	Strategy of neutrophil detection	Outcome of neutrophil depletion	Ref.
C57BL/6	Transgenic *P.berghei* ANKA expressing ovalbumin (PbTg) infected RBC/5*10^4/i.v	250 µg of anti-GR1(day 0 of infection or day 3-5 p.i for 30 mins i. p^1)	Flow cytometry on blood samples: $CD11b^+$ $Ly6C^{int}$ $Ly6G^+$	CM developed on day 6 post infection, survival rate was 80% and no effect on parasitemia level.	(74)
C57BL/6	Transgenic *P.berghei* ANKA expressing ovalbumin (PbTg) infected RBC/5*10^4/i.v.	250 µg of anti-GR1(day 3 and day 5 i.p)	Flow cytometry on blood samples: CD45+ $Ly6C^{int}$ Ly6G+	Decreased CM development on day 6 p.i, high survival rate and no effect on parasitemia level.	(74)
C57BL/6	*P.berghei* -ANKA infected RBC/1*10^6/i.p.	200 µg of anti-CXCL10 (between day 3 and 9 p.i)	Flow cytometry on spleen samples: Ly6G+	High CM, low survival rate and low parasitemia level.	(68)
C57BL/6	*P.berghei* -ANKA infected RBC/1*10^5/i.v.	Pulmozyme (5mg/kg for every 8h i.p.)	Not Applicable	Low survival rate at 20%, 100% mortality by day 10 post infection and parasitemia increased day 6 p.i.	(49)
C57BL/6, BALB/c	*P.berghei* -ANKA and NK65 infected RBC/1*10^6/i.p.	Immunization with r*Pb*TatD or rPcTatD (50 µg intramuscularly every 14 days).	Not Applicable	100% survival rate and reduced parasitemia level.	(52)
CBA/ NSlc	*P.berghei* -ANKA infected RBC/1*10^6/i.p.	250 µg of anti-GR1 (day 1 or day 5 i.p.)	Tail blood	no CM development (low hemorrhage), survival rate was 90% by day 10 post infection and no effect on parasitemia level.	(67)
DBA/2	*P.berghei* -ANKA infected RBC/1*10^6/NA	anti-GR1(0.2mg on day 1 p.i)	Flow cytometry on blood samples and microscopy of blood smear	Low MA-ARDS development, survival rate was 90% by day 10 post infection and no effect on parasitemia level.	(17)
129/Ola + C57BL/ 6J mice	*P.berghei* -ANKA infected RBC/1*10^7/NA	anti-GR1(1mg on day 6 post infection i.p.)	Flow cytometry on blood samples: GR1+	There was 60%-80% of CM development and survival rate was 0% after 24h of CM development.	(75)
CBA/Ca	*P.berghei* -ANKA infected RBC/1*10^6/i.p.	anti-GR1(0.5mg on day 5 post infection i.p.)	Microscopy of blood smear	BBB was not disrupted, delayed death and high survival rate (80%).	(76)
BALB/c	PyMDR/NA	anti-GR1(day 3 until day 7 post infection i.p.)	Not Applicable	Low liver injury (low AST, ALT and ALP $levels^2$).	(77)
C57BL/6	*P.chabaudi* AS infected RBC/ 1*10^4/i.v.	$DNase^{-/-}$	Flow cytometry on blood samples: CD45+ CD3− Ly6G/ Chi	Low liver injury, low AST level and no effect on parasitemia level.	(53)
C57BL/6	*P.chabaudi* AS infected RBC/ 1*10^4/i.v.	NE/PR3−/−	Flow Cytometry on blood samples: CD45+ CD3− Ly6G/ Chi	Low liver injury, low AST level and no effect on parasitemia level.	(53)
C57BL/6	*P.chabaudi* AS infected RBC/ 1*10^4/i.v.	Anti-G-CSF (day 7 post infection i.v.)	Flow Cytometry on blood samples: CD45+ CD3− Ly6G/ Chi	Low liver injury, low AST level.	(53)
C57BL/6	*P. yoelli* 17XNL infected RBC/2*10^4/i.v.	MPO−/−	Not Applicable	Not determine, however no effect on parasitemia level on day 6-12 post infection, parasitemia level increased after day 12 post infection.	(78)
C57BL/6 + *Py*17XNL	*P. yoelli* 17XNL infected RBC/2*10^4/i.v.	Anti-Ly6G (500 µg i.p.)	Flow Cytometry on blood samples: CD11b+ Ly6Cint GR1+	Not determine, however no effect on parasitemia level.	(78)

i.p., Intraperitoneal; i.v., Intravenously; p.i, Post infection; i.m., Intramuscularly; AST, aspartate aminotransferase; ALT, alanine aminotransferase; ALP, alkaline phosphatase.

sections was performed in 10 high power fields (HPF). While in Pai study, neutrophils were quantified in real time using 2-photon intravital microscopy. Another contradiction is the link between neutrophil depletion and survival rate in murine CM model. For example, some *in vivo* studies demonstrated that depletion of neutrophils using anti-CD11a resulted in an increased survival rate and slowed down the rate of CM development (67, 80) (**Table 1**). In these studies, depletion of neutrophils was done using anti-CD11A or anti-GR1 before parasite infection, which depleted neutrophils and other leukocytes. In contrast, when anti-GR1 was administered late during the infection, the authors still observed CM development in their model except for a study by Senaldi and colleague (76). In contrast, another study showed that when specific anti-Ly6G antibody was used for neutrophil depletion, no CM development was observed (74) (Table 1). Interestingly, neutrophil released CXCL10 is known to recruit pathogenic $CD8^+$ T cells to the brain in murine CM (68). The indirect effect on CD8+ T cells in the murine CM by the anti-GR1 antibody might explain the contradicting data. Therefore, there is a need for more in depth studies to elucidate whether neutrophils count plays a role in the development of CM.

Malaria co-infection with bacteria: Any neutrophil link?

Salmonella co-infection is a common bacterial infection, and it remains a global health concern. One well-documented risk factor for *Salmonella* is *Plasmodium falciparum* malaria (25). It's often a lethal complication of *P. falciparum* infection in Sub-Saharan Africa. In Gambia, the incidence of invasive NTS infection mirrors that of malaria, and about 43% of children with *Salmonella* bacteremia had concurrent *P. falciparum* infections (81). In Tanzania, invasive NTS in young children is highly associated with recent malaria infection (26). Interestingly evidence from co-infection models supports this idea (**Table 2**). For example, a study by Cunnington and colleagues demonstrated that prior infection of mice with non-lethal *P. yoelii* resulted in decreased survival of *S. typhimurium* in the mice. Though the authors suggested that the decrease in the survival rate of the mice was a result of impaired ROS production in neutrophils (85), the mechanism underlying the neutrophil-associated immune suppression remains unclear.

Underlying mechanisms of neutrophil associated immune suppression during malaria

During malaria infection, the parasite continuously breaks down RBCs followed by eryptosis of many uninfected RBCs (87). The direct destruction of RBC leads to the release of hemoglobin, or its breakdown product heme, into the plasma. Free heme is prooxidant and highly cytotoxic, contributing to endothelial injury (88). Intracellular heme is then degraded into equimolar amounts of iron, carbon monoxide, and biliverdin through the action of heme oxygenase (HO). Significantly, plasma heme is raised during both acute (89) and subclinical (90) *P. falciparum* malaria infections in humans and during acute *P. yoelii* infection in mice (85) https://jlb.onlinelibrary.wiley.com/doi/full/10.1002/JLB.3RI1018-400R - jlb10293-bib-0063. Studies have shown that hemolysis might be responsible for inhibiting neutrophil functions during malaria. For example, Cunnington and colleagues using a malaria mouse model demonstrated that neutrophils from malaria-infected mice could phagocytose S. typhimurium; however, their ability to kill was impaired.

The authors further reported that the phagocytosed bacteria remained viable and replicated within the phagosome due to deficient ROS production (85). In another study, neutrophils from children with acute malaria were observed to exhibit impaired ROS production. The authors recorded that the dysfunctional ROS production persists for up to 8 weeks after drug treatment (89). The authors suggested that this might explain why children with acute malaria remain susceptible to secondary bacterial infection (27). Several studies have shown that during malaria infection, the migration of neutrophils into the infected tissues, including blood (85), intestine (82), and liver (84) is impaired. Neutrophils precursors of *Plasmodium*-infected mice have been shown to express heme oxygenase-1(HO-1) (85), which has been reported to reduce neutrophil migration into the inflamed lung (91), thus suggesting an association between HO-1 and neutrophil migration.

During the parasite life cycle in the RBC, the malaria parasite feeds on the hemoglobin and packages the waste product hemozoin in an organelle designated the digestive vacuole (DV) (92). Large numbers of DVs are released into blood circulation during severe malaria infection. Some reports have implicated the role of DVs in suppressing the host immune system *via* the inhibition of neutrophil functions. For example, a study by Dasari and colleagues demonstrated that phagocytosed

TABLE 2 Showing studies on malaria and salmonella co-infection.

Plasmodium spp.	Bacteria Strain	Bacteria load	Route of bacteria challenge	Time of bacteria Co infection	End point	Bacteria-related Outcome	Animal strain	Ref.
P. yoelii nigeriensis	*S.* typhimurium strain (IR715)	1×10^8 CFU^3.	Intragastric	Day 10	Day 14	Reduced intestinal inflammation to NTS	CBA/J	(82)
P. yoelii nigeriensis	*S.* typhimurium strain (IR715)	Not available	Intragastric	Day 10	Day 11	Increased NTS colonization in feces.	C57BL/6J	(83)
P. yoelii nigeriensis	*S.* typhimurium strain (IR715)	1×10^8 CFU.	Intra-peritoneal	Day 10	Day 12, 13	Increased CFU in liver.	CBA/J	(84)
P. fragile	*S.* typhimurium strain (IR715)	1×10^8 CFU.	Ligated ilieal loops	Day 14, 15	8h	Reduced intestinal inflammation to NTS.	*Macaca mulatta*	(82)
P. yoelii nigeriensis	*S.* typhimurium strain (IR715)	1×10^8 CFU.	Intragastric	Day 0	Day 5	Increased CFU in liver, spleen and peyer's patch and spleen	CBA/J	(84)
P. yoelii 17XNL	12023-GFP	1×10^5 CFU	Intra-peritoneal	Day 15	18h	Increased CFU in blood, spleen, and liver.	C57BL/6	(85)
P. yoelii 17XNL	*S.* typhimurium strain (BRD509)	1×10^8 CFU.	Intravenous	Day 14, 28	Day 17, 31	Increased CFU in liver	C57BL/6	(86)

CFU, Colony Forming Unit.

DVs induce oxidative burst in human neutrophils. However, the capacity to generate a subsequent ROS response to kill phagocytose bacteria was impaired (34). Thus, the anti-microbicidal activity was compromised. They suggested that DV might explain the risk of developing bacterial sepsis in patients with severe malaria. However, much more work is needed to fully characterize the content of these DVs and their effect on neutrophil migration during malaria infection.

Future direction and conclusion

Neutrophils in malaria remain understudied and they play a double-edge sword role in malaria. During malaria infection, neutrophils may be involved in defense mechanisms against parasites *via* phagocytosis and ROS production. On the other hand, neutrophils might also be involved in the pathogenesis of severe malaria *via* NETs and toxic granule proteins release. Therefore, more research studies are required to understand the specific roles of neutrophils in malaria.

During malaria, small extracellular vesicles (EVs) are secreted by *Plasmodium* infected RBC (iRBCs). EVs contribute to the immune regulation by transferring cargoes including RNAs from the iRBCs to immune cells, resulting in immune suppression or immune activation depending on the cellular context. Currently, it's not clear if these EVs are involved in the observed immune suppression *via* the modulation of neutrophil functions in malaria patients. It will be interesting to know if EVs can deliver their biological cargoes to neutrophils which in turn maybe responsible for the observed immune suppression.

There seems to be a lot of contradicting neutrophil data using both *in vitro* and *in vivo* malaria models. We suggest that a novel *ex vivo* microfluidic platform, modelling the *in vivo* malaria infection microenvironment, will allow studying the interaction of neutrophils and malaria at single cell resolution and in real time. Such platform should allow the investigation of neutrophil migration, NETs release and parasite killing during neutrophil-parasite interaction.

Author contributions

KB conceptualized the review. KB and OA drafted the review. KB prepared the figure and we read and adapted the manuscript and approved the final version.

Funding

This work is supported by the Swiss National funding (P500PB_203002) and a grant from the Jubilee Foundation of the Swiss Life Insurance and Pension Fund for Public Health and Medical Research to KB.

Conflict of interest

The authors declare that the research was conducted in the absence of any commercial or financial relationships that could be construed as a potential conflict of interest.

Publisher's note

References

1. Schofield L, Grau GE. Immunological processes in malaria pathogenesis. *Nat Rev Immunol* (2005) 5:722–35. doi: 10.1038/nri1686

2. World Health Organization. *WHO World Malaria Report 2021. Malaria report 2021*. (2021).

3. Adebayo JO, Krettli AU. Potential antimalarials from Nigerian plants: A review. *J Ethnopharmacol* (2011) 133:289–302. doi: 10.1016/j.jep.2010.11.024

4. Laishram DD, Sutton PL, Nanda N, Sharma VL, Sobti RC, Carlton JM, et al. The complexities of malaria disease manifestations with a focus on asymptomatic malaria. *Malar J* (2012) 11:1475–2875. doi: 10.1186/1475-2875-11-29

5. Balaji S, Deshmukh R, Trivedi V. Severe malaria: Biology, clinical manifestation, pathogenesis and consequences. *J Vector Borne Dis* (2020) 57:1–13. doi: 10.4103/0972-9062.308793

6. Moxon CA, Gibbins MP, McGuinness D, Milner DA, Marti M. New insights into malaria pathogenesis. *Annu Rev Pathol Mech Dis* (2020). doi: 10.1146/annurev-pathmechdis-012419-032640

7. Babatunde KA, Yesodha Subramanian B, Ahouidi AD, Martinez Murillo P, Walch M, Mantel PY. Role of extracellular vesicles in cellular cross talk in malaria. *Front Immunol* (2020) 11. doi: 10.3389/fimmu.2020.00022

8. Aly ASI, Vaughan AM, Kappe SHI. Malaria parasite development in the mosquito and infection of the mammalian host. *Annu Rev Microbiol* (2009) 63:195–221. doi: 10.1146/annurev.micro.091208.073403

9. Cowman AF, Crabb BS. Invasion of red blood cells by malaria parasites. *Cell* (2006) 124:755–86. doi: 10.1016/j.cell.2006.02.006

10. Baker DA. Malaria gametocytogenesis. *Mol Biochem Parasitol* (2010) 172:56–65. doi: 10.1016/j.molbiopara.2010.03.019

11. Mooney JP, Galloway LJ, Riley EM. Malaria, anemia, and invasive bacterial disease: A neutrophil problem? *J Leukoc Biol* (2019) 105:644–55. doi: 10.1002/JLB.3RI1018-400R

12. Kruger P, Saffarzadeh M, Weber ANR, Rieber N, Radsak M, von Bernuth H, et al. Neutrophils: Between host defence, immune modulation, and tissue injury. *PloS Pathog* (2015) 11:e1004651. doi: 10.1371/journal.ppat.1004651

13. Sollberger G, Tilley DO, Zychlinsky A. Neutrophil extracellular traps: The biology of chromatin externalization. *Dev Cell* (2018) 44:542–53. doi: 10.1016/j.devcel.2018.01.019

14. Rosales C. Neutrophil: A cell with many roles in inflammation or several cell types? *Front Physiol* (2018) 9. doi: 10.3389/fphys.2018.00113

15. Babatunde KA, Ayuso JM, Kerr SC, Huttenlocher A, Beebe DJ. Microfluidic systems to study neutrophil forward and reverse migration. *Front Immunol* (2021) 12. doi: 10.3389/fimmu.2021.781535

16. Jenne CN, Wong CHY, Zemp FJ, McDonald B, Rahman MM, Forsyth PA, et al. Neutrophils recruited to sites of infection protect from virus challenge by releasing neutrophil extracellular traps. *Cell Host Microbe* (2013) 13:169–80. doi: 10.1016/j.chom.2013.01.005

17. Sercundes MK, Ortolan LS, Debone D, Soeiro-Pereira PV, Gomes E, Aitken EH, et al. Targeting neutrophils to prevent malaria-associated acute lung Injury/Acute respiratory distress syndrome in mice. *PloS Pathog* (2016) 13:e1006730. doi: 10.1371/journal.ppat.1006054

18. Silvestre-Roig C, Braster Q, Wichapong K, Lee EY, Teulon JM, Berrebeh N, et al. Externalized histone H4 orchestrates chronic inflammation by inducing lytic cell death. *Nature* (2019) 569:263–240. doi: 10.1038/s41586-019-1167-6

19. Csepregi JZ, Orosz A, Zajta E, Kása O, Németh T, Simon E, et al. Myeloid-specific deletion of mcl-1 yields severely neutropenic mice that survive and breed in homozygous form. *J Immunol* (2018) 201:3793–803. doi: 10.4049/jimmunol.1701803

20. Hedrick CC, Malanchi I. Neutrophils in cancer: heterogeneous and multifaceted. *Nat Rev Immunol* (2022) 22:173–87. doi: 10.1038/s41577-021-00571-6

21. De Oliveira S, Rosowski EE, Huttenlocher A. Neutrophil migration in infection and wound repair: Going forward in reverse. *Nat Rev Immunol* (2016) 16:378–91. doi: 10.1038/nri.2016.49

22. Deroost K, Pham TT, Opdenakker G, Van den Steen PE. The immunological balance between host and parasite in malaria. *FEMS Microbiol Rev* (2016) 40:208–57. doi: 10.1093/femsre/fuv046

23. Aitken EH, Alemu A, Rogerson SJ. Neutrophils and malaria. *Front Immunol* (2018) 9:3005. doi: 10.3389/fimmu.2018.03005

24. Takem EN, Roca A, Cunnington A. The association between malaria and nontyphoid salmonella bacteraemia in children in sub-Saharan Africa: A literature review. *Malar J* (2014) 13:475–2875. doi: 10.1186/1475-2875-13-400

25. Church J, Maitland K. Invasive bacterial co-infection in African children with plasmodium falciparum malaria: A systematic review. *BMC Med* (2014) 12:1741–7015. doi: 10.1186/1741-7015-12-31

26. Mtove G, Amos B, Von Seidlein L, Hendriksen I, Mwambuli A, Kimera J, et al. Invasive salmonellosis among children admitted to a rural Tanzanian hospital and a comparison with previous studies. *PloS One* (2010) 5:e9244. doi: 10.1371/journal.pone.0009244

27. Biggs HM, Lester R, Nadjm B, Mtove G, Todd JE, Kinabo GD, et al. Invasive salmonella infections in areas of high and low malaria transmission intensity in Tanzania. *Clin Infect Dis* (2014) 58:638–47. doi: 10.1093/cid/cit798

28. Bronzan RN, Taylor TE, Mwenechanya J, Tembo M, Kayira K, Bwanaisa L, et al. Bacteremia in Malawian children with severe malaria: Prevalence, etiology, HIV coinfection, and outcome. *J Infect Dis* (2007) 195:895–904. doi: 10.1086/511437

29. Dale DC, Boxer L, Conrad Liles W. The phagocytes: Neutrophils and monocytes. *Blood* (2008) 112:935–45. doi: 10.1182/blood-2007-12-077917

30. Feng G, Wines BD, Kurtovic L, Chan JA, Boeuf P, Mollard V, et al. Mechanisms and targets of fcgamma-receptor mediated immunity to malaria sporozoites. *Nat Commun* (2021) 12:1742. doi: 10.1038/s41467-021-21998-4

31. Sun T, Chakrabarti C. Schizonts, merozoites, and phagocytosis in falciparum malaria. *Ann Clin Lab Sci* (1985) 15:465–9.

32. Wickramasinghe SN, Phillips RE, Looareesuwan S, Warrell DA, Hughes M. The bone marrow in human cerebral malaria: parasite sequestration within sinusoids. *Br J Haematol* (1987) 66:295–306. doi: 10.1111/j.1365-2141.1987.00295.x

33. Zelter T, Strahilevitz J, Simantov K, Yajuk O, Adams Y, Jensen AR, et al. Neutrophils impose strong immune pressure against PfEMP1 variants implicated in cerebral malaria. *EMBO Rep* (2022) 23:e53641. doi: 10.15252/embr.202153641

34. Dasari P, Reiss K, Lingelbach K, Baumeister S, Lucius R, Udomsangpetch R, et al. Digestive vacuoles of plasmodium falciparum are selectively phagocytosed by and impair killing function of polymorphonuclear leukocytes. *Blood* (2011). 118:4946–56 doi: 10.1182/blood-2011-05-353920

35. Tannous S, Ghanem E. A bite to fight: front-line innate immune defenses against malaria parasites. *Pathog Glob Health* (2018) 112:1–12. doi: 10.1080/20477724.2018.1429847

36. Kumaratilake LM, Rathjen DA, Mack P, Widmer F, Prasertsiriroj V, Ferrante A. A synthetic tumor necrosis factor-α agonist peptide enhances human polymorphonuclear leukocyte-mediated killing of plasmodium falciparum *in vitro* and suppresses plasmodium chabaudi infection in mice. *J Clin Invest* (1995) 95:2315–23. doi: 10.1172/JCI117923

37. Garcia-Senosiain A, Kana IH, Singh S, Das MK, Dziegiel MH, Hertegonne S, et al. Neutrophils dominate in opsonic phagocytosis of p. falciparum blood-stage merozoites and protect against febrile malaria. *Commun Biol* (2021) 4:984. doi: 10.1038/s42003-021-02511-5

38. Kumaratilake LM, Ferrante A. Opsonization and phagocytosis of plasmodium falciparum merozoites measured by flow cytometry. *Clin Diagn Lab Immunol* (2000) 7:9–13. doi: 10.1128/cdli.7.1.9-13.2000

39. Celada A, Cruchaud A, Perrin LH. Phagocytosis of plasmodium falciparum-parasitized erythrocytes by human polymorphonuclear leukocytes. *J Parasitol* (1983) 69:49–53. doi: 10.2307/3281273

40. Healer J, Graszynski A, Riley E. Phagocytosis does not play a major role in naturally acquired transmission-blocking immunity to plasmodium falciparum malaria. *Infect Immun* (1999) 67:2334–9. doi: 10.1128/iai.67.5.2334-2339.1999

41. Dupré-Crochet S, Erard M, Nüβe O. ROS production in phagocytes: why, when, and where? *J Leukoc Biol* (2013) 94:657–70. doi: 10.1189/jlb.1012544

42. Llewellyn D, Miura K, Fay MP, Williams AR, Murungi LM, Shi J, et al. Standardization of the antibody-dependent respiratory burst assay with human neutrophils and plasmodium falciparum malaria. *Sci Rep* (2015) 5: 14081. doi: 10.1038/srep14081

43. Nnalue NA, Friedman MJ. Evidence for a neutrophil-mediated protective response in malaria. *Parasite Immunol* (1988) 10:47–58. doi: 10.1111/j.1365-3024.1988.tb00202.x

44. Hoppenbrouwers T, Autar ASA, Sultan AR, Abraham TE, Van Cappellen WA, Houtsmuller AB, et al. *In vitro* induction of NETosis: Comprehensive live imaging comparison and systematic review. *PloS One* (2017) 12:e0176472. doi: 10.1371/journal.pone.0176472

45. Asahi H, Kanazawa T, Kajihara Y, Takahashi K, Takahasht T. Hypoxanthine: A low molecular weight factor essential for growth of erythrocytic plasmodium falciparum in a serum-free medium. *Parasitology* (1996). doi: 10.1017/s0031182000066233

46. Heath WR, Carbone FR. Immunology: dangerous liaisons. *Nature* (2003). doi: 10.1038/425460a

47. Dunst J, Kamena F, Matuschewski K. Cytokines and chemokines in cerebral malaria pathogenesis. *Front Cell Infect Microbiol* (2017) 7. doi: 10.3389/fcimb.2017.00324

48. Percário S, Moreira DR, Gomes BAQ, Ferreira MES, Gonçalves ACM, Laurindo PSOC, et al. Oxidative stress in malaria. *Int J Mol Sci* (2012) 13:16346–372. doi: 10.3390/ijms131216346

49. Rodrigues DAS, Prestes EB, Gama AMS, de Souza Silva L, Pinheiro AAS, Ribeiro JMC, et al. CXCR4 and MIF are required for neutrophil extracellular trap release triggered by plasmodium-infected erythrocytes. *PloS Pathog* (2020) 16: e1008230. doi: 10.1371/JOURNAL.PPAT.1008230

50. Baker VS, Imade GE, Molta NB, Tawde P, Pam SD, Obadofin MO, et al. Cytokine-associated neutrophil extracellular traps and antinuclear antibodies in plasmodium falciparum infected children under six years of age. *Malar J* (2008) 7: 41. doi: 10.1186/1475-2875-7-41

51. Kho S, Minigo G, Andries B, Leonardo L, Prayoga P, Poespoprodjo JR, et al. Circulating neutrophil extracellular traps and neutrophil activation are increased in proportion to disease severity in human malaria. *J Infect Dis* (2019) 219:1994–2004. doi: 10.1093/infdis/jiy661

52. Chang Z, Jiang N, Zhang Y, Lu H, Yin J, Wahlgren M, et al. The TatD-like DNase of plasmodium is a virulence factor and a potential malaria vaccine candidate. *Nat Commun* (2016) 7: 11537. doi: 10.1038/ncomms11537

53. Knackstedt SL, Georgiadou A, Apel F, Abu-Abed U, Moxon CA, Cunnington AJ, et al. Neutrophil extracellular traps drive inflammatory pathogenesis in malaria. *Sci Immunol* (2019) 4: 397. doi: 10.1126/SCIIMMUNOL.AAW0336

54. Feintuch CM, Saidi A, Seydel K, Chen G, Goldman-Yassen A, Mita-Mendoza NK, et al. Activated neutrophils are associated with pediatric cerebral malaria vasculopathy in Malawian children. *MBio* (2016) 7:e01300-–5. doi: 10.1128/mBio.01300-15

55. Lee HJ, Georgiadou A, Walther M, Nwakanma D, Stewart LB, Levin M, et al. Integrated pathogen load and dual transcriptome analysis of systemic host-pathogen interactions in severe malaria. *Sci Transl Med* (2018) 10:eaar3619. doi: 10.1126/scitranslmed.aar3619

56. Yang JJ, Kettritz R, Falk RJ, Jennette JC, Gaido ML. Apoptosis of endothelial cells induced by the neutrophil serine proteases proteinase 3 and elastase. *Am J Pathol* (1996) 149:1617–26.

57. Dietmann A, Helbok R, Lackner P, Issifou S, Lell B, Matsiegui PB, et al. Matrix metalloproteinases and their tissue inhibitors (TIMPs) in plasmodium falciparum malaria: Serum levels of TIMP-1 are associated with disease severity. *J Infect Dis* (2008) 197:1614–20. doi: 10.1086/587943

58. Van Den Steen PE, Van Aelst I, Starckx S, Maskos K, Opdenakker G, Pagenstecher A. Matrix metalloproteinases, tissue inhibitors of MMPs and TACE in experimental cerebral malaria. *Lab Investig* (2006) 86:873–88. doi: 10.1038/labinvest.3700454

59. Amulic B, Moxon CA, Cunnington AJ. A more granular view of neutrophils in malaria. *Trends Parasitol* (2020) 36: 501–3. doi: 10.1016/j.pt.2020.03.003

60. Amodu OK, Adeyemo AA, Olumese PE, Gbadegesin RA. Intraleucocytic malaria pigment and clinical severity of malaria in children. *Trans R Soc Trop Med Hyg* (1998) 92:54–6. doi: 10.1016/S0035-9203(98)90952-X

61. Phu NH, Day N, Diep PT, Ferguson DJP, White NJ. Intraleucocytic malaria pigment and prognosis in severe malaria. *Trans R Soc Trop Med Hyg* (1995) 89:200–4. doi: 10.1016/0035-9203(95)90496-4

62. Lyke KE, Diallo DA, Dicko A, Kone A, Coulibaly D, Guindo A, et al. Association of intraleukocytic plasmodium falciparum malaria pigment with disease severity, clinical manifestations, and prognosis in severe malaria. *Am J Trop Med Hyg* (2003) 69:253–9. doi: 10.4269/ajtmh.2003.69.253

63. Lin JW, Sodenkamp J, Cunningham D, Deroost K, Tshitenge TC, McLaughlin S, et al. Signatures of malaria-associated pathology revealed by high-resolution whole-blood transcriptomics in a rodent model of malaria. *Sci Rep* (2017) 7:41722. doi: 10.1038/srep41722

64. Lovegrove FE, Gharib SA, Peña-Castillo L, Patel SN, Ruzinski JT, Hughes TR, et al. Parasite burden and CD36-mediated sequestration are determinants of acute lung injury in an experimental malaria model. *PloS Pathog* (2008) 4: e1000068. doi: 10.1371/journal.ppat.1000068

65. Chen L, Sendo F. Cytokine and chemokine mRNA expression in neutrophils from CBA/NSlc mice infected with plasmodium berghei ANKA that induces experimental cerebral malaria. *Parasitol Int* (2001) 50:139–43. doi: 10.1016/S1383-5769(01)00063-0

66. Nacer A, Movila A, Sohet F, Girgis NM, Gundra UM, Loke P, et al. Experimental cerebral malaria pathogenesis–hemodynamics at the blood brain barrier. *PloS Pathog* (2014) 10:e1004528. doi: 10.1371/journal.ppat.1004528

67. Chen L, Zhang ZH, Sendo F. Neutrophils play a critical role in the pathogenesis of experimental cerebral malaria. *Clin Exp Immunol* (2000) 120:125–33. doi: 10.1046/j.1365-2249.2000.01196.x

68. Ioannidis LJ, Nie CQ, Ly A, Ryg-Cornejo V, Chiu CY, Hansen DS. Monocyte- and neutrophil-derived CXCL10 impairs efficient control of blood-stage malaria infection and promotes severe disease. *J Immunol* (2016) 196:1227–38. doi: 10.4049/jimmunol.1501562

69. Jain V, Armah HB, Tongren JE, Ned RM, Wilson NO, Crawford S, et al. Plasma IP-10, apoptotic and angiogenic factors associated with fatal cerebral malaria in India. *Malar J* (2008) 7: 83. doi: 10.1186/1475-2875-7-83

70. Wilson NO, Jain V, Roberts CE, Lucchi N, Joel PK, Singh MP, et al. CXCL4 and CXCL10 predict risk of fatal cerebral malaria. *Dis Markers* (2011) 30:39–49. doi: 10.3233/DMA-2011-0763

71. Campanella GSV, Tager AM, El Khoury JK, Thomas SY, Abrazinski TA, Manice LA, et al. Chemokine receptor CXCR3 and its ligands CXCL9 and CXCL10 are required for the development of murine cerebral malaria. *Proc Natl Acad Sci U.S.A.* (2008) 105:4812–19. doi: 10.1073/pnas.0801544105

72. Wilson NO, Solomon W, Anderson L, Patrickson J, Pitts S, Bond V, et al. Pharmacologic inhibition of CXCL10 in combination with anti-malarial therapy eliminates mortality associated with murine model of cerebral malaria. *PloS One* (2013) 8:e60898. doi: 10.1371/journal.pone.0060898

73. Miu J, Mitchell AJ, Müller M, Carter SL, Manders PM, McQuillan JA, et al. Chemokine gene expression during fatal murine cerebral malaria and protection due to CXCR3 deficiency. *J Immunol* (2008) 180:1217–30. doi: 10.4049/jimmunol.180.2.1217

74. Schumak B, Klocke K, Kuepper JM, Biswas A, Djie-Maletz A, Limmer A, et al. Specific depletion of Ly6Chi inflammatory monocytes prevents immunopathology in experimental cerebral malaria. *PloS One* (2015) 10: e0124080.. doi: 10.1371/journal.pone.0124080

75. Belnoue E, Kayibanda M, Vigario AM, Deschemin J-C, van Rooijen N, Viguier M, et al. On the pathogenic role of brain-sequestered αβ CD8 + T cells in experimental cerebral malaria. *J Immunol* (2002) 169:6369–75. doi: 10.4049/jimmunol.169.11.6369

76. Senaldi G, Vesin C, Chang R, Grau GE, Piguet PF. Role of polymorphonuclear neutrophil leukocytes and their integrin CD11a (LFA-1) in the pathogenesis of severe murine malaria. *Infect Immun* (1994) 62:1144–9. doi: 10.1128/iai.62.4.1144-1149.1994

77. Dey S, Bindu S, Goyal M, Pal C, Alam A, Iqbal MS, et al. Impact of intravascular hemolysis in malaria on liver dysfunction. *J Biol Chem* (2012) 287:26630–46. doi: 10.1074/jbc.m112.341255

78. Theeß W, Sellau J, Steeg C, Klinke A, Baldus S, Cramer JP, et al. Myeloperoxidase attenuates pathogen clearance during plasmodium yoelii nonlethal infection. *Infect Immun* (2017) 85:e00475–16. doi: 10.1128/IAI.00475-16

79. Pai S, Qin J, Cavanagh L, Mitchell A, El-Assaad F, Jain R, et al. Real-time imaging reveals the dynamics of leukocyte behaviour during experimental cerebral malaria pathogenesis. *PloS Pathog* (2014) 10:e1004236.. doi: 10.1371/journal.ppat.1004236

80. Porcherie A, Mathieu C, Peronet R, Schneider E, Claver J, Commere PH, et al. Critical role of the neutrophil-associated high-affinity receptor for IgE in the pathogenesis of experimental cerebral malaria. *J Exp Med* (2011) 208: 2225–236. doi: 10.1084/jem.20110845

81. Mabey DCW, Brown A, Greenwood BM. Plasmodium falciparum malaria and salmonella infections in gambian children. *J Infect Dis* (1987) 155:1319–21. doi: 10.1093/infdis/155.6.1319

82. Mooney JP, Butler BP, Lokken KL, Xavier MN, Chau JY, Schaltenberg N, et al. The mucosal inflammatory response to non-typhoidal salmonella in the intestine is blunted by IL-10 during concurrent malaria parasite infection. *Mucosal Immunol* (2014) 7:1302–11. doi: 10.1038/mi.2014.18

83. Mooney JP, Lokken KL, Byndloss MX, George MD, Velazquez EM, Faber F, et al. Inflammation-associated alterations to the intestinal microbiota reduce colonization resistance against non-typhoidal salmonella during concurrent malaria parasite infection. *Sci Rep* (2015) 5:14603. doi: 10.1038/srep14603

84. Lokken KL, Mooney JP, Butler BP, Xavier MN, Chau JY, Schaltenberg N, et al. Malaria parasite infection compromises control of concurrent systemic non-typhoidal salmonella infection *via* IL-10-Mediated alteration of myeloid cell function. *PloS Pathog* (2014) 10:e1004049. doi: 10.1371/journal.ppat.1004049

85. Cunnington AJ, de Souza JB, Walther M, Riley EM. Malaria impairs resistance to salmonella through heme- and heme oxygenase–dependent dysfunctional granulocyte mobilization. *Nat Med* (2011) 18:120–7. doi: 10.1038/nm.2601

86. Mooney JP, Lee SJ, Lokken KL, Nanton MR, Nuccio SP, McSorley SJ, et al. Transient loss of protection afforded by a live attenuated non-typhoidal salmonella vaccine in mice Co-infected with malaria. *PloS Negl Trop Dis* (2015) 9:e0004027. doi: 10.1371/journal.pntd.0004027

87. Price RN, Simpson JA, Nosten F, Luxemburger C, Hkirjaroen L, Kuile FT, et al. Factors contributing to anemia after uncomplicated falciparum malaria. *Am J Trop Med Hyg* (2001) 65:614–22. doi: 10.4269/ajtmh.2001.65.614

88. Jeney V, Balla J, Yachie A, Varga Z, Vercellotti GM, Eaton JW, et al. Pro-oxidant and cytotoxic effects of circulating heme. *Blood* (2002) 100:879–87. doi: 10.1182/blood.V100.3.879

89. Cunnington AJ, Njie M, Correa S, Takem EN, Riley EM, Walther M. Prolonged neutrophil dysfunction after plasmodium falciparum malaria is related to hemolysis and heme oxygenase-1 induction. *J Immunol* (2012) 189:5336–46. doi: 10.4049/jimmunol.1201028

90. Mooney JP, Barry A, Gonçalves BP, Tiono AB, Awandu SS, Grignard L, et al. Haemolysis and haem oxygenase-1 induction during persistent "asymptomatic" malaria infection in burkinabé children. *Malar J* (2018) 17: 253. doi: 10.1186/s12936-018-2402-6

91. Konrad FM, Knausberg U, Höne R, Ngamsri KC, Reutershan J. Tissue heme oxygenase-1 exerts anti-inflammatory effects on LPS-induced pulmonary inflammation. *Mucosal Immunol* (2016) 9:98–111. doi: 10.1038/mi.2015.39

92. Bannister LH, Hopkins JM, Fowler RE, Krishna S, Mitchell GH. A brief illustrated guide to the ultrastructure of plasmodium falciparum asexual blood stages. *Parasitol Today* (2000) 6:427–33. doi: 10.1016/S0169-4758(00)01755-5

frontiers | Frontiers in Pharmacology

TYPE Original Research
PUBLISHED 08 August 2022
DOI 10.3389/fphar.2022.949264

OPEN ACCESS

EDITED BY
Galina Sud'ina,
Lomonosov Moscow State University, Russia

REVIEWED BY
Sachiko Sato,
Laval University, Canada
Jerka Dumić,
Faculty of Pharmacy and Biochemistry, University of Zagreb, Croatia

*CORRESPONDENCE
Alison C. Mackinnon,
AM@Galecto.com

SPECIALTY SECTION
This article was submitted to Inflammation Pharmacology, a section of the journal Frontiers in Pharmacology

RECEIVED 20 May 2022
ACCEPTED 30 June 2022
PUBLISHED 08 August 2022

CITATION
Humphries DC, Mills R, Boz C, McHugh BJ, Hirani N, Rossi AG, Pedersen A, Schambye HT, Slack RJ, Leffler H, Nilsson UJ, Wang W, Sethi T and Mackinnon AC (2022), Galectin-3 inhibitor GB0139 protects against acute lung injury by inhibiting neutrophil recruitment and activation.
Front. Pharmacol. 13:949264.
doi: 10.3389/fphar.2022.949264

Galectin-3 inhibitor GB0139 protects against acute lung injury by inhibiting neutrophil recruitment and activation

Duncan C. Humphries[1,2], Ross Mills[1], Cecilia Boz[1], Brian J. McHugh[1], Nikhil Hirani[1], Adriano G. Rossi[1], Anders Pedersen[3], Hans T. Schambye[3], Robert J. Slack[4], Hakon Leffler[5], Ulf J. Nilsson[6], Wei Wang[7], Tariq Sethi[3,7] and Alison C. Mackinnon[1,2]*

[1]Centre for Inflammation Research, University of Edinburgh, Edinburgh, United Kingdom, [2]Galecto Inc. Nine Edinburgh BioQuarter, Edinburgh, United Kingdom, [3]Galecto Inc, Copenhagen, Denmark, [4]Galecto Inc, Stevenage, United Kingdom, [5]Department of Laboratory Medicine, Lund University, Lund, Sweden, [6]Department of Chemistry, Lund University, Lund, Sweden, [7]Department of Asthma, Allergy and Respiratory Science, King's College London, Guy's Hospital, London, United Kingdom

Rationale: Galectin-3 (Gal-3) drives fibrosis during chronic lung injury, however, its role in acute lung injury (ALI) remains unknown. Effective pharmacological therapies available for ALI are limited; identifying novel concepts in treatment is essential. GB0139 is a Gal-3 inhibitor currently under clinical investigation for the treatment of idiopathic pulmonary fibrosis. We investigate the role of Gal-3 in ALI and evaluate whether its inhibition with GB0139 offers a protective role. The effect of GB0139 on ALI was explored *in vivo* and *in vitro*.

Methods: The pharmacokinetic profile of intra-tracheal (*i.t.*) GB0139 was investigated in C57BL/6 mice to support the daily dosing regimen. GB0139 (1–30 µg) was then assessed following acute *i.t.* lipopolysaccharide (LPS) and bleomycin administration. Histology, broncho-alveolar lavage fluid (BALf) analysis, and flow cytometric analysis of lung digests and BALf were performed. The impact of GB0139 on cell activation and apoptosis was determined *in vitro* using neutrophils and THP-1, A549 and Jurkat E6 cell lines.

Results: GB0139 decreased inflammation severity via a reduction in neutrophil and macrophage recruitment and neutrophil activation. GB0139 reduced LPS-mediated increases in interleukin (IL)-6, tumor necrosis factor alpha (TNFα) and macrophage inflammatory protein-1-alpha. *In vitro*, GB0139 inhibited Gal-3-induced neutrophil activation, monocyte IL-8 secretion, T cell apoptosis and the upregulation of pro-inflammatory genes encoding for IL-8, TNFα, IL-6 in alveolar epithelial cells in response to mechanical stretch.

Conclusion: These data indicate that Gal-3 adopts a pro-inflammatory role following the early stages of lung injury and supports the development of GB0139, as a potential treatment approach in ALI.

KEYWORDS

galectin-3, acute lung injury, neutrophiils, cytokine, LPS

Introduction

Galectin-3 (Gal-3) is a pro-fibrotic, mammalian ß-galactoside binding lectin, which is highly upregulated in the injured lung (MacKinnon et al., 2012). Gal-3 is elevated in the plasma and broncho-alveolar lavage fluid (BALf) of patients with idiopathic pulmonary fibrosis (IPF) (Nishi et al., 2007; MacKinnon et al., 2012), and is further upregulated in the plasma of patients undergoing an acute exacerbation of IPF (AE-IPF) (MacKinnon et al., 2012). Furthermore, in a cohort of 2025 patients from the Framingham Heart study, elevated plasma Gal-3 was associated with restrictive lung disease, decreased lung volumes and altered gas exchange (Ho et al., 2016), suggesting a potential role for Gal-3 in the early stages of pulmonary fibrosis.

Preclinical data supports the role of Gal-3 as an important regulator of lung fibrosis; global deletion of Gal-3 in mice was shown to reduce bleomycin-induced fibrosis compared to wild-type mice (MacKinnon et al., 2012). *In vitro* findings also suggest a role for Gal-3 in fibrogenesis as Gal-3 stimulates migration and collagen synthesis in fibroblasts (Nishi et al., 2007), and promotes alternative, pro-fibrotic, macrophage activation (MacKinnon et al., 2008). Gal-3 is also a key regulator in the induction of epithelial to mesenchymal transition (EMT) in lung epithelial cells (MacKinnon et al., 2012), and has a role in neutrophil activation and neutrophil apoptosis (Yamaoka et al., 1995; Kuwabara and Liu, 1996; Almkvist and Karlsson, 2002; Farnworth et al., 2008; Sundqvist et al., 2018). In mouse models of inflammation, elevated levels of Gal-3 in exudates correlates with increased neutrophil recruitment to the inflammatory site (Sano et al., 2000); such persistent neutrophil activation and delay of apoptosis could result in an overall exacerbation of tissue injury and failure of resolution.

In lung epithelial cells, Gal-3 activates ERK, AKT and JAK/STAT1 signaling pathways, leading to the release of pro-inflammatory cytokines during influenza and *Streptococcus pneumoniae* co-infection (Nita-Lazar et al., 2015), and enhances the pathogenic effects of H5N1 avian influenza virus by promoting host inflammatory responses via an interaction with NLRP3 inflammasome in macrophages (Chen et al., 2018). Mice deficient in Gal-3 develop less severe inflammation and interleukin (IL)-1β production than wild-type mice (Chen et al., 2018). In dendritic cells (DC) Gal-3 serves as a pattern-recognition receptor, regulating proinflammatory cytokine production and downregulation of Gal-3 in DCs inhibits expression of IL-6, IL-1β, and IL-23 and subsequent Th17 and Th2 development (Chen et al., 2015).

Currently, no targeted therapies exist for ALI and so treatment is limited to best supportive care. Based on available data, the combined effects of Gal-3 on macrophages, lung epithelial cells and neutrophil function, suggest that the inhibition of Gal-3 may serve as a potential strategy for the treatment of ALI. Recently we showed that conditional myeloid deletion of Gal-3 led to a significant reduction in Gal-3 expression in alveolar macrophages and neutrophils which decreased pulmonary inflammation and neutrophil recruitment into the interstitium (Humphries et al., 2021). GB0139 (formerly TD139), is a novel, inhalable, small molecule Gal-3 inhibitor, which reduces bleomycin-induced fibrosis in mice (MacKinnon et al., 2012; Delaine et al., 2016). In a Phase I/IIa study, GB0139 had a manageable safety profile and demonstrated good target engagement with alveolar macrophages in patients with IPF (Hirani et al., 2021). GB0139 is currently undergoing Phase IIb clinical evaluation for the treatment of IPF (NCT03832946). Here, we investigate the impact of Gal-3 and GB0139, on ALI models in mice, and on neutrophil and epithelial cell activation *in vitro*.

Methods and materials

In-vivo studies

Animals: 8-week-old male C57BL/6 mice were purchased from Harlan (Harlan Ltd, United Kingdom) and given 1 week to acclimatize prior to experimentation. Mice were maintained in 12-h light/12-h dark cycles with free access to food and water. All experimental animal procedures were approved by the University of Edinburgh and were performed in accordance with Home Office guidelines [Animal (Scientific Procedures) Act 1986].

GB0139 pharmacokinetics

For full details on GB0139 lung and plasma pharmacokinetics following intra-tracheal (*i.t.*) delivery see online supplement.

Induction of ALI and administration of GB0139

To induce ALI, mice received 10 µg lipopolysaccharide ([LPS] serotype 0127:B8, L4516, Sigma-Aldrich, Missouri, United States) from *E. coli*, or 33 µg bleomycin (BI3543, Apollo Scientific, United Kingdom), respectively, via *i.t.* administration. LPS/bleomycin ± GB0139 (in 50 µL 0.9% NaCl), was inserted into the needle via a pipette, and delivered into the lungs with a 2 × 100 µL bolus of air (using a 1 ml syringe). GB0139 was subsequently administered every 24 h until sacrifice.

Bronchoalveolar lavage

BALf was collected as previously described (Dhaliwal et al., 2012).

Histology and immunohistochemistry preparation

For full details of histology and immunohistochemistry preparation, see online supplement. Total inflammation score and fibrosis score were assessed according to protocols (Murao et al., 2003; Hübner et al., 2008). Quantitative analysis of histological and immunohistochemical samples was performed blinded to the investigator.

Total protein

Total protein within BALf was performed using a Pierce BCA Total Protein Assay Kit (23227; ThermoFisher Scientific, Waltham, MA, United States) as per the manufacturer's instructions.

Flow cytometric analysis of lung digests

Tissue digests and flow cytometry methods were performed according to published methodology (Humphries et al., 2018). See online supplement for further details.

Cytokine analysis

The mouse magnetic luminex assay (LXSAMSM, R&D Systems, Minneapolis, MN, United States) was used according to the manufacturer's instructions.

Enzyme Linked immunosorbent assay (ELISA)

ELISA kit for the measurement of IL-8 or Gal-3 in BALf samples (DuoSet; R&D Systems) was used according to the manufacturer's instructions.

Gal-3 synthesis

Gal-3 was synthesized in house. Recombinant human full length Gal-3 was produced in *E. Coli* BL21 Star (DE3) cells and purified by affinity chromatography on lactosyl-sepharose columns, as previously described (Salomonsson et al., 2010). To remove endotoxin contamination, 1% Triton X114 (X114, Sigma-Aldrich) was added to Gal-3 solution for 30 min (min) at 4°C prior to 10 min incubation at 37°C. After centrifugation at 5000 *g* for 5 min, the aqueous solution was removed. This process was repeated 3 times. GB0139 (Bis (3-deoxy-3-(3-fluorophenyl-1*H*-1,2,3-triazol-1-yl)-β-D-galactopyranosyl) sulfane) was provided by Galecto Inc. The purity of GB0139 was >99% as determined by analytical high-performance liquid chromatography.

Cell culture

Cell lines (THP-1, A549 and Jurkat E6 cells) were purchased from the European Collection of Authenticated Cell Cultures and were cultured at 37°C in 5% CO_2 (95% air) in Dulbecco's Modified Eagle's Medium (A549) or Roswell Park Memorial Institute medium (THP1, Jurkat E6) supplemented with 10% fetal calf serum, 1% L-glutamine, and 1% penicillin/streptomycin.

Monocyte IL-8 secretion

THP-1 monocyte-like cells (ATCC, Middlesex, United Kingdom) were activated with 100 nM phorbol 12-myristate 13-acetace ([PMA] P8139, Sigma-Aldrich) overnight and allowed to adhere. The following day cells were washed x three with phosphate buffered saline (PBS) and treated with Gal-3 ± 10 μM GB0139 for 24 h. Levels of IL-8 within media were quantified using IL-8 ELISA (DY208, R&D Systems).

Isolation of human neutrophils/monocytes

Peripheral human neutrophils and mononuclear cells were isolated from whole blood using Percoll gradients (Dorward et al., 2017). To isolate monocytes, the pan monocyte isolation kit (130-096-537, Miltenyi Biotec, Germany) was used as per the manufacturer's instructions.

Macrophage RNA analysis

For full details of macrophage polarization and RNA analysis, see online supplement.

Luminol ROS assay

Human peripheral neutrophils were primed with 10 ng/ml tumor necrosis factor alpha ([TNFα] 210-TA, R&D Systems) for 30 min at 37°C prior to addition of GB0139 for a further 10 min. To quantify reactive oxygen species (ROS) release, neutrophils were mixed with Horse Radish Peroxidase (P8375, Sigma-Aldrich)/Luminol (A8511, Sigma-Aldrich) and incubated with 30 μg/ml Gal-3, with luminescence measured using a Synergy plate reader (BioTek, Winooski, VT, United States).

Neutrophil/Jurkat apoptosis

Neutrophils or Jurkat cells were cultured for 20 h in the presence of 10 μg/ml or 20 μg/ml Gal-3, respectively, ± GB0139. Rates of apoptosis were determined using Annexin V (11828681001, Roche, Switzerland)/PI (P4170, Sigma-Aldrich) staining. Samples were assessed using the FACSCalibur flow cytometer (BD Biosciences, United Kingdom) and analyzed using FlowJo software (Tree Start Inc., OR, United States).

Stretch-induced gene changes in human lung epithelial cells in vitro

Human lung epithelial A549 cells were plated in 6-well collagen Bioflex culture plates (Flexcell International Corporation, Germany) ± 10 μg/ml Gal-3 ± 10 μM GB0139. Cyclic mechanical stretch was applied using a Flexcell FX-4000T Tension Plus system (Flexcell International Corporation, Germany) set to deliver 15% elongation at 1 Hz for 4 h. After the stretch procedure, RNA was isolated from the cells and analyzed by quantitative polymerase

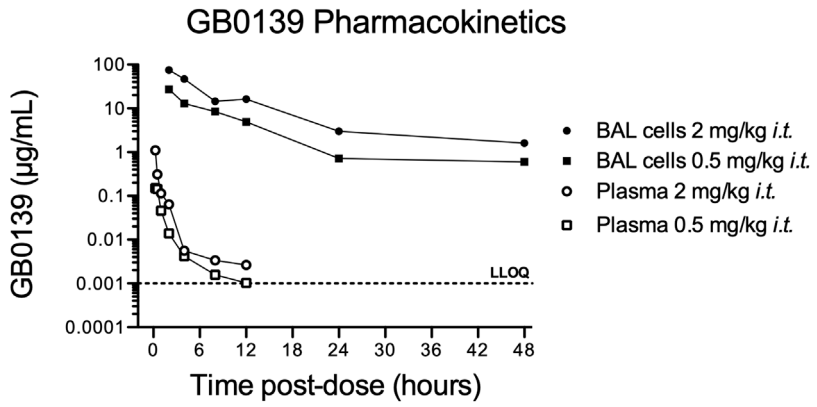

FIGURE 1
Pharmacokinetic profile of GB0139 in female C57BL/6 mice following *i.t.* administration. BAL cell and total blood concentrations of GB0139 were determined by LC-MS/MS overtime following single *i.t.* Administrations of 0.5 mg/kg and 2 mg/kg. Data shown are the mean values of three animals in each time point. BAL = broncho-alveolar lavage; *i.t.* = intra-tracheal; LC-MS/MS = liquid chromatography-tandem mass spectrometry; LLOQ = lowest level of quantification (1 ng/ml).

chain reaction array. For full details of the gene set see online supplement.

Statistics

Data are represented as mean ± the standard error of the mean (SEM). Statistical comparisons were made using two-tailed Students t-test or one-way/two-way analysis of variance (ANOVA) with Bonferroni post-test for multiple comparisons. A p value <0.05 was considered statistically significant (* = $p < 0.05$, ** = $p < 0.01$, *** = $p < 0.001$, **** = $p < 0.0001$). All graphs and statistics were performed using the statistical package GraphPad Prism five for Windows (GraphPad Software, CA, United States).

Results

GB0139 pharmacokinetic data support *i.t.* daily dosing

The pharmacokinetic profile of GB0139 was assessed in naïve mice. GB0139 was retained at high concentrations in the lung for up to 48 h following *i.t.* dosing of 0.5 mg/kg and 2 mg/kg (Figure 1). This supported daily dosing of 0.3–1 mg/kg (9–30 µg per mouse) to be taken forward into ALI models.

GB0139 reduces inflammatory cell recruitment following LPS-induced ALI

LPS administration resulted in significant pulmonary inflammation at 24 h, as seen by alveolar membrane thickening, capillary congestion, intra-alveolar hemorrhage and interstitial and alveolar neutrophil infiltration. Histology inflammation score was significantly reduced in a dose-dependent manner with GB0139 when compared with the LPS treatment only group (Figure 2A–D). No significant differences in vascular permeability were observed, however a trend of increased BALf total protein was seen following LPS, which was partially reduced following GB0139 (Figure 2E). Although absent following PBS, neutrophils were detected within the alveolar space following LPS administration and were reduced with 30 µg GB0139 (Figure 2F).

LPS administration upregulated several pro-inflammatory and pro-fibrotic cytokines within BALf, however administration of 10–30 µg GB0139 significantly reduced TNFα, IL-6, granulocyte-colony stimulating factor, C-C motif chemokine ligand (CCL) 5, macrophage inflammatory protein-1-alpha (MIP-1α), and matrix metallopeptidase 8 (MMP8) in a dose-dependent manner (Figure 2G–L, Supplementary Figure S1A, B).

The reduction of pulmonary inflammation seen with 30 µg GB0139 was associated with a significant decrease in interstitial neutrophil recruitment (identified as $CD11b^+$, $LY\text{-}6G^+$) and activation, as seen by a significant reduction in CD11b expression (Figures 3A–C) – for gating strategies see Supplementary Figures S2–4. A significant reduction in interstitial cytotoxic T cells ($CD3^+$, $CD8^+$) was also seen with LPS, which was reversed with 30 µg GB0139 (Figure 3D).

To identify alveolar and interstitial macrophage populations, a flow cytometric staining protocol was used (Misharin et al., 2013). LPS-induced ALI significantly reduced alveolar macrophage numbers whilst increasing inflammatory

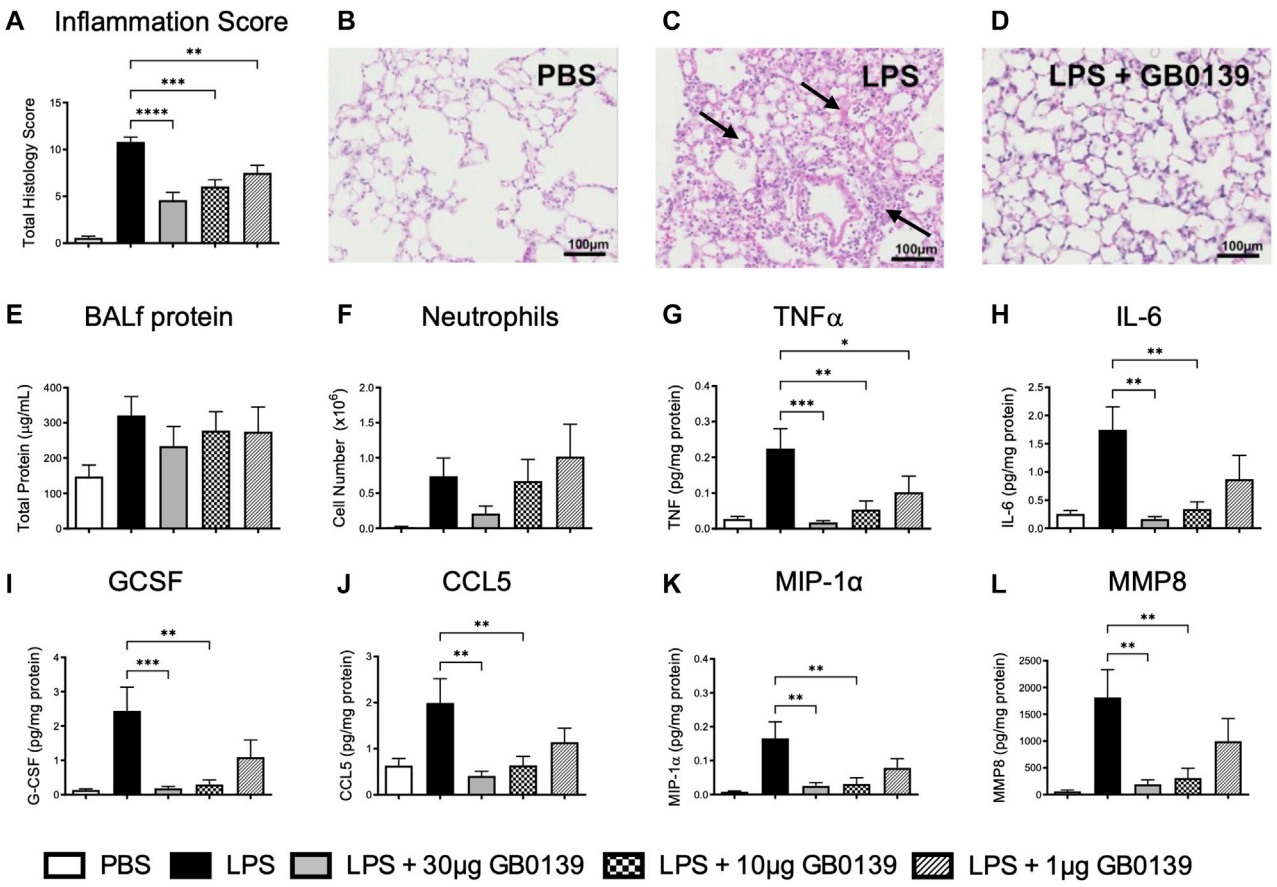

FIGURE 2
Histological and BALf analysis following LPS-induced lung inflammation. 10 μg LPS was administered alongside 1, 10 or 30 μg GB0139 *i.t.* and tissue retrieved 24 h later. Cytokine levels were normalised against total BALf protein. **(A–D)** Histology inflammation score and representative images of H and E stained lung tissue sections. Arrows indicate areas of pulmonary inflammation (alveolar membrane thickening, capillary congestion and alveolar neutrophil infiltration). Inflammation score was based on the presence of alveolar membrane thickening, capillary congestion, intra-alveolar haemorrhage, interstitial neutrophil infiltration and alveolar neutrophil infiltration. **(E)** BALf total protein. **(F)** BALf neutrophil numbers. **(G–J)** BALf pro-inflammatory cytokine profiles. **(K–L)** BALf pro-fibrotic cytokine profiles. Data represented as mean ± SEM. Analysed via 1-way ANOVA (n = 6, *$p < 0.05$, **$p < 0.01$, ***$p < 0.001$, ****$p < 0.0001$). Images taken at ×200 magnification. ANOVA = analysis of variance; BALf = broncho-alveolar lavage fluid; CCL = C-C motif chemokine ligand; E = eosin; G-CSF = granulocyte-colony stimulating factor; H = hematoxylin; h = hours; IL = interleukin; *i.t.* = intra-tracheal; LPS = lipopolysaccharide; MIP-1α = macrophage inflammatory protein-1-alpha; MMP = matrix metallopeptidase; PBS = phosphate bufferd saline; SEM = standard error of the mean; TNF = tumor necrosis factor.

interstitial macrophage recruitment (measured as both % of total interstitial cells and proportion of total macrophages) (Figures 3E,F). Both effects were partially inhibited with 30 μg GB0139, although the data were not statistically significant. CD80, a marker of inflammatory M1 macrophages, was seen to increase following LPS treatment and was significantly reduced with 30 μg GB0139 (Figure 3G).

Similar results were also seen at the 48 h timepoint, with GB0139 reducing histology inflammation score, pulmonary neutrophil number and activation (Supplementary Figure S5A–C). A significant increase in the proportion of alveolar macrophages alongside a significant reduction in interstitial macrophage recruitment was observed with GB0139 compared with the LPS only group (Supplementary Figure S5D, E). Analysis of the prototypical markers for M1 (CD80) and M2 (CD206) macrophages showed that Gal-3 inhibition was also found to non-significantly reduce CD80 expression on both alveolar and interstitial macrophages, whilst significantly increasing CD206 expression on interstitial macrophages. This suggests Gal-3 inhibition may have an M2-mediated protective role following LPS-induced ALI.

Flow cytometric analysis of BALf (Figures 4A–D) revealed GB0139 treatment did not affect the overall numbers of neutrophils but did reduce neutrophil activation as measured by a increase in neutrophil CD62L and decrease in CD11b expression when compared with LPS-treated mice (Figures 4E,F). Cell surface Gal-3 expression (geometric mean fluorescence intensity measured via flow cytometry) was also

decreased by GB0139 and there was a reduction in both recruitment and Gal-3 expression on CD11b$^+$, LY-6G$^-$, inflammatory monocytes in BALf (Figures 4G,H).

Bleomycin-induced acute lung injury

We have previously shown that global genetic deletion of Gal-3 and therapeutic administration of GB0139 reduces chronic inflammation and fibrosis induced by bleomycin (MacKinnon et al., 2012; Delaine et al., 2016). We examined the effect of GB0139 on the acute inflammatory phase following bleomycin injury in mice treated daily with 30 µg GB0139. Following bleomycin-induced injury, significantly lower inflammation scores were observed at day 3 in the GB0139-treated group versus the bleomycin only group (Figures 5A–C). Flow cytometric analysis of lung digests showed that GB0139 significantly reduced Gal-3 expression on interstitial neutrophils and macrophages and reduced interstitial neutrophil accumulation following bleomycin (Figures 5D–F). GB0139 reduced neutrophil activation as determined by an increase in CD62L expression (Figure 5G) and reduced inflammatory M1 macrophage polarization (decrease in CD80 expression; Figure 5H).

GB0139 has anti-inflammatory properties *in vitro*

We sought to define the mechanism of action of GB0139 on cell types known to drive ALI. *In vitro* addition of 10–30 µg/ml Gal-3 to human THP-1 monocyte-like cells led to a significant increase in IL-8 secretion, which was inhibited with 10 µM

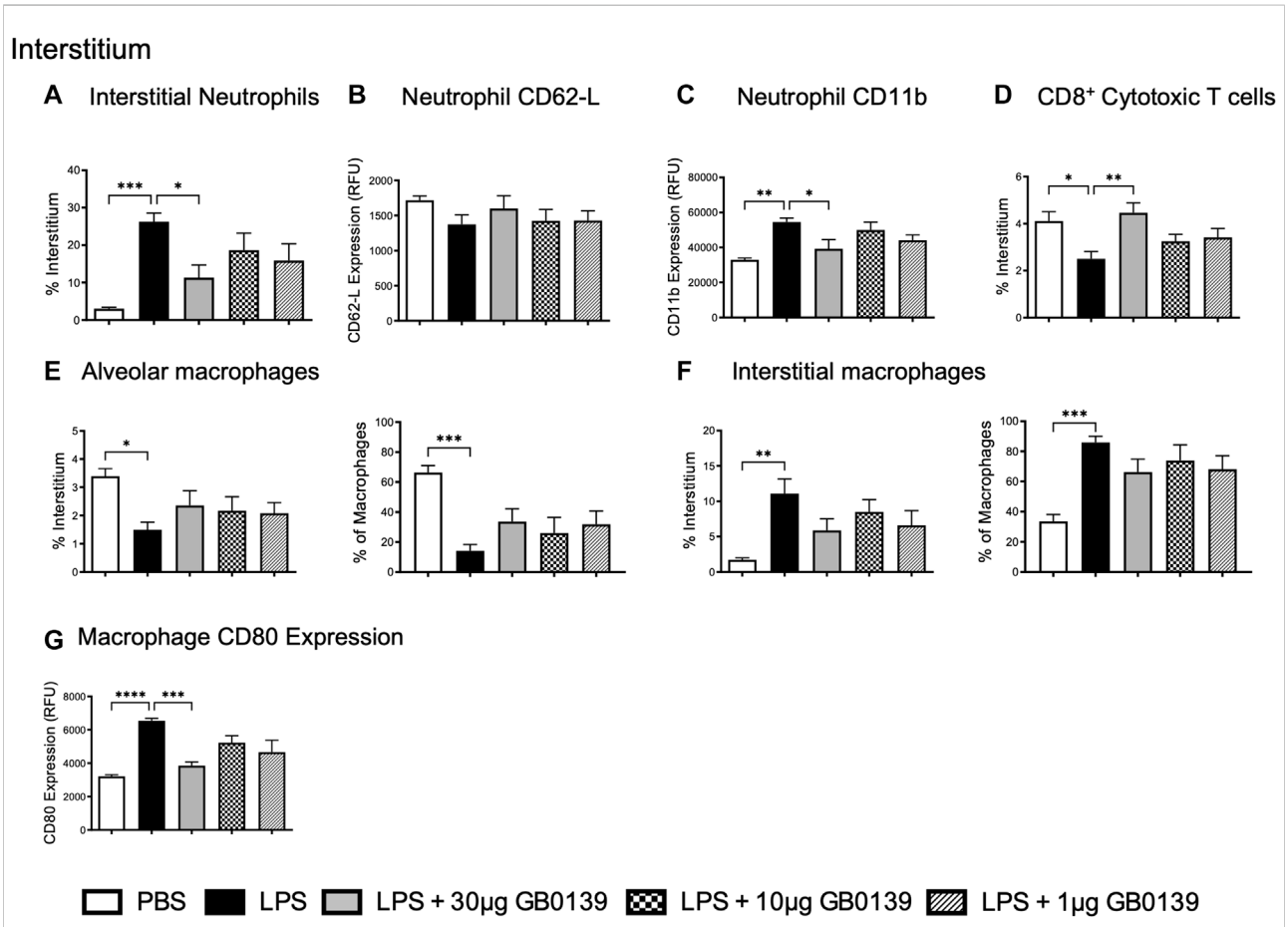

FIGURE 3
Flow cytometric analysis of whole lung digests following LPS-induced lung inflammation. 10 µg LPS was administered alongside 1, 10 or 30 µg GB0139 *i.t.* and tissue retrieved 24 h later. **(A–C)** Interstitial neutrophil numbers and activation parameters (CD62L and CD11b). **(D)** Interstitial CD8$^+$ cytotoxic T-cell accumulation. **(E–F)** Alveolar and interstitial macrophage accumulation, and **(G)** CD80 expression. Data represented as mean ± SEM. Analysed via 1-way ANOVA (n = 6, *$p < 0.05$, **$p < 0.01$, ***$p < 0.001$, ****$p < 0.0001$). ANOVA = analysis of variance; h = hours; *i.t.* = intra-tracheal; LPS = lipopolysaccharide; RFU = relative fluorescence units; SEM = standard error of the mean.

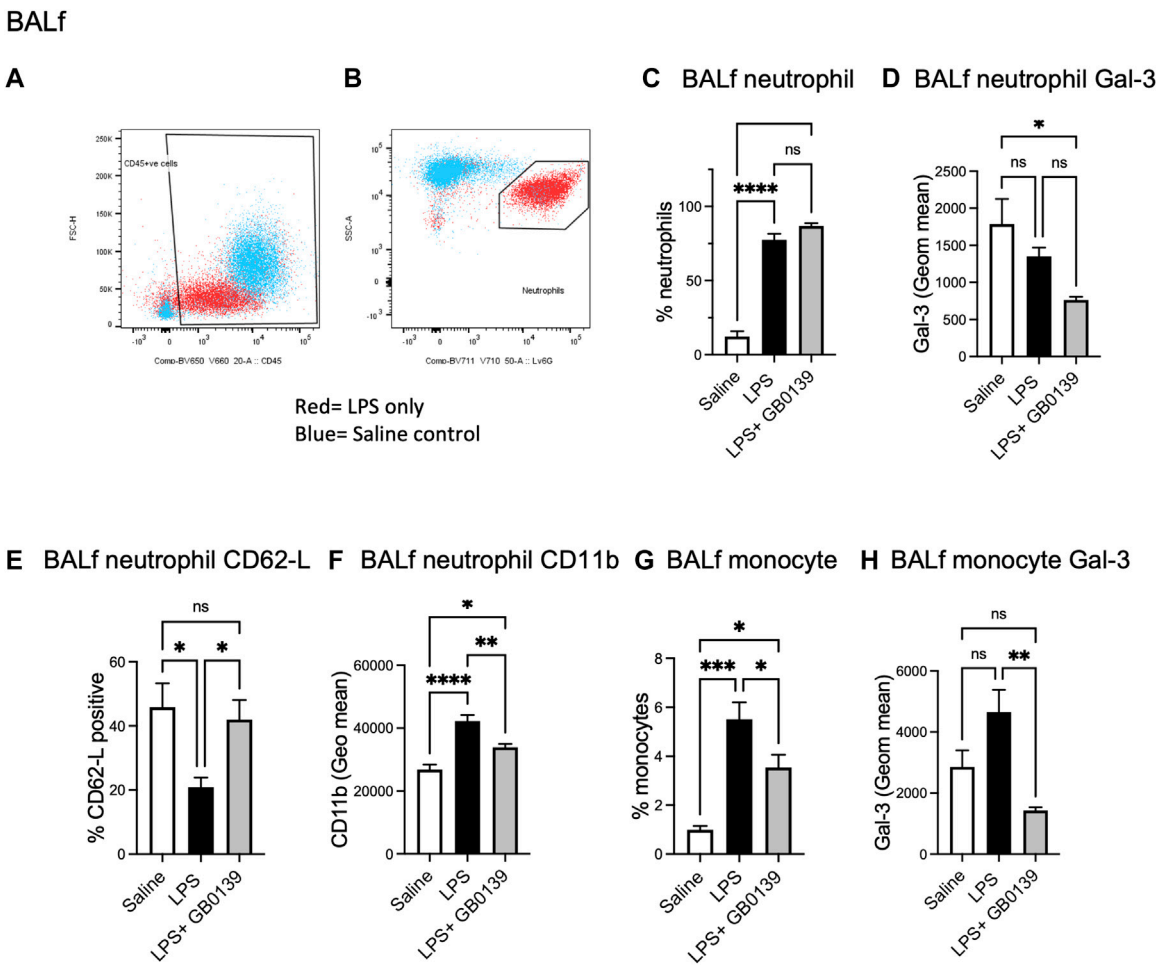

FIGURE 4
Flow cytometric analysis of BALf following LPS-induced lung inflammation. 10 μg LPS was administered alongside 30 μg GB0139 *i.t.* and tissue retrieved 24 h later. **(A–B)** Gating strategy to identify $CD45^+$ cells (left panel) and $LY\text{-}6G^+$ neutrophils (right panel) in BALf. **(C)** BALf neutrophil numbers, **(D)** Gal-3 expression and **(E–F)** activation parameters (CD62L and CD11b). **(G–H)** BALf monocytes and Gal-3 expression. Data represented as mean ± SEM. Analysed via 1-way ANOVA (n = 6, $*p < 0.05$, $**p < 0.01$, $***p < 0.001$, $****p < 0.0001$). ANOVA = analysis of variance; BALf = broncho-alveolar lavage fluid; Gal-3 = galectin-3; h = hours; *i.t.* = intra-tracheal; LPS = lipopolysaccharide; SEM = standard error of the mean.

GB0139 (Figure 6A). Human monocyte-derived macrophages upregulated TNFα gene expression when polarized towards an M1 phenotype by culturing in the presence of LPS and interferon gamma (IFNγ), which was reduced with 10 μM GB0139 (Figure 6B). Human neutrophils primed with TNFα increased ROS production in response to 30 μg/ml Gal-3 (Figure 6C). This was significantly inhibited with GB0139 (IC_{50} 0.8 μM; Figure 6D). Gal-3 also significantly delayed rates of neutrophil apoptosis that was partially inhibited with GB0139 (Figure 6E). The opposite was seen in Jurkat cells (an immortalized human T-cell line). Gal-3 (20 μg/ml) significantly increased apoptosis from 11% to 65% (Figure 6F). This was inhibited with GB0139 (IC_{50} 0.54 μM).

Epithelial cells play a key role in inflammation and repair in the diseased lung. To assess the effects of epithelial damage *in vitro*, human lung epithelial (A549) cells were exposed to a period of cyclic mechanical stretch. Stretch induced a significant upregulation of several genes encoding for pro-inflammatory cytokines, in particular IL-8, IL-6 and TNFα, and chemokines such as CCL20 and regulatory molecules (vascular endothelial growth factor, transforming growth factor beta-2) (Figure 6G). The addition of 10 μg/ml Gal-3 produced a further upregulation of IL-6, IL-8 and TNFα, and chemokines C-X-C motif chemokine ligand 1 (CXCL1) and CXCL2 (Figure 6H). Co-incubation with 10 μM GB0139 abolished these Gal-3-mediated changes and further reduced colony-stimulating factor-2 (CSF2) expression (Figure 6I). Gal-3 inhibition therefore reduces inflammation by inhibiting neutrophil activation, accelerating neutrophil apoptosis and inhibiting pro-inflammatory M1 macrophage activation, whilst reducing pro-inflammatory cytokine release from injured epithelial cells.

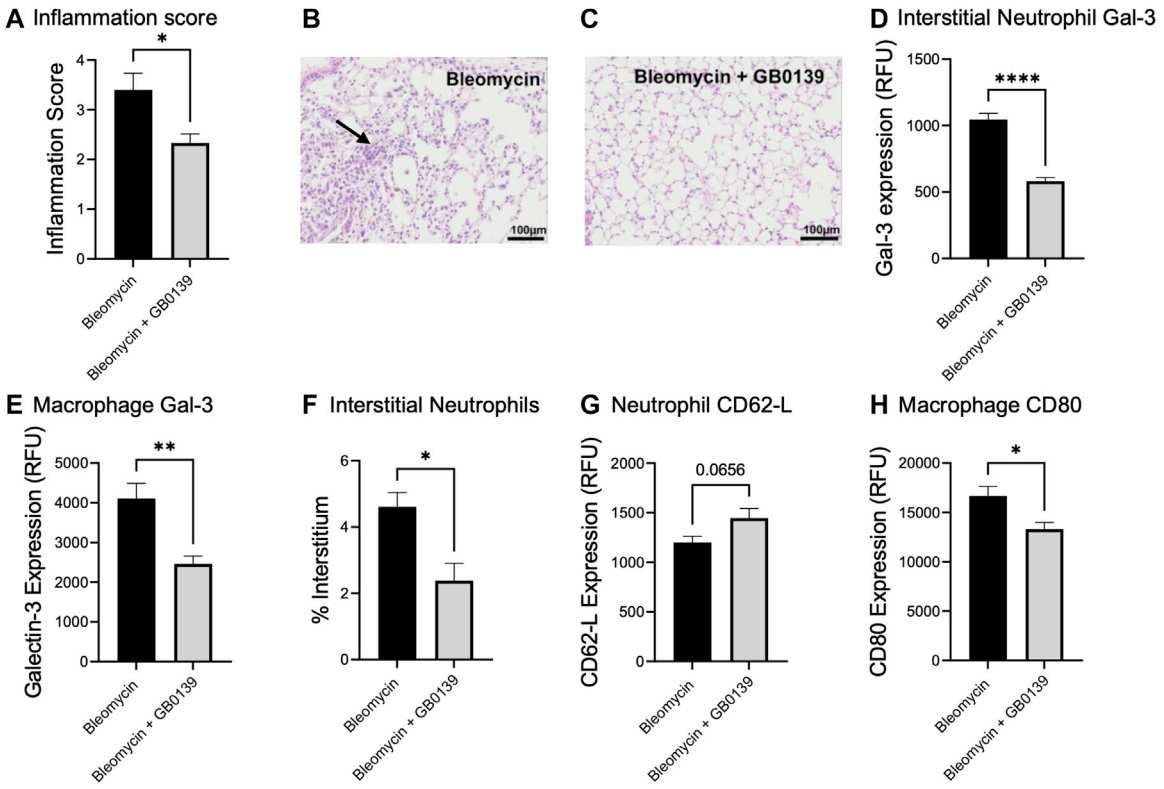

FIGURE 5
Effect of GB0139 on bleomycin-induced lung inflammation. 33 μg bleomycin was administered *i.t.* with further administration of 30 μg GB0139 every 24 h and lung tissue retrieved at day 3. **(A–C)** Histology inflammation score and representative H and E sections following administration of bleomycin with/without GB0139. Arrow indicates areas of pulmonary inflammation (alveolar membrane thickening, capillary congestion and alveolar neutrophil infiltration). **(D)** Gal-3 expression on interstitial neutrophils. **(E)** Gal-3 expression on macrophages. **(F)** Interstitial neutrophil accumulation. **(G)** Expression of CD62L on neutrophils. **(H)** Expression of the M1 marker, CD80 on macrophages. Data represented as mean ± SEM. Analysed via Student's t-test (n = 5, *$p < 0.05$, **$p < 0.01$, ***$p < 0.001$, ****$p < 0.0001$). Images taken at ×200 magnification. E = eosin; H = haematoxylin; h = hours; *i.t.* = intra-tracheal; RFU = relative fluorescence units; SEM = standard error of the mean.

Discussion

ALI is a condition with limited treatment options and so identifying novel therapeutic targets is essential. The accumulation and activation of neutrophils is considered key to the progression of ALI into the life-threatening acute respiratory distress syndrome (ARDS) (Abraham, 2003). This study examined the effect of the Gal-3 inhibitor, GB0139, on LPS- and bleomycin-induced ALI in mice and explored its mechanism of action *in vitro* in human inflammatory cell types known to trigger ALI. When evaluated *in vivo* and *in vitro*, GB0139 was found to decrease inflammation severity whilst accelerating neutrophil apoptosis to promote resolution. Gal-3 may serve as a potential therapeutic target for ALI and should be explored further.

GB0139 reduced interstitial neutrophil accumulation following LPS-induced lung inflammation. GB0139 was found to reduce both interstitial and alveolar neutrophil recruitment at least at the highest dose of GB0139. This is in keeping with our previous observations that global Gal-3 deletion reduced neutrophil recruitment into both compartments, whereas myeloid specific deletion only impacted interstitial recruitment (Humphries et al., 2021). This would suggest that GB0139 can additionally inhibit Gal-3 in the alveolar space derived from other non-myeloid cells (Humphries et al., 2021). Gal-3 derived from stromal cells has also been shown to mediate neutrophil extravasation into the alveolar space following *Aspergillus fumigatus* infection (Snarr et al., 2020). We also show that GB0139 inhibits Gal-3-induced delay of neutrophil apoptosis, which may be one mechanism whereby GB0139 reduces LPS-induced inflammation. The expression of Gal-3 and the number of inflammatory monocytes recruited into the alveolar space was also inhibited by GB0139. The reduction in CSF2 expression in injured alveolar epithelial cells suggests a mechanism whereby GB0139 may inhibit monocyte and neutrophil recruitment into the lung.

GB0139 also demonstrates affinity for Gal-1 (MacKinnon et al., 2012; Peterson et al., 2018). It is therefore conceivable that

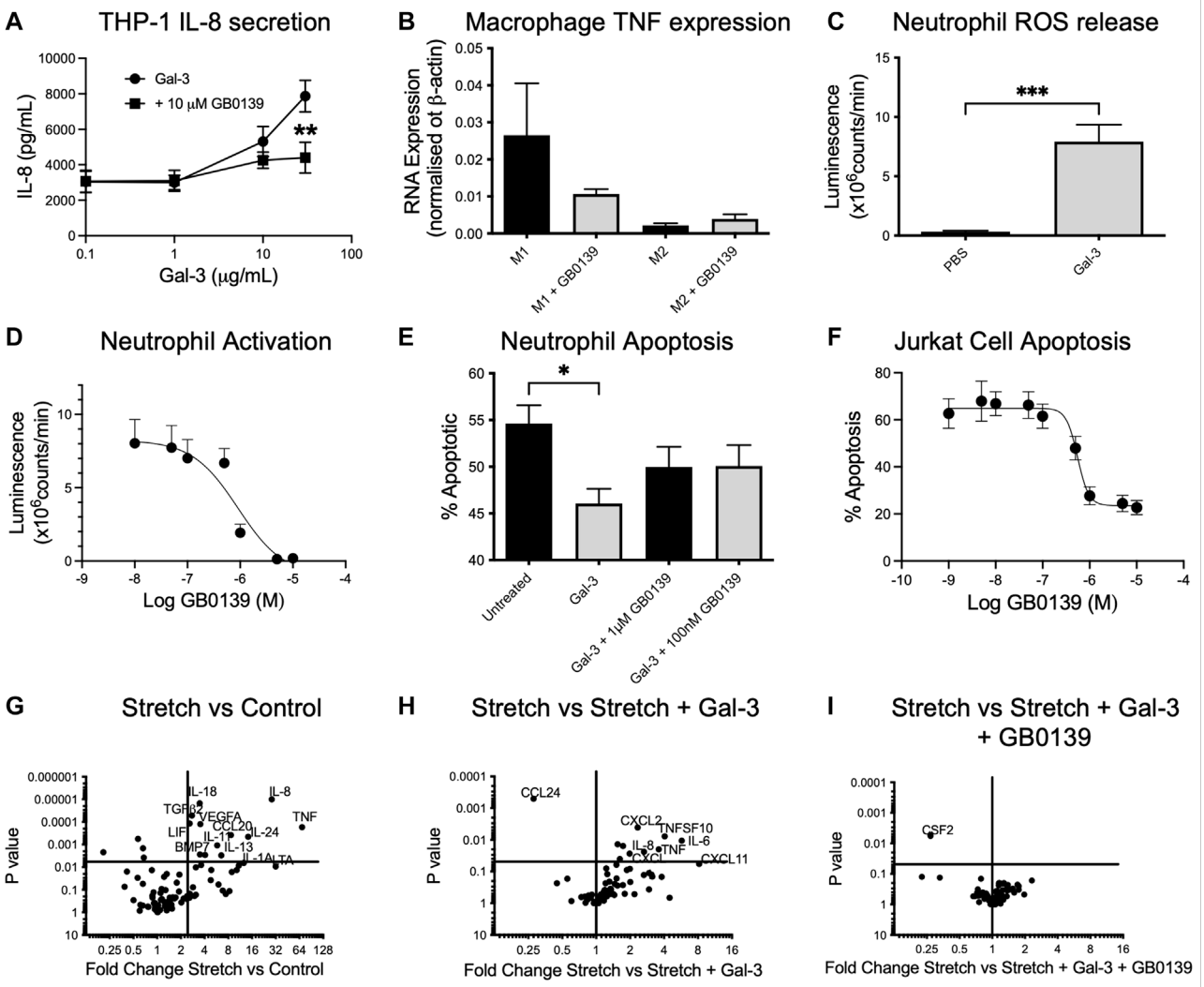

FIGURE 6
Effects of GB0139 *in vitro*. **(A)** THP-1 monocyte IL-8 secretion. THP-1 cells were differentiated with 10 nM PMA and treated with human recombinant Gal-3 ± 10 μM GB0139 for 24 h. **(B)** Human monocyte-derived macrophages were cultured in the presence of GM-CSF (M1) or M-CSF (M2) for 6 days and then further activated with IFN-γ/LPS (M1) or IL-4 (M2) ± 10 μM GB0139 for 48 h. **(C)** Neutrophil ROS production. Neutrophils were primed with TNFα (10 ng/ml), prior to stimulation with 30 μg/ml Gal-3. **(D)** GB0139 inhibition of Gal-3-induced neutrophil activation. **(E)** Neutrophil apoptosis. Neutrophils were cultured for 20 h in the presence of 10 μg/ml Gal-3 ± GB0139. **(F)** Jurkat cell apoptosis. Jurkat cells were cultured for 20 h in the presence of 20 μg/ml Gal-3 ± GB0139. Data represented as mean ± SEM. Analyzed via 2-way ANOVA (Figure 6A), 1-way ANOVA (Figures 6B,E), students t-test (Figure 6C) (n = 4–9, *$p < 0.05$, **$p < 0.01$, ***$p < 0.001$). The effects of stretch-induced gene expression in human lung epithelial cells following GB0139 treatment are shown in Figure 6G–I. Human epithelial A549 cells underwent a period of cyclic mechanical stretch ±10 μg/ml Gal-3 and/or 10 μM GB0139 prior to gene analysis. **(G)** Gene expression in human lung epithelial cells following mechanical stretch. **(H)** Effect of Gal-3 on stretch-induced changes in gene expression. **(I)** Effect of GB0139 on Gal-3-induced gene expression following stretch. Data (gene expression fold-change associated *p* value) represented as a dot plot. ANOVA = analysis of variance; Gal-3 = galectin-3; GM-CSF = granulocyte macrophage colony stimulating factor; h = hours; IFN-γ = interferon gamma; IL = interleukin; LPS = lipopolysaccharide; PMA = phorbol 12-myristate 13-acetate; ROS = reactive oxygen species; SEM = standard error of the mean; TNFα = tumor necrosis factor alpha.

GB0139 may also target Gal-1 in the lung, however, we have not shown significant upregulation of Gal-1 in the BALf or on the surface of BAL cells following LPS or bleomycin acute injury (data not shown). Our view is that the activated cells that are recruited into the lung in response to LPS or bleomycin injury have elevated Gal-3 (principally from monocytes). GB0139 inhibits recruitment and activation of these cells and as a result Gal-3 is itself reduced whereas the level of soluble Gal-1 in BALf is not elevated by injury or inhibited by GB0139. In addition, the effect we see is similar to that seen in the global Gal-3 deficient mouse (Humphries et al., 2021) so we conclude the effect of GB0139 is largely down to inhibition of Gal-3. Increased Gal-1 has however been associated with worse prognosis in other interstitial lung disease (ILD) (d'Alessandro et al., 2020) and COVID-19 induced inflammation (Markovic et al.,

2022). We would therefore surmise that a co-inhibition of galectin-1 would have a beneficial effect although this requires further study.

We have shown that Gal-3 deletion and inhibition of Gal-3 with GB0139 inhibits IL-4-induced M2 macrophage activation (MacKinnon et al., 2008). However, in human monocytes, exogenously added Gal-3 induces production of superoxide (Liu et al., 1995) and acts as an autocrine ligand for toll-like receptor (TLR)4 and induces TLR4-mediated activation (Burguillos et al., 2015). We show that GB0139 reduced the predominance of the pro-inflammatory M1 phenotype, as seen via a reduction in CD80 expression on interstitial macrophages and reduced the recruitment of inflammatory monocytes into the alveolar space. Therefore, in response to M1 macrophage stimuli, Gal-3 may adopt a pro-inflammatory role. Previous studies have shown that Gal-3 binding to M1 and M2 macrophages has differential carbohydrate dependence (Lepur et al., 2012). Based on our findings, we propose that GB0139 inhibits M1 macrophage responses during acute injury whilst reducing the profibrotic M2 macrophage phenotype during chronic injury. Modulation of macrophage polarization has important implications during ALI such as in AE-IPF where cytokines produced by both M1-and M2-like macrophages are elevated (Schupp et al., 2015).

In addition, GB0139 maintained alveolar macrophage numbers, which have been shown to inhibit neutrophil recruitment following LPS-induced lung injury (Beck-Schimmer et al., 2005), preserved $CD8^+$ T-cell populations and inhibited T-cell apoptosis *in vitro*. GB0139 may have a role in preserving $CD8^+$ T-cell function and so promote the resolution of inflammation. Plasma levels of Gal-3 are significantly elevated in patients with COVID-19 infection (de Biasi et al., 2020) and it has been suggested that GB0139 may have utility in reducing viral-induced lung injury and preventing fibrosis following COVID-19 infection (George et al., 2020).

GB0139 inhibited several pro-inflammatory cytokines/chemokines, including IL-6, IL-8 and TNFα, which are considered typical biomarkers of ALI (Parsons et al., 2005). IL-8 predicts ARDS following major trauma (Donnelly et al., 1993; Folkesson et al., 1995) and is considered one of the most potent neutrophil chemo-attractants in inflammation (Hoffmann et al., 2002), and blocking IL-8 has been shown to protect rabbits from acid-aspiration-induced lung injury (Folkesson et al., 1995). Here, we show that GB0139 inhibits Gal-3-induced IL-8 secretion from monocytes. IL-6 is an important cytokine in ALI and stimulates profibrotic M2 macrophage activation during the fibrotic phase of bleomycin-injury (Ayaub et al., 2017). IL-6 may therefore be an important mediator of pro-fibrotic signaling in response to an acute injury. GB0139 decreased several pro-fibrotic mediators in the BALf including MMP8, tissue inhibitor matrix metalloproteinase 1 (TIMP-1) and MIP-1α, which are indicative of an early fibrotic signature (Marshall et al., 2000; Kolb et al., 2001). This suggests that GB0139 may inhibit an early fibrotic response to an acute injury.

Consistent with our findings, clinical data from a Phase I/IIa clinical trial in patients with IPF demonstrated that inhaled GB0139 impacts on several key fibrotic mediators in the lung. As well as having an acceptable safety profile, GB0139 is able to reach the alveolar compartment to reduce alveolar macrophage Gal-3 expression and reduce biomarkers associated with IPF progression. GB0139 has a manageable safety profile and is associated with a favorable cytokine profile in patients with SARS-CoV-2 infection (Gaughan et al., 2021).

In conclusion, our data show that when Gal-3 levels are high (such as following ALI), GB0139 decreases inflammation and promotes resolution by reducing inflammatory cell recruitment and pro-inflammatory cytokine release whilst accelerating neutrophil apoptosis. These data indicate a potential opportunity to exploit Gal-3 as a therapeutic target in ALI and support the progression of GB0139 into the Phase IIb GALACTIC-1 study (NCT03832946) in patients with IPF.

Data availability statement

The raw data supporting the conclusions of this article will be made available by the authors, without undue reservation.

Ethics statement

The animal study was reviewed and approved by Animal Welfare Ethical Review Body.

Author contributions

AR, NH, TS and AM conceived the project. DH and AM designed the experiments and DH, RM, CB, BM, RS, WW performed the experiments. DH and AM provided the methodology and AP, HS, UN, and HL provided guidance and reagents. AR, TS, RS provided guidance and edited the manuscript. DH and AM drafted the manuscript.

Funding

This work was financially supported by the U.S. Army Medical Research and Materiel Command (#W81XWH-15-1-0499) and Galecto Inc.

Acknowledgments

The authors would like to thank the Queen's Medical Research Institute (QMRI) Flow Cytometry and Histology Facilities at the University of Edinburgh for their assistance.

Conflict of interest

AM and TS report personal fees from Galecto Biotech, outside the submitted work and AP, RS and HS report personal fees from Galecto Biotech, outside the submitted work. UN and HL are consultants of and shareholders in Galecto Biotech. NH received grants from Galecto Biotech. AR, BM, CB, DH, RM, WW declare that the research was conducted in the absence of any commercial or financial relationships that could be construed as a potential conflict of interest. Galecto Biotech AB is fully the owner of granted patents US9243021, US9580456, US9688713, US7700763, US86977862, US10369136, US10307403, US10799482, EP2914269, EP2297174, EP2679595, CA2794066, CA2724064, IN279934, CN102066393, CN103497228, JP6863984 and pending patent applications WO2020260351, EP16809870, CA3004632, CN2016800710578, JP2021062805, IN201817023621, IN2573/DELNP/2015, US17/221201.

Publisher's note

All claims expressed in this article are solely those of the authors and do not necessarily represent those of their affiliated organizations, or those of the publisher, the editors and the reviewers. Any product that may be evaluated in this article, or claim that may be made by its manufacturer, is not guaranteed or endorsed by the publisher.

Supplementary material

The Supplementary Material for this article can be found online at: https://www.frontiersin.org/articles/10.3389/fphar.2022.949264/full#supplementary-material

References

Abraham, E. (2003). Neutrophils and acute lung injury. *Crit. Care Med.* 31, S195–S199. doi:10.1097/01.CCM.0000057843.47705.E8

Almkvist, J., and Karlsson, A. (2002). Galectins as inflammatory mediators. *Glycoconj. J.* 19, 575–581. doi:10.1023/B:GLYC.0000014088.21242.e0

Ayaub, E. A., Dubey, A., Imani, J., Botelho, F., Kolb, M. R. J., Richards, C. D., et al. (2017). Overexpression of OSM and IL-6 impacts the polarization of pro-fibrotic macrophages and the development of bleomycin-induced lung fibrosis. *Sci. Rep.* 7, 13281. doi:10.1038/s41598-017-13511-z

Beck-Schimmer, B., Schwendener, R., Pasch, T., Reyes, L., Booy, C., Schimmer, R. C., et al. (2005). Alveolar macrophages regulate neutrophil recruitment in endotoxin-induced lung injury. *Respir. Res.* 6, 61. doi:10.1186/1465-9921-6-61

Burguillos, M. A., Svensson, M., Schulte, T., Boza-Serrano, A., Garcia-Quintanilla, A., Kavanagh, E., et al. (2015). Microglia-secreted galectin-3 acts as a toll-like receptor 4 ligand and contributes to microglial activation. *Cell Rep.* 10, 1626–1638. doi:10.1016/j.celrep.2015.02.012

Chen, S.-S., Sun, L.-W., Brickner, H., and Sun, P.-Q. (2015). Downregulating galectin-3 inhibits proinflammatory cytokine production by human monocyte-derived dendritic cells via RNA interference. *Cell. Immunol.* 294, 44–53. doi:10.1016/j.cellimm.2015.01.017

Chen, Y. J., Wang, S. F., Weng, I. C., Hong, M. H., Lo, T. H., Jan, J. T., et al. (2018). Galectin-3 enhances avian H5N1 influenza A virus–induced pulmonary inflammation by promoting NLRP3 inflammasome activation. *Am. J. Pathol.* 188, 1031–1042. doi:10.1016/j.ajpath.2017.12.014

d'Alessandro, M., de Vita, E., Bergantini, L., Mazzei, M. A., di Valvasone, S., Bonizzoli, M., et al. (2020). Galactin-1, 3 and 9: potential biomarkers in idiopathic pulmonary fibrosis and other interstitial lung diseases. *Respir. Physiol. Neurobiol.* 282, 103546. doi:10.1016/j.resp.2020.103546

de Biasi, S., Meschiari, M., Gibellini, L., Bellinazzi, C., Borella, R., Fidanza, L., et al. (2020). Marked T cell activation, senescence, exhaustion and skewing towards TH17 in patients with COVID-19 pneumonia. *Nat. Commun.* 11, 3434. doi:10.1038/s41467-020-17292-4

Delaine, T., Collins, P., MacKinnon, A., Sharma, G., Stegmayr, J., Rajput, V. K., et al. (2016). Galectin-3-Binding glycomimetics that strongly reduce bleomycin-induced lung fibrosis and modulate intracellular glycan recognition. *ChemBioChem* 17, 1759–1770. doi:10.1002/cbic.201600285

Dhaliwal, K., Scholefield, E., Ferenbach, D., Gibbons, M., Duffin, R., Dorward, D. a., et al. (2012). Monocytes control second-phase neutrophil emigration in established lipopolysaccharide-induced murine lung injury. *Am. J. Respir. Crit. Care Med.* 186, 514–524. doi:10.1164/rccm.201112-2132OC

Donnelly, S. C., Haslett, C., Strieter, R. M., Kunkel, S. L., Walz, A., Robertson, C. R., et al. (1993). Interleukin-8 and development of adult respiratory distress syndrome in at-risk patient groups. *Lancet* 341, 643–647. doi:10.1016/0140-6736(93)90416-E

Dorward, D. A., Lucas, C. D., Doherty, M. K., Chapman, G. B., Scholefield, E. J., Conway Morris, A., et al. (2017). Novel role for endogenous mitochondrial formylated peptide-driven formyl peptide receptor 1 signalling in acute respiratory distress syndrome. *Thorax* 72, 928–936. doi:10.1136/thoraxjnl-2017-210030

Farnworth, S. L., Henderson, N. C., MacKinnon, A. C., Atkinson, K. M., Wilkinson, T., Dhaliwal, K., et al. (2008). Galectin-3 reduces the severity of pneumococcal pneumonia by augmenting neutrophil function. *Am. J. Pathol.* 172, 395–405. doi:10.2353/ajpath.2008.070870

Folkesson, H. G., Matthay, M. A., Hebert, C. A., and Broaddus, V. C. (1995). Acid aspiration-induced lung injury in rabbits is mediated by interleukin- 8-dependent mechanisms. *J. Clin. Invest.* 96, 107–116. doi:10.1172/JCI118009

Gaughan, E., Sethi, T., Quinn, T., Hirani, N., Mills, A., Bruce, A. M., et al. (2021). GB0139, an inhaled small molecule inhibitor of galectin-3, in COVID-19 pneumonitis: a randomised, controlled, open-label, phase 2a experimental medicine trial of safety, pharmacokinetics, and potential therapeutic value. *medRxiv*. 2021.12.21.21267983. doi:10.1101/2021.12.21.21267983

George, P. M., Wells, A. U., and Jenkins, R. G. (2020). Pulmonary fibrosis and COVID-19: the potential role for antifibrotic therapy. *Lancet. Respir. Med.* 8, 807–815. doi:10.1016/S2213-2600(20)30225-3

Hirani, N., MacKinnon, A. C., Nicol, L., Ford, P., Schambye, H., Pedersen, A., et al. (2021). Target inhibition of galectin-3 by inhaled TD139 in patients with idiopathic pulmonary fibrosis. *Eur. Respir. J.* 57, 2002559. doi:10.1183/13993003.02559-2020

Ho, J. E., Gao, W., Levy, D., Santhanakrishnan, R., Araki, T., Rosas, I. O., et al. (2016). Galectin-3 is associated with restrictive lung disease and interstitial lung abnormalities. *Am. J. Respir. Crit. Care Med.* 194, 77–83. doi:10.1164/rccm.201509-1753OC

Hoffmann, E., Dittrich-Breiholz, O., Holtmann, H., and Kracht, M. (2002). Multiple control of interleukin-8 gene expression. *J. Leukoc. Biol.* 72, 847–855.

Hübner, R. H., Gitter, W., el Mokhtari, N. E., Mathiak, M., Both, M., Bolte, H., et al. (2008). Standardized quantification of pulmonary fibrosis in histological samples. *Biotechniques* 44, 507–511. doi:10.2144/000112729

Humphries, D. C., O'Neill, S., Scholefield, E., Dorward, D. A., Mackinnon, A. C., Rossi, A. G., et al. (2018). Cerebral concussion primes the lungs for subsequent neutrophil-mediated injury. *Crit. Care Med.* 46, e937–44. doi:10.1097/CCM.0000000000003270

Humphries, D. C., Mills, R., Dobie, R., Henderson, N. C., Sethi, T., Mackinnon, A. C., et al. (2021). Selective myeloid depletion of galectin-3 offers protection against acute and chronic lung injury. *Front. Pharmacol.* 12, 715986. doi:10.3389/fphar.2021.715986

Kolb, M., Margetts, P. J., Anthony, D. C., Pitossi, F., and Gauldie, J. (2001). Transient expression of IL-1β induces acute lung injury and chronic repair leading to pulmonary fibrosis. *J. Clin. Invest.* 107, 1529–1536. doi:10.1172/JCI12568

Kuwabara, I., and Liu, F. T. (1996). Galectin-3 promotes adhesion of human neutrophils to laminin. *J. Immunol.* 156, 3939–3944.

Lepur, A., Carlsson, M. C., Novak, R., Dumić, J., Nilsson, U. J., Leffler, H., et al. (2012). Galectin-3 endocytosis by carbohydrate independent and dependent pathways in different macrophage like cell types. *Biochim. Biophys. Acta* 1820, 804–818. doi:10.1016/j.bbagen.2012.02.018

Liu, F. T., Hsu, D. K., Zuberi, R. I., Kuwabara, I., Chi, E. Y., Henderson, W. R., et al. (1995). Expression and function of galectin-3, a β-galactoside-binding lectin, in human monocytes and macrophages. *Am. J. Pathol.* 147, 1016–1028.

MacKinnon, A. C., Farnworth, S. L., Hodkinson, P. S., Henderson, N. C., Atkinson, K. M., Leffler, H., et al. (2008). Regulation of alternative macrophage activation by galectin-3. *J. Immunol.* 180, 2650–2658. doi:10.4049/jimmunol.180.4.2650

MacKinnon, A. C., Gibbons, M. A., Farnworth, S. L., Leffler, H., Nilsson, U. J., Delaine, T., et al. (2012). Regulation of transforming growth factor-β1-driven lung fibrosis by galectin-3. *Am. J. Respir. Crit. Care Med.* 185, 537–546. doi:10.1164/rccm.201106-0965OC

Markovic, S. S., Gajovic, N., Jurisevic, M., Jovanovic, M., Jovicic, B. P., Arsenijevic, N., et al. (2022). Galectin-1 as the new player in staging and prognosis of COVID-19. *Sci. Rep.* 12, 1272. doi:10.1038/s41598-021-04602-z

Marshall, R. P., Bellingan, G., Webb, S., Puddicombe, A., Goldsack, N., McAnulty, R. J., et al. (2000). Fibroproliferation occurs early in the acute respiratory distress syndrome and impacts on outcome. *Am. J. Respir. Crit. Care Med.* 162, 1783–1788. doi:10.1164/ajrccm.162.5.2001061

Misharin, A. V., Morales-Nebreda, L., Mutlu, G. M., Budinger, G. R. S., and Perlman, H. (2013). Flow cytometric analysis of macrophages and dendritic cell subsets in the mouse lung. *Am. J. Respir. Cell Mol. Biol.* 49, 503–510. doi:10.1165/rcmb.2013-0086MA

Murao, Y., Loomis, W., Wolf, P., Hoyt, D. B., and Junger, W. G. (2003). Effect of dose of hypertonic saline on its potential to prevent lung tissue damage in a mouse model of hemorrhagic shock. *Shock* 20, 29–34. doi:10.1097/01.shk.0000071060.78689.f1

Nishi, Y., Sano, H., Kawashima, T., Okada, T., Kuroda, T., Kikkawa, K., et al. (2007). Role of galectin-3 in human pulmonary fibrosis. *Allergol. Int.* 56, 57–65. doi:10.2332/allergolint.O-06-449

Nita-Lazar, M., Banerjee, A., Feng, C., and Vasta, G. R. (2015). Galectins regulate the inflammatory response in airway epithelial cells exposed to microbial neuraminidase by modulating the expression of SOCS1 and RIG1. *Mol. Immunol.* 68, 194–202. doi:10.1016/j.molimm.2015.08.005

Parsons, P. E., Eisner, M. D., Thompson, B. T., Matthay, M. A., Ancukiewicz, M., Bernard, G. R., et al. (2005). Lower tidal volume ventilation and plasma cytokine markers of inflammation in patients with acute lung injury. *Crit. Care Med.* 33, 1–6. doi:10.1097/01.ccm.0000149854.61192.dc

Peterson, K., Kumar, R., Stenström, O., Verma, P., Verma, P. R., Håkansson, M., et al. (2018). Systematic tuning of fluoro-galectin-3 interactions provides thiodigalactoside derivatives with single-digit nM affinity and high selectivity. *J. Med. Chem.* 61, 1164–1175. doi:10.1021/acs.jmedchem.7b01626

Salomonsson, E., Carlsson, M. C., Osla, V., Hendus-Altenburger, R., Kahl-Knutson, B., Oberg, C. T., et al. (2010). Mutational tuning of galectin-3 specificity and biological function. *J. Biol. Chem.* 285, 35079–35091. doi:10.1074/jbc.M109.098160

Sano, H., Hsu, D. K., Yu, L., Apgar, J. R., Kuwabara, I., Yamanaka, T., et al. (2000). Human galectin-3 is a novel chemoattractant for monocytes and macrophages. *J. Immunol.* 165, 2156–2164. doi:10.4049/jimmunol.165.4.2156

Schupp, J. C., Binder, H., Jäger, B., Cillis, G., Zissel, G., Müller-Quernheim, J., et al. (2015). Macrophage activation in acute exacerbation of idiopathic pulmonary fibrosis. *PLoS One* 10, e0116775. doi:10.1371/journal.pone.0116775

Snarr, B. D., St-Pierre, G., Ralph, B., Lehoux, M., Sato, Y., Rancourt, A., et al. (2020). Galectin-3 enhances neutrophil motility and extravasation into the airways during *Aspergillus fumigatus* infection. *PLoS Pathog.* 16, e1008741. doi:10.1371/journal.ppat.1008741

Sundqvist, M., Welin, A., Elmwall, J., Osla, V., Nilsson, U. J., Leffler, H., et al. (2018). Galectin-3 type-C self-association on neutrophil surfaces; the carbohydrate recognition domain regulates cell function. *J. Leukoc. Biol.* 103, 341–353. doi:10.1002/JLB.3A0317-110R

Yamaoka, A., Kuwabara, I., Frigeri, L. G., and Liu, F. T. (1995). A human lectin, galectin-3 (epsilon bp/Mac-2), stimulates superoxide production by neutrophils. *J. Immunol.* 154, 3479–3487.

frontiers | Frontiers in Immunology

TYPE Original Research
PUBLISHED 15 September 2022
DOI 10.3389/fimmu.2022.928312

OPEN ACCESS

EDITED BY
Roman A. Zinovkin,
Lomonosov Moscow State University, Russia

REVIEWED BY
Cassiano Felippe Gonçalves-de-Albuquerque,
Rio de Janeiro State Federal University, Brazil
Xianfei Ding,
First Affiliated Hospital of Zhengzhou University, China
Guojun Zhang,
Fifth Affiliated Hospital of Zhengzhou University, China

*CORRESPONDENCE
Yongnan Li
1449417219@qq.com
Xingdong Cheng
861470395@qq.com
Bingren Gao
ery_gaobr@lzu.edu.cn

†These authors have contributed equally to this work

SPECIALTY SECTION
This article was submitted to Inflammation, a section of the journal Frontiers in Immunology

RECEIVED 25 April 2022
ACCEPTED 29 August 2022
PUBLISHED 15 September 2022

CITATION
Huang J, Wang B, Tao S, Hu Y, Wang N, Zhang Q, Wang C, Chen C, Gao B, Cheng X and Li Y (2022) D-tagatose protects against oleic acid-induced acute respiratory distress syndrome in rats by activating PTEN/PI3K/AKT pathway.
Front. Immunol. 13:928312.
doi: 10.3389/fimmu.2022.928312

D-tagatose protects against oleic acid-induced acute respiratory distress syndrome in rats by activating PTEN/PI3K/AKT pathway

Jian Huang[1†], Bingjie Wang[2†], Shaoyi Tao[3†], Yuexia Hu[2], Ning Wang[2,4], Qiaoyun Zhang[1], Chunhui Wang[2], Chen Chen[2], Bingren Gao[1*], Xingdong Cheng[1*] and Yongnan Li[1*]

[1]Department of Cardiac Surgery, Lanzhou University Second Hospital, Lanzhou University, Lanzhou, China, [2]Department of Anesthesiology, The Forth Affiliated Hospital of Anhui Medical University, Hefei, China, [3]Department of Plastic Repair Burn Surgery Dermatology, The Second People's Hospital of Hefei, Hefei Hospital Affiliated to Anhui Medical University, Hefei, China, [4]Key Laboratory of Anesthesiology and Perioperative Medicine of Anhui Higher Education Institutes, Anhui Medical University, Hefei, China

Acute respiratory distress syndrome (ARDS) is characterized by disruption of the alveolar–capillary barrier, resulting in severe alveolar edema and inflammation. D-tagatose (TAG) is a low-calorie fructose isomer with diverse biological activities whose role in ARDS has never been explored. We found that TAG protects lung tissues from injury in the oleic acid-induced rat model of ARDS. Seventeen male Sprague–Dawley rats were randomly assigned to 3 groups: Sham (n = 5), ARDS (n = 6), and TAG + ARDS (n = 6). The treatment groups were injected with oleic acid to induce ARDS, and the TAG + ARDS group was given TAG 3 days before the induction. After the treatments, the effect of TAG was evaluated by blood gas analysis and observing the gross and histological structure of the lung. The results showed that TAG significantly improved the oxygenation function, reduced the respiratory acidosis and the inflammatory response. TAG also improved the vascular permeability in ARDS rats and promoted the differentiation of alveolar type II cells, maintaining the stability of the alveolar structure. This protective effect of TAG on the lung may be achieved by activating the PTEN/PI3K/AKT pathway. Thus, TAG protects against oleic acid-induced ARDS in rats, suggesting a new clinical strategy for treating the condition.

KEYWORDS

D-tagatose, acute respiratory distress syndrome, PTEN/PI3K/AKT pathway, oleic acid, alveolar

Introduction

ARDS is considered a significant health and economic burden. The incidence of ARDS in the intensive care units (ICUs) of 50 countries was 10.4% (1). ARDS involves a cascade of secondary inflammatory injury and secondary diffuse lung parenchymal injury mediated by various inflammatory mediators and effector cells (2–4). Despite numerous studies in recent years, the mortality of ARDS is still very high due to the complexity of etiology and pathogenesis (2). The alveolar epithelial barrier and the pulmonary microvascular endothelial barrier are the two central physiological barriers in the lung (3). During lung injury, pulmonary microvascular permeability increases from barrier damage, and protein-rich fluid exudes from the alveolar space, causing pulmonary edema and promoting the formation of hyaline membranes (2, 4). Evidence suggests that the alveolar epithelial barrier is more resistant to injury than the pulmonary microvascular endothelial (5). Therefore, promoting the repair of the alveolar epithelial barrier is crucial for improving lung injury in patients with ARDS. To seek an effective therapeutic approach to ARDS, it is important to study the pathological mechanisms of ARDS in ARDS animal model (6). Oleic acid (OA)-induced lung injury is a relevant model to study ARDS because this fatty acid acts directly on the lung cells or lung endothelium and triggers activation of different innate immune receptors (7).

The PI3K/AKT signaling pathway promotes cell growth, survival, and differentiation (8). According to previous studies, activating it protects lung epithelial cells under oxidative stress and prevents stress-induced apoptosis (9, 10). Phosphatase and tensin homolog (PTEN) is a major negative regulator of the PI3K/AKT pathway (8). It dephosphorylates PIP3 through phospholipase activity, inhibiting the pathway (11).

D-tagatose (TAG) is a rare fructose isomer and has recently been used as a new functional sweetener (12). It has a low caloric value and hypoglycemic, intestinal flora-regulating, prevent colon cancer, and lower cholesterol properties (13, 14). The heat generated is only 1/3 that of sucrose, and the energy value is 1.5 kcal/g (12). In 2001, the US Food and Drug Administration appointed TAG as a generally recognized safe food (15). It is a promising sugar substitute because it reduces the detrimental effects of fructose on the metabolic profile and the associated cardiac susceptibility to ischemia/reperfusion injury (16). In this study, the rat ARDS model induced by OA was used to evaluate the protective effect of TAG on lung tissues to provide a basis for further exploring its underlying mechanism.

Material and methods

Experimental animals

Seventeen male Sprague-Dawley rats (320 g ± 50 g) were randomly divided into three groups: Sham (n = 5), ARDS (n = 6), and TAG + ARDS (n = 6). They were placed in cages with a controlled temperature range (20°C–22°C) and a 12-hour light-dark cycle. The animals were given free water and food. The study protocol was approved by the Laboratory Animal Ethics Committee of Anhui Medical University (License No: LISC20180351) and performed according to the ARRIVE guidelines for animal experiments.

Experimental protocol

TAG was purchased from Selleck (Houston, USA) and dissolved in normal saline (NS). A flow chart of the experimental procedure is shown in Figure 1A. The rats were anesthetized intraperitoneally with 30 mg/kg of pentobarbital, followed by separating and exposing the right femoral artery and vein. A 24-gauge catheter was catheterized into the right femoral artery to continuously monitor mean arterial pressure (MAP) and heart rate (HR) using an electrocardiogram (ECG) monitor. Those in the TAG + ARDS group were given 300 mg/kg of TAG and the 300 mg/kg of saline was given to the ARDS group by gavage for three days before OA administration. The rats in the ARDS group were treated with highly pure (99.9%) OA (Sigma, USA) by slowly injecting it into the right femoral vein with a microsyringe at a 100 mg/kg dose. The same doses of NS were provided to the Sham group. All rats were given carprofen (5 mg/kg) for postoperative analgesia. After 8 hours, the animals were euthanized with an intravenous overdose of pentobarbital. Subsequently, bronchoalveolar lavage fluid (BALF), lung tissues, and blood samples were collected for further evaluation.

Blood gas analysis, BALF protein concentration, and Wet/Dry weight ratio

Blood samples collected from the right femoral artery were analyzed using a blood analyzer and EG7+ cartridges (Abbott, USA) to assess the oxygenation and metabolic state in each treatment group. Lungs were lavaged using 2.0 mL normal saline to collect BALF. Protein levels were quantified using a bicinchoninic acid kit (Solarbio, China). The left lung was weighed to determine the wet weight and placed in an oven at 70°C for 72 hours. When completely dehydrated, it was weighed to estimate the dry weight. Finally, the Wet/Dry weight ratio of the left lung was calculated. The oxygenation index (OI) was determined with the PaO_2/FiO_2 ratio.

Enzyme-linked immunosorbent assay

The levels of TNF-α, IL-1β, IL-6, and IL-8 were quantified in the BALF and lung tissues using ELISA assay (Enzyme-linked Biotechnology, China) following the manufacturer's instructions.

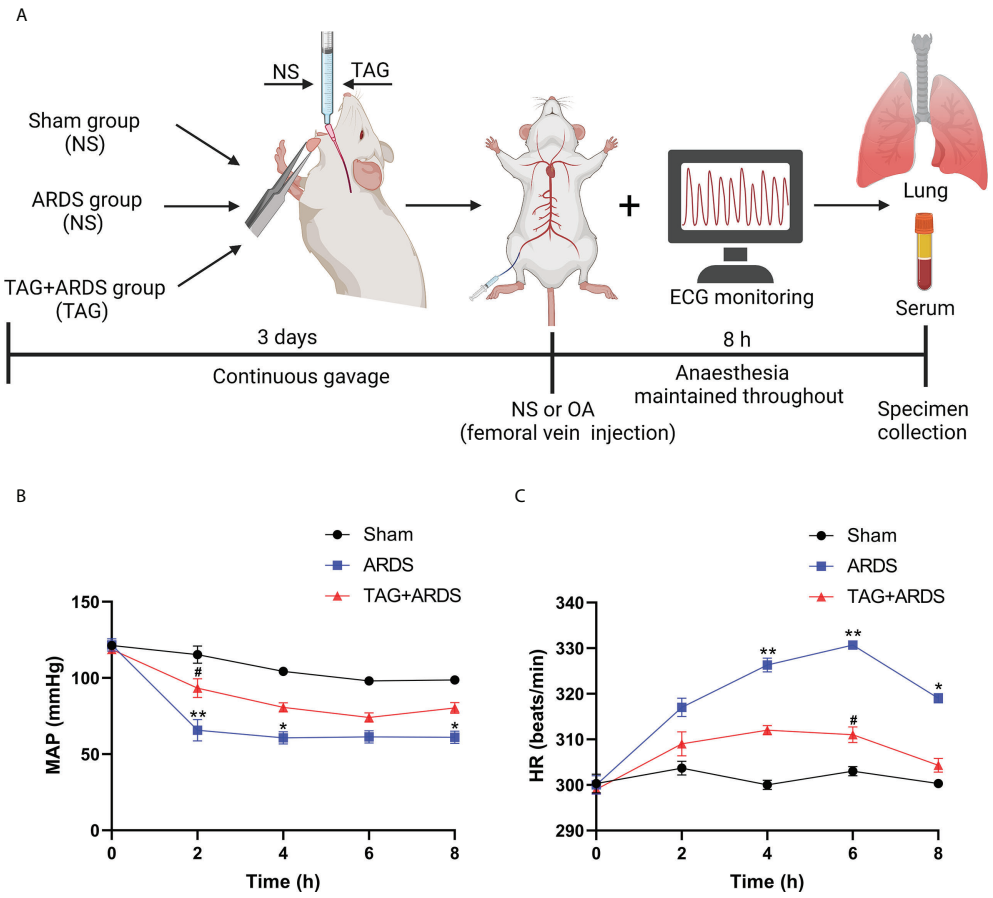

FIGURE 1
(A) Flow chart of the experimental procedure. **(B, C)** An ECG monitor was used to monitor MAP and HR changes throughout the experiment. Data are presented as the mean ± SD. $^{*}p < 0.05$, $^{**}p < 0.01$, compared with the Sham group; $^{\#}p < 0.05$, compared with the ARDS group. Illustrations were created using BioRender (biorender.com). ECG monitor, electrocardiogram monitor; TAG, D-tagatose; OA, oleic acid; NS, normal saline; ARDS, acute respiratory distress syndrome; MAP, mean arterial pressure; HR, heart rate.

Histopathological evaluation

The isolated lung was fixed in 4% paraformaldehyde at 4°C for 48 hours, embedded in paraffin, and sectioned at a 5 μm thickness. The sections were stained with hematoxylin-eosin, immunofluorescence, etc. For the hematoxylin–eosin staining, lung injury was determined by evaluating alveolar congestion, edema, inflammatory cell infiltration, and interstitial thickening. The lung injury score was defined as follows: none, 0; mild, 1; moderate, 2; and severe, 3. For the immunofluorescence staining, the sections were incubated with the primary antibodies: anti-surfactant protein C (anti-SPC) (1:200; Santa Cruz Biotechnology, USA), anti-aquaporin 5 (anti-AQP5) (1:4000; Abcam, USA), anti-Claudin 4 (1:200; Proteintech, China), anti-Keratin 8 (1:200; Proteintech, China) and anti-CD31 (1:200; Servicebio, China) at 4°C overnight. The images were obtained with a confocal microscope (Carl Zeiss, Germany). For the immunohistochemistry staining, the sections were incubated with an anti-myeloperoxidase (anti-MPO) primary antibody (1:2000; Abcam, USA). Histopathological evaluation was double blinded and performed by two pathologists.

Apoptosis assay

Apoptotic cells in the lung tissue sections were quantified with TUNEL (terminal-deoxynucleotidyl transferase-mediated biotin-deoxyuridine triphosphate nick-end labeling) staining according to the manufacturer's instructions. Five visual regions were randomly selected in each sample and recorded using a fluorescence microscope (Olympus, Japan). The TUNEL-positive rate was presented by the ratio of positively stained nuclei to total nuclei using ImageJ software (version 1.51; National Institutes of Health, USA).

Western blot analysis

Total proteins were extracted from lung tissues using a radioimmunoprecipitation assay buffer (Beyotime, China) supplemented with protease and phosphatase inhibitors (Biosharp, China). Their levels were quantified using a bicinchoninic acid kit. Proteins were separated with sodium dodecyl sulfate–polyacrylamide gel and transferred to polyvinylidene fluoride membranes. They were blocked in 5% skim milk at 37 °C for 1 hour and incubated overnight at 4°C with primary antibodies: anti-PTEN (1:2000; Abcam, USA), anti-AKT (1:4000; Proteintech, China), anti-p-AKT (1:4000; Proteintech, China), anti-Bcl-2 (1:1000; Proteintech, China), anti-Bax (1:2000; Abcam, USA), anti-Cleaved Caspase 3 (1:2000; CST, USA), anti-SPC (1:1000; Proteintech, China), anti-AQP5 (1:1000; Proteintech, China), anti-Claudin 4 (1:4000; Proteintech, China) and anti-Keratin 8 (1:4000; Proteintech, China). β-actin (1:10000; Proteintech, China) was used as a reference protein. The membranes were incubated with a horseradish peroxidase-conjugated secondary antibody (1:10000; Proteintech, China) at 37 °C for 1 hour. Protein bands were detected with enhanced chemiluminescence detection reagents (Millipore, USA) and analyzed using ImageJ software (version 1.51; National Institutes of Health, USA).

Reverse-transcription quantitative PCR (RT-qPCR) assay

Total RNA from lung tissues was extracted using Trizol reagent (Takara, Japan) and reversely transcribed into cDNA with a reverse transcription kit. Spectrophotometer (Thermo Fisher, USA) was used to estimate the RNA yield. The CFX96TM Real-time Detection system (Bio-RAD, USA) and TB Green qPCR Mix Plus (Takara, Japan) were used to detect mRNA levels. The PCR results were normalized to expression of β-actin. Primer sequences for PCR are shown in Table 1.

Statistical analysis

All data were presented as mean ± standard deviation (SD). To determine data normality, the Shapiro-Wilk normality test was used. The unpaired Students *t*-test was used to compare two groups with data that had a normal distribution and similar variances. For abnormal data distribution, a nonparametric test, such as the Mann-Whitney U test was used. All statistical analyses were performed using SPSS (version 22.0, California, USA) and GraphPad Prism (version 9.2.0, California, USA) software. p values < 0.05 were considered statistically significant.

Results

Perioperative hemodynamics and metabolic parameters

Figures 1B, C shows dynamic changes of MAP and HR throughout the experiment. MAP in the ARDS group was significantly lower than in the Sham at 2 h, 4 h and 8 h, whereas they markedly improved in the TAG + ARDS group at 2 h (TAG + ARDS *vs.* ARDS, $p < 0.05$). HR was remarkably higher in the ARDS group compared with the Sham at 4 h, 6 h and 8 h and markedly lower under the TAG pretreatment at 6 h (TAG + ARDS *vs.* ARDS, $p < 0.05$). Table 2 summarizes the oxygenation and metabolic parameters in each group. The PaO_2, SaO_2, pH levels in the ARDS group were lower than in the Sham, whereas they markedly improved in the TAG + ARDS group (TAG + ARDS *vs.* ARDS, $p < 0.001$, $p < 0.01$, $p < 0.01$, respectively). The $PaCO_2$ in the ARDS group was higher than in the Sham, whereas they significantly reduced in the TAG + ARDS group (TAG + ARDS *vs.* ARDS, $p < 0.01$).

Effects of TAG on OA-induced lung injury

We established a rat model of OA-induced ARDS to assess whether TAG affects lung injury. As shown in Figure 2A, the lung tissues in the ARDS group showed dark-red congestion, edema, and exudation compared with those in the Sham group. All three signs significantly improved under the TAG pretreatment. Moreover, histological analysis of lung tissues

TABLE 1 RT-qPCR primers.

Target gene	Primer sequence
pten	Forward: 5′-AGGGACGAACTGGTGTAATGA-3′
	Reverse: 5′-CTGGTCCTTACTTCCCCATAGAA-3′
pi3k	Forward: 5′-GCCCAGGCTTACTACAGAC-3′
	Reverse: 5′-AAGTAGGGAGGCATCTCG-3′
akt	Forward: 5′-AGTCCCCACTCAACAACTTCT-3’
	Reverse: 5′-AAGTAGGGAGGCATCTCG-3′
β-actin	Forward: 5′-TGATGATATCGCCGCGCTC-3’
	Reverse: 5′-CCATCACGCCCTGGTGC-3′
spc	Forward: 5′-AAGAGATCCCTCTCCCAGCA-3′
	Reverse: 5′-TGGGGTTTGCCGCCATC-3′
aqp5	Forward: 5′-CCCTGCGGTGGTCATGAA-3′
	Reverse: 5′-CAGTCCTCCTCCGGCTCATA-3′
claudin4	Forward: 5′-CTCTCGCCTCCTCCACGTTACTC-3′
	Reverse: 5′-AGGGTAGGTGGGTGGGTAAG-3′
keratin8	Forward: 5′-CTCCGGCAGATCCATGAAGA-3′
	Reverse: 5′-GCTCGGCTGCGATTGG-3′

spc, surfactant protein C; aqp5, aquaporin 5.

indicated that increased infiltration of inflammatory cells in the alveolar cavity, edema, and interstitial thickening observed in the ARDS group considerably improved in the TAG + ARDS group (Figure 2B). Lung injury score was also significantly lower in the TAG + ARDS group than in the ARDS (TAG + ARDS, 2.77 ± 0.40 *vs.* ARDS, 4.69 ± 0.20, $p < 0.01$; Figure 2C). The protein levels in BALF were higher in the ARDS group than in the Sham and were significantly reduced by the TAG pretreatment (TAG + ARDS, 6.76 ± 0.61 *vs.* ARDS, 12.18 ± 0.89, $p < 0.001$; Figure 2D). Similarly, the Wet/Dry ratio of lung tissues in the ARDS group was higher than that in the Sham and significantly decreased under the TAG pretreatment (TAG + ARDS, 7.80 ± 0.60 *vs.* ARDS, 11.39 ± 0.85, $p < 0.01$; Figure 2E). OI of all animal groups was lower than 300 after establishing the ARDS model and markedly improved in the TAG + ARDS group versus the ARDS (ARDS, 140.30 ± 8.51 *vs.* TAG + ARDS, 363.30 ± 18.56, $p < 0.001$; Figure 2F). The $PaCO_2$ level was significantly higher in the ARDS group compared with the Sham and the TAG pretreatment decreased the level (TAG + ARDS, 48.09 ± 2.71 vs. ARDS, 64.22 ± 2.83, $p < 0.01$; Figure 2G). The pH level was significantly lower in the ARDS group compared with the Sham and the TAG pretreatment increased the level (ARDS, 7.18 ± 0.02 *vs.* TAG + ARDS, 7.32 ± 0.02, $p < 0.01$; Figure 2H).

Effects of TAG on ARDS-induced inflammation

To determine whether TAG also affects ARDS-induced inflammation, we performed immunohistochemistry staining and ELISA. The results revealed that more cells were positive for the neutrophil-specific marker MPO in the ARDS group than in the Sham, and their number significantly reduced under the TAG pretreatment (TAG + ARDS, 27.49 ± 3.29 *vs.* ARDS, 62.25 ± 7.12, $p < 0.01$; Figures 3A, B). Furthermore, the levels of TNF-α, IL-1β, IL-6, and IL-8 in BALF and lung tissues were higher in the ARDS group than in the Sham, and the TAG pretreatment decreased their levels (TAG + ARDS *vs.* ARDS, 62.82 ± 3.53 *vs.* 74.69 ± 3.89, 56.53 ± 6.89 *vs.* 77.55 ± 6.63, 38.34 ± 2.56 *vs.* 45.68 ± 3.11, and 65.83 ± 3.05 *vs.* 77.56 ± 3.22 for the BALF, respectively, $p < 0.05$; TAG + ARDS *vs.* ARDS, 44.62 ± 4.22 *vs.* 65.76 ± 3.72, $p < 0.01$, 51.74 ± 4.52 *vs.* 67.68 ± 7.19, $p < 0.05$, 29.36 ± 1.77 *vs.* 37.94 ± 2.47, $p < 0.01$, and 53.22 ± 2.87 *vs.* 65.00 ± 3.47, $p < 0.05$ for the lung, respectively; Figures 3C, D).

Effects of TAG on ARDS-induced apoptosis and PTEN/PI3K/AKT pathway

We also performed TUNEL staining to detect apoptotic cells in lung tissues (Figure 4A). We found more apoptotic cells in the ARDS group than in the Sham and observed significantly fewer apoptotic cells in the TAG + ARDS group (TAG + ARDS, 13.31 ± 2.50 *vs.* ARDS, 37.98 ± 7.85, $p < 0.01$; Figure 4B). In addition, we quantified the expression levels of apoptosis-related and central proteins in the PTEN/PI3K/AKT pathway with western blotting (Figure 4C). The expression levels of PTEN, Bax/Bcl-2 and Cleaved-Caspase3 were significantly downregulated in the TAG + ARDS group compared with the ARDS, confirming TAG relieves apoptosis (TAG + ARDS *vs.* ARDS, 0.45 ± 0.06 *vs.* 0.87 ± 0.08, 0.88 ± 0.06 *vs.* 1.36 ± 0.17, 0.63 ± 0.06 *vs.* 0.87 ± 0.05, respectively, $p < 0.01$; Figure 4D). Conversely, the TAG pretreatment remarkably upregulated p-AKT/AKT expression (ARDS, 0.64 ± 0.09 *vs.* TAG + ARDS, 1.06 ± 0.05, $p < 0.01$; Figure 4D). The RT-qPCR results show that the levels of *pten* mRNA were lower than in the TAG + ARDS group compared with the ARDS group (TAG + ARDS *vs.* ARDS, 0.59 ± 0.23 *vs.* 5.87 ± 0.51, $p < 0.001$, 0.98 ± 0.13 *vs.* 1.05 ± 0.07, $p > 0.05$, respectively; Figure 4E). However, TAG pretreatment markedly upregulated level of *pi3k* mRNA compared with the ARDS group (ARDS, 0.66 ± 0.15 *vs.* TAG + ARDS, 0.94 ± 0.08, $p < 0.05$; Figure 4E).

TABLE 2 Metabolic changes in each group throughout the procedure.

Biochemical parameters	Sham	ARDS	TAG + ARDS
pH	7.37 ± 0.01	7.18 ± 0.02***	7.32 ± 0.02$^{\#\#}$
$PaCO_2$ (mmHg)	42.65 ± 2.56	64.22 ± 2.83***	48.09 ± 2.71$^{\#\#}$
PaO_2 (mmHg)	86.44 ± 1.04	29.48 ± 2.21***	76.40 ± 1.81$^{\#\#\#}$
SaO_2 (%)	98.52 ± 0.91	95.49 ± 0.72**	97.25 ± 0.65$^{\#\#}$
Na^+ (mmol/l)	137.50 ± 0.88	140.40 ± 2.17	141.50 ± 2.05
K^+ (mmol/l)	4.37 ± 0.07	4.85 ± 0.09	4.57 ± 0.21
Ca^{2+} (mmol/l)	1.39 ± 0.01	1.36 ± 0.02	1.28 ± 0.01
Hct (%)	40.18 ± 0.14	41.57 ± 0.89	40.41 ± 0.99
Hb (g/dL)	14.41 ± 0.08	14.58 ± 0.20	14.25 ± 0.09
Lac	0.56 ± 0.09	1.64 ± 0.19	1.00 ± 0.02

$PaCO_2$, arterial partial pressure of CO_2; PaO_2, arterial partial pressure of O_2; Hct, Hematocrit; Hb, Hemoglobin. **p < 0.01, ***p < 0.001 versus Sham group; $^{\#\#}$p < 0.01, $^{\#\#\#}$p < 0.001 versus ARDS group.

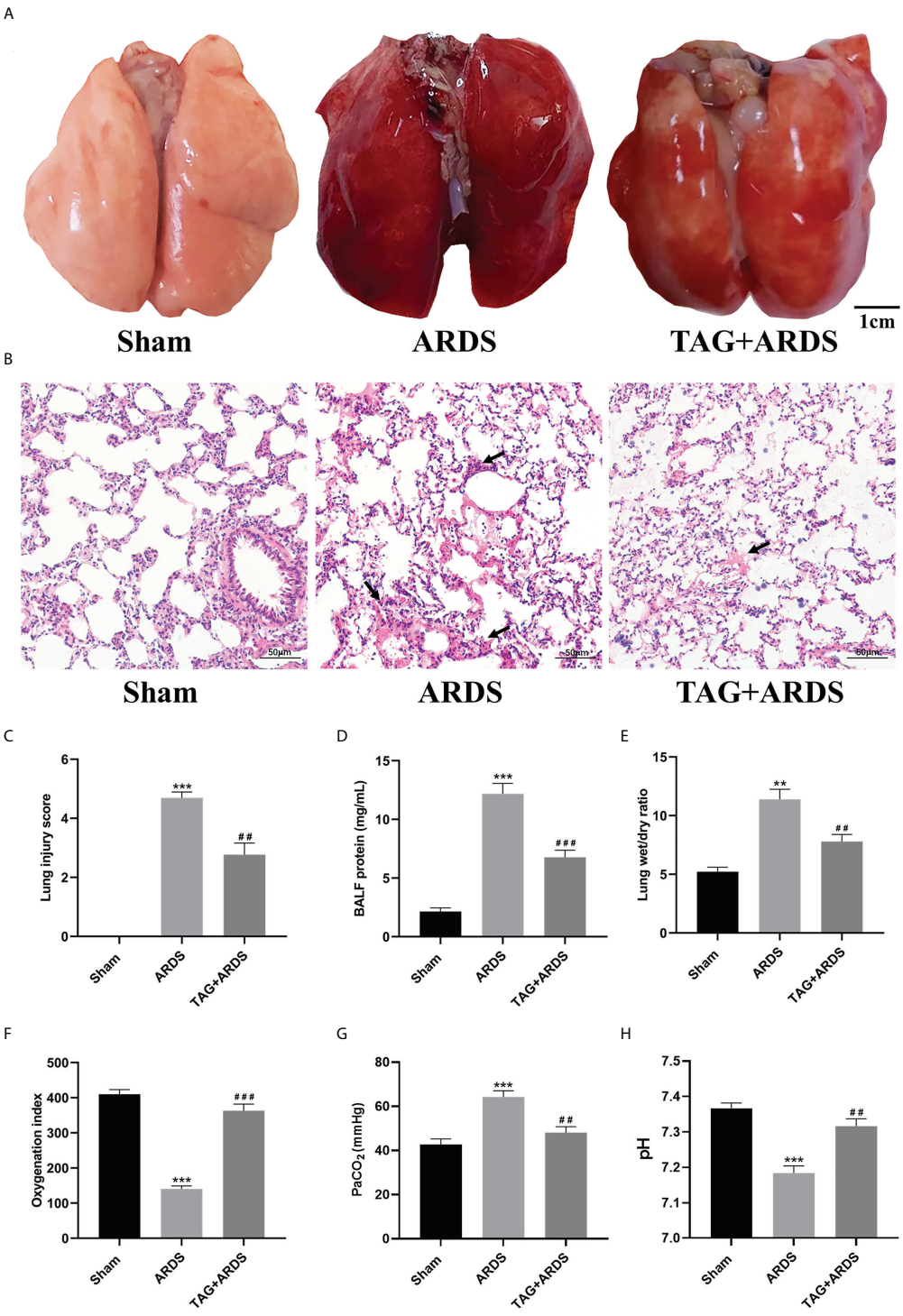

FIGURE 2
TAG pretreatment protects from OA-induced lung injury in Sprague-Dawley rats. **(A)** Gross pathological images of lung injury across experimental animal groups (scale bar = 1 cm): Sham, ARDS, and TAG+ ARDS (pretreated with TAG 3 days before ARDS induction). **(B, C)** Representative histological images of lung and lung injury score in the groups (scale bar = 50 μm). Arrows represent edema and inflammatory cell infiltration in alveolar cavity. **(D)** Protein levels in BALF in each group. **(E)** Wet/Dry weight ratio of the left lung. **(F–H)** OI, $PaCO_2$ and pH determined for each group. Data are presented as the mean ± SD. $^{**}p < 0.01$, $^{***}p < 0.001$, compared with the Sham group; $^{\#\#}p < 0.01$, $^{\#\#\#}p < 0.001$, compared with the ARDS group. TAG, D-tagatose; OA, oleic acid; ARDS, acute respiratory distress syndrome; BALF, bronchoalveolar lavage fluid; OI, Oxygenation indexes.

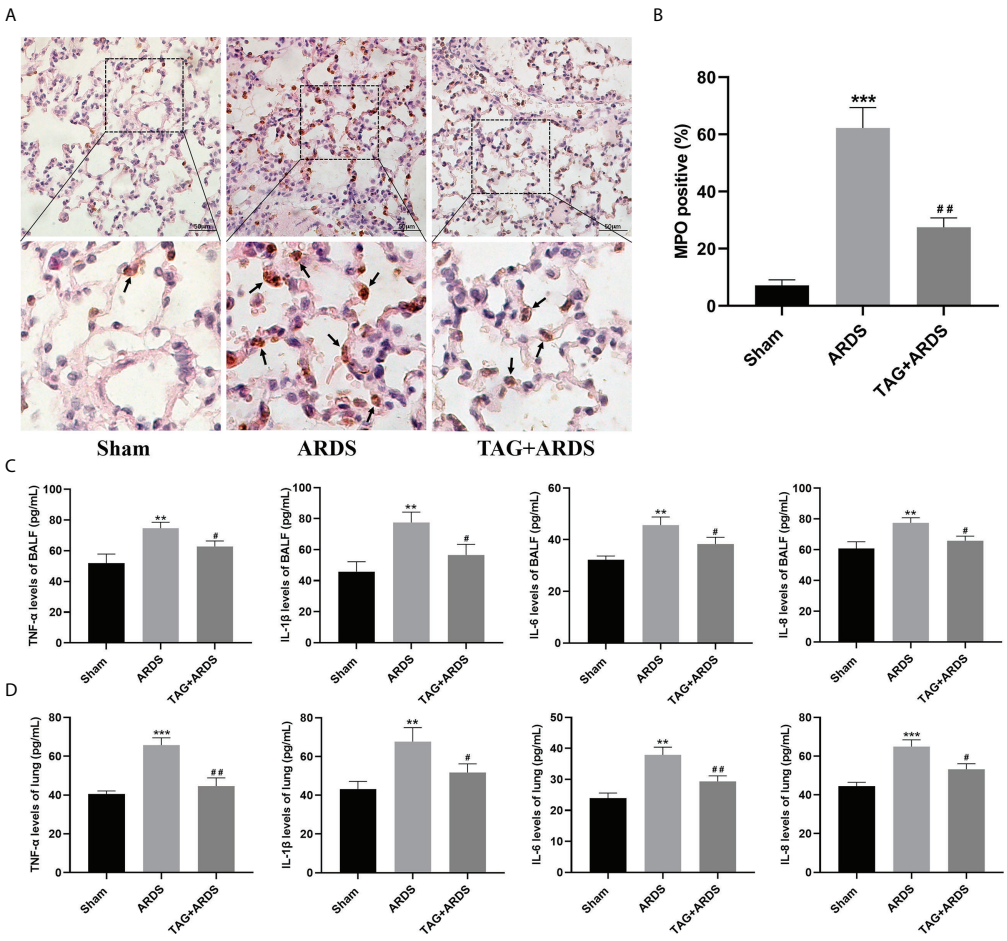

FIGURE 3
Effects of TAG on ARDS-induced inflammation. **(A, B)** Representative images of MPO-positive lung cells and their quantification in experimental animal groups: Sham, ARDS, and TAG + ARDS. Arrows represent neutrophil infiltrations (scale bar = 50 μm). **(C, D)** Levels of TNF-α, IL-1β, IL-6, and IL-8 in BALF and lung tissues assessed by ELISA. Data are presented as mean ± SD. $^{**}p < 0.01$, $^{***}p < 0.001$, compared with the Sham group; $^{\#}p < 0.05$, $^{\#\#}p < 0.01$, compared with the ARDS group. MPO, myeloperoxidase; TAG, D-tagatose; ARDS, acute respiratory distress syndrome; IHC, immunohistochemistry.

Effects of TAG on ARDS-induced alveolar and endothelial damage

Next, we performed immunofluorescence staining and western blotting to determine whether TAG affects the alveolar structure and the juxtaposed endothelium under inflammatory conditions. We double-stained alveolar epithelial cells for markers of alveolar type I and II cells (AQP5 and SPC) (Figure 5A). Results show that the expression levels of SPC and AQP5 in the ARDS group were lower than in the Sham but significantly higher on the TAG pretreatment (ARDS, 14.41 ± 4.65 *vs.* TAG + ARDS, 41.40 ± 4.33, $p < 0.01$; Figure 5B). We also stained vascular endothelial cells for the vascular marker CD31 and found numerous vascular endothelial cells in the TAG + ARDS group compared with the ARDS (ARDS, 10.76 ± 1.96 *vs.* TAG + ARDS, 16.88 ± 2.01, $p < 0.01$; Figures 5C, D). The expression levels of SPC and AQP5 proteins in the ARDS group were lower than in the Sham but increased under the TAG pretreatment (ARDS vs. TAG + ARDS, 0.28 ± 0.08 vs. 0.71 ± 0.04 and 0.49 ± 0.08 vs. 0.79 ± 0.08, respectively, $p < 0.01$; Figures 5E, F). The RT-qPCR results show that the levels of *spc*, *aqp5*, *claudin4 and keratin8* mRNA are markedly higher in the TAG + ARDS group compared with the ARDS group (ARDS *vs.* TAG + ARDS, 0.26 ± 0.09 *vs.* 0.76 ± 0.12, 0.44 ± 0.06 *vs.* 0.71 ± 0.05, 0.32 ± 0.06 *vs.* 0.59 ± 0.05, and 0.48 ± 0.11 *vs.* 0.72 ± 0.09, respectively, $p < 0.01$; Figures 5G, 6G).

Effects of TAG on differentiation of alveolar type II cells

The transitional state of alveolar type II cells was marked by Claudin 4 and Keratin 8 (Figures 6A, C). We identified significantly

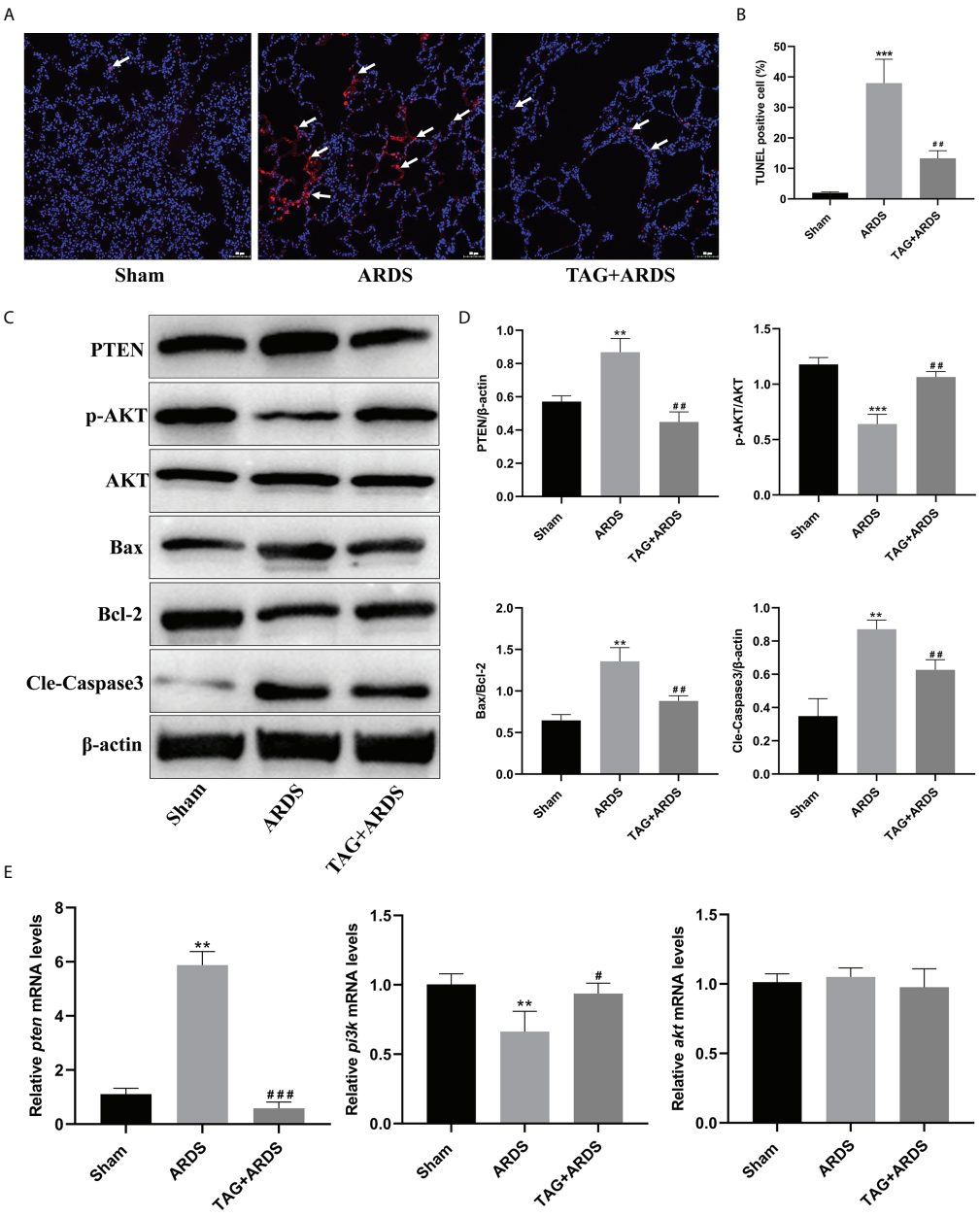

FIGURE 4
Effects of TAG on ARDS-induced apoptosis and PTEN/PI3K/AKT pathway. **(A, B)** Representative images of TUNEL-stained cells and their quantitation in lung tissue sections of 3 experimental animal groups: Sham, ARDS, and TAG + ARDS. Arrows represent apoptotic cells (scale bar = 50 μm). **(C, D)** Representative WB images and quantitation of PTEN, p-AKT/AKT, Bax/Bcl-2, and Cleaved Caspase 3 protein expression levels. **(E)** RT-qPCR results show that the transcripts levels for *pten*, *pi3k*, and *akt* mRNA. Data are presented as mean ± SD. $p > 0.05$, $^{**}p < 0.01$, $^{***}p < 0.001$, compared with the Sham group; $p > 0.05$, $^{\#}p < 0.05$, $^{\#\#}p < 0.01$, $^{\#\#\#}p < 0.001$, compared with the ARDS group. TAG, D-tagatose; ARDS, acute respiratory distress syndrome.

more ATII cells in the transitional state in the TAG + ARDS group than in the ARDS (ARDS *vs.* TAG + ARDS, 9.34 ± 2.94 *vs.* 25.52 ± 3.03, $p < 0.01$, 6.63 ± 1.45 *vs.* 27.23 ± 2.51, $p < 0.001$, respectively; Figures 6B, D). In addition, the expression levels of Claudin 4 and Keratin 8 proteins in the ARDS group were lower than in the Sham but increased under the TAG pretreatment (ARDS *vs.* TAG + ARDS, 0.48 ± 0.07 *vs.* 0.72 ± 0.06 and 0.44 ± 0.06 *vs.* 0.77 ± 0.05, respectively, $p < 0.01$; Figures 6E, F).

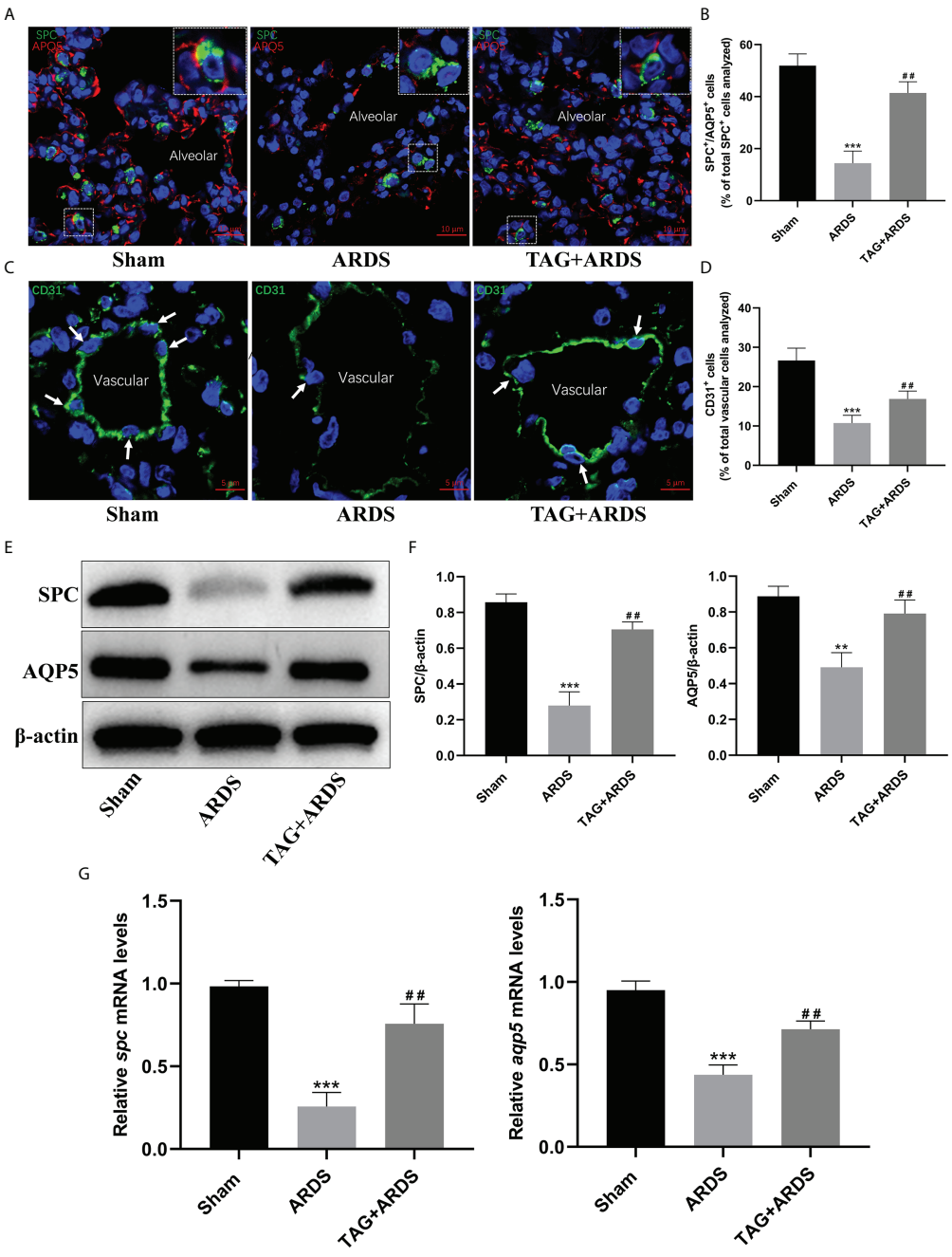

FIGURE 5
Effects of TAG on ARDS-induced alveolar and endothelial damage. **(A, B)** Representative immunofluorescence images and quantification of alveolar type I and II epithelial cells in Sham, ARDS, and TAG + ARDS groups. The lungs were co-immunostained for SPC and AQP5 alveolar epithelial-specific markers (scale bar = 10 μm). The marker-positive cells were quantified with a confocal microscope. **(C, D)** Representative immunofluorescence images and quantification of CD31-positive vascular endothelial cells in each group. Arrows represent vascular endothelial cells (scale bar = 5 μm). **(E, F)** Representative WB images and assessment of SPC and AQP5 protein expression levels in each group. **(G)** RT-qPCR results show that the transcripts levels for *spc* and *aqp5* mRNA. Data are presented as mean ± SD. $^{**}p < 0.01$, $^{***}p < 0.001$, compared with the Sham group; $^{\#\#}p < 0.01$, compared with the ARDS group. TAG, D-tagatose; ARDS, acute respiratory distress syndrome; SPC, surfactant protein C; AQP5, aquaporin 5.

Discussion

The specific mechanism of ARDS remains unclear, and effective drugs for treating ARDS are lacking. Thus, an OA-induced rat model of ARDS was established to explore a possible protective effect of TAG on lung injury. It is widely used in scientific research because it faithfully simulates the pathophysiological manifestations of ARDS patients and is simple, stable, and reliable (7). Subjecting the animals with OA-induced ARDS to a TAG pretreatment for 3 days significantly reduced pulmonary edema, improved gas exchange, increased the oxygenation index, reduced respiratory acidosis, and alleviated inflammation. Moreover, TAG promoted the repair of damaged alveolar epithelial and endothelial cells, inhibiting the expression of apoptosis-related proteins and activating the PTEN/PI3K/AKT pathway. These results suggest that TAG reduces OA-induced ARDS in rats, opening a new way for treating the condition.

TAG is a low-calorie sweetener and a promising novel functional food product (11). Recently, few studies explored its potential as a therapeutic drug for diseases. In one study, for example, TAG reduced the susceptibility to cardiovascular disease, but its role in respiratory diseases was unknown (15). OA induces ARDS in rats. It causes excessive protein-rich fluid exudation, extensive hyperemia, and edema, accompanied by inflammation (7). The Wet/Dry ratio of the lung is an indicator of pulmonary edema (17). We showed that TAG reduces it in OA-induced ARDS rats, which we confirmed with hematoxylin–eosin staining, among other methods. Neutrophils are crucial inflammatory cells in acute inflammation and the first-recruited cells in ARDS (18). They release proteases that cause the initial tissue damage and further migrate to the lungs for degranulation. This process releases inflammatory mediators (e.g., bactericidal proteins, cytokines, and reactive oxygen species), aggravating the inflammatory response (19, 20). Therefore, neutrophil content in alveoli reflects the degree of inflammation in the lung. We discovered that a 3-day TAG pretreatment reduces the exudation of MPO in the alveolar tissue under inflammatory conditions. This observation suggests that TAG relieves excessive ARDS-promoted secretion of inflammatory mediators in the lung. Under exacerbated pulmonary inflammation, activated alveolar macrophages release TNF-α and IL-1β, stimulating other alveolar cells (e.g., alveolar epithelial cells, macrophages, etc.) to secrete chemokines and activate the inflammatory cascade, causing continuous migration of inflammatory cells to the lungs (21). Consequently, further damage to the lung occurs. Tumor necrosis factor-alpha is a central pro-inflammatory factor in ARDS. It increases capillary permeability and initiates substantial fluid exudation, causing extensive pulmonary edema and endothelial disruption (22). Our results revealed that the expression of pro-inflammatory factors TNF-α, IL-1β, IL-6, and IL-8 in BALF and lung tissues reduces if the tissues were pretreated with TNF-α, suggesting its anti-inflammatory effect.

The PTEN/PI3K/AKT signaling pathway protects lung epithelial cells and relieves lung inflammation (23). Its activation can significantly delay the onset of acute lung injury, increasing the survival rate of animals. In humans, deleting PTEN stimulates the proliferation of malignant cells through polymorphic mutation or gene deletion, identifying the protein as a proto-oncogene (24). Although the permanent loss of PTEN function may have adverse consequences, the temporary, controllable inhibition of PTEN in lung epithelial cells is helpful for the regeneration of lung epithelium after injury (23). Moreover, the activation of PI3K/AKT signaling pathway in human lung epithelial cells occurs after PTEN is inhibited, and no agonists are later added in the process (25). We found that the PI3K/AKT signaling is inhibited in lung tissues of rats with ARDS. Pretreating the animals with TAG inhibits PTEN and activates the PI3K/AKT cascade, consistent with previous results. Thus, TAG can be used as a temporary, controllable pharmacological inhibitor of PTEN that activates the PI3K/AKT pathway and protects from lung tissue damage.

Normal alveoli are mainly composed of alveolar type I and alveolar type II cells. Alveolar type I cells are large and flat, accounting for more than 95% of the alveolar area and having an important role in gas exchange (26). Alveolar regeneration commences after acute lung injury in many mammal species. After the injury, alveolar type II cells assume stem cell properties, rapidly proliferating and differentiating into alveolar type II cells (27). Hence, they replenish the alveolar epithelium. We discovered that the number of alveolar type II cells positive increases significantly in TAG-administered rats with ARDS, suggesting enhanced proliferation of alveolar type II cells. When human and mouse lungs are injured, alveolar type II cells acquire a transient intermediate state before trans-differentiating into alveolar type I cells (28–30). Three markers for the intermediate state of alveolar type II cells are known: Claudin 4, Stratifin, and Keratin 8 (31). Interestingly, none are expressed in alveolar type II cells under physiological conditions. We found that few alveolar type II cells were in the intermediate state in lung tissues of rats with ARDS compared with control animals, indicating a compromised regenerative potential. Nonetheless, their levels increased significantly under the TAG pretreatment, suggesting that TAG promotes the repair of damaged alveoli.

Our study has several drawbacks and should be interpreted in the specific context of prophylactic administration of TAG for treating ARDS. First, it does not suggest any information on the sustained efficacy of the TAG. Second, although TAG can be administered safely over a range of doses without evident side effects, our study used only a single one (300 mg/kg) for the TAG pretreatment. Third, Oleic acid is an acid that can increase H^+ in

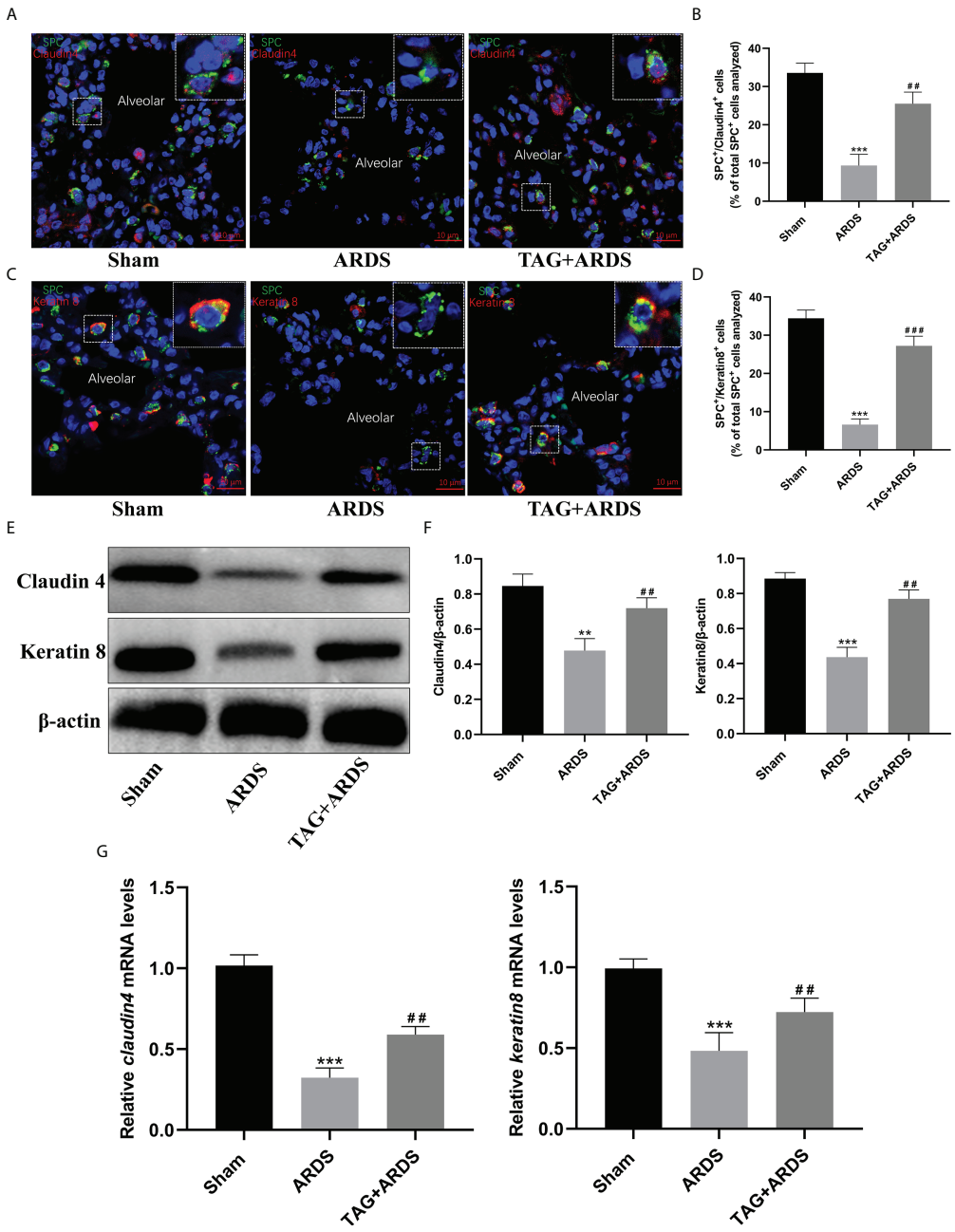

FIGURE 6
Effects of TAG on differentiation of alveolar type II cells under lung injury. **(A–D)** Representative immunofluorescence images of alveolar type II epithelial cells in the alveolar type II cells–alveolar type I cells transitional state (SPC^+–Claudin 4^+ and SPC^+–Keratin 8^+) across 3 experimental groups: Sham, ARDS, and TAG + ARDS (scale bar = 10 μm). The marker-positive cells were quantified with a confocal microscope. **(E, F)** Representative WB and quantification of Claudin 4 and Keratin 8 protein expression levels in each group. **(G)** RT-qPCR results show that the transcripts levels for *claudin 4* and *keratin 8* mRNA. Data are presented as mean ± SD. $^{**}p < 0.01$, $^{***}p < 0.001$, compared with the Sham group; $^{\#\#}p < 0.01$, $^{\#\#\#}p < 0.001$, compared with the ARDS group. TAG, D-tagatose; ARDS, acute respiratory distress syndrome; SPC, surfactant protein C.

blood and cause acidosis and tissue damage, so it cannot completely simulate the pathophysiological process of human ARDS. Nonetheless, our data still provide valuable information for the development of drugs to treat ARDS.

Conclusions

In conclusion, TAG pretreatment protects lung tissues from OA-induced ARDS in rats. This protective effect may be related to

reducing inflammation, inhibiting apoptosis, activating the PI3K/AKT pathway, and improving alveolar and microvascular permeability. However, further experiments are necessary to identify its underlying mechanism. Our study represents the basis for developing novel therapeutic strategies for managing ARDS.

Data availability statement

The original contributions presented in the study are included in the article/supplementary material. Further inquiries can be directed to the corresponding authors.

Ethics statement

The animal study was reviewed and approved by the Committee of Ethics on Animal Experiments at the Anhui Medical University. Written informed consent was obtained from the owners for the participation of their animals in this study.

Author contributions

YL, BG, and XC designed the study. JH, BW, and ST performed the experiments. YH and NW performed the statistical analysis. JH, BW and ST drafted the article. YL, BG, XC, CW and CC supervised the experimental work. All authors contributed to the article and approved the submitted version.

Funding

This work was supported by the Basic and Clinical Cooperative Research Promotion Program of Anhui Medical University (2020xkjT046), the research fund of Anhui Medical University (2019xkj144), the Open Research fund of Key Laboratory of Anesthesiology and Perioperative Medicine of Anhui Higher Education Institutes, Anhui Medical University (MZKF202003), Lanzhou Science and Technology Bureau, science and technology planning project of Lanzhou (2020-XG-59).

Acknowledgments

We would like to thank Home for Researchers for providing language help and writing assistance. In addition, we also thank Li Zhang and Gao Cheng for their help with the literature search and sample processing.

Conflict of interest

The authors declare that the research was conducted in the absence of any commercial or financial relationships that could be construed as a potential conflict of interest.

Publisher's note

References

1. Zhang Q, Wang Y, Qu D, Yu J, Yang J. Role of HDAC6 inhibition in sepsis-induced acute respiratory distress syndrome (Review). *Exp Ther Med* (2021) 21:781874(5). doi: 10.3389/fphys.2021.781874

2. Meyer NJ, Gattinoni L, Calfee CS. Acute respiratory distress syndrome. *Lancet* (2021) 398(10300):622–37. doi: 10.1016/s0140-6736(21)00439-6

3. Dutra Silva J, Su Y, Calfee CS, Delucchi KL, Weiss D, McAuley DF, et al. Mesenchymal stromal cell extracellular vesicles rescue mitochondrial dysfunction and improve barrier integrity in clinically relevant models of Ards. *Eur Respir J* (2021) 58(1):2002978. doi: 10.1183/13993003.02978-2020

4. Rothberg AD, Smith J, Lubbe W. Evidence of an active cushing reflex in a preterm neonate with hyaline membrane disease: A case report. *J Med Case Rep* (2021) 15(1):592. doi: 10.1186/s13256-021-03161-1

5. Mendez MP, Morris SB, Wilcoxen S, Du M, Monroy YK, Remmer H, et al. Disparate mechanisms of sicam-1 production in the peripheral lung: Contrast between alveolar epithelial cells and pulmonary microvascular endothelial cells. *Am J Physiol Lung Cell Mol Physiol* (2008) 294(4):L807–14. doi: 10.1152/ajplung.00398.2007

6. Jiang Z, Chen Z, Li L, Zhou W, Zhu L. Lack of SOCS3 increases LPS-induced murine acute lung injury through modulation of Ly6C(+) macrophages. *Respir Res* (2017) 18(1):217. doi: 10.1186/s12931-017-0707-6

7. Gonçalves-de-Albuquerque CF, Silva AR, Burth P, Castro-Faria MV, Castro-Faria-Neto HC. Acute respiratory distress syndrome: Role of oleic acid-triggered lung injury and inflammation. *Mediators Inflamm* (2015) 2015:260465. doi: 10.1155/2015/260465

8. Jung SY, Kim DY, Yune TY, Shin DH, Baek SB, Kim CJ. Treadmill exercise reduces spinal cord injury-induced apoptosis by activating the Pi3k/Akt pathway in rats. *Exp Ther Med* (2014) 7(3):587–93. doi: 10.3892/etm.2013.1451

9. Lai JP, Bao S, Davis IC, Knoell DL. Inhibition of the phosphatase pten protects mice against oleic acid-induced acute lung injury. *Br J Pharmacol* (2009) 156(1):189–200. doi: 10.1111/j.1476-5381.2008.00020.x

10. Han X, Zhuang Y. Pm2.5 induces autophagy-mediated cell apoptosis *Via* Pi3k/Akt/Mtor signaling pathway in mice bronchial epithelium cells. *Exp Ther Med* (2021) 21(1):1. doi: 10.3892/etm.2020.9433

11. Zhang J, Gao X, Schmit F, Adelmant G, Eck MJ, Marto JA, et al. Crkl mediates P110β-dependent Pi3k signaling in pten-deficient cancer cells. *Cell Rep* (2017) 20(3):549–57. doi: 10.1016/j.celrep.2017.06.054

12. Wanarska M, Kur J. A method for the production of d-tagatose using a recombinant pichia pastoris strain secreting β-D-Galactosidase from arthrobacter chlorophenolicus and a recombinant l-arabinose isomerase from arthrobacter sp. 22c. *Microb Cell Fact* (2012) 11:113. doi: 10.1186/1475-2859-11-113

13. Guo Q, An Y, Yun J, Yang M, Magocha TA, Zhu J, et al. Enhanced d-tagatose production by spore surface-displayed l-arabinose isomerase from isolated lactobacillus brevis Pc16 and biotransformation. *Bioresour Technol* (2018) 247:940–6. doi: 10.1016/j.biortech.2017.09.187

14. Bertelsen H, Jensen BB, Buemann B. D-Tagatose–a novel low-calorie bulk sweetener with prebiotic properties. *World Rev Nutr Diet* (1999) 85:98–109. doi: 10.1159/000059685

15. Levin GV. Tagatose, the new gras sweetener and health product. *J Med Food* (2002) 5(1):23–36. doi: 10.1089/109662002753723197

16. Durante M, Sgambellone S, Lucarini L, Failli P, Laurino A, Collotta D, et al. D-tagatose feeding reduces the risk of sugar-induced exacerbation of myocardial I/R injury when compared to its isomer fructose. *Front Mol Biosci* (2021) 8:650962. doi: 10.3389/fmolb.2021.650962

17. Peng LY, Yuan M, Shi HT, Li JH, Song K, Huang JN, et al. Protective effect of piceatannol against acute lung injury through protecting the integrity of air-blood barrier and modulating the Tlr4/Nf-κb signaling pathway activation. *Front Pharmacol* (2019) 10:1613. doi: 10.3389/fphar.2019.01613

18. Dupuis J, Sirois MG, Rhéaume E, Nguyen QT, Clavet-Lanthier M, Brand G, et al. Colchicine reduces lung injury in experimental acute respiratory distress syndrome. *PloS One* (2020) 15(12):e0242318. doi: 10.1371/journal.pone.0242318

19. Prame Kumar K, Nicholls AJ. Wong CHY. partners in crime: Neutrophils and Monocytes/Macrophages in inflammation and disease. *Cell Tissue Res* (2018) 371(3):551–65. doi: 10.1007/s00441-017-2753-2

20. Potey PM, Rossi AG, Lucas CD, Dorward DA. Neutrophils in the initiation and resolution of acute pulmonary inflammation: Understanding biological function and therapeutic potential. *J Pathol* (2019) 247(5):672–85. doi: 10.1002/path.5221

21. Matthay MA, Zemans RL, Zimmerman GA, Arabi YM, Beitler JR, Mercat A, et al. Acute respiratory distress syndrome. *Nat Rev Dis Primers* (2019) 5(1):18. doi: 10.1038/s41572-019-0069-0

22. Scott BNV, Kubes P. Death to the neutrophil! a resolution for acute respiratory distress syndrome? *Eur Respir J* (2018) 52(2):1801274. doi: 10.1183/13993003.01274-2018

23. Lai JP, Dalton JT, Knoell DL. Phosphatase and tensin homologue deleted on chromosome ten (Pten) as a molecular target in lung epithelial wound repair. *Br J Pharmacol* (2007) 152(8):1172–84. doi: 10.1038/sj.bjp.0707501

24. Tu K, Liu Z, Yao B, Han S, Yang W. Microrna-519a promotes tumor growth by targeting Pten/Pi3k/Akt signaling in hepatocellular carcinoma. *Int J Oncol* (2016) 48(3):965–74. doi: 10.3892/ijo.2015.3309

25. Bao S, Wang Y, Sweeney P, Chaudhuri A, Doseff AI, Marsh CB, et al. Keratinocyte growth factor induces akt kinase activity and inhibits fas-mediated apoptosis in A549 lung epithelial cells. *Am J Physiol Lung Cell Mol Physiol* (2005) 288(1):L36–42. doi: 10.1152/ajplung.00309.2003

26. Gupte VV, Ramasamy SK, Reddy R, Lee J, Weinreb PH, Violette SM, et al. Overexpression of fibroblast growth factor-10 during both inflammatory and fibrotic phases attenuates bleomycin-induced pulmonary fibrosis in mice. *Am J Respir Crit Care Med* (2009) 180(5):424–36. doi: 10.1164/rccm.200811-1794OC

27. Hogan BL, Barkauskas CE, Chapman HA, Epstein JA, Jain R, Hsia CC, et al. Repair and regeneration of the respiratory system: Complexity, plasticity, and mechanisms of lung stem cell function. *Cell Stem Cell* (2014) 15(2):123–38. doi: 10.1016/j.stem.2014.07.012

28. Wu H, Yu Y, Huang H, Hu Y, Fu S, Wang Z, et al. Progressive pulmonary fibrosis is caused by elevated mechanical tension on alveolar stem cells. *Cell* (2020) 180(1):107–21.e17. doi: 10.1016/j.cell.2019.11.027

29. Riemondy KA, Jansing NL, Jiang P, Redente EF, Gillen AE, Fu R, et al. Single cell rna sequencing identifies tgfβ as a key regenerative cue following lps-induced lung injury. *JCI Insight* (2019) 5(8):e123637. doi: 10.1172/jci.insight.123637

30. Jiang P, Gil de Rubio R, Hrycaj SM, Gurczynski SJ, Riemondy KA, Moore BB, et al. Ineffectual type 2-to-Type 1 alveolar epithelial cell differentiation in idiopathic pulmonary fibrosis: Persistence of the Krt8(Hi) transitional state. *Am J Respir Crit Care Med* (2020) 201(11):1443–7. doi: 10.1164/rccm.201909-1726LE

31. Chen J, Wu H, Yu Y, Tang N. Pulmonary alveolar regeneration in adult covid-19 patients. *Cell Res* (2020) 30(8):708–10. doi: 10.1038/s41422-020-0369-7

frontiers | Frontiers in Immunology

TYPE Brief Research Report
PUBLISHED 20 October 2022
DOI 10.3389/fimmu.2022.993720

OPEN ACCESS

EDITED BY
Roman A. Zinovkin,
Lomonosov Moscow State University, Russia

REVIEWED BY
Akrivi Chrysanthopoulou,
Akrivi Chrysanthopoulou, Greece
Meraj Alam Khan,
University of Toronto, Canada
Taisheng Li,
Peking Union Medical College Hospital (CAMS), China

*CORRESPONDENCE
Jorge Adrian Masso-Silva
jmassosilva@ucsd.edu

SPECIALTY SECTION
This article was submitted to Inflammation, a section of the journal Frontiers in Immunology

RECEIVED 14 July 2022
ACCEPTED 30 September 2022
PUBLISHED 20 October 2022

CITATION
Masso-Silva JA, Sakoulas G, Olay J, Groysberg V, Geriak M, Nizet V, Crotty Alexander LE and Meier A (2022) Abrogation of neutrophil inflammatory pathways and potential reduction of neutrophil-related factors in COVID-19 by intravenous immunoglobulin. *Front. Immunol.* 13:993720. doi: 10.3389/fimmu.2022.993720

Abrogation of neutrophil inflammatory pathways and potential reduction of neutrophil-related factors in COVID-19 by intravenous immunoglobulin

Jorge Adrian Masso-Silva[1,2]*, George Sakoulas[3,4], Jarod Olay[1,2], Victoria Groysberg[5], Matthew Geriak[6], Victor Nizet[5,7], Laura E. Crotty Alexander[1,2] and Angela Meier[8]

[1]Section of Pulmonary and Critical Care, Veterans Affairs (VA) San Diego, La Jolla, CA, United States, [2]Division of Pulmonary, Critical Care, Sleep and Physiology, University of California San Diego (UCSD), La Jolla, CA, United States, [3]Department of Infectious Disease, Sharp Rees-Stealy Medical Group, San Diego, CA, United States, [4]Department of Pediatrics, School of Medicine, University of California San Diego, San Diego, CA, United States, [5]Division of Host-Microbe Systems and Therapeutics, Department of Pediatrics, University of California (UC) San Diego, La Jolla, CA, United States, [6]Department of Research, Sharp Healthcare, San Diego, CA, United States, [7]Skaggs School of Pharmacy and Pharmaceutical Sciences, University of California (UC) San Diego, La Jolla, CA, United States, [8]Department of Anesthesiology, Division of Critical Care, UCSD, La Jolla, CA, United States

Pathogenesis of lung injury in COVID-19 is not completely understood, leaving gaps in understanding how current treatments modulate the course of COVID-19. Neutrophil numbers and activation state in circulation have been found to correlate with COVID-19 severity, and neutrophil extracellular traps (NETs) have been found in the lung parenchyma of patients with acute respiratory distress syndrome (ARDS) in COVID-19. Targeting the pro-inflammatory functions of neutrophils may diminish lung injury in COVID-19 and ARDS. Neutrophils were isolated from peripheral blood of healthy donors, treated *ex vivo* with dexamethasone, tocilizumab and intravenous immunoglobulin (IVIG) and NET formation, oxidative burst, and phagocytosis were assessed. Plasma from critically ill COVID-19 patients before and after clinical treatment with IVIG and from healthy donors was assessed for neutrophil activation-related proteins. While dexamethasone and tocilizumab did not affect PMA- and nigericin-induced NET production *ex vivo*, IVIG induced a dose-dependent abrogation of NET production in both activation models. IVIG also reduced PMA-elicited reactive oxygen species production, but did not alter phagocytosis. COVID-19 patients were found to have elevated levels of cell-free DNA, neutrophil elastase and IL-8 as compared to healthy controls. Levels of both cell-free DNA and neutrophil elastase were lower 5 days after 4 days of daily treatment with IVIG. The lack of impact of dexamethasone or tocilizumab

on these neutrophil functions suggests that these therapeutic agents may not act through suppression of neutrophil functions, indicating that the door might still be open for the addition of a neutrophil modulator to the COVID-19 therapeutic repertoire.

KEYWORDS

intravenous immunoglobulin (IVIG), neutrophils, NETosis, oxidative burst, COVID-19, corticosteroids, dexamethasone, tocilizumab

Introduction

Neutrophils are the most abundant immune cells in circulation and are key for host immune responses. Neutrophils are promptly recruited to sites of infection and key in shaping adaptive immune responses (1, 2). Despite their vital role in clearing infections, neutrophils can cause significant collateral tissue damage if not properly controlled (3, 4). This is evidenced by the pathologic role of neutrophils in many infections and autoimmune diseases (5–7). In the context of infections, our research and others recently identified neutrophilia and neutrophil activity as prognostic factors in COVID-19 and associated with increased disease severity (8). Acute respiratory distress syndrome (ARDS) is the heterogeneous condition at the center of COVID-19 pathophysiology, where inflammatory cells such as neutrophils are recruited to the lung, contributing to tissue damage, ultimately leading to respiratory failure (8–11).

As phagocytes, neutrophils engulf pathogens within phagosomes, merge them with lysosomes, leading to killing of pathogens *via* oxidative burst (producing reactive oxygen species or ROS), low pH, antimicrobial molecules and degrading enzymes (12). Another key antimicrobial function is the production of neutrophil extracellular traps (NETs), which are formed by expulsion of DNA with adherent antimicrobial proteins including myeloperoxidase (MPO), elastase, histones, LL-37, etc. (13). In addition, neutrophils can release ROS, which can modify extracellular targets and affect the function of neighboring cells (14). Both NETosis and oxidative burst have been implicated in tissue damage (3–5) and are highly pro-inflammatory (4, 13, 14).

Corticosteroids are commonly used to treat inflammatory diseases to limit tissue damage (*e.g.* bacterial meningitis, brain tumors, and connective tissue diseases) (15). Dexamethasone is a widely used corticosteroid and became a standard treatment during the COVID-19 pandemic. Dexamethasone was found to lower 28-day mortality among COVID-19 patients who were receiving either invasive mechanical ventilation or oxygen alone (16, 17). Other therapeutic approaches in COVID-19 involve the use of biologics that target pro-inflammatory cytokines, such as IL-6, IL-1, GM-CSF, and TNFα (18). Tocilizumab, a monoclonal antibody against the IL-6 receptor, was the first biologic agent with proven efficacy in COVID-19 and is now an approved therapy (18). However, a recent randomized controlled trial (RCT) found that tocilizumab does not improve clinical outcomes or decrease mortality at 28 days (19), although the findings of another RCT supports the use of tocilizumab for patients with moderate-to-severe COVID-19 and high c-reactive protein (CRP) levels (20). Nevertheless, despite the implementation of these and other therapies, COVID-19 mortality rate remains high in patients with critical illness (21).

Intravenous immunoglobulins (IVIG) have been used primarily in the treatment of autoimmune diseases, with favorable results. In many of these diseases, including systemic lupus erythematosus, antiphospholipid syndrome and multiple sclerosis, neutrophils have been found to be important drivers of exacerbations (22–25). Multiple small clinical trials of IVIG as a treatment in COVID-19 have shown beneficial effects by reducing mortality and time of hospitalization (26–34), while one RCT found that treatment with IVIG (added to hydroxychloroquine and lopinavir/ritonavir therapies for all trial subjects) found that earlier IVIG administration correlated with shorter hospital and ICU stays (35). On the other hand, the results of another large and randomized clinical trial have suggested that IVIG treatment may lead to increased mortality and increased frequency of serious adverse events (36).

IVIG modulates the activation of multiple leukocytes, including monocytes/macrophages (37, 38), dendritic cells (38), T cells (39) and B cells (40). Interestingly, *ex vivo* treatment of leukocytes with IVIG has been shown to reduce production of ROS (41). In the context of neutrophils, early studies found that IVIG can activate neutrophils, leading to production of ROS (42–44), release of MPO (45) and elastase (46), and alterations in surface markers (47). More recently, Bohländer *et al*, found that IVIG treatment decreases inflammation in neutrophil-like HL-60 cells *via* reduction in release of cytokines (48), and Uozumi et al. observed that IVIG treatment of human neutrophils led to reduced NETosis by fluorescence microscopy (49). However, there are significant differences in the experimental designs of all those studies.

Based on the proven anti-inflammatory effects of IVIG observed in patients with autoimmune diseases, the

discrepancies across prior *ex vivo* and *in vitro* assessments of IVIG on neutrophil function, and our previous observation of the contribution of neutrophils to ARDS immunopathology in COVID-19 (8), we undertook this study to define the impact of IVIG and anti-inflammatory treatments used in COVID-19 (dexamethasone and tocilizumab) on key pro-inflammatory and antimicrobial neutrophil functions. Further, we assessed NET components within plasma of COVID-19 patients whose therapy was complemented with IVIG.

Materials and methods

Study design and oversight

Patients admitted to a single center in San Diego, CA with COVID-19 confirmed by a PCR test (nasal or pharyngeal sample) who developed rapid hypoxemic respiratory failure from ARDS and requiring mechanical ventilation were considered for off-label IVIG therapy (0.5g/kg adjusted body weight per day for 4 consecutive days) < 72 hours from onset of mechanical ventilation. Patients with any baseline chronic organ failure comorbidities (*e.g.* heart failure, renal failure, stroke, dementia, or active malignancy) were excluded. A protocol entitled "Pilot study of the use of IVIG in patients with severe COVID-19 requiring mechanical ventilation and to assess their biological responses to IVIG therapy" (clincaltrials.gov NCT04616001) allowed for patient or next of kin consent for analysis of blood samples for this study that were obtained before, during, and after IVIG therapy. Blood analyzed consisted of residuals from samples drawn as part of routine daily blood work. Other than receipt of off-label IVIG, patients received standard of care diagnostic and therapeutic management contemporary for the time in the pandemic (December 2020-March 2021). The study was reviewed and approved by the Sharp Healthcare Internal Review Board (#2010902). *Ex vivo* neutrophil and plasma studies were conducted with VASDHS institutional review board (IRB) approval B200003, a non-human subject research waiver from the UCSD Institutional Review Board (IRB), and in accordance with the Helsinki Declaration of the World Medical Association.

Plasma and neutrophil collection

Blood from healthy donors or COVID-19 patients was drawn in heparinized tubes and plasma was isolated by centrifugation at 1000 x g for 10 minutes. Plasma was aliquoted and stored at -80°C. For neutrophil isolation, blood from healthy donors was drawn and layered onto Polymorphprep™ (PROGEN) per manufacturer's instructions. Briefly, 20 ml whole blood was gently layered onto 20 ml of Polymorphprep™ in a 50 ml conical tube and centrifuged at 500 x g for 30 min at room temperature (RT), sans brake. The granulocyte layer was collected and washed with $HBSS^{Ca-/Mg-}$ and centrifuged at 400 x g for 10 min at RT. Cell pellet was re-suspended in 1 ml of $HBSS^{Ca-/Mg-}$ and cells were counted using an hemocytometer. Average neutrophil purity across samples was 90%. Finally, neutrophils were resuspended at $2x10^6$ cells/ml for functional assays.

Drug preparations (IVIG, dexamethasone, and tocilizumab)

Up to 4 final concentrations of IVIG (Octagam® 10% from Octapharma USA, Inc), were used (0.2, 1, 5 and 10 mg/ml). For dexamethasone, we used a 4 mg/ml stock (Fresenius Kabi) and diluted to 100, 500 and 1000 ng/ml. Tocilizumab was prepared from 20mg/ml (Actemra) and diluted to 20, 200 and 400 µg/ml. All diluted stocks were prepared in $HBSS^{Ca+/Mg+}$.

Quantification of Cell-Free DNA from plasma of patients and for ex vivo NETosis assays

Neutrophils ($2x10^5$ in 100 µl $HBSS^{Ca+/Mg+}$) were plated in 96-well plates and incubated at 37°C with 5% CO_2 with and without IVIG for 30 min, followed by stimulation with either phorbol 12-myristate 13-acetate (PMA) at 25 nM or Nigericin at 15 µM. All conditions were run in triplicate. After 2 hours, 500 mU/ml of micrococcal nuclease was added to each well and incubated for 10 min at 37°C with 5% CO_2. Next, after addition of EDTA, plates were centrifuged at 200 x g for 8 min, and 100 µl supernatant was collected and transferred to a fresh 96-well plate. For quantification of NETs (from *ex vivo* assay) and cell-free DNA (from plasma of patients) the Quant-iT™ PicoGreen™ dsDNA Assay Kit (Invitrogen) was used, following the manufacturer's protocol. Fluorescence was measured using the Infinite M200 (TECAN) plate reader with 480ex/520em.

Imaging of NETs

Neutrophils at $2x10^5$ in 100 µl/well were seeded in an 8-chamber glass slide (Nunc™ Lab-Tek™ II Chamber Slide™ System) and incubating at 37°C with 5% CO_2 for 30 min with and without IVIG. Neutrophils were stimulated with 25 nM PMA and incubated at 37°C with 5% CO_2 for 2 hours. All conditions were run in duplicate. Cells were fixed with 4% Paraformaldehyde and stored at 4°C overnight. To stain for NETs, wells were washed with 1x PBS and then blocked with 2% bovine serum albumin (BSA) and 2% goat serum in PBS for 45min. Cells were incubated for 1 hour with rabbit anti-human

MPO primary antibody (1:300 in 2% PBS-BSA; Dako North America, Inc.), and then with Alexa Fluor 488 goat anti-rabbit IgG secondary antibody (1:500 in 2% PBS-BSA; Life Technologies) for 45 min. Finally, cells were washed and incubated 10 min with 1 µM Hoechst-33342-trihydrochloride. Three washes with 1x PBS were performed after each staining step. Images were obtained using a Zeiss AxioObserver D1 microscope equipped with an LD A-Plan 20x/0.45 Ph1 and 10x/0.30 Ph1 objectives.

Quantification of oxidative burst

We placed 1.2 ml of $2x10^6$ neutrophils/ml in 1.5 ml siliconized tubes and incubated with 10 µM 2',7'-dichlorodihydrofluorescein diacetate for 20 min at 37°C on an orbital shaker. Cells were centrifuged at 500 x g for 8 min and resuspended in the original volume with $HBSS^{Ca-/Mg-}$. Neutrophils at $2x10^5$ in 100 µl were seeded in a 96-well plate and pre-treated with IVIG or dexamethasone for 30 min. Cells were then stimulated with 25 nM of PMA. Each condition was run in triplicate. Cells were incubated at 37°C and 5% CO_2 and fluorescence measured using an Infinite M200 (TECAN) plate reader with 495ex/520em, every 15 min for 2 hours.

Quantification of phagocytosis

Neutrophils were seeded in a 96-well plate at $2x10^5$ per well. Cells were pre-treated with IVIG or dexamethasone for 30 min and cells were washed once with 1x $HBSS^{Ca-/Mg-}$ to remove IVIG or dexamethasone prior to adding bioparticles. Cells were resuspended at 1:1 with pHrodo™ Red *Staphylococcus aureus* Bioparticles™ (Invitrogen) diluted in $HBSS^{Ca+/Mg+}$, centrifuged at 1200 rpm for 5 min and incubated at 37°C and 5% CO_2. Fluorescence was measured with 560ex/585em every 15 min for 2 hours. To exclude background signal, fluorescence of wells containing either HBSS, cells and pHrodo™ Red *S. aureus* Bioparticles was also measured.

Quantification of NET and neutrophil activation related markers in the plasma of COVID-19 subjects

To measure granulocyte-derived elastase, plasma at 1:100 was assessed *via* the PMN Elastase Human ELISA kit (Abcam), following the manufacturer's protocol. For quantification of MPO-DNA, a 96 well plate was coated with 50µl/well of.01 µg/ml anti-MPO mAb (Upstate) and incubated overnight at 4°C. Wells were washed twice with 1x PBS and blocked with 2% BSA for 2 hours. Wells were washed three times and 100µl of plasma samples were added at 1:4 dilutions and incubated at 4°C overnight. Peroxidase-labeled anti-DNA mAb (Cell Death ELISAPLUS, Roche) at a dilution of 1:25 in 100µl of assay buffer was added and plates incubated for 2 hours with shaking at 300 rpm at RT. Wells were washed 3 times and 100 µl of peroxidase substrate was added and incubated for 20 min at RT in the dark. The reaction was stopped with 50µl of 160mM sulfuric acid, and absorbance measured at 405nm. IL-8 was quantified from plasma at a 1:2 dilution using the DuoSet human IL-8/CXCL8 ELISA kit (R&D Systems) following the manufacturer's instructions.

Statistical analysis

Statistical analyses were performed using GraphPad Prism Version 8.4.3 (San Diego). Plasma cytokine levels and NETosis in controls and COVID-19 subjects were analyzed with Mann-Whitney tests. ROS production and phagocytosis assays were analyzed using a 2-way ANOVA with Geisser-Greenhouse correction and Dunnett's multiple comparisons test for each timepoint. Two-sided tests and α level of 0.05 were used to determine significance.

Results

IVIG diminishes NETosis

In order to assess the potential mechanistic effects of IVIG on neutrophil functions, and thus identify further immunomodulatory properties of IVIG, we pre-treated primary human neutrophils with IVIG prior to inducing NETosis. Our assays were performed with isolated neutrophils from healthy donors with over 90% of both live cells (defined at the end of assay in untreated cells) and purity (Supplementary Figures 1A, B). Pre-treatment with IVIG leads to a significant reduction in NETosis, which was dose-dependent after activation of NETosis through different pathways since both PMA- and nigericin-activated neutrophils abrogated NETosis when treated with IVIG (Figures 1A, D). In addition, treatment with IVIG was also able to abrogate spontaneous NETosis on unstimulated neutrophils (Supplementary Figure 2A). On the other hand, therapeutic concentrations of tocilizumab (19) (Figures 1B, E) and dexamethasone (16) (Figures 1C, F) did not affect NETosis using both types of activation. Furthermore, concomitant exposure of neutrophils to IVIG and dexamethasone does not show a synergistic effect on reducing NETs (Supplementary Figure 2B). Upon visualizing NETs *via* fluorescence microscopy, similar findings were seen, with reduction of NETs by IVIG treatment visualized by staining of MPO (a major component of NETs) in a dose-dependent manner (Figure 1G).

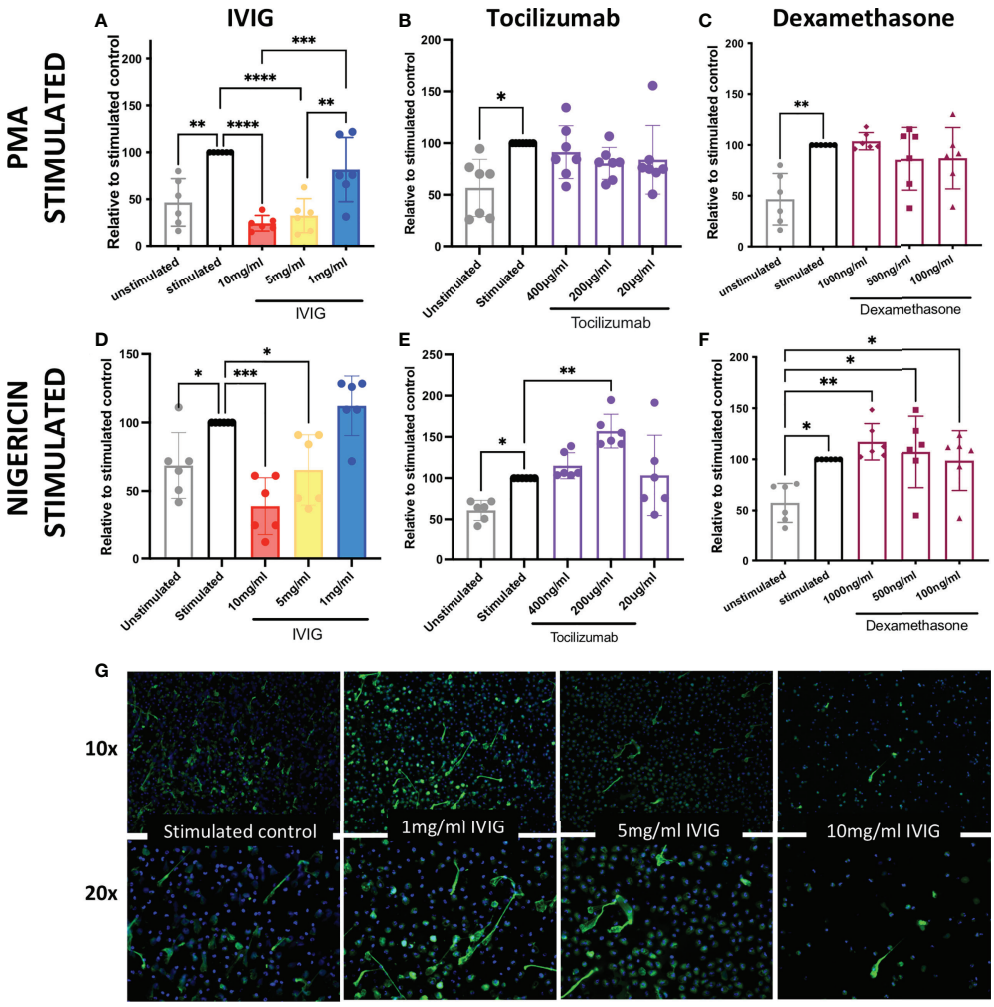

FIGURE 1
IVIG has a dose-dependent suppressive effect on NETosis, which suggests that it may be a complimentary treatment in acute lung injury. *Ex vivo* functional assays of healthy neutrophils stimulated with either PMA or nigericin shows that abrogation of NETosis is induced in a dose-dependent manner by: IVIG **(A, D)**, but not tocilizumab **(B, E)** or dexamethasone **(C, F)**. An alternative approach of assessing NETosis using fluorescence microscopy of neutrophils stained for myeloperoxidase (green; a key component of NETs) shows clear inhibition of NETosis by IVIG **(G)**. Data in panels A–F was analyzed with one-way ANOVA with multiple comparisons. Data are presented as individual data points ± SD with n = 6–7 individuals per group. Error bars represent 95% confidence interval. *P < .05, **P < .01, ***P < .001, ****P < .0001.

IVIG diminishes neutrophil oxidative burst

The production of ROS is a key mechanism used to kill pathogens and is involved in NETosis, which leads to significant inflammation in host tissues. Similar to the impact on NETosis, pre-treatment of neutrophils with IVIG led to reduced production of ROS in a dose-dependent manner, with the highest concentration tested (10mg/ml of IVIG) approaching the low levels of ROS observed in unstimulated controls (Figure 2A). Pre-treatment of neutrophils with varying concentrations of dexamethasone did not impact ROS production (Figure 2A).

Treatment with IVIG preserves neutrophil phagocytosis

Besides NETosis and ROS production, neutrophils also utilize phagocytosis as a primarily antimicrobial mechanism. In the context of COVID-19, we previously found that neutrophils circulating in the blood of critically ill COVID-19 patients had increased phagocytic activity relative to healthy controls (8). Preserving or even increasing phagocytosis is important in COVID-19 and across ARDS patients in general, as these patients are at risk for opportunistic and nosocomial infections. In these studies, we found that neither treatment with

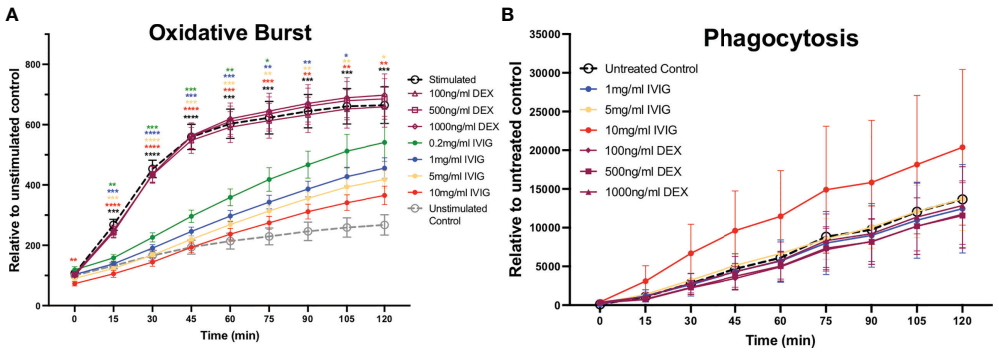

FIGURE 2
Treatment of primary human neutrophils with IVIG inhibits oxidative burst in a dose-dependent manner, while preserving phagocytosis. Circulating neutrophils from healthy controls were used to assess antimicrobial functions including reactive oxygen species production (oxidative burst) and phagocytosis. **(A)** Neutrophil oxidative burst, while being an important antimicrobial function can cause significant collateral damage to tissues, was inhibited in a dose-dependent manner by IVIG (solid circle markers) but not by dexamethasone (hollow purple markers). **(B)** Neutrophil phagocytosis was retained (unaffected) by treatment with IVIG or dexamethasone. Data were analyzed with a 2-way ANOVA with Geisser-Greenhouse correction and Dunnett's multiple comparisons test. Data are presented as individual data points ± SEM with n = 9 and n = 5 individuals per group in oxidative burst and phagocytosis assays, respectively. Error bars represent 95% confidence interval. *P < .05, **P < .01, ***P < .001, ****P < .0001.

IVIG nor dexamethasone had a significant effect on the phagocytic activity of neutrophils (Figure 2B). It is important to mention that IVIG was removed from the assay prior adding the *S. aureus* bioparticles in order to focus on intrinsic changes to neutrophil phagocytic activity, since IVIG can opsonize *S. aureus* bioparticles thus leading to increased phagocytosis.

IVIG treatment and neutrophil-related factors in the circulation of COVID-19 patients

Cell-free DNA and PMN elastase were significantly elevated in COVID-19 patients prior to IVIG treatment, as compared to healthy controls (Figures 3A, C, respectively). After 5 days of IVIG treatment, both cell-free DNA and PMN elastase were significantly reduced (Figures 3B, D, respectively). MPO-DNA complexes were not increased in COVID-19 subjects relative to healthy controls, and did not change across time or when compared prior to the first IVIG dose versus 5 days later (Figures 3E, F, respectively). Finally, IL-8, a key cytokine for neutrophil activation and recruitment, was elevated in COVID-19 patients as compared to healthy controls (Figure 3G), with the IL-8 level at 5 days post IVIG treatment having a non-significant downward trend (Figure 3H).

Discussion

Neutrophils have a "dark side" capable to induce significant immunopathology in different inflammatory settings (3, 4, 7). In the context of COVID-19, a wide variety of studies established neutrophils and their activity with detrimental effects during the disease (8, 10). In COVID-19 and other respiratory diseases, avoiding the development of ARDS is critical (50). ARDS is a very heterogeneous clinical picture with no specific treatment and management of ARDS patients is reduced to supportive therapy (9, 51). During ARDS development, inflammatory cells cause tissue damage affecting lung function (9). Neutrophils have been associated with the development of ARDS in COVID-19 and to worsen the prognosis of the disease (8, 10, 11).

During the course of COVID-19, it is crucial to avoid exacerbation of inflammation, which can lead to organ failure, including ARDS. Thus, the use of corticosteroids in COVID-19 has been widely used worldwide (52). Dexamethasone is one of the most commonly used corticosteroid to diminish and control inflammation in the context of COVID-19 (16, 52). Clinical data supports the use of dexamethasone in patients receiving either invasive mechanical ventilation or oxygen alone (reducing 28-day mortality), although not in those receiving no respiratory support (16). This suggests that clinical situation of the patient and the timing of intervention during the disease course is important to achieve positive results. In the context of neutrophils and their potential contribution to exacerbation of inflammation, here, we show through our established *ex vivo* functional assays that dexamethasone does not have effect in three major neutrophil pathways associated to inflammation, NETosis, oxidative burst and phagocytosis (Figures 1C, 2A, B, respectively). It has been shown that dexamethasone can inhibit *S. aureus*-induced NETosis but not PMA-induced, although that study used a concentration 4 times higher (10μM, thus around 4000 ng/ml) than our highest concentration (1000ng/ml) (53), reaching levels significantly higher that are not probably

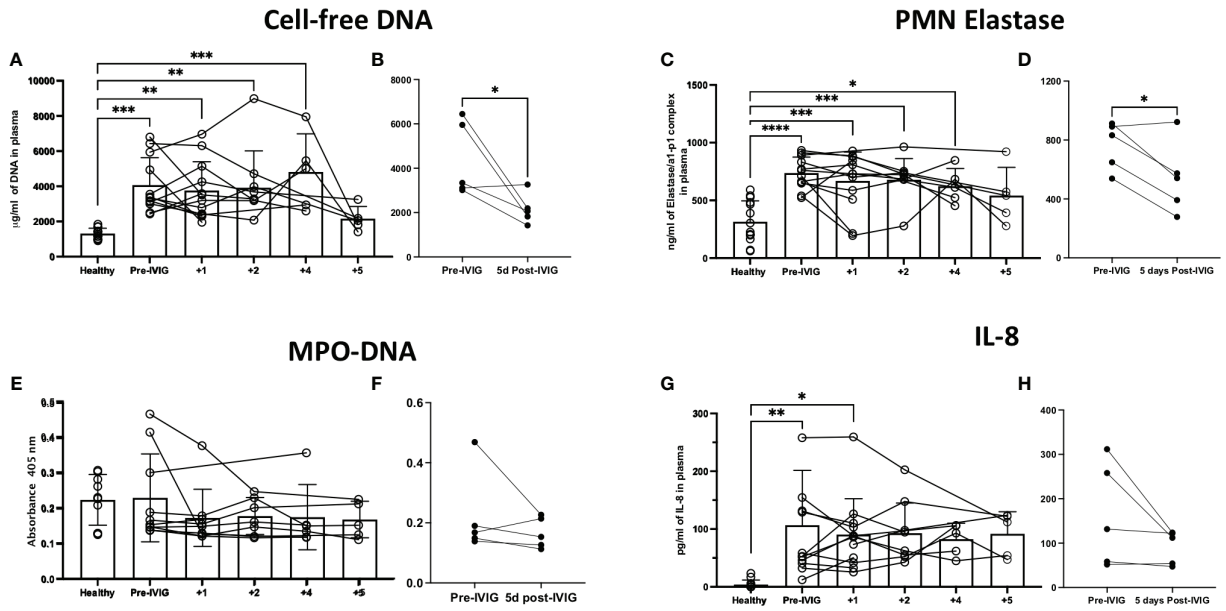

FIGURE 3
Treatment of severe COVID-19 with IVIG may lead to decreased NET-related factors and IL-8 in the circulation of patients. We assessed NET related components in the circulation of IVIG-treated COVID-19 patients, hours before the first IVIG dose and up to 5 days after treatment with IVIG. Moreover, we did a paired comparison of pre-IVIG plasma versus 5 days post-IVIG. We assessed NET components such as cell-free DNA **(A, B)**, neutrophil elastase **(C, D)**, and myeloperoxidase (MPO)-DNA complexes **(E, F)**. Cell-free DNA and neutrophil elastase were significantly elevated in COVID-19 patients relative to controls **(A, C)**, and decreased after IVIG treatment **(B, D)**. MPO-DNA was not elevated in the plasma of patients with severe COVID-19 and did not change after IVIG treatment **(E, F)**. The neutrophil chemokine and activating cytokine IL-8 was elevated in the plasma of COVID-19 patients **(G)** but did not significantly decrease after IVIG treatment **(H)**. Data for panels A, C, E, and G was analyzed *via* one-way ANOVA with Tukey's multiple comparisons test, although data points from same patients are connected to observe data trends. Data for panels B, D, F and H was analyzed with paired t-tests. Data are presented as individual data points ± SD with healthy controls (n = 10-14) and COVID-19 (n = 12). Error bars represent 95% confidence interval. *P < .05, **P < .01, ***P < .001, ****P < .0001.

achieved physiologically during COVID-19 treatment, which is usually 6 mg of dexamethasone per day (23). Recently, it has been reported that in the context of COVID-19, dexamethasone can downregulate interferon-stimulated genes and activated IL-1R2^{+} in neutrophils, and to expand immunosuppressive immature neutrophils (54), thus the mechanism by which dexamethasone can diminish neutrophil activity is by affecting their functions toward a immunosuppressive phenotype. Similar to dexamethasone, tocilizumab, a monoclonal antibody against the interleukin-6 receptor (IL-6R) used to abrogate IL-6 signaling, does not have any effect in NETosis when used within the range of therapeutic concentrations (Figure 1C). Although, tocilizumab are also immunoglobulins as IVIG, tocilizumab in a monoclonal population of IgGs that are used at a lower concentrations than IVIG due to its specificity for the IL-6R, hence the effect on neutrophils may not be achieve at the used concentrations and by the nature of formulation of tocilizumab. On the other hand, IVIG is able to significantly abrogate NETosis (under both PMA and nigericin activation) and oxidative burst in a dose-dependent manner (Figures 1A, D, G, 2A), which suggests that complementation of standard treatment with IVIG might account for the lower mortality rate observed in IVIG-treated patients through diminishing neutrophil-mediated immunopathology, having implications in other conditions with neutrophil-mediated immunopathology. Interestingly, neither dexamethasone, tocilizumab nor IVIG seem to have an effect in changing the phagocytic activity of neutrophils. This data concur with our previous findings showing that neutrophils isolated from COVID-19 have enhanced phagocytic activity as compared to healthy controls, even when some COVID-19 patients received dexamethasone and/or tocilizumab (8). IVIG have shown to be able to modulate neutrophil functions, although in contrary to our results, early studies showed that IVIG can induce the production of ROS (42–44), NETs (myeloperoxidase and elastase) (45, 46) and increased activation status defined by changes in surface markers (47). However, recently, Bohländer et al, found that IVIG can decrease inflammation in the neutrophil-like HL60 cells by reducing the release of cytokines such as IL-10, MCP-1 and IL-8 (48); and Uozumi et al. observed that treatment of human neutrophils with 5ml/ml of human sulfo-immunoglobulins lead to decreased production of NETs defined by staining of DNA with SYTOX (49), a different approach that this study for NET assessment. Nevertheless,

there are significant differences in the experimental designs of all those studies. For instance, although most studies used isolated neutrophils (31, 43–45), some studies used whole blood (47) or a neutrophil-like cell line (48). Moreover, neutrophil activation varied from using live bacteria (15, 45), LPS (47), TNFα (21, 46) and even SARS-CoV-2-like particles associated to SARS-CoV-2 spike protein specific IgG, IgA, and IgM antibodies (48). In this study, we used PMA, which is commonly used in leukocyte activation studies, and studying neutrophils is not the exception, particularly in assessing NETosis and oxidative burst (55, 56).

IVIG has been used for a while to treat autoimmune diseases, evidencing its immunomodulatory properties (25). Hence, early attempts to introduce IVIG to counteract hyperinflammation in COVID-19 were expected. However, contradictory conclusions have arisen, from being beneficial by reducing mortality and time of hospitalization (26–34), to showing no differences in mortality rate (35), to even suggesting a tendency to be associated with an increased frequency of serious adverse events (36). Nevertheless, differences between these studies may account for their opposite conclusions. For instance, there are differences in dosage of IVIG, length of treatment, timing of first dose upon admission, the formulation of IVIG, additional treatments, amount of subjects and subject heterogeneity.

Despite ambiguous results at the global level, our specific clinical experience with IVIG has been highly successful when niche-applied early to patients without end-organ comorbidities or advanced age (57, 58). As part of quality measurements by Sharp Healthcare, data was collected to assess clinical outcomes in patients with COVID-19 at different stages of the pandemic. Review of these data has demonstrated a survival benefit in IVIG recipients ≤70 years of age with severe to critical COVID-19 (receipt of high-flow oxygen or greater oxygen requirement, WHO severity score 5-7). In these patients, receipt standard of care alone (remdesivir, glucocorticoids) was 21%, receipt of adjunctive tocilizumab mortality was 23%, and only 7% in IVIG recipients (p=0.03, Fisher exact test, unpublished observations). Although limited in sample size and a single-center retrospective assessment, this clinical experience coupled with our findings showing IVIG attenuation of neutrophil-driven inflammation clearly sets the stage for important more rigorous future clinical study of IVIG. Interestingly, we previously showed that COVID-19 treated with tocilizumab have increased IL-6 in circulation (8), which correlates with a numerically higher mortality in tocilizumab recipients, and also aligns with a larger study showing no improvement on the clinical status or lower mortality (19).

The inconsistent results of IVIG benefit in COVID-19 rest largely on the broad heterogeneity of COVID-19 patient types. COVID-19 therapeutics are likely impactful only in younger patients at high-risk for COVID-19 disease with comorbidities like obesity, hypertension, and diabetes mellitus but without end-organ damage. In settings of advanced age and/or baseline organ failure, mortality from COVID-19 may be significantly less modifiable, not only due to direct COVID-19 factors, but due to the increased risk of secondary complications such as cardiovascular, thrombotic, or secondary bacterial or fungal infections, and even adverse drug reactions. Unfortunately, large prospective clinical trials may be underpowered to be able to address specific patient subtypes within their cohorts (36, 59). Thus, more studies are needed to consider IVIG as part of standard therapy for COVID-19 (and perhaps viral ARDS), specifically addressing subpopulations who may benefit. Related to this, there is evidence showing that the beneficial effects of IVIGs might depend on the composition of the IVIG preparation, the immune status of the patient, and the severity of the disease (60). Although the majority of the studies use IVIG based on IgGs, other studies have shown that IVIG containing relevant amounts of IgM and IgA (in addition to IgG) can modulate the release of pro-inflammatory cytokines in neutrophil-like HL60 cell line better than IVIG containing mostly IgGs (48). Nevertheless, in our cohort of patients we found that neutrophil-related factors, such as those involved in NETosis, including cell-free DNA and PMN elastase seem to be reduced upon complementation with IVIG (Figures 3A–D), although even when cell-free DNA is a well-accepted indicator of NET in circulation, it can also come from other sources such as dead cells. Moreover, MPO-DNA did not show significant differences although trend over time appears to be downward, and interestingly there was no difference between healthy donors and COVID-19 patients (Figures 3E, F). Similarly, IL-8, a strong chemoattractant and activator of neutrophils also showed a trend down over time, but in this case there was a significant difference between COVID-19 and healthy plasma (Figures 3G, H), which aligns to our previous findings and others associating increased IL-8 in the severity of COVID-19 (8).

Currently, different trials are attempting to inhibit or block neutrophil pathways to control inflammation. Several current trials are targeting NETosis, since they are highly pro-inflammatory (61). Some trials are addressing the use of DNase (61–64), which tackle NETs effects once they are released, (but may not directly inhibit proteolytic enzymes coating the DNA strands) in contrary to IVIG, which prevent their release according to our *ex vivo* assays. Related to this, a recent non-randomized open-label study evaluated the complementation with inhaled DNase plus tocilizumab and baricitinib (JAK1/2 inhibitor), finding association with lower in-hospital mortality and intubation rate, shorter duration of hospitalization, and prolonged overall survival; in addition, in an *in vitro* approach, plasma from those COVID-19 patients undergoing the complemented treatment induced less tissue factor/thrombin pathway in primary lung fibroblasts as compared to standard-of-care (64). Nevertheless, it is important to consider that the anti-inflammatory effect of IVIG also occurs in other leukocytes and that this study is strictly limited to neutrophils. Thus, more studies are needed to address the questions to the overall impact of IVIG in COVID-19 patients and other inflammatory conditions.

This study has limitations such as the small cohort of COVID-19 patients, the lack of some samples from each time point, limited

to components in circulation (even when neutrophils are phenotypically different from circulation to lung tissue (65). Our *ex vivo* studies utilized two activation stimuli, which may not accurately reflect all NET compositions, as such compositions can change depending on the stimulus (66, 67). Furthermore, there was no comparator group of similar illness severity and similar points of illness who did not receive IVIG or received placebo in its place. Regardless of the limitations, this study established the foundation of the effect of IVIG in three key functions of neutrophils and along with data from IVIG-treated patients suggests that complementation of IVIG to standard therapy for COVID-19 may diminish neutrophil pro-inflammatory pathways, which are not affected by the commonly used corticosteroid, dexamethasone.

Data availability statement

The raw data supporting the conclusions of this article will be made available by the authors, without undue reservation.

Ethics statement

The study was reviewed and approved by the Sharp Healthcare Internal Review Board (#2010902). Ex vivo neutrophil and plasma studies were conducted with VASDHS institutional review board (IRB) approval B200003, a non-human subject research waiver from the UCSD Institutional Review Board (IRB), and in accordance with the Helsinki Declaration of the World Medical Association. The patients/participants provided their written informed consent to participate in this study.

Author contributions

JM-S, AM, VN and LC contributed to conception and design of the study. JM-S and AM organized the database. JM-S, JO and VG performed the experiments. JM-S and LC performed the statistical analysis. JM-S wrote the first draft of the manuscript. GS wrote sections of the manuscript. GS and MG provide key samples. All authors contributed to manuscript revision, read, and approved the submitted version.

Funding

This work was supported by a Veterans Affairs Merit Award 1I01BX004767 (LC), NIH NHLBI K24HL155884 and R01HL137052 (LC), TRDRP Award T30IP0965 (LC), and UCSD ACTRI 1KL2TR001444 (AM).

Acknowledgments

Octagam 10% for this study both for patient administration and for *in vitro* work was provided by Octapharma USA (Hoboken, NJ).

Conflict of interest

Author GS has received consulting and research fees from Octapharma USA (Hoboken, NJ).

The remaining authors declare that the research was conducted in the absence of any commercial or financial relationships that could be construed as a potential conflict of interest.

Publisher's note

Supplementary material

The Supplementary Material for this article can be found online at: https://www.frontiersin.org/articles/10.3389/fimmu.2022.993720/full#supplementary-material

SUPPLEMENTARY FIGURE 1
Cell viability and purity of neutrophils for functional assays. Upon isolation of neutrophils, viability was assessed by staining with propidium iodide and analyze by flow cytometric analysis, observing over 90% live cells **(A)**. In addition, over 90% purity was obtained in isolated cells, which was observed by cytospining cells and staining with Giemsa, a representative picture is shown **(B)**.

SUPPLEMENTARY FIGURE 2
IVIG alone can inhibit spontaneous NETosis and dexamethasone does not show synergistic inhibitory effect with IVIG. Isolated neutrophils were incubated with increasing concentrations of IVIG for 3.5 h and no activation stimuli was added to cell culture, observing that IVIG can also diminish spontaneous NETosis in a dose-dependent manner. In addition, a potential synergistic effect was assessed by incubating neutrophils with IVIG and dexamethasone concomitantly; observing that dexamethasone at 500 ng/ml does not enhance NETosis abrogation caused by IVIG **(B)**. Data was analyzed with one-way ANOVA with multiple comparisons. Data are presented as individual data points ± SD with n=6 individuals per group. Error bars represent 95% confidence interval. **P<.01, ***P<.001, ****P<.0001.

References

1. Mantovani A, Cassatella MA, Costantini C, Jaillon S. Neutrophils in the activation and regulation of innate and adaptive immunity. *Nat Rev Immunol* (2011) 11(8):519–31. doi: 10.1038/nri3024

2. Leliefeld PHC, Koenderman L, Pillay J. How neutrophils shape adaptive immune responses. *Front Immunol* (2015) 6. doi: 10.3389/fimmu.2015.00471

3. Sorensen OE, Borregaard N. Neutrophil extracellular traps - the dark side of neutrophils. *J Clin Invest.* (2016) 126(5):1612–20. doi: 10.1172/JCI84538

4. Mitsios A, Arampatzioglou A, Arelaki S, Mitroulis I, Ritis K. NETopathies? unraveling the dark side of old diseases through neutrophils. *Front Immunol* (2017) 7. doi: 10.3389/fimmu.2016.00678

5. Mortaz E, Alipoor SD, Adcock IM, Mumby S, Koenderman L. Update on neutrophil function in severe inflammation. *Front Immunol* (2018) 9. doi: 10.3389/fimmu.2018.02171

6. Gupta S, Kaplan MJ. The role of neutrophils and NETosis in autoimmune and renal diseases. *Nat Rev Nephrology* (2016) 12(7):402–13. doi: 10.1038/nrneph.2016.71

7. Fousert E, Toes R, Desai J. Neutrophil extracellular traps (NETs) take the central stage in driving autoimmune responses. *Cells* (2020) 9(4):1–20. doi: 10.3390/cells9040915

8. Masso-Silva JA, Moshensky A, Lam MTY, Odish MF, Patel A, Xu L, et al. Increased peripheral blood neutrophil activation phenotypes and neutrophil extracellular trap formation in critically ill coronavirus disease 2019 (COVID-19) patients: A case series and review of the literature. *Clin Infect Dis* (2021) 74(3):479–89. doi: 10.1093/cid/ciab437

9. Saguil A, Fargo MV. Acute respiratory distress syndrome: Diagnosis and management. *Am Fam Physician* (2020) 101(12):730–8.

10. McKenna E, Wubben R, Isaza-Correa JM, Melo AM, Mhaonaigh AU, Conlon N, et al. Neutrophils in COVID-19: Not innocent bystanders. *Front Immunol* (2022) 13. doi: 10.3389/fimmu.2022.864387

11. Chiang C-C, Korinek M, Cheng W-J, Hwang T-L. Targeting neutrophils to treat acute respiratory distress syndrome in coronavirus disease. *Front Pharmacol* (2020) 11. doi: 10.3389/fphar.2020.572009

12. Rosales C. Neutrophil: A cell with many roles in inflammation or several cell types? *Front Physiol* (2018) 9. doi: 10.3389/fphys.2018.00113

13. Delgado-Rizo V, Martínez-Guzmán M, Iñiguez-Gutierrez L, García-Orozco A, Alvarado-Navarro A, Fafutis-Morris M. Neutrophil extracellular traps and its implications in inflammation: an overview. *Front Immunol* (2017) 8. doi: 10.3389/fimmu.2017.00081

14. Winterbourn CC, Kettle AJ, Hampton MB. Reactive oxygen species and neutrophil function. *Annu Rev Biochem* (2016) 85:765–92. doi: 10.1146/annurev-biochem-060815-014442

15. Barnes PJ. How corticosteroids control inflammation: Quintiles prize lecture 2005. *Br J Pharmacol* (2006) 148(3):245–54. doi: 10.1038/sj.bjp.0706736

16. Horby P, Lim WS, Emberson JR, Mafham M, Bell JL, Linsell L, et al. Dexamethasone in hospitalized patients with covid-19. *N Engl J Med* (2021) 384 (8):693–704. doi: 10.1056/NEJMoa2021436

17. Närhi F, Moonesinghe SR, Shenkin SD, Drake TM, Mulholland RH, Donegan C, et al. Implementation of corticosteroids in treatment of COVID-19 in the ISARIC WHO clinical characterisation protocol UK: prospective, cohort study. *Lancet Digital Health* (2022) 4(4):e220–e34. doi: 10.1016/S2589-7500(22)00018-8

18. Cavalli G, Farina N, Campochiaro C, De Luca G, Della-Torre E, Tomelleri A, et al. Repurposing of biologic and targeted synthetic anti-rheumatic drugs in COVID-19 and hyper-inflammation: A comprehensive review of available and emerging evidence at the peak of the pandemic. *Front Pharmacol* (2020) 11. doi: 10.3389/fphar.2020.598308

19. Rosas IO, Bräu N, Waters M, Go RC, Hunter BD, Bhagani S, et al. Tocilizumab in hospitalized patients with severe covid-19 pneumonia. *N Engl J Med* (2021) 384(16):1503–16. doi: 10.1056/NEJMoa2028700

20. Mariette X, Hermine O, Tharaux P-L, Resche-Rigon M, Steg PG, Porcher R, et al. Effectiveness of tocilizumab in patients hospitalized with COVID-19: A follow-up of the CORIMUNO-TOCI-1 randomized clinical trial. *JAMA Internal Med* (2021) 181(9):1241–3. doi: 10.1001/jamainternmed.2021.2209

21. Johnson AG, Amin AB, Ali AR, Hoots B, Cadwell BL, Arora S, et al. COVID-19 incidence and death rates among unvaccinated and fully vaccinated adults with and without booster doses during periods of delta and omicron variant emergence - 25 U.S. jurisdictions, April 4-December 25, 2021. *MMWR Morb Mortal Wkly Rep* (2022) 71(4):132–8. doi: 10.15585/mmwr.mm7104e2

22. Kaplan MJ. Neutrophils in the pathogenesis and manifestations of SLE. *Nat Rev Rheumatol* (2011) 7(12):691–9. doi: 10.1038/nrrheum.2011.132

23. Knight JS, Meng H, Coit P, Yalavarthi S, Sule G, Gandhi AA, et al. Activated signature of antiphospholipid syndrome neutrophils reveals potential therapeutic target. *JCI Insight* (2017) 2(18):1–13. doi: 10.1172/jci.insight.93897

24. Maugeri N, Capobianco A, Rovere-Querini P, Ramirez Giuseppe A, Tombetti E, Valle Patrizia D, et al. Platelet microparticles sustain autophagy-associated activation of neutrophils in systemic sclerosis. *Sci Trans Med* (2018) 10 (451):eaao3089. doi: 10.1126/scitranslmed.aao3089

25. Shoenfeld Y, Katz U. IVIg therapy in autoimmunity and related disorders: our experience with a large cohort of patients. *Autoimmunity* (2005) 38(2):123–37. doi: 10.1080/08916930500059633

26. Herth FJF, Sakoulas G, Haddad F. Use of intravenous immunoglobulin (Prevagen or octagam) for the treatment of COVID-19: Retrospective case series. *Respiration* (2020) 99(12):1145–53. doi: 10.1159/000511376

27. Sakoulas G, Geriak M, Kullar R, Greenwood KL, Habib M, Vyas A, et al. Intravenous immunoglobulin plus methylprednisolone mitigate respiratory morbidity in coronavirus disease 2019. *Crit Care Explor* (2020) 2(11):1–7. doi: 10.1097/CCE.0000000000000280

28. Gharebaghi N, Nejadrahim R, Mousavi SJ, Sadat-Ebrahimi S-R, Hajizadeh R. The use of intravenous immunoglobulin gamma for the treatment of severe coronavirus disease 2019: a randomized placebo-controlled double-blind clinical trial. *BMC Infect Dis* (2020) 20(1):786. doi: 10.1186/s12879-020-05507-4

29. Raman RS, Bhagwan Barge V, Anil Kumar D, Dandu H, Rakesh Kartha R, Bafna V, et al. A phase II safety and efficacy study on prognosis of moderate pneumonia in coronavirus disease 2019 patients with regular intravenous immunoglobulin therapy. *J Infect Diseases.* (2021) 223(9):1538–43. doi: 10.1093/infdis/jiab098

30. Shao Z, Feng Y, Zhong L, Xie Q, Lei M, Liu Z, et al. Clinical efficacy of intravenous immunoglobulin therapy in critical ill patients with COVID-19: a multicenter retrospective cohort study. *Clin Transl Immunol* (2020) 9(10):e1192–e. doi: 10.1002/cti2.1192

31. Esen F, Özcan PE, Orhun G, Polat Ö, Anaklı İ, Alay G, et al. Effects of adjunct treatment with intravenous immunoglobulins on the course of severe COVID-19: results from a retrospective cohort study. *Curr Med Res Opin* (2021) 37 (4):543–8. doi: 10.1080/03007995.2020.1856058

32. Cao W, Liu X, Hong K, Ma Z, Zhang Y, Lin L, et al. High-dose intravenous immunoglobulin in severe coronavirus disease 2019: A multicenter retrospective study in China. *Front Immunol* (2021) 12. doi:10.3389/fimmu.2021.627844

33. Daneshpazhooh M, Soori T, Isazade A, Noormohammadpour P. Mucous membrane pemphigoid and COVID-19 treated with high-dose intravenous immunoglobulins: a case report. *J Dermatolog Treat* (2020) 31(5):446–7. doi: 10.1080/09546634.2020.1764472

34. Mohtadi N, Ghaysouri A, Shirazi S, Sara A, Shafiee E, Bastani E, et al. Recovery of severely ill COVID-19 patients by intravenous immunoglobulin (IVIG) treatment: A case series. *Virology* (2020) 548:1–5. doi: 10.1016/j.virol.2020.05.006

35. Tabarsi P, Barati S, Jamaati H, Haseli S, Marjani M, Moniri A, et al. Evaluating the effects of intravenous immunoglobulin (IVIg) on the management of severe COVID-19 cases: A randomized controlled trial. *Int Immunopharmacology* (2021) 90:107205. doi: 10.1016/j.intimp.2020.107205

36. Mazeraud A, Jamme M, Mancusi RL, Latroche C, Megarbane B, Siami S, et al. Intravenous immunoglobulins in patients with COVID-19-associated moderate-to-severe acute respiratory distress syndrome (ICAR): multicentre, double-blind, placebo-controlled, phase 3 trial. *Lancet Respir Med* (2022) 10 (2):158–66. doi: 10.1016/S2213-2600(21)00440-9

37. Saha C, Kothapalli P, Patil V, ManjunathaReddy GB, Kaveri SV, Bayry J. Intravenous immunoglobulin suppresses the polarization of both classically and alternatively activated macrophages. *Hum Vaccin Immunother.* (2020) 16(2):233–9. doi: 10.1080/21645515.2019.1602434

38. Das M, Karnam A, Stephen-Victor E, Gilardin L, Bhatt B, Kumar Sharma V, et al. Intravenous immunoglobulin mediates anti-inflammatory effects in peripheral blood mononuclear cells by inducing autophagy. *Cell Death Disease.* (2020) 11(1):50. doi: 10.1038/s41419-020-2249-y

39. MacMillan HF, Lee T, Issekutz AC. Intravenous immunoglobulin G-mediated inhibition of T-cell proliferation reflects an endogenous mechanism by which IgG modulates T-cell activation. *Clin Immunol* (2009) 132(2):222–33. doi: 10.1016/j.clim.2009.04.002

40. Mitrevski M, Marrapodi R, Camponeschi A, Cavaliere FM, Lazzeri C, Todi L, et al. Intravenous immunoglobulin and immunomodulation of b-cell - *in vitro* and *in vivo* effects. *Front Immunol* (2015) 6:4–. doi: 10.3389/fimmu.2015.00004

41. Basyreva LY, Brodsky IB, Gusev AA, Zhapparova ON, Mikhalchik EV, Gusev SA, et al. The effect of intravenous immunoglobulin (IVIG) on ex vivo

activation of human leukocytes. *Hum Antibodies* (2016) 24(3-4):39–44. doi: 10.3233/HAB-160293

42. Maródi L, Kalmár A, Karmazsin L. Stimulation of the respiratory burst and promotion of bacterial killing in human granulocytes by intravenous immunoglobulin preparations. *Clin Exp Immunol* (1990) 79(2):164–9. doi: 10.1111/j.1365-2249.1990.tb05173.x

43. Jarius S, Eichhorn P, Albert MH, Wagenpfeil S, Wick M, Belohradsky BH, et al. Intravenous immunoglobulins contain naturally occurring antibodies that mimic antineutrophil cytoplasmic antibodies and activate neutrophils in a TNFα-dependent and fc-receptor–independent way. *Blood* (2007) 109(10):4376–82. doi: 10.1182/blood-2005-12-019604

44. Nemes E, Teichman F, Roos D, Maródi L. Activation of human granulocytes by intravenous immunoglobulin preparations is mediated by FcgammaRII and FcgammaRIII receptors. *Pediatr Res* (2000) 47(3):357–61. doi: 10.1203/00006450-200003000-00012

45. Itoh H, Matsuo H, Kitamura N, Yamamoto S, Higuchi T, Takematsu H, et al. Enhancement of neutrophil autophagy by an IVIG preparation against multidrug-resistant bacteria as well as drug-sensitive strains. *J Leukoc Biol* (2015) 98(1):107–17. doi: 10.1189/jlb.4A0813-422RRR

46. Teeling JL, De Groot ER, Eerenberg AJM, Bleeker WK, Van Mierlo G, Aarden LA, et al. Human intravenous immunoglobulin (IVIG) preparations degranulate human neutrophils in vitro. *Clin Exp Immunol* (1998) 114(2):264–70. doi: 10.1046/j.1365-2249.1998.00697.x

47. Casulli S, Topçu S, Fattoum L, von Gunten S, Simon H-U, Teillaud J-L, et al. A differential concentration-dependent effect of IVIg on neutrophil functions: Relevance for anti-microbial and anti-inflammatory mechanisms. *PloS One* (2011) 6(10):e26469. doi: 10.1371/journal.pone.0026469

48. Bohländer F, Riehl D, Weißmüller S, Gutscher M, Schüttrumpf J, Faust S. Immunomodulation: Immunoglobulin preparations suppress hyperinflammation in a COVID-19 model *via* FcγRIIA and FcαRI. *Front Immunol* (2021) 12:700429. doi: 10.3389/fimmu.2021.700429

49. Uozumi R, Iguchi R, Masuda S, Nishibata Y, Nakazawa D, Tomaru U, et al. Pharmaceutical immunoglobulins reduce neutrophil extracellular trap formation and ameliorate the development of MPO-ANCA-associated vasculitis. *Mod Rheumatol* (2020) 30(3):544–50. doi: 10.1080/14397595.2019.1602292

50. Yadav H, Thompson BT, Gajic O. Fifty years of research in ARDS. is acute respiratory distress syndrome a preventable disease? *Am J Respir Crit Care Med* (2017) 195(6):725–36. doi: 10.1164/rccm.201609-1767CI

51. Wilson JG, Calfee CS. ARDS subphenotypes: Understanding a heterogeneous syndrome. *Crit Care* (2020) 24(1):102. doi: 10.1007/978-3-030-37323-8_5

52. Annane D. Corticosteroids for COVID-19. *J Intensive Med* (2021) 1(1):14–25. doi: 10.1016/j.jointm.2021.01.002

53. Wan T, Zhao Y, Fan F, Hu R, Jin X. Dexamethasone inhibits s. aureus-induced neutrophil extracellular pathogen-killing mechanism, possibly through toll-like receptor regulation. *Front Immunol* (2017) 8:60. doi: 10.3389/fimmu.2017.00060

54. Sinha S, Rosin NL, Arora R, Labit E, Jaffer A, Cao L, et al. Dexamethasone modulates immature neutrophils and interferon programming in severe COVID-19. *Nat Med* (2022) 28(1):201–11. doi: 10.1038/s41591-021-01576-3

55. Blanter M, Gouwy M, Struyf S. Studying neutrophil function *in vitro*: Cell models and environmental factors. *J Inflamm Res* (2021) 14:141–62. doi: 10.2147/JIR.S284941

56. Vorobjeva NV, Chernyak BV. NETosis: Molecular mechanisms, role in physiology and pathology. *Biochem (Mosc)* (2020) 85(10):1178–90. doi: 10.1134/S0006297920100065

57. Geriak M, McGrosso D, Gonzalez DJ, Dehner M, Sakoulas G. Case series of successful intravenous immunoglobulin (IVIG) treatment in 4 pregnant patients with severe COVID-19-Induced hypoxia. *Am J Case Rep* (2022) 23:e936734. doi: 10.12659/AJCR.936734

58. Poremba M DM, Perreiter A, Semma A, Mills K, Sakoulas G. Intravenous immunoglobulin in treating nonventilated COVID-19 patients with moderate-to-Severe hypoxia: A pharmacoeconomic analysis. *J Clin Outcomes Management.* (2022) 29(3):123–9. doi: 10.12788/jcom.0094

59. Wilfong EM, Matthay MA. Intravenous immunoglobulin therapy for COVID-19 ARDS. *Lancet Respir Med* (2022) 10(2):123–5. doi: 10.1016/S2213-2600(21)00450-1

60. Kindgen-Milles D, Feldt T, Jensen BEO, Dimski T, Brandenburger T. Why the application of IVIG might be beneficial in patients with COVID-19. *Lancet Respir Med* (2022) 10(2):e15. doi: 10.1016/S2213-2600(21)00549-X

61. Barnes BJ, Adrover JM, Baxter-Stoltzfus A, Borczuk A, Cools-Lartigue J, Crawford JM, et al. Targeting potential drivers of COVID-19: Neutrophil extracellular traps. *J Exp Med* (2020) 217(6):1–7. doi: 10.1084/jem.20200652

62. Weber AG, Chau AS, Egeblad M, Barnes BJ, Janowitz T. Nebulized in-line endotracheal dornase alfa and albuterol administered to mechanically ventilated COVID-19 patients: a case series. *Mol Med* (2020) 26(1):91. doi: 10.1186/s10020-020-00215-w

63. Lee YY, Park HH, Park W, Kim H, Jang JG, Hong KS, et al. Long-acting nanoparticulate DNase-1 for effective suppression of SARS-CoV-2-mediated neutrophil activities and cytokine storm. *Biomaterials* (2021) 267:120389–. doi: 10.1016/j.biomaterials.2020.120389

64. Gavriilidis E, Antoniadou C, Chrysanthopoulou A, Ntinopoulou M, Smyrlis A, Fotiadou I, et al. Combined administration of inhaled DNase, baricitinib and tocilizumab as rescue treatment in COVID-19 patients with severe respiratory failure. *Clin Immunol* (2022) 238:109016. doi: 10.1016/j.clim.2022.109016

65. Christoffersson G, Phillipson M. The neutrophil: one cell on many missions or many cells with different agendas? *Cell Tissue Res* (2018) 371(3):415–23. doi: 10.1007/s00441-017-2780-z

66. Hoppenbrouwers T, Autar ASA, Sultan AR, Abraham TE, van Cappellen WA, Houtsmuller AB, et al. *In vitro* induction of NETosis: Comprehensive live imaging comparison and systematic review. *PloS One* (2017) 12(5):e0176472. doi: 10.1371/journal.pone.0176472

67. Pruchniak MP, Demkow U. Potent NETosis inducers do not show synergistic effects in vitro. *Cent Eur J Immunol* (2019) 44(1):51–8. doi: 10.5114/ceji.2019.84017

Frontiers in Pharmacology

Explores the interactions between chemicals and living beings

The most cited journal in its field, which advances access to pharmacological discoveries to prevent and treat human disease.

Discover the latest Research Topics

See more →

Frontiers

Avenue du Tribunal-Fédéral 34
1005 Lausanne, Switzerland
frontiersin.org

Contact us

+41 (0)21 510 17 00
frontiersin.org/about/contact